Cellular Metabolism and the NLRP3 Inflammasome as Therapeutic Targets in Cystic Fibrosis

Thomas Edward Scambler

Submitted in accordance with the requirements for the degree of

Doctor of Philosophy

The University of Leeds

Faculty of Medicine and Health

September 2018

The candidate confirms that the work is his own and that appropriate credit has been given where reference has been made to the work of others.

This copy has been supplied on the understanding that it is copyright material and that no quotation from the thesis may be published without proper acknowledgement.

Acknowledgments

I would like to thank and acknowledge those people without whom this project would not have been possible. Firstly, I would like to thank my three supervisors Professor Michael McDermott, Professor Daniel Peckham and Dr Sinisa Savic. Michael first supported my scholarship through unwavering guidance, support and encouragement, which continued throughout my time at the University of Leeds. Daniel has provided expert knowledge to the project that has proven time and time again to be invaluable. Sinisa offered excellent scientific critique during the project, which I feel has led to the quality of my research to improve substantially. All three supervisors were fully dedicated to the project as well as my development as a scientist and have given me honest advice that was always appreciated.

I would like to thank Dr Chi Wong who has taught me how to be a bench scientist, not only regarding technical knowledge but how to conduct myself in the lab as an honest and hardworking scientist. Chi was always available for questions, for which I cannot thank him enough.

I would also like to thank Dr Heledd Jarosz-Griffiths, Mr Samuel Lara Reyna, Mr Jonathan Holbrook, Dr Stephanie Harrison and Ms Shelly Pathak. Their friendship made looming deadlines, troubleshooting impossible experiments and cleaning tissue culture tolerable and made conferences, lab successes and publishing papers a real joy.

Finally, I would like to acknowledge my wife, Devon. Her scientific, editorial and psychological support sustained me on the marathon that is a PhD, a journey that we both started and finished together.

Abstract

Cystic Fibrosis (CF) is caused by mutations in the gene encoding the CFTR protein, an anion channel that conducts Cl^- and $HCO3^-$ and regulates amiloride-sensitive Na^+ channels. In both animal and *in vitro* models, CFTR dysfunction results in excessive neutrophilic inflammation, Na^+ absorption and inflammasome activation, with a strong interleukin (IL)-1 signature.

This study's hypothesis is that CF is associated with a pathogenic increase in Na^+ transport, which occurs due to the loss of CFTR-dependent inhibition of amiloride-sensitive Na^+ channels and drives excessive inflammation and metabolism at the molecular and systemic level.

Primary human monocytes, macrophages and bronchial epithelial cell lines, with characterised CF-associated mutations, were cultured *in vitro* and stimulated for NLRP3 inflammasome activation. Differentiated macrophages were characterised using flow cytometry. Cytokines, ion fluxes and metabolites were measured from *in vitro* stimulations using colorimetric and fluorometric assays.

Patients with CF were observed to have a systemic proinflammatory cytokine signature accompanied by an *in vitro* hyperactivation of the NLRP3 inflammasome and metabolic pathways associated with proinflammatory immune phenotypes. Excessive Na^+ influx in cells with CF-associated mutations, which created a propensity for excessive K^+ efflux and cellular energy demand upon stimulation, was observed in this study. Primary CF monocytes and epithelial cell lines hyper-responded to NLRP3 stimulation with disproportionate IL-1β and IL-18 secretion, inhibited by pre-treatment with small molecule and peptide inhibitors of Na^+ channels, metabolic pathways and the NLRP3 inflammasome. In addition, a small cohort of

patients with CF-associated mutations on a 3-month study of small molecule CFTR modulator therapy showed a reduction in inflammation and glycolysis.

This is the first study to demonstrate a link between excess Na$^+$ absorption, a characteristic intrinsic feature of CF, and increased inflammation and metabolism. Future therapies will need to focus on rectifying Na$^+$ absorption if they are to obtain maximal therapeutic benefit.

Table of Contents

List of figures

List of tables

Abbreviations

2-DG	2-Deoxy-D-glucose
A20	Tumour necrosis factor, alpha-induced protein 3
AGS	Aicardi-Goutières syndrome
AIM2	Absent in melanoma 2
ALR	AIM2-like receptor
AMPK	Adenosine monophosphate-activated protein kinase
ASC	Apoptosis-associated speck-like protein containing a caspase recruitment domain (or Pycard)
ASL	Airway surface liquid
ATP	Adenosine triphosphate
BALF	Bronchoalveolar lavage fluid
BCC	Burkholderia cepacia complex
Ca^{2+}	Calcium
CARD	Caspase activation and recruitment domain
CAPS	Cryopyrin-associated periodic syndromes
CCL/CXCL	Chemokine
CD	Cluster of differentiation
CF	Cystic fibrosis
CFTR	Cystic fibrosis transmembrane conductance regulator
Cl^-	Chloride
COX2	Cyclooxygenase 2
CRAC	Calcium release activated channel

DAD	Diaphanous autoregulatory domain
DAMP	Damage-associated molecular pattern molecules
DNA	Deoxyribonucleic acid
dsDNA	Double stranded Deoxyribonucleic acid
EIPA	5-(N-Ethyl-N-isopropyl) amiloride
ELISA	Enzyme-linked immunosorbent assay
ENaC	Epithelial sodium channel
ER	Endoplasmic reticulum
ETC	Electron transport chain
GLUT	Glucose transporter
GSDMD	Gasdermin D
$FADH_2$	Flavin adenine dinucleotide
FCAS	Familial cold autoinflammatory syndrome
FMF	Familial Mediterranean fever
H^+	Hydrogen
HAMP	Homeostasis altering molecular process
HBEC	Human bronchial epithelial cell
HC	Healthy control
HCO_3^-	Bicarbonate
HIDS	Hyper IgD Syndrome
HIF1α	Hypoxia-inducible factor 1-alpha
IFN	Interferon
IL	Interleukin
IL-1R	Interleukin 1 receptor
IL-1Ra	Interleukin 1 receptor antagonist

K$^+$	Potassium
KEAP1	Kelch-like ECH-associated protein 1
LDH	Lactate dehydrogenase
LPS	Lipopolysaccharide
LRR	Leucine rich repeat
MAVS	Mitochondrial antiviral-signalling protein
MCT2	Monocarboxylate transporter 2
MEFV	Mediterranean fever
mROS	Mitochondrial reactive oxygen species
mtDNA	Mitochondrial Deoxyribonucleic acid
MWS	Muckle-Wells syndrome
Na$^+$	Sodium
NACHT	NAIP (neuronal apoptosis inhibitor protein), C2TA [class 2 transcription activator, of the MHC, HET-E (heterokaryon incompatibility) and TP1 (telomerase-associated protein 1)
NADH	Nicotinamide adenine dinucleotide (reduced form of NAD$^+$)
NBD	Nucleotide binding domain
NCFB	Non-cystic fibrosis bronchiectasis
NET	Neutrophil extracellular trap
NF-κB	Nuclear factor kappa-light-chain-enhancer of activated B cells
NK cell	Natural killer cell
NLRC4	NLR family CARD domain-containing protein 4
NLRP 1/3	NACHT, LRR and PYD domains-containing protein 1/3
NRF2	Nuclear factor (erythroid-derived 2)-like 2
O$_2$	Oxygen

OXPHOS	Oxidative phosphorylation
P2X7	P2X purinoceptor 7
PAAND	Pyrin-Associated Autoinflammation with Neutrophilic Dermatosis
PAMP	Pathogen-associated molecular patterns
PBMC	Peripheral blood mononuclear cell
PGE$_2$	Prostaglandin E 2
PRR	Pattern recognition receptors
PYD	Pyrin domain
R-domain	Regulatory domain (CFTR)
RET	Reverse electron transport
ROS	Reactive oxygen species
RNA	Ribonucleic acid
SAID	Systemic Autoinflammatory Disease
SDH	Succinate dehydrogenase
siRNA	Small interfering ribonucleic acid
SLC26A9	Solute Carrier Family 26 Member 9
SOCE	Store operated calcium entry
SPLUNC1	Short palate and nasal epithelial clone 1 (also known as Bactericidal/permeability-increasing fold-containing family A1 (BPIFA1))
STIM	Stromal interaction molecule 1
T2D	Type 2 diabetes
TCA	The Citric Acid (cycle)
TCR	T-cell receptor
Tg (mouse)	Transgenic

Th cell	T-helper cell
TLR	Toll like receptor
TMBD	Transmembrane domain
TNF	Tumour necrosis factor
UPR	Unfolded protein response
uSAID	Undiagnosed/undifferentiated Systemic Autoinflammatory Disease
WT	Wild Type

Chapter 1

Introduction

1.1 Cystic Fibrosis Pathophysiology

The cystic fibrosis transmembrane conductance regulator (CFTR) is a membrane-associated N-linked glycoprotein, which functions as a Cl$^-$ and HCO3$^-$ channel and a regulator of amiloride-sensitive Na$^+$ channels (Cheng et al., 1990, Berdiev et al., 2009, Bhalla and Hallows, 2008, Donaldson et al., 2002, Garcia-Caballero et al., 2009, Hobbs et al., 2013, König et al., 2002, Konstas et al., 2003, Kunzelmann, 2003). CFTR is highly expressed on the apical surface of epithelia (Riordan et al., 1989), but is also expressed by many other cell types, such as neurons and lymphocytes (Besancon et al., 1994, Bonfield et al., 2012, Cafferata et al., 2000, Collaco et al., 2013, Dong et al., 2015, Ettorre et al., 2014, Gao and Su, 2015, Kulka et al., 2002, Painter et al., 2006, Sorio et al., 2011, Su et al., 2011, Weyler et al., 1999, Zaidi et al., 2004). Innate immune cells, such as monocytes and neutrophils, increase CFTR expression when they encounter danger signals and enter tissue from the blood. This migration differentiates the monocyte cell into an active macrophage, which has been shown to have increased CFTR expression compared to its monocytic precursor (Del Porto et al., 2011).

When mutated, the CFTR is responsible for the multisystem disease that characterises cystic fibrosis (CF). The identification of the CF gene to locus 7cen-q22 was first described in 1985 (Wainwright et al., 1985) and the CFTR gene was identified as the cause of CF in 1989 (Kerem et al., 1989, Riordan et al., 1989, Rommens et al., 1989), establishing the underlying molecular basis of CF (Cheng et al., 1990). There are six molecular classes of CFTR mutation

that are classified depending on the severity of the cellular defect they cause. There are currently 2028 CFTR mutations (http://www.genet.sickkids.on.ca) which have been grouped into seven classes according their functional defect (Table 1).

CLASS	MOLECULAR ABNORMALITY	EXAMPLE MUTATION	CELL LINE	APPROVED CORRECTIVE DRUG
I	No functioning CFTR produced	W1282X	**IB3-1**	No
II	Impaired protein folding	F508del	**CuFi-1,** CFNPE14o-	Correctors
III	Problems with gating	G551D, R117H, F508del	CFBE45o- **CuFi-4**	Potentiators
IV	Poor Conductance	R347H, R117H	CFBE45o-	No
V	Abnormal Splicing	621+1G>T, R117H	CFBE45o-	No
VI	Poor Stability	S1455X, F508del	**CuFi-1,** CF14o-	No
VII	No mRNA	dele2,3(21kb)	KO cell line	No

Table 1: The molecular classification of *CFTR* mutations. Mutations are classified according to functional defects. Examples of mutations and classes of mutations are shown in this table. A summary of available cell lines used in this thesis are highlighted in bold. Each cell line has at least one allele of one of the associated mutations for that class and also share the cellular abnormality for that class (Ratjen et al., 2015). The cell lines highlighted in bold are used in this study.

The severity of the cellular defect directly impacts upon the severity of disease and clinical manifestations. This is evident in individuals with severe class I or class VII mutations where no protein (or mRNA with class VII) is produced causing complete abrogation of CFTR function (De Boeck and Amaral, 2016). These classes of mutation also pose therapeutic problems as there is no CFTR protein to target with small molecule correctors or potentiators. Carriers of a single mutated CFTR allele alongside a wild type CFTR allele remain asymptomatic, also indicating that 50% of wild type CFTR expression is enough to avoid a CF pathology. There are some reports that there is an increased prevalence of CFTR mutations in diseases such as idiopathic pancreatitis (Sosnay et al., 2013). The phenotypic expression of CF varies widely, even in patients with the same mutations. This may be attributable to both environmental factors and epigenetics (Brennan and Schrijver, 2016).

In order to describe the variations in the function of CFTR between mutations, it is necessary to understand the structure and function of the CFTR transmembrane protein. The *CFTR* gene is a member of the transport system ATP-binding cassette super-family. The CFTR protein functions as an anion channel for Cl^- and $HCO3^-$. The CFTR contains two sites that are able to bind and hydrolyse ATP, and also a series of transmembrane domains that form the channel in the plasma membrane (Figure 1.1.1).
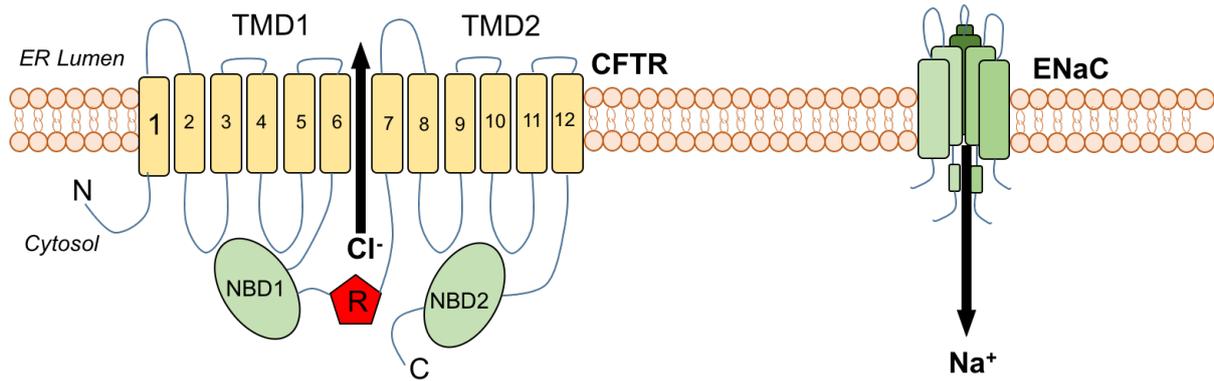
Figure 1.1.1: The CFTR and ENaC ion channels. The CFTR (cystic fibrosis transmembrane conductance regulator) has 5 domains: the TMBD (transmembrane domain) 1, which has six transmembrane peptides, the NBD (nucleotide binding domain) 1, which has ATP hydrolytic activity, the R (regulatory) domain, which as phosphorylation sites that control channel activity, followed by TMD2 and NBD2. When active the channel opens briefly to allow Cl^- and $HCO3^-$ to efflux from the cell. The ENaC (epithelial Na^+ channel) has 3 subunits and allows Na^+ ion influx (Kim and Skach, 2012).

The dysfunctional class III mutations (Table 1) weaken ATP hydrolysis, and the class IV mutations cause inferior Cl^- conductance across the membrane. Other mutation classes affect the stability and structure of CFTR and result in diminished expression on the cell surface. This may be due to alterations in the *CFTR* gene, terminating transcription, or reduced protein stability due to atypical splicing or protein mis-folding in the endoplasmic reticulum (ER) (Ratjen et al., 2015). The varying levels of CFTR expression and function affect the successful cellular transport of Cl^- ions, causing organ-specific manifestations. As CFTR is highly expressed in glandular epithelial cells, the primary organs affected by mutations in the CFTR are the lungs, pancreas, gastrointestinal tract and male reproductive system.

Lung disease remains the most common cause of morbidity and mortality in patients with CF. This is a result of an absence or reduction in CFTR function, which predisposed

patients to recurrent pulmonary infections, airway inflammation and defective mucociliary clearance. Pulmonary colonisation and infections due to *Staphylococcus aureus*, *Haemophilus Influenzae*, *Pseudomonas aeruginosa* (*P. aeruginosa*) and B*urkholderia cepacia* complex (BCC) are particularly common (Coutinho et al., 2008). Male infertility is a characteristic feature in the majority of males with CF and results from obstructive azoospermia due to ductal obstructions and reduced mucociliary transport (Cohen and Prince, 2012, Ratjen et al., 2015). Reduced bicarbonate efflux due to CFTR dysfunction contributes to highly adherent and viscous mucous.

There is a wide variation in the phenotypic expression of CF which is largely due to the impact of the various genotypes on CFTR protein folding, quantity of functioning CFTR and the amount of stable CFTR, which is able to anchor to the cell surface (Mehta, 2005, Farinha et al., 2013). The CFTR is a glycoprotein expressed on the apical membrane of epithelial surfaces and is the only large adenine nucleotide-binding cassette (ABC) protein family member to act as an ion channel (Valdivieso and Santa-Coloma, 2013). The CFTR has two transmembrane domains (TMD) and two nucleotide-binding domains (NBD) in addition to a regulatory (R) domain (Kim and Skach, 2012). The R-domain contains phosphorylation sites that regulate the activity of the ion channel. It is the phosphorylation of the R-domain by protein kinase A (PKA) that allows the NBDs to interact, causing a conformational change within the TMDs, opening the channel. The CFTR does have ATPase activity that contributes to channel activity, but the hydrolysis of ATP does not seem to be required for channel opening (Collaco et al., 2013). The idea that the CFTR is able to function as an ATP channel is unfounded. Chloride ions (Cl-), glutathione and bicarbonate (HCO3) efflux through the active and open CFTR channel. In the presence of a mutated CFTR, the efflux of these anions is dysfunctional causing dysregulated hydration and control of pH at epithelial cell surfaces. The multisystem manifestations in CF are generated by this epithelial surface disruption.

Secondary functions of the CFTR protein exist in non-epithelial, non-polarised cells such as immune cells (Riordan, 2008). There is evidence that the CFTR has a role in phagocytosis and may contribute to poor clearance of pathogens in CF (Bonfield et al., 2012, Van de Weert-van Leeuwen et al., 2013). The CFTR is also considered to be a receptor for certain pathogens, such as *Chlamydia trachomatis* and S*almonella typhi* (Pier et al., 1998)*,* to gain entry into host cells.

A lack of CFTR is also associated with certain downstream events that are thought to contribute to disease. Na^+ influx is enhanced on epithelial surfaces in CF through the epithelial Na^+ channel (ENaC). There is strong evidence that CFTR is able to inhibit ENaC activity through a variety of mechanisms, although the precise method of inhibition is unclear (Berdiev et al., 2009, Donaldson et al., 2002, Garcia-Caballero et al., 2009, König et al., 2002, König et al., 2001, Konstas et al., 2003, Kunzelmann, 2003, Mall et al., 2004). One potential mechanism is through a secreted protein that inhibits ENaC via its extracellular domains causing αγ-subunit internalisation, termed short palate and nasal epithelial clone 1 (SPLUNC1) (also known as Bactericidal/permeability-increasing fold-containing family A1 (BPIFA1)). SPLUNC1 is an allosteric inhibitor of ENaC and forms a complex with the β-subunit of ENaC whilst the αγ-subunits are internalised (Kim et al., 2018). SPLUNC1 has been described as an innate defence protein capable of autocrine ENaC inhibition (Hobbs et al., 2013). SPLUNC1 has bactericidal permeability increasing protein (BPI) structure that has been shown to be degraded by the high level of airway proteases, particularly neutrophil elastase in the CF and COPD airways (Jiang et al., 2013). The augmented Na^+ absorption is responsible for the dehydration of the epithelial airway surface and accumulation of acidic mucous in CF (Riordan, 2008). This fact is enforced by the CF mouse model that overexpresses β-chain of the ENaC channel and displays a comparable lung phenotype to human CF (Mall et al., 2004).

Recent publications have described the CFTR interactome, with the mutated ΔF508 CFTR having distinctly different protein-protein interactions compared to wild-type (WT) CFTR (Pankow et al., 2015). Interesting changes in the CFTR interactome exist in metabolic pathways and evidence from other studies have described important mitochondrial dysfunction and altered calcium metabolism. This is important to the pathophysiology of CF as mitochondrial dysfunction will have knock-on effects on the clearance of airway pathogens. Examples of this are reactive oxygen species (ROS) generation, antioxidant secretion, and defects in autophagy in CF cells. All of these examples will make the airway environment more susceptible to oxidative damage in CF.

As CFTR is a plasma membrane protein expressed on the surface of cells, once translated the peptide will follow the secretory pathway of protein trafficking to reach its destination and native conformation. However, this does not mean that the CFTR protein's vigorous trafficking checkpoints finish at the Golgi apparatus. Farinha *et al.* propose five conformation checkpoints that the CFTR is required to pass in order to be successfully expressed on the cell surface (Farinha et al., 2013). The initial checkpoints are localized to the ER, where heat shock proteins check for basic CFTR conformation and protein folding. Calnexin examines the CFTR for correct glycosylation, in a second checkpoint. Once these two checkpoints are passed, the CFTR enters the secretory pathway, where two further checkpoints inspect CFTR for ER retention motifs and positive secretory signals such as di-acidic (DAD) motifs. The final checkpoint that Farinha *et al.* describe involves chaperone attachment at the plasma membrane. Prolonged chaperone attachment to CFTR, due to incorrect CFTR docking or vesicle fusion to the plasma membrane, causes CFTR to be targeted for endocytosis. These chaperones include the Rab GTPases (Farinha et al., 2013).

With the recent advances in knowledge of the ER export and folding of CFTR, new molecular therapies have been brought to the market for the treatment of CF. The Vertex®

Pharmaceutical drugs VX-770 (ivacaftor) (Wainwright et al., 2015) and VX-809 (lumacaftor) are used in combination (Orkambi) to treat certain genotypes of CF. VX-770 is a potentiator, that improves the transport of Cl^- through the channel, keeping the CFTR permanently open via unconventional gating. VX-809 is a corrector that acts as a chaperone molecule, increasing the number of CFTR molecules (regardless of functionality) at the cell surface (Figure 1.1.2). There is no current cure for CF but new small molecule therapies are being developed to treat the underlying defect. Ivacaftor is approved for gating and residual function mutations and a combination of ivacaftor with either lumacaftor or tezacaftor for class III mutations (Table 1). Phase 2 results for triple therapy using VX-659 or VX-445 in combination with tezacaftor and ivacaftor have resulted in significant improvement in lung function and sweat Cl^- in both patients homozygous and heterozygous to Phe508del (https://investors.vrtx.com/) (Table 1). To date, gene therapy in CF has only been proof-of-principle, and CFTR gene expression has not been of the required efficiency to have a therapeutic benefit (Lee et al., 2005, Alton et al., 2015).
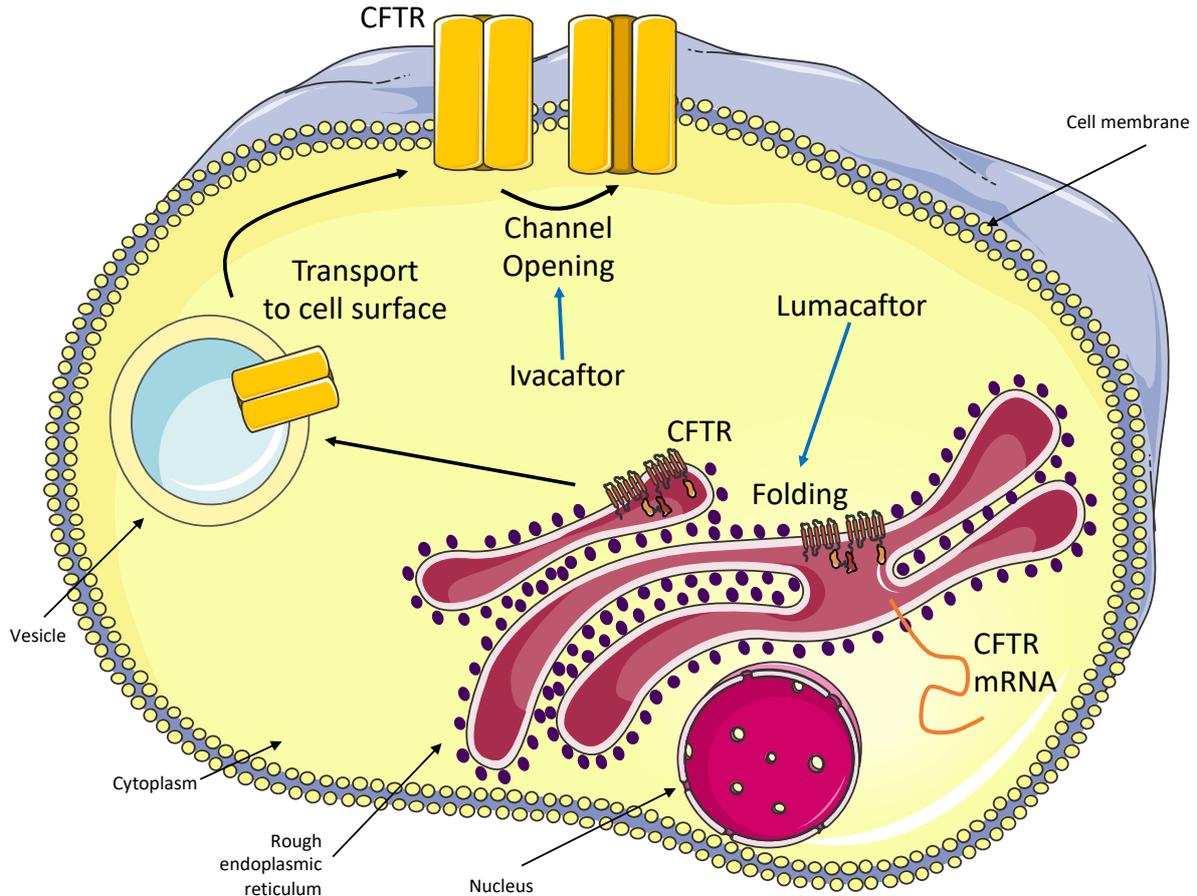
Figure 1.1.2: Molecular targets of ivacaftor and lumacaftor. Vertex® Pharmaceutical drugs VX-770 (ivacaftor) and VX-809 (lumacaftor) are used in combination (Orkambi) to treat certain genotypes of CF. Ivacaftor is a potentiator, that improves the transport of Cl^- through the channel, keeping the CFTR permanently open via unconventional gating. Lumacaftor is a corrector that acts as a chaperone molecule, increasing the number of CFTR molecules (regardless of functionality) at the cell surface by improving CFTR folding in the ER. CFTR-Cystic fibrosis transmembrane conductance regulator.

1.2 Inflammation in CF

The body's first line in defence from invading pathogens is the innate immune system. This refers to the myeloid-derived immune cells and anatomical barriers that are designed to combat and control constant pathogenic invasions from being established. The respiratory tract is a biological barrier that uses ciliated epithelial cells, resident macrophages and peripheral, migrating neutrophils and monocytes as the first line of airway defence (Whitsett and Alenghat, 2015). In CF, airway dehydration, defective mucociliary transport, low pH levels of mucus, denaturing of defensins and impairment of granule trafficking in neutrophils and reduced bactericidal abilities of macrophages, all contribute to the inadequate clearance of respiratory infections (Ratjen et al., 2015, Bonfield et al., 2012, Bruscia and Bonfield, 2016a, Bruscia et al., 2009, Del Porto et al., 2011, Keiser et al., 2015, Lubamba et al., 2015, Downey et al., 2009, Hayes et al., 2011, Law and Gray, 2017, Machen, 2006, Ng et al., 2014, Painter et al., 2006, Pohl et al., 2014, Taylor et al., 2016, Watt et al., 2005). As a result, patients with CF develop recurrent pulmonary infections due to bacteria, fungi and viruses. The immunological status of CF lungs is pro-inflammatory, with continual release of reactive oxygen species (ROS), neutrophil extracellular traps (NETs) (Marcos et al., 2015), inflammatory cytokines and chemokines that all function in the recruitment of inflammatory immune cell subsets, such as the T Helper 17 (Th17) cell (Dubin et al., 2007). Further indications of airway inflammation in CF can be characterised by increased neutrophil infiltrations and an increase in related pro-inflammatory cytokines, such as tumour necrosis factor (TNF), interleukin (IL)-6, IL-8 (Greally et al., 1993) and IL-1β and IL-18 (Grassmé et al., 2014, Clauzure et al., 2014, Fritzsching et al., 2015, Iannitti et al., 2016, Levy et al., 2009, Reiniger et al., 2007, Rimessi et al., 2015). In addition, the anti-inflammatory cytokine IL-10 is decreased in CF bronchial

alveolar lavage (BAL) fluid compared to healthy controls (HC) (Bonfield et al., 1995). The multitudinous neutrophils within the CF lung create a perfect storm of inflammatory mediators, releasing oxidants, proteinases and DNA, which stimulate further release of inflammatory cytokines (Devaney et al., 2003).

The origin or cause of this persistent pro-inflammatory state is debated: whether the recurrent infections maintain the inflammation or whether intrinsic dysfunction of the epithelium or immune cells predisposes effected organs to become inflamed, even when sterile. Both hypotheses are valid, with CF infants presenting with inflamed and infected lungs in early disease stage (Koehler et al., 2004) (Table 2). In favour of pathogen-led inflammation is the fact that macrophage phagocytosis is fully functional regardless of CFTR mutation (Del Porto et al., 2011). Additionally, haematopoietic cells have been observed as the major source of pro-inflammatory cytokines in response to live bacteria, with airway epithelial cells responding weakly to microbial challenge in CF (Tang et al., 2012). This viewpoint attributes the origins of inflammation and its maintenance to indirect effects of the mutated CFTR on inflammatory pathways (Machen, 2006). Indirect mechanisms include increased acidification and oxidation of mucous in the airways, allowing the colonisation of pathogenic colonies and biofilm formation. In contrast, there are many examples of intrinsic defects related to CF, that could contribute to an augmented inflammatory state, including increased NF-κB activity (Venkatakrishnan et al., 2000, Weber et al., 2001), however this has been refuted (Tang et al., 2012). Experimental studies have developed sterile murine models with an overexpression of the Na^+ ion channel ENaC, causing a CF-like lung disease prior to infection, indicating an intrinsic CF-defect in which loss of CFTR-dependent ENaC inhibition induces mucous dehydration and inflammatory processes independent of infection (Mall et al., 2004). However, this animal model does not present with a disease that is truly representative of human CF due to the presence of fully functional CFTR. Irrespective of the basis of the inflammation, it is

agreed that the CF lungs are a highly inflammatory site, with many immune cell infiltrates and pro-inflammatory cytokines.

1.3 The inflammasomes

One of the most potent proinflammatory cytokines is IL-1β. It is part of a superfamily of cytokines denoted as the IL-1 cytokines, comprising seven pro-inflammatory members and four anti-inflammatory members (Palomo et al., 2015). An IL-1 cytokine will bind to its specific receptor from the IL-1 receptor (IL-1R) family, triggering co-receptor recruitment and downstream intracellular signalling. Due to the proinflammatory members' highly potent inflammatory effects, IL-1 cytokines are highly regulated, by IL-1 antagonists, decoy receptors and a tight control over production and maturation of IL-1 cytokine release (Palomo *et al.* 2015). One of the forms of cellular control over IL-1 cytokine production is a type of cellular rheostat, known as the inflammasomes (Martinon et al., 2002, Muruve et al., 2008, Tschopp and Schroder, 2010). Classical cytokine secretion involves gene transcription and translation of biologically active peptides that are secreted via the endoplasmic reticulum (ER)-Golgi pathway. However, IL-1 cytokines, specifically proinflammatory IL-1β and IL-18, are formed as inactive pro-peptides that require cleavage at their N-terminal and are secreted via a non-classical pathway. The required cleavage is facilitated by inflammasomes, large multimeric protein structures, although proteinase-3, elastase and chymase have all been observed performing the required cleavage in myeloid cells (Palomo et al., 2015). Inflammasome formation is initiated when intracellular pattern recognition receptors (PRR) (Table 3), such as the AIM2-like receptor (ALR) and nucleotide-binding domain and leucine-rich repeat containing (NLR) receptor, detect pathogen associated molecular patterns (PAMPs) and danger

associated molecular patterns (DAMPs) (De Nardo et al., 2014). The inflammasome is utilised by myeloid cells primarily, as well as stromal epithelial cells that are capable of detecting pathogens using PRRs. Downstream signalling from PRRs upregulate inflammatory proteins in response to the detected PAMPs or DAMPs. A group of these inflammatory proteins is able to assemble into what is known as an inflammasome complex. The primary purpose of canonical and non-canonical inflammasomes is to cleave inactive pro-caspase-1 or pro-caspases-4/-5 (pro-caspase-11 in mouse) respectively, into their active forms. When active, caspase-1 cleaves pro-IL-1 cytokines, whereas both capase-1 and caspases-4/-5 or -11 are capable of inducing cell pyroptosis, a type of controlled, inflammation-driven cell death (Bergsbaken et al., 2009, de Gassart and Martinon, 2015, He et al., 2015, Miao et al., 2010, Yang et al., 2015). However, there is evidence that caspases-4/-5 or -11 are required for IL-1β and IL-18 secretion in response to gram-negative bacterial PAMPs (Kayagaki et al., 2015). The recruitment of pro-caspases to an inflammasome requires large pro-caspase pro-domains, such as the caspase activation and recruitment domain (CARD) (Lamkanfi, 2011, Lamkanfi and Dixit, 2014). When recruited, pro-caspases develop enzymatic activity and mature into active caspases. The two members of the IL-1 family that are cleaved and activated by caspase-1 are: IL-1β and IL-18. IL-1β has a role in inducing T-cell differentiation into Th1 and Th17 cells, as well as aiding antibody production. Pro-IL-1β transcription is induced by NF-κB activity whereas pro-IL-18 is constitutively expressed in macrophages (Puren et al., 1999). When active, IL-18 is able to skew T-cells towards a Th17 subset and promotes pro-inflammatory IL-17 secretion (Palomo et al., 2015). Inflammasomes are characterised by the PRRs that form their scaffold and detects specific PAMPs or DAMPs. The AIM2 inflammasome contains the ALR PRR and the NLRP1, NLRP3 and NLRC4 inflammasomes contain the NLR PRR (Table 3). There are other inflammasomes that have been described, such as the pyrin inflammasome,

but they are not as well characterised (Aubert et al., 2016). The Pyrin inflammasome is activated by bacterial modifications of Rho GTPases, such as the glucosyltransferase cytotoxin B secreted by *C. difficile* (TcdB) (Xu et al., 2014, Aubert et al., 2016, Park et al., 2016). This type of molecular pattern has been described as a homeostasis altering molecular process (HAMP) (Liston and Masters, 2017). NLRP2, NLRP6, NLRP7 and NLRP12 have also been described as orchestrating caspase-1 dependent IL-1β secretion but are not well characterised (Broz and Dixit, 2016, Lamkanfi and Dixit, 2014).

A recent publication by He *et al.* described a new component of the inflammasome, gasdermin D (GSDMD) (He et al., 2015). GSDMD was found to have a role in IL-1β and IL-18 secretion as well as pyroptosis. The authors suggest that GSDMD may function through the puncturing of holes in the cell surface, facilitating both cytokine secretion and pyroptosis. The authors also show that GSDMD has a role in suppressing apoptosis, favouring pyroptotic cell death (Kayagaki et al., 2015). Depending on the PRR at the basis of the inflammasome, different PAMPs and DAMPs will stimulate its formation. Inflammasomes are highly evolutionarily conserved within mammals, however drawing conclusions from animal models and relating the findings to human disease may be flawed, as inflammasome activation differs between species such as the structure and activity of the caspases between human and mouse, for example.

The NLRP3 inflammasome has been characterised most comprehensively, as it is the basis of one of the monogenic autoinflammatory diseases, Muckle-Wells syndrome (MWS) (Agostini et al., 2004). Two signals are required to activate the NLRP3 inflammasome: (1) a signal that activates NF-κB transcription factor, which induces expression of NLRP3 inflammasome components and IL-1β and IL-18, and (2) a signal that stimulates the activation of NLRP3 and the formation of the NLRP3 inflammasome (Figure 1.4.1) (Mathews et al.,

2014). The range of activators for NLRP3 is broad, with a large variety of PAMPs and DAMPs from various sources able to trigger NLRP3 inflammasome assembly. It is therefore unlikely that NLRP3 is specific to all of the stimulants, and it has hence been hypothesised that NLRP3 detects indirect cellular changes caused by the presence of the PAMP or DAMP (Table 3) (Shi et al., 2016). Mutations within the *NLRP3* gene are responsible for the autoinflammatory disease MWS (Agostini et al., 2004). It was within this disease model that the relationship of NLRP3 and ASC was first described, with the mutation triggering constitutive NLRP3 inflammasome activation and spontaneous IL-1β secretion from MWS macrophages. Autoinflammatory diseases are characterised by the activation of innate immune cells causing self-directed inflammation and tissue damage (McDermott, 2004, McDermott and Aksentijevich, 2002, McDermott et al., 1999, McGonagle and McDermott, 2006, Pathak et al., 2016, Peckham et al., 2017, Savic et al., 2012). Autoinflammatory diseases are successfully treated using recombinant IL-1RA (Church et al., 2008) and are discussed further in section 6.1.

TAXONOMIC RANK		DESCRIPTION OF INFECTION	PRR
MYCOBACTERIUM SPECIES	Bacteria	Most commonly *Mycobacterium avium*. Has been associated with low *Pseudomonas aeruginosa* colonisation and therefore good prognosis.	TLR-1, TLR-2, TLR-4, TLR-9, RIG-1, NOD2, DECTIN-1, Mannose receptor and DC-SIGN
STAPHYLOCOCCUS AUREUS	Bacteria	Highly prevalent in children with CF, causing damage to airways and co-infect with *Pseudomonas aeruginosa*.	TLR-2, TLR-1, TLR-6, TLR-7 and TLR-9
PSEUDOMONAS AERUGINOSA	Bacteria	This gram-negative motile rod-shaped bacterium colonises approximately 50% of CF patients. It is an opportunistic member of the normal respiratory microbiota. Biofilms are commonly formed releasing alginate polymers, which facilitates antibiotic avoidance.	TLR-2, TLR-4, TLR-5, TLR-9, NOD1, NLRC4/IPAF and CFTR
BURKHOLDERIA CEPACIA	Bacteria	These gram-negative rod-shaped bacteria, thought to be passed on via oral transmission through kissing. It has a highly mutated genome, with high antibiotic resistance rates. It is also difficult to genotype due to difficulties in cell culture.	TLR-4, TLR-5
RESPIRATORY SYNCYTIAL VIRUS	Paramyxovirus	Major pathogen in children with CF. Increased epithelial damage and IL-18 secretion. Increased neutrophil infiltration and elastase release.	TLR2, TLR-6, TLR-4, TLR-3, TLR-7, RIG-1, NOD2, NLRP3
INFLUENZA	Orthomyxovirus	Major pathogen in older children and adults with CF.	TLR-3, TLR-7, TLR-8, TLR-9, RIG-1, MDA5, NLRX1, IPS-1, NLRP3
RHINOVIRUS	Picornavirus	Increased IL-8 and increased neutrophil myeloperoxidase.	TLR2, TLR-7, TLR-8, RIG1, MDA5

Table 2: Common pathogenic infections in CF. Pathogens that cause the most common/severe infections in CF (Killick et al., 2013, van 't Wout et al., 2015, Sutterwala et al., 2007, Blohmke et al., 2008, Coutinho et al., 2008, Kim and Lee, 2014, Kozutsumi et al., 1988, Stokes et al., 2016).
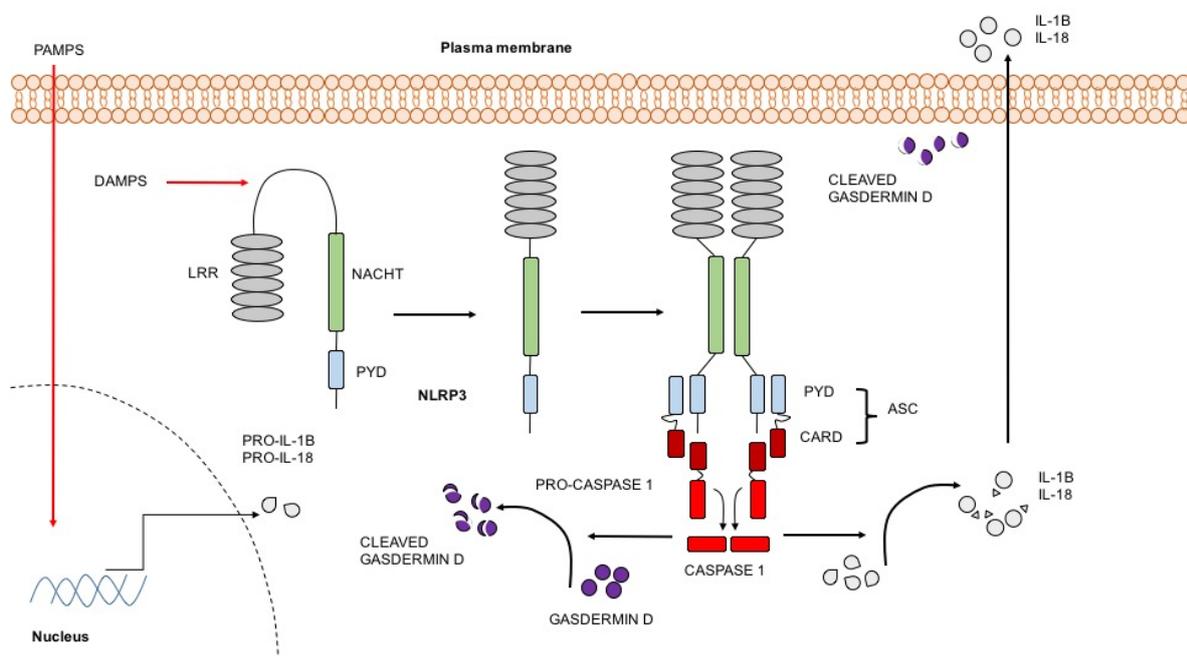
Figure 1.4.1: The NLRP3 inflammasome. PAMPs (pattern associated molecular pattern) from pathogens will be recognised by the cell via innate immune receptors causing cytokine transcription and translation. DAMP (danger associated molecular pattern) such as ATP will open K$^+$ channels and cause activation of the inflammasome components: LRR (leucine rich repeats), NACHT (NAIP, CIITA, HET-E and TP1) and PYD (pyrin domain). The NACHT domain becomes exposed and is removed from LRR auto-repression. The NLRP3 will then oligomerise and recruit ASC (apoptosis-associated speck-like protein containing a carboxy-terminal CARD) via its CARD (caspase-recruitment domain) domain. ASC is then able to recruit pro-caspase 1 which auto-cleaves and becomes active. Active caspase is then able to cleave pro-IL (interleukin)-1B, pro-IL-18 and gasdermin D (GSDMD). The active IL-1B and IL-18 are then secreted, which is GSDMD (cleaved) dependent (based on (Tschopp and Schroder, 2010)).

INFLAMMASOME	PRR	SCAFFOLD PROTEINS	CASPASE	CYTOKINE RELEASED	STIMULANT	SPECIFIC PATHOGEN	OTHER FUNCTIONS AND STIMULI
AIM2	ALR	p10, p20, CARD, PYD, ASC, HIN200	Caspase-1	IL-18 IL-1β	Intracellular DNA	*Francisella tularensi; cytomegalovirus; Vaccinia virus; Listeria monocytogenes*	Links with systemic lupus erythematosus pathology
NLRP1	NLR	p10, p20, CARD, FIIND, NACHT	Caspase-1	IL-18 IL-1β	Nlrp1 cleavage	*Lymphocytic choriomeningitis virus (LCMV); Bacillus anthracis*	LeTx toxin cleaves Nlrp1b in mouse models, suggesting this may be an important event in activation
NLRP3	NLR	p10, p20, CARD, PYD, ASC, NACHT	Caspase-1	IL-18 IL-1β	Bacterial, viral and fungal PAMPs; Crystals, β-amyloid plaques, ATP, hyaluronan DAMPs	Primarily detects LPS via TLR4	Detect cellular changes associated with the presence of PAMPs and DAMPs. K^+ ion efflux, mitochondrial translocation, ROS production, mtDNA, cathepsins and cardiolipin. Requires two signals
NLRC4	NLR (Naip)	p10, p20, CARD, NACHT	Caspase-1	IL-18 IL-1β	Flagellin and bacterial T3SS and T4SS	*Salmonella Typhimurium, Shigella flexneri, Pseudomonas aeruginosa, Burkholderia thailandensis, and Legionella pneumophila*	Significant differences between mouse and human homologs. The murine Naip loci are highly polymorphic compared to the single human homolog. Nlrc4 phosphorylation also is thought to activate this inflammasome

Table 3: Canonical NLRP3 inflammasome components and stimulants. ROS: reactive oxygen species, mtDNA: mitochondrial DNA (Cai et al., 2014, D'Osualdo et al., 2015, Fernandes-Alnemri et al., 2009, Grinstein et al., 2015, Hornung et al., 2009, Munoz-Planillo et al., 2009, Munoz-Planillo et al., 2013, Yang et al., 2013a)

1.5 Mitochondrial metabolism

The study of mitochondrial metabolism has been dominated by the field of oncology, with advances in the understanding of how a cancerous cell is able to switch from oxidative phosphorylation (OXPHOS) to glycolysis (Bertaux et al., 2018, Wen et al., 2012, Khalid et al., 2017). A cell primarily uses OXPHOS during a resting, senescent or memory state, which provides a cell with continuous, efficient, high-yield ATP production. Glycolysis on the other hand provides an active, effector cell with fast ATP production to carry out rapid cellular functions. A cancerous cell will utilise glycolysis, termed the Warburg effect, due to oncogene activation allowing the cell to proliferate quickly and migrate during metastasis, a cancer cell's effector functions (Khalid et al., 2017). Metabolism has become a valid target for new generation chemotherapies, to target this distinct metabolic profile of cancerous cells. Figure 1.5.1 summarises mitochondrial metabolism, with further details of the metabolic pathways in chapter 4.1.2.
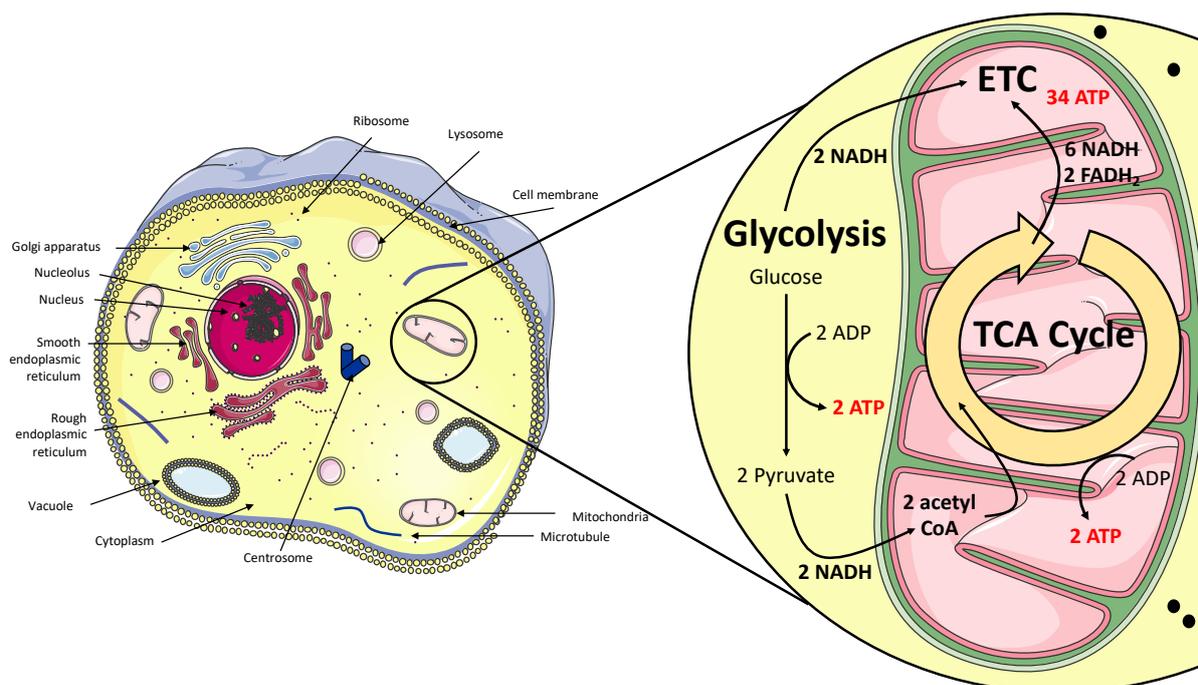
Figure 1.5.1: Cellular metabolism- Glycolysis, TCA cycle and OXPHOS. Cellular metabolism takes place within the cytoplasm and mitochondria. Glucose is metabolised into pyruvate during glycolysis and transported into the mitochondria to fuel TCA cycle. Metabolites such as NADH and FADH produced by the intermediate TCA steps then fuel OXPHOS, which transports electrons across the mitochondrial inner membrane, termed the ETC. ADP- Adenosine di-phosphate; ATP- Adenosine tri-phosphate; TCA- The citric acid; ETC- Electron transport chain; NADH- Nicotinamide adenine dinucleotide (reduced form of NAD$^+$); FADH- Flavin adenine dinucleotide.

Immune cells also utilise glycolysis, or the Warburg effect, when activated into an effector phenotype (Norata et al., 2015, Everts et al., 2012, Lamkanfi, 2011, Tannahill et al., 2013a, Wen et al., 2012). Therefore, measuring the activity of metabolic pathways can provide a marker of the inflammatory state of an immune cell population. Interestingly, recent publications in the field of immunometabolism have not only supported the metabolic profile of active or senescent immune cells but have made molecular links between the accumulation of certain metabolites during metabolic switching and downstream inflammatory pathway

activation (Buck et al., 2016, Kelly and O'Neill, 2015, Mills et al., 2016, Mills et al., 2017, Mills and O'Neill, 2016, Mills et al., 2018, O'Neill, 2016, O'Neill, 2015, Tannahill et al., 2013b). Both systems, metabolism and inflammation, are inextricably linked and exist in a reciprocal relationship where one system's activation or will influence the other and vice versa. These studies focus on the *in vitro* activation of the macrophage and elucidate the influence glycolysis in particular has on proinflammatory pathways such as the inflammasome.

Immune cells, such as macrophages do not become resistant to insulin as they use the glucose transporter (GLUT) 1 (Macintyre et al., 2014, Tannahill et al., 2013a), which is independent of insulin control, whereas many other tissues such as muscle and adipose utilise the insulin-dependent GLUT4. This observation highlights the importance of glucose as a fuel for macrophage survival and effector function. The availability of glucose for macrophage metabolism is not limited by, or under the control of insulin. In the disease type-2 diabetes (T2D), insulin resistance is chronic and therefore macrophage glucose-dependent activation occurs. Notably, fatty acid oxidation decreases with glycolysis as adipose is created rather than metabolised as fuel (Wen et al., 2012).

Mills *et al* describe how LPS stimulated M1-type macrophages switch to glycolytic metabolism, which also induces a subsequent break in the TCA cycle, causing an accumulation of certain metabolites specific to these break-points (Mills et al., 2017, Mills et al., 2016). The breakpoint at complex 2 (SDH), which converts succinate to fumarate as part of the TCA cycle (Figure 1.5.2), begins to oxidise succinate, which accumulates and induces reverse electron transport (RET). Electrons transfer from complex 2 to complex 1, increasing mitochondrial ROS (mROS) production by complex 1. mROS has been shown to induce the activation of transcription factor HIF1α. *IL1β* is a known transcriptional target of HIF1α. Inhibition of SDH, complex 1 or RET inhibits this HIF1α-induced *IL1B* expression. The glycolytic switch within myeloid cells in *HIF1α* knockout-mice is impaired, with reduced ATP and impaired

macrophage functions in anaerobic environments (Cramer et al., 2003). These investigations elucidated the mechanisms behind LPS induced M1-type macrophage activation, NLRP3 inflammasome assembly and mROS production (Chouchani et al., 2014, Littlewood-Evans et al., 2016, Mills et al., 2016, Tannahill et al., 2013a).
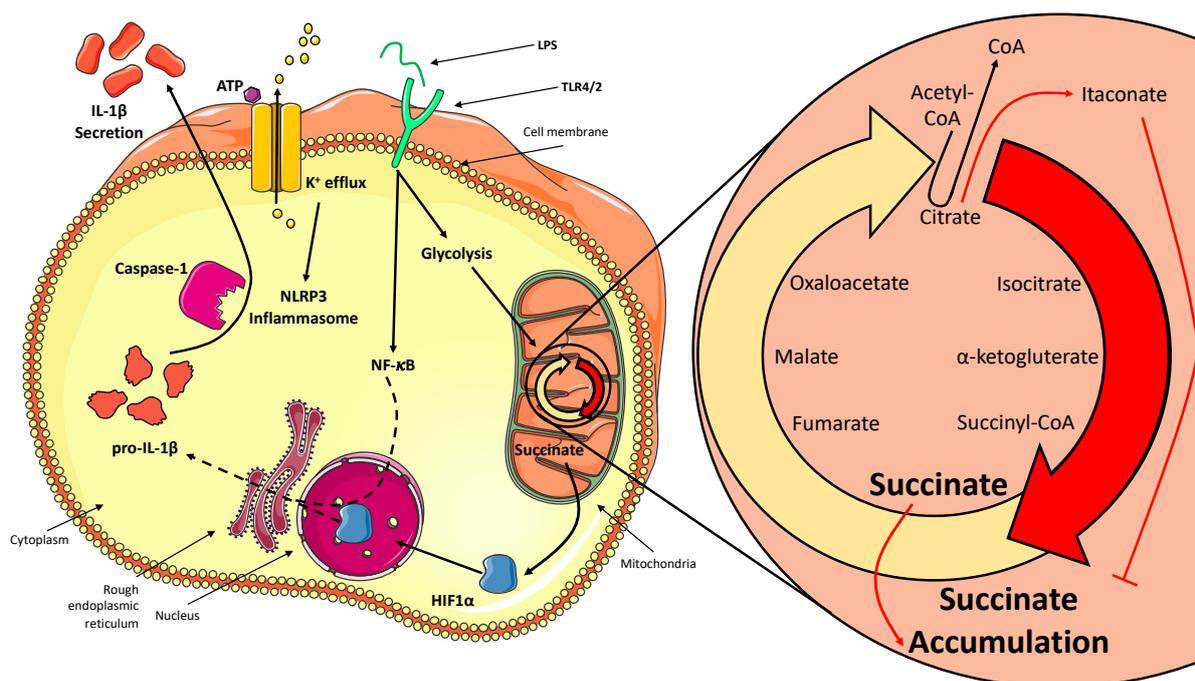
Figure 1.5.2: Glycolysis drives inflammation through succinate-dependent IL-1β production. LPS stimulated macrophages switch to glycolytic metabolism. A subsequent break in TCA cycle, causing an accumulation of specific metabolites at these break-points which have inflammatory consequences, such as HIF1α-dependent IL-1β expression. LPS-Lipopolysaccharide; TLR- Toll like receptor; ATP- Adenosine tri-phosphate; IL- Interleukin; HIF1α- hypoxia-inducible factor 1 alpha.

A second point in TCA cycle has been identified where metabolism and inflammation meet. In a resting or senescent cell isocitrate dehydrogenase converts citrate into succinate, instead of itaconate. M1-type macrophages prevent this conversion, allowing an accumulation

of itaconate. The accumulation of itaconate has been shown to have inhibitory effects on RET and SDH-dependent succinate oxidation. Pre-treatment of a soluble derivative of itaconate (4-octyl itaconate) was able to also inhibit SDH in M1-type macrophages, inhibiting mROS-driven *IL1B* expression *in vitro* and *in vivo* (Cordes et al., 2016, Lampropoulou et al., 2016, Mills et al., 2018). Interestingly, other SDH inhibitors did not activate the anti-inflammatory transcription factor nuclear factor erythroid 2-related factor 2 (NRF2) in macrophages, whereas itaconate at its derivative did. NRF2 induces an anti-inflammatory program in macrophages by inducing antioxidants. The authors observed that the known NRF2 regulator, kelch-like ECH-associated protein 1 (KEAP1) binds to NRF2 and targets it for proteasomal degradation. Itaconate and fumarate, a similar metabolite, were found to inhibit KEAP1 via novel covalent modifications, known as dicarboxypropylation, such as multiple alkylations on multiple cysteines and a lysine. Itaconate's post-translational upregulation of NRF2 decreased IL-1β and HIF1α but not TNF or NF-κB. Therefore, itaconate can be considered an anti-inflammatory metabolite promoting cell survival through prevention of chronic oxidative stress and subsequent inhibition of specific proinflammatory cytokine expression (Cordes et al., 2016, Lampropoulou et al., 2016, Mills et al., 2018).

It is clear that not only is metabolism a marker of inflammation in immune cells, but that the two systems regulate one another, contributing to the other's activity and fate.

1.6 Current therapies for CF

Commonly used treatments for CF target the inflammation and infection in the lung as well as the comorbidities associated with CF (© Cystic Fibrosis Trust Registered Charity No. (England and Wales) 1079049, 2018). Various oral and nebulised antibiotics are used on a daily basis to reduced pulmonary exacerbations, decline in lung function and improve quality

of life. Anti-inflammatory agents such as low dose macrolides steroids and high dose NSAID are also used (Coutinho et al., 2008). Mucolytic agents such as DNase and hypertonic saline help improve mucociliary clearance (Elborn, 2016). Pancreatic malabsorption is common in CF with pancreatitis occurring in some patients with pancreatic sufficiency. As a result, many patients have malabsorption and require pancreatic enzyme replacement. Nutritional requirements are increased in CF, in part due to malabsorption. As a result, patients are prescribed a high calorie and high-fat diet with pancreatic enzyme and fat-soluble vitamin supplementation. Gastrointestinal complications such as distal intestinal obstruction syndrome is also relatively common.

Despite treatments, patients with CF will often deteriorate due to progression of bronchiectasis and lung damage. Suitable patients with end-stage lung disease can be considered for lung transplantation, which carries a 50%, 10-year survival. The median age of patients with CF in the UK is 20 years with predicted life expectancy for people born between 2012-2016 increasing to 47-years old, (Jeffery, 2017). This is a huge improvement from 40-years ago when individuals with CF died in infancy. However, the median age of death remains around 30 years of age, with a significant number of younger patients still dying. In addition, median life expectancy does not consider the intensity of treatment and the impact of CF on quality of life. Additionally, to prevent cross-infection, patients with CF are isolated from other individuals with CF, as they are at a particular risk of spreading the specific infections (Table 2) that colonise the CF lung (Duff, 2002). This creates a painful and somewhat lonely existence where it can be difficult to share experiences face-to-face with fellow patients with CF. To date ivacaftor is the only highly efficacious drug available to treat CFTR dysfunction in patients with CF. Treatment is limited to gating and residual function mutations and can result in significantly increases life-expectancy and quality of life.

New therapies are in the pipe-line, including more advanced small molecules and gene therapies, discussed in section 5.1 in detail.

1.7 Targeting autoinflammation- current therapeutics

Established biologic therapies are now in use for highly efficacious treatment of autoinflammatory diseases (sections 1.3 and 6.1). These biologics target IL-1β through IL-1 blockade with either an anti-IL-1β antibody (canakinumab) or a recombinant, soluble receptor antagonist, IL-1Ra (anakinra) (Dinarello et al., 2012, Dinarello and van der Meer, 2013, Hawkins et al., 2003, Palomo et al., 2015, Schlesinger, 2014). The majority of patients with diagnosed systemic autoinflammatory disease (SAID) benefit from IL-1 blockade, with evidence that many undiagnosed or undifferentiated SAID (uSAID) patients would also benefit from IL-1 blockade and anakinra may prove useful for diagnosing uSAID patients (Harrison et al., 2015).

1.8 Targeting metabolism- current therapeutics

As previously discussed, metabolism and inflammatory responses are inextricably linked with metabolic reprogramming occurring synchronously with activation of inflammatory pathways and differentiation into proinflammatory phenotypes (Bettencourt and Powell, 2017). Metabolism is therefore a possible therapeutic target that has significant potential. In addition to being able to target the inflammatory response, metabolism is differentially active in proinflammatory, and potentially pathogenic immune cells providing a degree of selectivity with non-specific small molecule administration. Further selectivity exists between innate and adaptive immune cells in terms of the metabolic pathways used for distinct

types of activation in the two arms of the immune system. Theoretically, innate immune-driven autoinflammation can be specifically targeted using small molecule drugs against metabolic pathways and metabolites.

Elevated glycolysis is a common feature of both innate and adaptive immune cell activation. Innate immune cells use this type of rapid ATP production to induce responsive cytokine secretion and phenotypic functions such as chemotaxis and phagocytosis. This was shown by reduced IL-1β secretion when the glycolytic enzyme hexokinase was inhibited with the small molecule with 2-deoxy-glucose (2DG), but TNF was not supporting the fact that metabolism is a dynamic and complex system that can be specifically and accurately targeted for specific therapeutic goals (Mills et al., 2016, Mills et al., 2017, Mills and O'Neill, 2016, Mills et al., 2018). The effects of 2DG are most likely due to the prevention of succinate accumulation, limiting succinate's role in modulating HIF1α-dependent innate immune inflammatory pathways, which has been extensively descried in section 1.4. Further evidence that innate immune inflammation can be targeted specifically by disturbing metabolic networks with small molecules exists with ROS. NO is elevated during glycolysis, with effects on the inhibition of OXPHOS, activation of NLRP3 and bacterial killing (Mills et al., 2017). Treatment with metformin, a drug that activates AMPK and has been used in diabetes is able to decrease ROS production specifically. Itaconate has been recently described as an anti-inflammatory metabolite (section 1.4) that functions by competitive inhibition of succinate dehydrogenase (SDH).

By using the above molecules to inhibit key points in innate immune cell metabolism, not only will proinflammatory innate immune cells be inhibited but anti-inflammatory immune cells may be promoted. M2-type macrophages are characterised as anti-inflammatory macrophages and typically use OXPHOS rather than glycolysis that proinflammatory M1-type macrophages employ. In addition, the use of ROS, succinate and HIF1α-dependent IL-1β

secretion are pathways that are specific to the innate immune system and therefore their inhibition would not, theoretically effect adaptive immune cells.

1.9 Hypotheses

The following hypotheses were formulated based on the current literature and clinical observations made at Cystic Fibrosis Adult Ward, St James Hospital, Leeds.

1.9.1 List of Hypotheses

1. A proinflammatory, innate immune-driven, cytokine signature exists *in vivo* and *in vitro* in patients and cells with CF-associated mutations that is associated with inflammasome activation.

2. The NLRP3 inflammasome is hyper-responsive in cells with CF-associated mutations due to intrinsic CFTR-dependent defects.

3. Immune cells with CF-associated mutations have a proinflammatory phenotype, characterised by cytokine secretion, cell surface markers and active metabolic pathways.

4. Modulating the intrinsic CFTR-dependent defect with small molecules ivacaftor and lumacaftor regulates the proinflammatory phenotype of cells with CF-associated mutations.

1.9.2 Aims and Objectives

Hypothesis 1:

a. To establish the serum cytokine signature from patients with CF-associated mutations in comparison to healthy control (HC), non-CF bronchiectasis (NCFB) and SAID cohorts.

b. To establish the secreted, *in vitro* cytokine signature from monocytes from patients with CF-associated mutations in comparison to HC, NCFB and SAID cohorts, as well as human bronchial epithelial cell (HBEC) lines with and without CF-associated mutations.

c. To understand whether the inflammatory response/signature in CF is dependent on CFTR intrinsic defects by the use of small molecule inhibition of multiple ion channels known to be pathogenic in CF.

Hypothesis 2:

a. To establish the activity of multiple inflammasomes (including NLRP3) in monocytes from patients with CF-associated mutations in comparison to HC, NCFB and SAID cohorts, as well as HBEC lines with and without CF-associated mutations.

b. To characterise the inflammatory phenotype of monocytes from patients with CF-associated mutations in comparison to HC, NCFB and SAID cohorts, by cytokine secretion and cell surface markers.

Hypothesis 3:

    a. To characterise the inflammatory phenotype of monocytes from patients with CF-associated mutations in comparison to HC, NCFB and SAID cohorts, as well as HBEC lines with and without CF-associated mutations by the activity of metabolic pathways.

    b. To explore whether inhibition of certain metabolic pathways can modulate inflammatory cytokine secretion in monocytes from patients with CF-associated mutations in comparison to HC, NCFB and SAID cohorts, as well as HBEC lines with and without CF-associated mutations.

Hypothesis 4:

    a. To explore whether ivacaftor and lumacaftor can modulate inflammatory cytokine secretion in monocytes from patients with CF-associated mutations in comparison to HC, NCFB and SAID cohorts, as well as HBEC lines with and without CF-associated mutations.

    b. To explore whether ivacaftor and lumacaftor can modulate metabolism in PBMCs from patients with CF-associated mutations over 3-months.

Chapter 2

2.0 Materials and Methods

2.1 Patient Cohorts

Patients with cystic fibrosis (CF) were recruited from the Adult Cystic Fibrosis Unit at St James's University Hospital, Leeds. All patients had two disease-causing CFTR mutations and clinical features consistent with the diagnosis of CF. (F508del/F508del, n = 34; F508del/c.1521_1523delCTT, n =3; 3849+10KB C>T/F508del, n=1; c.1040G>C/R347P, n=1; F508del/621+1 (G>T), n=1) (table 4).

We saw no statistically significant difference in terms of serum cytokines between stable patients (n=14) and those who had acute arthritis or infection (n=26). Patients included in Figs 2-4 were all F508del/F508del with no sign of infection. Patients with NCFB and SAID were recruited from the Leeds Regional bronchiectasis unit and Department of Clinical Immunology and Allergy, respectively. All patients with a SAID had characterised mutations in a known disease-causing gene (TRAPS n=2, Muckle-Wells n=2, A20 haploinsufficiency n=1, PAAND n=1, MEFV n=2, FMF n=2, HIDS n=2 and Schnitzler syndrome n=1). Age and sex matched healthy controls were recruited from the research laboratories at the Wellcome Trust Benner Building, St James's University Hospital, Leeds, UK.

All patient samples collected are approved by the Health Research Authority REC reference 17/YH/0084. All patients enrolled on this study provided their full consent for their samples to be used for research purposes, detailed in the above REC reference.

Code	Gender	Age	Genotype	Sweat Chloride (mmol/l)	FEV1 l/s	FEV1 (%)	Weight (kg)	BMI (kg/m2)	Anti-inflammatory Medication	Antibiotics	CRP	Active Joint symptoms	Bacteria	CFA diagnosis ever	CFRD	Figures
CF001	F	27	Phe508del/Phe508del	N/A	1.23	47	47.3	18.4	Azithromycin 500 mg 3-times a week	Elective IV antibiotics / mild exacerbation started on 13/07/2015 Tigecycline and Meropenem for 2 weeks	8.7	Joint pain in right hip and left shoulder the previous week. Asymptomatic at time of bloods.	Stenotrophomonas maltophilia	Yes	No	3.3.1.1 3.3.4.1
CF002	M	24	Phe508del/Phe508del	N/A	0.64	15	51.2	16.6	None	None	17.5	None	Chronic Pseudomonas aeruginosa	No	No	3.3.1.1 3.3.4.1 3.4.1.1 – 3.5.2.1 3.8.1.1 – 3.9.3.2
CF003	M	26	Phe508del/Phe508del	N/A	1.48	35	63.6	21.3	None	Start of iv antibiotics 14/07/2015. IV Aztreonam and temocillin	140	Some aching in knee joints but no clear CFA	Bcc - multivorans	Yes	No	3.3.1.1 3.3.4.1 3.6.1 – 3.6.2 3.7.1.1
CF004	M	38	Phe508del/Phe508del	N/A	1.38	36	57.5	19.6	None	Ending IV antibiotics 23/06/2015 to 20/07/2015. Ceftazidime, colomycin and teicoplanin	8.3	None	Chronic Pseudomonas aeruginosa	Yes	Yes	3.3.1.1 3.3.4.1 3.4.1.1 – 3.5.2.1 3.8.1.1 – 3.9.3.2 3.6.1 – 3.6.2 3.7.1.1 Appendix Figure 5

CF005	M	31	Phe508del/Phe508del	N/A	2.2	63	81.5	28.9	Azithromycin 500 mg 3-times a week / methotrexate	Start of IV antibiotics. Blood pre-dose. Chest symptoms and joint pain	<5	Active joint pain	Chronic Pseudomonas aeruginosa	Yes. Rheumatoid Arthritis	No	3.3.1.1 3.3.4.1
CF006	M	21	Phe508del/Phe508del	N/A	1.67	38	49.8	15.9	None	Started IV antibioitcs with mild pulmonary exacerbation. Colomycin and Aztreonam IV	22	Vasculitic rash lower limbs	Chronic Pseudomonas aeruginosa	Yes	No	3.3.1.1 3.3.4.1 3.4.1.1 – 3.5.2.1 3.8.1.1 – 3.9.3.2 3.6.1 – 3.6.2 3.7.1.1
CF007	F	21	Phe508del/Phe508del	N/A	0.62	19	46.3	17.0	Azithromycin 500 mg 3-times a week	Pulmonary exacerbation on meropenem and Tobramycin	46	None	Chronic Pseudomonas aeruginosa	Yes	No	3.3.1.1 3.3.4.1
CF008	M	34	Phe508del/Phe508del	N/A	3.28	79	70.0	22.1	None	None	Not available	Wrist and back pain	Chronic Pseudomonas aeruginosa	Yes	No	3.3.1.1 3.3.4.1 3.4.1.1 – 3.5.2.1 3.8.1.1 – 3.9.3.2
CF009	F	39	Phe508del/Phe508del	N/A	1.31	45	64.3	24.1	Montelukast - hydroxychloroquine - azithromycin 500 mg 3-times a week	Start iv antibiotics on 35/07/2015 for pulmonary exacerbation Teocoplanin / meropenem / tobramycin	<5	Joint pain elbow, wrists, hips, knees	Chronic Pseudomonas aeruginosa	Yes	Yes	3.3.1.1 3.3.4.1

CF010	M	20	Phe508del/Phe508del	N/A	1.96	49	39.4	13.6	None	Admitted 1/8/2015 with pulmonary exacerbation meropenem tobramycin cotrimoxazole	140	None	Achromobactin, mycobacterium abscessus	No	Yes	3.3.1.1 3.3.4.1
CF011	F	41	Phe508del/Phe508del	N/A	1.53	49	83.4	28.5	Azithromycin 500 mg 3-times a week. Prednisolone started on 16/9/2018 30 mg	Start of IV antibiotics on 16/9/2015 Tobramycin and ceftazidime	<5	Knee and small joint pain	Chronic Pseudomonas aeruginosa	Yes	Yes	3.3.1.1 3.3.3.1 3.3.4.1 3.6.1 – 3.6.2 3.7.1.1 Appendix Figure 5
CF012	M	33	Phe508del/Phe508del	N/A	1.23	29	78.0	24.7	None	Pulmonary exacerbation and started tobramycin and meropenem on 14/07/2015	286	None	Chronic Pseudomonas aeruginosa	No	Yes	3.3.1.1 3.3.3.1 3.3.4.1
CF013	F	22	Phe508del/Phe508del	86	2.58	80	54.3	20.4	Azithromycin 500 mg 3-times a week	Admitted 20/9/2015 tobramycin and ceftazidime mild pulmonry exacerbation	15.2	Joint pain throughout the body especially hips	Chronic Pseudomonas aeruginosa	No	No	3.3.1.1 3.3.3.1 3.3.4.1 3.6.1 – 3.6.2 3.7.1.1 Appendix Figure 5
CF014	F	33	Phe508del/Phe508del	N/A	1.52	56	51.9	21.2	None	Course of antibiotics colomycin and meropenem	8.4	Joint pain in knees and ankles	Chronic Pseudomonas aeruginosa	No	Yes	3.3.1.1 3.3.3.1 3.3.4.1 Appendix Figure 5

CF015	M	23	Phe508del/Phe508del	N/A	3.57	85	74.8	25.1	Montelukast	None		No joint pain	Achromobactin, mycobacterium abscessus	No	No	3.3.1.1 3.3.3.1 3.3.4.1 3.4.1.1 – 3.5.2.1 3.8.1.1 – 3.9.3.2
CF016	F	50	Phe508del/Phe508del	111	2.25	90	65.7	25.7	Ibuprofen	None	<5	Palindromic joint pain - all joints	Intermitted Pseudomonas aeruginosa	Yes	No	3.3.1.1 3.3.3.1 3.3.4.1 3.4.1.1 – 3.5.2.1 3.8.1.1 – 3.9.3.2
CF017	F	19	Phe508del/Phe508del	100	2.48	86	46.2	19.3	None	End home IV antibiotics on 19/01/2016 meropenem and colomycin	<5	Joint pain affecting wrists, fingers and knees. Often exacerbated by IV antibiotics	Chronic Pseudomonas aeruginosa	Yes	No	3.3.1.1 3.3.4.1 3.4.1.1 – 3.5.2.1 3.8.1.1 – 3.9.3.2 3.6.1 – 3.6.2 3.7.1.1 4.3.1- 4.6.2 Appendix Figure 5
CF018	F	25	Phe508del/Phe508del	116	1.13	35	47.9	17.9	Ibuprofen, Azithromycin 500 mg three times a week	None	37	Joint pains hands fingers, neck, spine	Chronic Pseudomonas aeruginosa	Yes	Yes	3.3.1.1 3.3.3.1 3.3.4.1
CF019	M	25	Phe508del/Phe508del	N/A	2.71	63	68.0	22.6	Montelukast	Admitted for IV antibiotics 21/01/2015 Fosfomycin and tobramycin	47	Ankles, knees wrist, shoulders	Chronic Pseudomonas aeruginosa	Yes	Yes	3.3.1.1 3.3.4.1

ID	Sex	Age	Genotype													
CF020	F	23	C.1521_1523delctt / Phe508del	N/A	2.16	70	55.8	21.8	None	End of IV antibiotics Tigecycline Tazocin and tobramycin started 11/01/2016. Tazocin rash on 26/01/2015 - allergy	58	Arthralgia on admission but resolved	Bcc - multivorans	No	No	3.3.1.1 3.3.3.1 3.3.4.1 3.4.1.1 – 3.5.2.1 3.8.1.1 – 3.9.3.2 3.6.1 – 3.6.2 3.7.1.1 4.3.1- 4.6.2
CF021	F	45	Phe508del/Phe508del	N/A	1.52	60	58.4	23.4	Post lung transplant Methotrexate prednisolone tacrolimus	None	25	Active joint pain	Chronic Pseudomonas aeruginosa	Yes	Yes	3.3.1.1 3.3.4.1
CF022	M	46	Phe508del/Phe508del	85	0.94	27	62.9	22.3	Azithromycin 500 mg 3-times a week	Influenza-A IV colomycin and tigecycline 4/2/2015 / Tamiflu	261	None	Stenotrophomonas maltophilia	Yes	No	3.3.1.1 3.3.3.1 3.3.4.1
CF023	F	37	Phe508del/Phe508del	N/A	0.76	26	56.7	21.1	Prednisolone 5 mg	26/2/2016 started 1/12 meropenem and aztreonam.	8.6	Active joint pains affecting most joints	Chronic Pseudomonas aeruginosa	Yes	No	3.3.1.1 3.3.4.1 3.6.1 – 3.6.2 3.7.1.1
CF024	F	28	Phe508del/Phe508del	N/A	0.6	21	57.9	26.0	Azithromycin 500 mg 3-times a week	IV antibiotics started on 12/2/2016 Colomycin and Fosfomycin. Fever	109	Aching joints knees, hips and wrists	Chronic Pseudomonas aeruginosa	Yes	Yes	3.3.1.1 3.3.3.1 3.3.4.1 3.6.1 – 3.6.2 3.7.1.1 4.3.1- 4.6.2
CF025	M	51	3849+10KB C>T/ Phe508del	50	0.56	16	92.4	32.3	None	IV for pulmonary exacerbation 9/2/2016 Ceftazidime Teicoplanin	51	None	Stenotrophomonas maltophilia, Staphylococcus, Haemophilus	No	No	3.3.1.1 3.3.3.1 3.3.4.1 3.4.1.1 – 3.5.2.1

																3.8.1.1 – 3.9.3.2 4.3.1- 4.6.2
CF026	F	20	Phe508del/Phe508del	115	1.21	39	59.2	23.1	Clarithromycin (part of NTM treatment), prednisolone 15 mg	Cefoxitin 3-times a week, clarithromycin, linezolid	5.5	Joint pains	Mycobacterium abscessus and steotrophomonas maltophilia	Yes	No	3.3.1.1 3.3.3.1 3.3.4.1 3.6.1 – 3.6.2 3.7.1.1 3.8.1.1 – 3.9.3.2
CF027	M	38	Phe508del/R347P	N/A	0.68	17	72.8	23.0	Montelukast	IV Fosfomycin and aztreonam	42	None	Chronic pseudomonas	No	Yes	3.3.1.1 3.3.4.1
CF028	F	43	Phe508del/Phe508del	N/A	0.54	21	51.5	20.1	Hydroxychloroquine	Fosfomycin and meropenem	69	Joint pain	Chronic pseudomonas	Yes	Yes	3.3.1.1 3.3.2.1 3.3.4.1
CF029	M	30	Phe508del/Phe508del	N/A	0.69	17	57.4	19.9	None	Meropenem, temocillin, tigecycline	66	None	Burkholdeeria multivorans	No	No	3.3.1.1 3.3.2.1 3.3.3.1 3.3.4.1 3.4.1.1 – 3.5.2.1
CF030	M	31	Phe508del/Phe508del	N/A	0.74	17	65.2	20.1	Azithromycin 500 mg 3-times a week	Pre orkambi IV imipenem and tobramycin 9-16/5/2016	27	None	Chronic pseudomonas maltophilia	No	Yes	3.3.1.1 3.3.2.1 3.3.4.1
CF031	F	36	Phe508del/Phe508del	N/A	0.86	35	55.1	23.2	Azithromycin 500 mg 3-times a week	Pre orkambi and post IV ceftazidime 9/6/2016	<5	None	Chronic pseudomonas, maltophilia	No	Yes	3.3.1.1 3.3.2.1 3.3.4.1
CF032	M	31	Phe508del/Phe508del	N/A	0.94	24	59.2	21.0	Azithromycin as part of NTM treatment	Pre orkambi. NTM treatment oral moxifloxacin, minocycline and azithromycin	13.1	None	Mycobacterium abscessus, intermittent pseudomonas, stenotrophomonas	No	No	3.3.1.1 3.3.2.1 3.3.4.1

CF033	F	41	Phe508del/Phe508del	N/A	0.6	25	46.4	20.0	None	Pre-orkambi no IV antibiotics	11.9	None	Chronic pseudomonas	No	Yes	3.3.1.1 3.3.2.1 3.3.3.1 3.3.4.1 3.4.1.1 – 3.5.2.1 3.8.1.1 – 3.9.3.2 4.3.1-4.6.2
CF034	M	34	Phe508del/Phe508del	N/A	1.85	43	76.8	23.4	Hydrocortisone oral Naproxen	IV ceftazidime	<5	Joint pain in hands and knees	Chronic pseudomonas	Yes	No	3.3.1.1 3.3.2.1 3.3.3.1 3.3.4.1
CF035	M	22	Phe508del/621+1 (G>T)	N/A	1.43	0	55.1	19.3	Montelukast, Azithromycin 500 mg 3-times a week	IV colomycin and meropenem. long term ceftazidime.	31	Joint pains shoulder hips back	Chronic pseudomonas stenotrophomonas maltophilia	Yes	Yes	3.3.1.1 3.3.2.1 3.3.3.1 3.3.4.1 4.3.1-4.6.2
CF036	M	29	C.1521_1523delctt / Phe508del	105	1.18	27	57.3	18.7	Azithromycin 500 mg 3-times a week	Pre-start of Orkambi and on last few days of IV antibiotics. Colomycin and tazocin	<5	None	Chronic pseudomonas and achromobactin	No	No	3.3.2.1 3.3.1.1 3.3.3.1 3.3.4.1 3.4.1.1 – 3.5.2.1 3.8.1.1 – 3.9.3.2
CF037	M	40	Phe508del/Phe508del	120	1.16	31	56.8	20.0	Prednisolone 10 mg	Pulmonary exacerbation. Colomycin, ciprofloxacin and septrin.	140	Joint pain	Achromobactin	Yes	No	3.3.1.1 3.3.2.1 3.3.3.1 3.3.4.1 4.3.1-4.6.2
CF038	F	41	Phe508del/Phe508del	N/A	0.62	0	47.9	20.7	Naproxen 250 mg Prednisolone 10 mg	Admitted for IV ceftazidime 2 g 2/11/2017 and	43	Joint pain. Small and large joint. Variable	Chronic Burkholderia cenocepacia	Yes	Yes	3.3.3.1 3.3.4.1 4.3.1-4.6.2

Study code	Gender	Age	Genotype	Sweat chloride	FEV1 l/s	FEV1 (%)	Weight	BMI	Anti-inflammatory medication	Antibiotics	CRP	Active joint symptoms	Bacteria	CFA	CFRD	Figures
										nebulised Azli						
CF039	M	36	Phe508del/Phe508del	N/A	1	0	58.0	20.8	Azithromycin 500 mg 3-times a week	Pre-orkambi.	<5	None	Chronic burkholderia multivorans	No	Yes	3.3.3.1 3.3.4.1 4.3.1-4.6.2
CF040	M	28	Phe508del/Phe508del	N/A	0.95	0	48.3	16.0	Azithromycin 500 mg 3-times a week	Aztreonam and tobramycin	31	None	Chronic Pseudomonas aeruginosa	No	No	3.3.3.1 3.3.4.1 4.3.1-4.6.2

Table 4: Available patient information form the CF cohort recruited to this study. Details of study code, genotype, anti-inflammatory medication, exacerbation status study code, gender, age, genotype, sweat chloride (mmol/l), FEV1 l/s, FEV1 (%), weight (kg), BMI (kg/m2), anti-inflammatory medication, antibiotics, C-reactive protein (CRP), active joint symptoms, bacteria, cystic fibrosis arthritis (CFA) diagnosis, cystic fibrosis related diabetes (CFRD) and which figures within this study the patient's samples and data are included. The clinical information was provided by the clinical team at St James Hospital Adult CF ward, Leeds.

2.2 Patient Sample Processing

Patient blood (50mL) were collected using 9mL Vacuette tubes (Greiner-bio-one) containing either clot activator or K_3EDTA. Blood in clot activator tubes were allowed to clot for 60 min followed by centrifuging at 1000xg for 10 min. Sera were collected into 1mL tubes for storage at -80°C. Blood collected in K3EDTA tubes were used for peripheral blood mononuclear cell (PBMC) isolation. EDTA treated blood were mixed with Phosphate-buffered saline (PBS) in a 1:1 ratio, carefully layered onto 13mL of Lymphoprep® (Axis-Shield) in 50mL Falcon tubes and centrifuged at room temperature, 1100xg for 20 mins without brakes. The PBMCs 'buffy layer' on top of the Lymphoprep® layer was extracted and washed in 3x volume PBS. PBMCs were passed through Miltenyi MS magnetic columns using the Miltenyi Monocyte isolation kit II to isolate peripheral monocytes. Isolated monocytes plated in 6 well plates, seeded at $1x10^6$ cells/mL/well in 1mL RPMI complete medium (Sigma) (supplemented with 10% (v/v) foetal bovine serum (FBS) (Gibco), 50 IU/ml penicillin, and 50 g/ml streptomycin (Sigma)).

2.3 Cell Lines

All cells were cultured in sterile conditions, using aseptic technique in a category two tissue culture hood and incubated in a humidified incubator at 37oC in 5% CO2 atmosphere. Four Human Bronchial Epithelial (HBE) cell lines were used: IB3-1 cells (a kind gift from Professor Eric Blair, Leeds, UK) with the CF mutation ΔF508/W1282X, CuFi-1 ΔF508/Phe508del (ATCC® CRL-4013TM), CuFi-4 ΔF508/G551D (ATCC® CRL-4015TM) and Beas-2B cells (ATCC® CRL-9609TM), the latter derived from a healthy control (HC),

and shown to express a full range of toll like receptors (TLR), including TLR4 (Ioannidis et al. 2013). IB3-1 and Beas-2B cell lines were cultured in basal LHC medium (Thermo Fisher Scientific) (supplemented with 10% (v/v) FBS (Gibco), 50 IU/ml penicillin, and 50 g/ml streptomycin (Sigma)). CuFi-1 and CuFi-4 cells were cultured in supplemented BEGM bullet kit (CC-3170, Lonza). The differential growth media formulations are optimised to ensure no significant differences in inflammation due to the growth media in appendix figure 11. All HBE cells were cultured in vented, positively charged T75 C+ flasks (Sarstedt), to promote adherence, until they reached 90% confluency. Once confluent, HBE cells removed from the flask using 0.5% trypsin (Sigma) for 10 min at 37°C. The trypsin was neutralised with equal amount of 10% FBS in PBS (or LHC complete medium). The cells were harvested by centrifuging at 300xg 5 min. The cells are resuspended in 5mL of BEGM medium and the number of cells counted and plated in 6-well positively charged plates (Sarstedt), seeded at 2×10^6 cells/mL/well overnight before stimulation/functional experiments.

2.4 Cell stimulations and inflammasome functional assay

Cells were pre-treated with the following compounds where indicated prior to NLRP3 stimulation; Amiloride (100mM, 1hour) (Cayman Chemical), MCC950 (15nM, 1 hour) (Cayman Chemical), 2-DG (0.5mM, 2 hours) (Agilent), EIPA (10μM, 1 hour) (Cayman Chemical), NPPB (100μM, 1 hour) (Cayman Chemical), S18 derived peptide (25μM, 4 hours) (a kind gift from Spyryx Biosciences, Inc ®), ouabain (100nM, 24 hours) (Cayman Chemical), digoxin (100nM, 24 hours) (Cayman Chemical), OxPAC (30μg/mL, 1 hour) (Invivogen), Ac-YVADD (2μg/mL, 1 hour) (Invivogen) and $CFTR_{172}$ (10μg/mL, 1 hour) (Cayman Chemical). Inflammasome stimulation was achieved using LPS (10ng/mL) (Ultrapure EK, Invivogen) for 4 hours with the addition of ATP (5mM, 30 minutes) (Invivogen), poly(dA:dT) dsDNA

(1µg/mL with Lipofectamine 2000, 1 hour) (Invivogen), TcdB (10ng/mL, 1 hour) (Cayman Chemical) or flagellin (10ng/mL with Lipofectamine 2000, 1 hour) (Invivogen) in the hour of the LPS stimulation.

Stimulant	Working concentration	Total incubation time
Lipopolysaccharide (LPS)	10 ng/mL	4 hours
ATP	5 mM	30 minutes
poly(dA:dT) dsDNA	1 µg/mL	1 hour
TcdB	10 ng/mL	1 hour
Flagellin	10 ng/mL	1 hour
Ouabain	100 nM	24 hours
Nigericin	1 µM	30 minutes
Amiloride	100 mM	1 hour
MCC950	15 nM	1 hour
2-DG	0.5 mM	2 hours
EIPA	10 µM	1 hour
NPPB	100 µM	1 hour
S18-derived peptide	25 µM	4 hours
Digoxin	100 nM	24 hours
OxPAC	30 µg/mL	1 hour
Ac-YVADD	2 µg/mL	1 hour
$CFTR_{172}$	10 µg/mL	1 hour

Table 5: Details of the *in vitro* stimulants and inhibitors used throughout this study, including the working concentration and incubation time.

2.5 ELISA

Cytokines (IL-1β, IL-18, IL-1Ra, TNF, IFN-γ and IL-6) from serum and cell culture supernatants were detected by ELISA kits (Invitrogen) using matched antibody pairs, as per the manufactures recommendations. Briefly capture antibodies were coated onto the plates and covered with a plate sealer overnight at room temperature. The wells were washed twice with PBS with 0.1% Tween 20 (PBST) and tapped dry. Sera (100µl) and/or supernatants (100µl)

from cell cultures were added to the plates in duplicate along with the cytokine standards and the plates covered with plate sealers. After 2 hrs incubation at room temperature the contents of the plates were aspirated off and the wells washed 3 times with PBST and tap dried. Anti-cytokine antibody-HRP conjugates were added to all wells at 100μl/well and the plate incubated for 2 hrs. The anti-cytokine antibody-HRP conjugates were removed by aspiration and the wells washed 5 times with PBST. Substrate reagents (100μl/well) were added to all wells and incubated for up to 30 min and the reaction stopped with 50μl/well of stop reagent. The absorbance of the wells was read at 450nm and the reference wavelength at 620nm. The one-site total curve was used to generate the calibration curve, based on the company cytokine standards, and interpolation of data points. All standard curves were compared to previous standard curves for that assay. All duplicate sample measurements were <10% of each other to ensure technical repeats were accurate and reliable.

2.6 RT-qPCR

Cells were washed in PBS, covered and suspended in TRIzol™ Reagent (Sigma) and stored at 4°C (short-term) or at -80°C (long-term). Cells were lysed in the TRIzol™ Reagent (Ambion Life technologies) or using cell lysis buffer from the PureLink RNA mini Kit (Ambion) or the *mir*Vana miRNA Isolation Kit (Ambion), which was then used to isolate the RNA from the samples. The RNA extraction was performed as per the manufacturers' protocol.

The High Capacity cDNA Reverse Transcription kit (Applied Biosystems) was used to convert the RNA to cDNA and the Taqman microRNA Reverse Transcription kit (Applied Biosystems) was used to convert the miRNAs to cDNA. The assay was performed as per the manufacturers' protocol. cDNA was stored at -20°C.

The SYBR Green PCR Master mix (Applied Biosystems) was used to analyse the expression of selected primers in the cDNA. The cDNA was defrosted from -20°C storage and mixed with SYBR Green master mix and specific forward and reverse primers to the genes of interest. The mix and cDNA sample were then loaded onto a 96 well PCR plate and loaded on to the PCR machine (Applied Biosystems 7500 Real Time PCR System) as per the manufacturers' protocol.

Primers for SYBR Green RT-qPCR were ordered from Sigma (see below) based on work by Dr Rebecca J Mathews, a previous student in the McDermott group at University of Leeds (Mathews *et al*. 2014).

Name	Sequence: (5' to 3')	Tm	GC%	MW	Length
IL1B F	GGCCTCAAGGAAAAGAATCTGTAC	64.9	45.8	7395	24
IL1B R	GGGATCTACACTCTCCAGCTGTAGA	65.7	52	7642	25
HPRT F	GGAAAGAATGTCTTGATTGTGGAAG	65.6	40	7825	25
HPRT R	GGATTATACTGCCTGACCAAGGAA	65.9	45.8	7386	24

The Taqman® primers used in this study are detailed below:

Gene	Assay ID	Dye
SCNN1B	Hs01548617_m1	FAM
IFNG	Hs00989291_m1	FAM

2.7 Western Blot

Samples were made up in dissociation buffer [1x dissociation buffer (100mM Tris-HCl, 2% (w/v) sodium dodecyl sulphate, 10% (v/v) glycerol, 100mM dithiothreitol, 0.02% (w/v)

bromophenol blue, pH 6.8] and heated at 95ºC for 5 min. Proteins were resolved by SDS-PAGE on 10% acrylamide Tris-glycine gels and then transferred to Hybond PVDF membranes (GE Healthcare). Following electrotransfer, the membranes were blocked for 1 h in PBST and 5% (w/v) non-fat milk and then incubated with primary antibody diluted in 2% BSA (w/v) PBST overnight at 4°C. Antigens were probed using the following primary antibodies: anti-SCNN1B (ARP72375_P050, Avia Systems Biology; 1ug/ml dilution). Primary antibodies were detected by incubation with horseradish peroxidase-conjugated secondary antibody anti-rabbit IgG (7074S; Cell Signalling Technology), in PBST containing 2% (w/v) BSA. Bound horseradish peroxidase conjugates were visualized using the ECL® detection system (Millipore Immobilon chemiluminescent HRP substrate, Merck) for 5 minutes, before being imaged with the ChemiDoc Imaging system (Bio-Rad).

2.8 Colorimetric assays for metabolites

Intracellular ATP (ATP Assay Kit, Abcam) and succinate (Succinate Assay Kit, Abcam) were measured using cell lysates and extracellular glucose (Glucose assay kit, Abcam) and L-lactate (L-Lactate assay kit, Abcam) were measured from cell supernatants, whereby by both standard curve and samples were quantified using colorimetric procedure at OD 570 nm. Both measurements were made using the manufacturer's recommendations.

2.9 Seahorse Metabolic Analyser

Live analysis of extracellular acidification rate (ECAR) and oxygen consumption rate (OCR) using the Cell Energy Phenotype kit on monocytes was performed, using the Seahorse XF-96 Extracellular Flux Analyser (Agilent Seahorse Bioscience). CD14+ monocytes were

purified from isolated PBMCs using MACS microbeads for negative selection, according to the manufacturer's instructions (Miltenyi Biotec) (section 2.2). Monocytes and HBECs were seeded in triplicate in XF-96 cell culture plates (2×10^5 cells/well and 5×10^4, respectively) using appropriate culture medium. CellTak (Corning) was used to attach both cell types to the cell culture plate and prepared according to the manufacturer's recommendations. The metabolism of monocytes and HBECs were analysed in four consecutive measurements in XF Base Medium (unbuffered DMEM with 5.5mM glucose and 2mM L-glutamine, pH adjusted to 7.4). After three basal measurements, three consecutive measurements were taken following the addition of 10μM oligomycin, carbonyl cyanide-4-(trifluoromethoxy) phenylhydrazone (FCCP) (5μM) in order to determine basal and maximum OCR and ECAR. All data is normalised to total cellular protein using a microplate reader. Cells are lysed and used for quantitation with Bradford protein detection reagent with a standard protein concentration curve to ensure accurate quantitation and allow absolute comparison of data from assay to assay. This method assumes that the *in vitro* stimulation does not alter total cellular protein content significantly. The total protein values calculated using the Bradford assay are then inserted into the WAVE software for normalisation of the OCR and ECAR values. Details of seahorse OCR and ECAR traces are described in appendix figure 8 and 9.

2.10 Lactate dehydrogenase (LDH) Cytotoxicity Assay

The LDH Cytotoxicity Assay Kit (Pierce) was used, as per the manufacturers' recommendations, with and without caspase-1 inhibitor, Ac-YVAD-cmk (InvivoGen), as a control for inflammasome-dependent cell death. Optimal cell density was calculated, and the chemical-mediated cytotoxicity assay was performed, whereby spontaneous and maximal LDH activity were calculated as controls for stimulation-mediated cytotoxicity. Absorbance

was measured at 490 nm and 680 nm and subtracted from each other. In order to quantify

pyroptosis and discriminate it from other forms of cell death, lactose dehydrogenase (LDH)

was measured with and without a caspase-1 inhibitor. LDH is released from a necrotic cell,

which provides a distinguishing feature between necrosis and programmed cell death (PCD),

such as apoptosis where LDH is contained within the apoptotic vesicles, or blebs. To further

distinguish pyroptosis from necrosis, a caspase-1 inhibitor was used in a control sample to

prevent pyroptosis. Any LDH that is detected in the presence of the caspase-1 inhibitor is then

termed necrosis and is taken away from the LDH release from the experimental sample,

without a caspase-1 inhibitor pre-treatment. The remaining LDH level is presented as caspase-

1-dependent pyroptosis, calculated as a percentage of complete necrotic cell death using lysis

buffer and water controls.

2.11 Transient Transfection

Beas-2B cells were transiently transfected with 5 or 10μg of SCNN1B cDNA

(Addgene) using Lipofectamine2000 reagent (Thermo Fisher Scientific) for 48h as per

manufacturer's instructions. Cells were harvested and immunoblotted for SCNN1B to confirm

expression.

2.12 Statistics

No statistical methods were used to predetermine sample size. All analyses were performed

using GraphPad Prism v 7. Differences were considered significant when $P < 0.05$. All bar

graphs were expressed as median 95% confidence intervals. The Mann-Whitney non-

parametric test was performed (p values * = ≤0.05, **= ≤0.01, ***= ≤0.001 and ****=

≤0.0001) when comparing non-parametric populations. A repeated measures 2-way ANOVA

statistical test was performed with Turkey's multiple comparisons test with Bennett's post-hoc

analysis was performed when calculating variance between samples (p values * = ≤0.05, **= ≤0.01, ***= ≤0.001 and ****= ≤0.0001).

Chapter 3

3.0 NLRP3 inflammasome activation in CF

3.1 Introduction

3.1.1 Activation of the inflammasomes - PAMPS, DAMPS and HAMPS

The inflammasomes and their structure, activation and regulation were discussed in detail in chapter 1, section 1.3. Briefly, inflammasomes are large, multi-protein complexes whose assembly requires two signalling events:

1. a priming signal, such as toll-like receptor (TLR) recognition of lipopolysaccharide (LPS) with downstream NF-κB signalling, for expression of the component parts of an inflammasome complex (Marshall et al., 1999).

2. a unique activating signal triggering assembly of the component parts of each unique inflammasome.

Assembled inflammasomes are centred around a sentinel protein, such as nucleotide-binding oligomerization domain (NOD)-like receptor (NLR) protein, which detects the unique activating signal and becomes active. Adapter proteins, such as apoptosis-associated, speck-like protein containing a CARD (ASC), are recruited to and oligomerise from the initial sentinel protein. ASC specks recruit pro-caspase-1 molecules, which auto-cleave into their active form. Active caspase-1 molecules cleave the zymogens pro-IL-1β, pro-IL18 and gasdermin D (GSDMD). GSDMD is then able to form pores in the plasma membrane to allow non-conventional secretion of IL-1β and IL-18 (Section 1.3) (Martinon et al., 2002, Aglietti et

al., 2016). Inflammasomes have been extensively studied *in vitro*, with well-defined procedures for stimulating each individual inflammasome. There are five well-characterised inflammasomes reported in the literature, with an established structure and activating signal. These inflammasomes are NLRP1, NLRP3, NLRC4 (IPAF), AIM2 and Pyrin.

NLRP1 is activated by lethal toxin (LeTx) from *Bacillus anthracis (B. anthracis)*. LeTx has two subunits: an antigen binding subunit and a catalytic subunit. When LeTx enters the cell through anthrax binding sites, it cleaves MAPK proteins at the n-terminal, inhibiting a major signalling pathway within the host cell. With compromised MAPK signalling, immune cells are unable to effectively secrete cytokines and chemokines. This lack of immune signalling impairs neutrophil chemotaxis and increases pro-apoptotic signalling. The NLRP1 inflammasome was not investigated in this study as there was no obvious biological relevance in CF pathology to justify its inclusion into the study's design.

There are a further four inflammasomes that have been described as being able to form a backbone of an inflammasome, but their precise activating signals are not yet characterised despite evidence of caspase-1 activation and IL-1β and IL-18 secretion (Broz and Dixit, 2016). These inflammasomes are NLRP2, NLRP6, NLRP7 and NLRP12 and were not investigated in this study due to the lack of data regarding their activating signal.

In this study, four inflammasomes were specifically studied *in vitro*: NLRP3, NLRC4, Pyrin and AIM2. CFTR defects induce various ionic imbalances, so this study's inflammasome of interest was NLRP3 due to its unique activating signal being K^+ efflux. The precise mechanisms of NLRP3 activation still remains unclear, although it is thought that NLRP3 detects changes in host-derived factors that are transmuted by a range of pathogens and environmental irritants. These altered host-derived factors include K^+ efflux, cathepsin release and mitochondrial ROS (mROS), DNA (mtDNA) or translocation. Many particulates such as aluminium, silica, monosodium urate (MSU), cholesterol, and amyloid-β escape

phagolysosomes and release cathepsin B, activating NLRP3. External necrotic cell death releases ATP into the extracellular milieu, which activates the K^+ channel P2X purinoceptor 7 (P2X7) and decrease the intracellular K^+ concentration to trigger NLRP3 inflammasome assembly (Munoz-Planillo et al., 2013).

Due to the nature of the recurrent pulmonary bacterial, viral and fungal infections that are characteristic of CF (Filkins and O'Toole, 2015), both flagellin (and therefore NLRC4) and dsDNA (and therefore AIM2) were also investigated in this study as potential inflammasome activating signals *in vitro*. The Pyrin inflammasome was also investigated, partly due to its novelty but also that Rho GTPases have an influential role in the trafficking of CFTR to the cell surface (Cheng et al., 2005) (section 1.3). In addition, it has been proposed that heterozygous carriers of a CF-associated mutation have a selective advantage in some infectious diseases (Meindl, 1987, Regelmann et al., 1991, Romeo et al., 1989) such as Vibrio cholera (*V. Cholera*) and Clostridium difficile (*C. difficile)*, which infect the digestive system causing diarrhoea, fluid loss and eventual dehydration through CFTR-dependent fluid loss (Hodges and Gill, 2010). However in the presence of a dysfunctional *CFTR* allele, roughly 50% of Cl^- transport will be lost in heterozygotes, thereby reducing fluid loss and providing a selective advantage for heterozygous carriers of a CF-associated mutation (Romeo et al., 1989). There are also published cases of asymptomatic *C. difficile* infection in patients with CF (Piccolo et al., 2017). With *C. difficile* TcdB being an established Pyrin inflammasome activating signal, this inflammasome was included in this study, to understand whether cells with CF-associated mutations may be protected from the inflammation associated with *C. difficile* TcdB as well as the associated fluid loss. Therefore, the NLRP3, NLRC4, AIM2 and Pyrin inflammasomes were investigated using the *in vitro* stimulation protocol discussed in section 2.4.

The initial, common priming signal to generate both the inflammasome sensor (e.g. NLRP3) and *IL1β* expression (*IL18* is constitutively expressed) is thought to be common to all inflammasomes. There is evidence to suggest that pro-caspase-1 and ASC, two common constituents of the majority of inflammasomes, are also constitutively expressed (Gurung et al., 2015). Priming of the inflammasome can also be through sterile cytokine signalling, with evidence that TNF may also have a role in providing this initial signal in sterile inflammation, such as during ageing or autoinflammatory diseases (Bauernfeind et al., 2016).

In vitro activation of the inflammasomes requires the addition of both the priming and activation signals sequentially. The NLRP3 inflammasome is commonly activated by K^+ efflux, which is achieved *in vitro* using adenosine triphosphate (ATP) stimulation in order to open the K^+ channel P2X7 and decrease the intracellular K^+ concentration to trigger NLRP3 inflammasome assembly (Munoz-Planillo et al., 2013). NLRC4 is activated by type-3 secretory system injection of flagellin, although the precise mechanism is still unclear (Zhao et al., 2011). *In vitro* the NLRC4 inflammasome is activated by transfected flagellin molecules. The Pyrin inflammasome is activated by bacterial modifications of Rho GTPases, such as the glucosyltransferase cytotoxin B secreted by *C. difficile* (TcdB) (Xu et al., 2014, Aubert et al., 2016, Park et al., 2016) (section 1.3). Therefore *in vitro* activation of the Pyrin inflammasome is achieved by the addition of purified TcdB. Finally, the AIM2 inflammasome is activated by dsDNA and primed by LPS or interferon (IFN)-γ (Fernandes-Alnemri et al., 2009, Hornung et al., 2009), which is also replicated *in vitro*. There are now many inflammasome inhibitors that are both potent and specific; in this study, a small molecule drug, named MCC950 that specifically inhibits NLRP3 activation, is used (mechanism unknown) (Coll et al., 2015).

Many cell types are able to produce an inflammasome response but the key cells in which inflammasome are assembled are cells of the myeloid and epithelial lineages. Both these cell types form part of the innate immune response with monocytes/macrophages and

neutrophils actively killing pathogens and the epithelial barrier maintaining tissue integrity as well as detecting invading organisms via pattern recognition receptor (PRR) detection of PAMPs and DAMPs (Whitsett and Alenghat, 2015). In this study both monocytes and epithelial cells are examined for *in vitro* NLRP3, NLRC4, AIM2 and Pyrin inflammasome activation.

3.1.2 Studying the inflammasomes in vitro

As previously discussed, ATP is a known activator of the NLRP3 inflammasome, via its opening of the P2X7 K^+ channel (Gong et al., 2018). However, there are numerous molecules that are known to instigate NLRP3 inflammasome assembly. In this study three other, well-described NLRP3 activating molecules were considered- monosodium urate (MSU), ouabain and nigericin toxin. The former is well described in disease models of gout, in which urate crystals accumulate and activate the NLRP3 inflammasome. The second stimulant, ouabain is a small, non-specific inhibitor of the Na^+/K^+ ATP-gated channel. The latter is a pore-forming toxin from *Streptomyces hygroscopicus*, and activates NLRP3 via pannexin-1. Including ATP, all four stimulants induce K^+ efflux and NLRP3 assembly and activation. During optimisation experiments (appendix figure 1), ATP and ouabain were the most potent and biologically relevant in terms of CF pathology: ATP and ouabain open and close ion channels respectively, making them pertinent molecules in the study of the NLRP3 inflammasome, in the context of channelopathy such as CF.

HBECs and monocytes were examined, under these conditions, from patients with CF, SAID and NCFB and age- and sex-matched HCs.
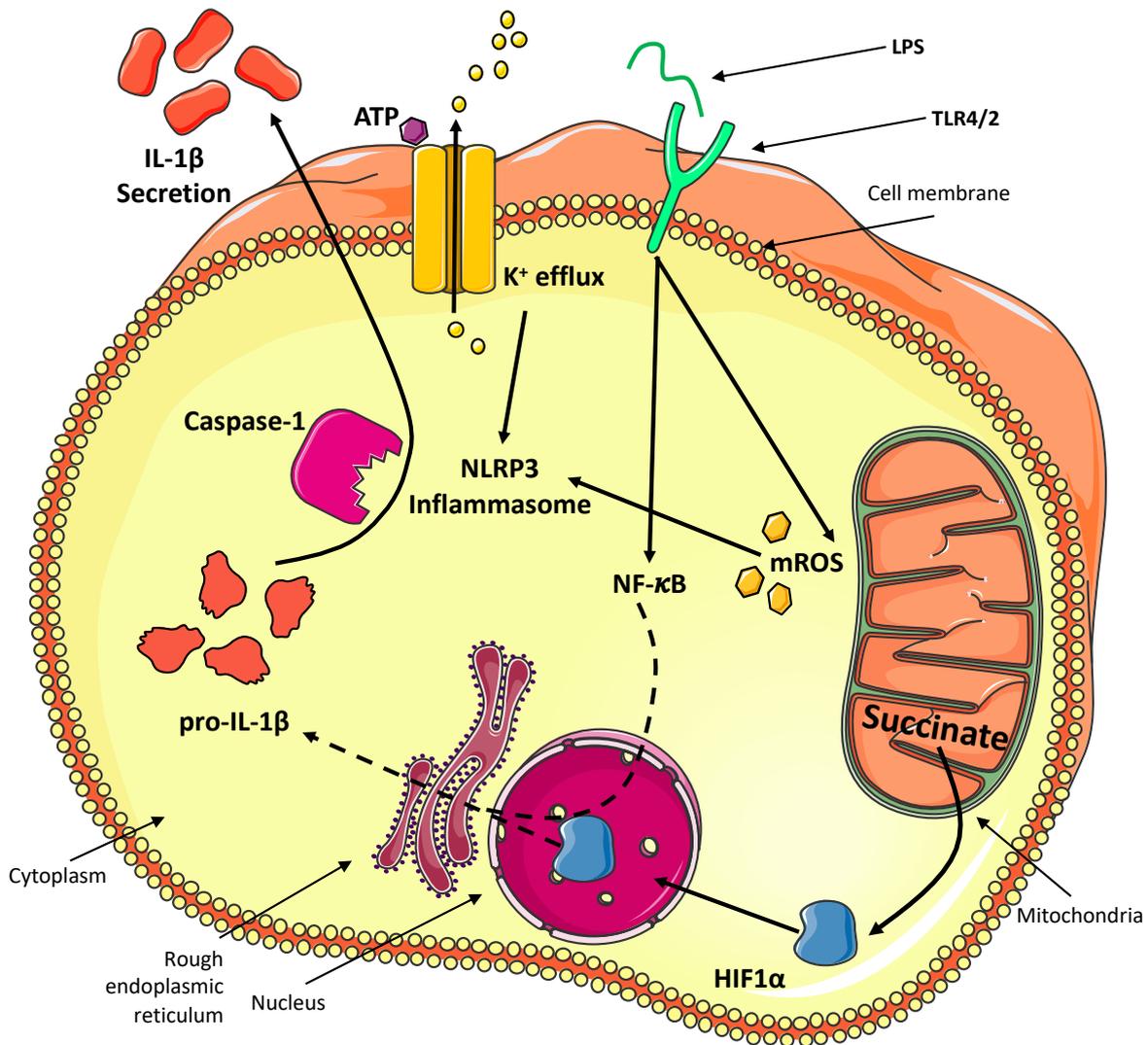
Figure 3.1.2: NLRP3 inflammasome priming and activation. The NLRP3 inflammasome requires two signals to be primed and activated. The first priming signal, such as LPS/TLR/NF-κB signaling or LPS/glycolysis/succinate/HIF1α signaling, generates the expression of *NLRP3* and *IL1B*. A second activating signal, such as K^+ efflux from P2X7 ATP-activated channel or mROS-dependent NLRP3 activation, assembles the component parts of the NLRP3 inflammasome. LPS- Lipopolysaccharide; TLR- Toll like receptor; mROS- mitochondrial ROS; K^+- potassium; IL- interleukin, HIF1α- hypoxia inducible factor 1 alpha.

3.1.3 In vitro inflammasome inhibition

It terms of the small molecule inhibition of NLRP3, MCC950 was used throughout due to its specificity and potency. Coincidently, the CFTR inhibitor 172 (CFTR$_{172}$) not only potently inhibits the CFTR Cl$^-$ channel but also is able to inhibit NLRP3 activation (Jiang et al., 2017). The fact that this small molecule inhibited the ATP binding site of both proteins made its use impractical in the investigation of the relationship between loss of CFTR activity and NLRP3 activity, although it was used as an NLRP3 inhibitor as well as in other, non-CFTR related experiments. In addition, TLR4 and caspase-1 small molecule inhibitors were used to inhibit NLRP3 inflammasome priming and IL-1β/IL-18 cleavage, respectively.

3.1.4 Pyroptotic cell death

Pyroptotic cell death is the terminal phase of chronic, sustained inflammasome activation. This unique form of cell death stems from the unique secretory pathway that the pyrogens, IL-1β and IL-18 use to exit the cell, after caspase-1 processing. Active caspase-1 not only cleaves and activates IL-1β and IL-18 but also cleaves a novel, small molecular weight protein, named gasdermin D (GSDMD) (Kayagaki et al., 2015, Shi et al., 2015, He et al., 2015, Aglietti et al., 2016). Active GSDMD forms pores in the plasma membrane, providing a secretory route for IL-1β and IL-18. When inflammasome activation is prolonged, GSDMD pore formation is also sustained. leading to a loss of cell integrity and cell death or pyroptosis. Pyroptosis is an inflammasome-dependent, caspase-1-dependent, inflammatory form of cell death, akin to necrosis. ASC speck release is thought to occur passively upon pyroptosis, rather than being an active secretory pathway (Baroja-Mazo et al., 2014, Franklin et al., 2014, Rowczenio et al., 2017). This is partly due to the large molecular weight of fully oligomerised

ASC, as well as the timing of ASC speck release being correlated with pyroptotic cell death. However, the field of ASC speck research is still in its infancy. Therefore, pyroptosis is an informative measure of systemic and sustained inflammasome activation, with many implications for the pathogenesis of inflammatory disease (Bergsbaken et al., 2009, Miao et al., 2010, Shi et al., 2015).

3.1.5 ASC specks

ASC is an integral protein, within many inflammasome complexes, as when it binds to a sensor molecule (e.g. NLRP3), ASC will oligomerise and form a macromolecular signalling platform for pro-caspase-1 recruitment (Fernandes-Alnemri and Alnemri, 2008, Dick et al., 2016). This oligomerisation can be observed using fluorescence microscopy, with large 'speck'-like macromolecules forming when an inflammasome is activated and assembled (Franklin et al., 2014). Under chronic or intense inflammasome activation, pyroptotic cell death will ensue- i.e., an inflammasome-dependent form of cell death. It has been previously reported that in cases of elevated pyroptosis the inflammasome components, particularly large ASC specks, can be detected using a flow cytometry-based assay (Fernandes-Alnemri and Alnemri, 2008, Fernandes-Alnemri et al., 2009, Baroja-Mazo et al., 2014, Franklin et al., 2014). The original study from Fernandes-Alnemri et al. used GFP-tagged ASC fusion proteins in human THP-1 monocytic cell lines to detect ASC specks, or pyroptosomes intracellularly. The authors go on to describe how pyroptosomes cause pyroptotic cell death through membrane rupture, with release of the cell contents, including IL-1β and ASC pyroptosomes. Other studies have progressed the study of extracellular ASC by investigating whether these macromolecules have any inflammatory functions, once released from the cytoplasm. Seminal studies into ASC speck function describe how ASC specks remain intact long after the host cell has been degraded post-pyroptosis (Kuri et al., 2017). ASC specks continue to recruit extracellular pro-

caspase-1 for auto-cleavage as well as processing pro-IL-1β into its active form, despite being released from the confines of a host cell. Extracellular ASC specks are able to disseminate inflammation beyond the local inflammatory environment. Multiple studies have detected ASC specks in the serum from a variety of inflammatory diseases, and even within macrophages that have phagocytosed extracellular ASC specks. These donor ASC specks are then able to escape endosomes and begin nucleating and oligomerising new pyroptosomes for capsase-1 and IL-1β/IL-18 cleavage in the recipient macrophage (Muñoz-Arias et al., 2015, Kofahi et al., 2016). In this study, a flow cytometry-based assay was used to detect extracellular ASC specks (see Methods section).

3.1.6 Macrophage polarisation

The capacity of human monocytes to differentiate into M1-type and M2-type macrophages *in vitro* can be utilised in order to understand whether there is any bias in differentiation state in specific diseases. M1-type macrophages are thought to have a proinflammatory role in peripheral tissues and are characterised by an inherent ability to produce proinflammatory IL-6 and TNF, whilst M2-type macrophages are archetypically associated with production of anti-inflammatory IL-10 cytokine. Peripheral monocytes were differentiated and activated to either M1-type or M2-type macrophages (Mia et al., 2014, Italiani and Boraschi, 2014) (figure 3.5.1.1). Macrophage cell surface markers and intracellular cytokines were measured using flow cytometry and ELISA (Tarique et al., 2017) and characterised into M1-type or M2-type (Tarique et al., 2017, Mills et al., 2000).

3.1.7 Pathogenic ion channel activity in CF

The CFTR protein is widely expressed in a variety of cells and tissues, where it acts as an anion channel, conducting Cl^- and HCO3-, and also a regulator of epithelial transport proteins (König et al., 2002, Konstas et al., 2003, König et al., 2001, Kunzelmann, 2003, Berdiev et al., 2009). In healthy lungs, CFTR inhibits the epithelial sodium channels (ENaC) and helps maintain normal volume and composition of airway surface liquid (ASL). Loss of ENaC inhibition in CF leads to increased sodium absorption, a hallmark of CF, with reduced ASL volume and defective mucociliary clearance (Althaus, 2013, Berdiev et al., 2009, Bhalla and Hallows, 2008, Donaldson et al., 2002, Garcia-Caballero et al., 2009, Gwoździńska et al., 2017, Hobbs et al., 2013, König et al., 2002, König et al., 2001, Konstas et al., 2003, Kunzelmann, 2003, Mall et al., 2004, Zhou et al., 2011, Zhou et al., 2008).

Several studies have provided insight into the potential importance of sodium homeostasis in the disease process. Overexpression of ENaC in mice results in a CF-like lung disease, with ASL dehydration and mucous obstruction (Althaus, 2013, Mall et al., 2004, Zhou et al., 2011, Zhou et al., 2008). In human patients, variants in the ENaC *SCNN1B* and *SCNN1G* genes have been associated with bronchiectasis and CF-like symptoms (Fajac et al., 2008). In contrast, rare mutations, which cause hypomorphic ENaC activity, can reduce disease progression in patients homozygous for F508del (Mall et al., 2004, Zhou et al., 2011, Donaldson and Boucher, 2007). Furthermore, reduced ENaC activity is associated with multisystem pseudohypoaldosteronism type-1, a disease that results in production of excessive amounts of ASL (Bhalla and Hallows, 2008).

Amiloride-sensitive Na^+ channels have diverse functions, and as macrophages modulate inflammation and spontaneous channel depolarisation in patients with CF, excessive cytokine secretion can be inhibited by amiloride therapy (Sorio et al., 2011, Rolfe et al., 1992).

In dendritic cells, channel activation triggers proinflammatory signalling through superoxide production (Barbaro et al., 2017).

3.2 Methods

3.2.1 ELISA

As in section 2.5.

Briefly, serum was isolated from whole blood using clot-activating blood collection tubes that were centrifuged to separate out the sera from the whole blood. Serum was aliquoted and stored long-term at -80°C. Serum from healthy controls and patients with CF, diagnosed SAID and NCFB were collected and serum cytokines measured by ELISA. The growth media supernatants from stimulated cell culture plates were stored at -20°C before being used to detect IL-1β and IL-18 cytokine secretion levels by ELISA.

3.2.2 ASC specks

Sera was separated from whole blood (see Methods section) and stored at -80°C before being thawed and incubated with an ASC-PE antibody and analysed using an optimised flow cytometric assay. The number of events was equated to the number of ASC specks, normalised to the volume of sample ran through the cytometer (standardised at 200μL) and expressed as extracellular ASC specks/μL. HC serum or CF patients' sera (200μl) were incubated with 5μl of anti-ASC-PE (TMS-1) antibody (Biolegend) and incubated for 1 hr at room temperature, and subsequently analysed on the LSRII flow cytometer instrument (BD Biosciences). Non-fluorescent 1μm microspheres (Thermo Fisher Scientific) were used as a guide to gate around

ASC specks for counting. ASC speck events were reported as total events in the set gate divided by 200 (ASC speck/µl) (Rowczenio et al., 2017).

3.2.3 Macrophage polarisation

PBMCs were isolated using the Lymphoprep®, as described in section 2.2. A total of $1x10^7$ PBMCs were seeded overnight into T150 flasks (Corning) in 'complete' RPMI media to allow monocytes to attach. On day 0, attached cells were washed with PBS and then detached using 5mM EDTA. In a 6-well plate, for each sample, two wells were seeded at $1x10^6$ cells/mL/well in 'complete' RPMI supplemented with either 20ng/mL human GM- CSF (PeproTech EC Ltd) for M1 differentiation or 20ng/mL human M-CSF (PeproTech EC Ltd) for M2 differentiation and incubated for 9 days, with supplemented-media changes every 3-days. On day 9, for M1 activation the complete RPMI medium was supplemented with 100ng/mL human IFN-γ (PeproTech EC Ltd), 100ng/mL TNF and 50ng/mL LPS or for M2 activation the medium was supplemented with 20ng/mL IL-13 and 20ng/mL IL-4 and incubated for 24 hours. Macrophages were periodically monitored for phenotypic changes using light microscopy: M1 macrophages display a rounded morphology, whilst M2 macrophages display a tortuous, dendritic morphology (Mia et al., 2014, Italiani and Boraschi, 2014). On day 10, macrophages were prepared for flow cytometry characterisation and day 10 supernatant stored for cytokine analysis using ELISA.

Differentiated and activated M1 and M2 macrophages were characterised by surface marker expression and detection of intracellular cytokines by flow cytometry. Macrophages were washed with complete RPMI media and cultured with complete RPMI media supplemented with Golgi plug for 4 hours. Cells were then detached using 5mM EDTA for 40 minutes on ice. EDTA was neutralised in complete RPMI and the cells were washed twice in

PBS. Cells were pelleted and suspended in Brilliant Stain buffer (BD Biosciences) supplemented with mouse and human serum (Sigma), to block Fc receptors. Cells were then washed and stained for surface markers for 30 minutes. Surface markers for M1-type (CD14$^+$ CD16$^+$ HLA-DR$^+$ CD274$^+$ CD86$^+$) and M2-type (CD14$^+$ CD16$^+$ CD206$^+$). Cells were then washed and fixed and permeabilised for 30 minutes. Cells were then washed and stained for intracellular markers (see below) for 30 minutes. The intracellular markers for M1-type and M2-type macrophages were the high expression of TNF and IL-10, respectively. Cells were then washed and suspended in brilliant stain buffer, ready for flow cytometry (BD Bioscience FACS Calibur). Monocytes were characterised as classical (CD14^{++}CD16$^−$), non-classical (CD14dimCD16^{++}), and intermediate (CD14^{++}CD16$^+$). Flow cytometry analysis for characterisation of macrophage and monocyte populations used the following antibodies: CD14 (V500 BD Horizon™, V500 Mouse Anti-Human, CD14 RUO M5E2, Lot: 561391), CD206 (Mannose Receptor) (FITC BD Pharmingen™, FITC Mouse Anti-Human, CD206, RUO 19.2, Lot: 551135), CD16 (FcγRIII) (APC-H7, BD Pharmingen™ APC-H7, Mouse Anti-Human CD16, RUO 3G8, Lot: 560195), TNF (BV421 BD Horizon™, BV421 Mouse Anti-Human TNF, RUO MAb11, Lot: 562783), CD274 (B7-H1) (APC, BD Pharmingen™ APC, Mouse Anti-Human CD274, RUO MIH1, Lot: 563741), CD86 (B7-2) (PE-Cy7, BD Pharmingen™ PE-Cy™7 Mouse Anti-Human CD86, RUO2331 (FUN-1), Lot: 561128), IL-10 (PE, BD Pharmingen™ PE Rat Anti-Human IL-10, RUO JES3-19F1, Lot: 559330) and HLA-DR (PerCP,Anti-HLA-DR PerCP, CE_IVD L243, Lot: 347402).

3.2.4 Ionic concentration assay

Sodium and potassium sensitive dyes, SBFI and PBFI, respectively (Molecular Probes) were used as cell permeant selective ion indicators for the fluorometric determination of Na$^+$

and K$^+$ concentrations. Monocytes and HBECs were allowed to adhere in black 96-well cell culture plates overnight. Cells were then washed and incubated in the appropriate low serum media (see above) (1%) for 1 hour. The dyes (10mM final concentration) were loaded with Pluronic® F-127 (Sigma) and incubated for 100 minutes. Stimulants were then added to the wells as indicated and described above. All wells were washed with NaCl solution. Excitation at 344nm and 400nm with emission at 500nm was measured immediately to calculate the percentage change in fluorescence compared to an untreated control (Andersson et al., 2006).

3.2.5 Capsase-1 activity

A colorimetric assay to determine caspase-1 activity via cleavage of a caspase-specific peptide conjugated to a colour reporter molecule p-nitroalinine (pNA). The assay was performed in protein lysates and serum.

3.2.6 Pyroptosis assay

As in section 2.10.

Briefly, the LDH Cytotoxicity Assay Kit (Pierce) was used, as per the manufacturer's recommendations, with and without caspase-1 inhibitor, Ac-YVAD-cmk (InvivoGen), as a control for inflammasome dependent cell death (pyroptosis). Optimal cell density was calculated, and the chemical-mediated cytotoxicity assay was performed, whereby spontaneous and maximal LDH activity were calculated as controls for stimulation-mediated cytotoxicity. Absorbance was measured at 490 nm and 680 nm and subtracted from each other.

3.2.7 in vitro NLRP3 inflammasome activation and inhibition

As in section 2.4.

Briefly, the growth media supernatants from stimulated cell culture plates were stored at -20°C before being used in the above assays. All stimulations were optimised using the THP-1 monocyte cell line, Beas-2b (WT) HBECs and HC PBMCs (appendix figure 1 and 2). The Don Whitley H35 Hypoxystation was used at 1% O_2 for hypoxic conditions. Cells were cultured in the hypoxystation overnight before stimulation. Stimulations were performed as described in section 2.4.

3.3 Inflammatory serum cytokine levels in patients with CF

3.3.1 Serum IL-1-family cytokines

Serum cytokine levels provide an insight into the systemic inflammatory state of an individual, acting as biomarkers for underlying, chronic or acute inflammation. Initially, selected cytokines from the IL-1 family were investigated due to the pathology of CF being related to an ion channel (CFTR) defect and the universal NLRP3 inflammasome activator being ionic flux (K^+ efflux). The IL-1 family of cytokines encompasses a large variety of both pro- and anti-inflammatory cytokines and chemokines. In this study, IL-18 and IL-1β were chosen as two potent proinflammatory cytokines that are cleaved and processed by active caspase-1 via inflammasome assembly. In patients with systemic autoinflammatory disease (SAID), these two cytokines are elevated in the serum before administration of the widely successful recombinant IL-1Ra therapy. The endogenous levels of this anti-inflammatory IL-1 family cytokine receptor, IL-1Ra was also studied to provide some understanding of the systemic resolution of this IL-1 driven inflammation. IL-1Ra will be secreted in response to NLRP3 inflammasome activation as a pro-resolution mechanism and so, therefore, provides additional evidence for the activity of the inflammasomes and downstream IL-1 cytokine family secretion in the systemic inflammation present in patients with CF (Medicine, 1997).
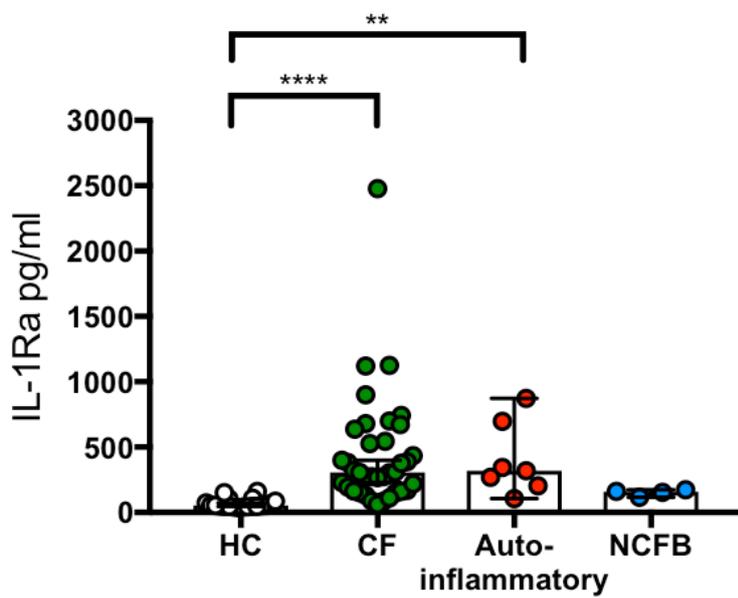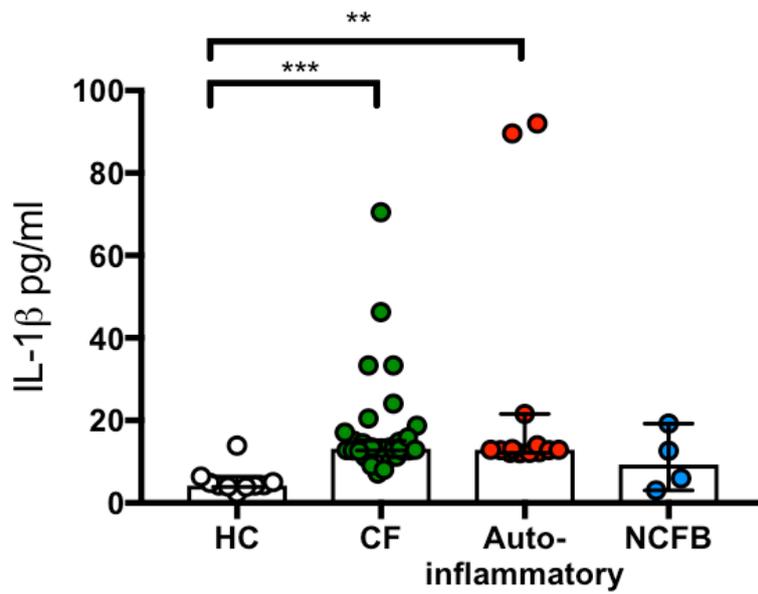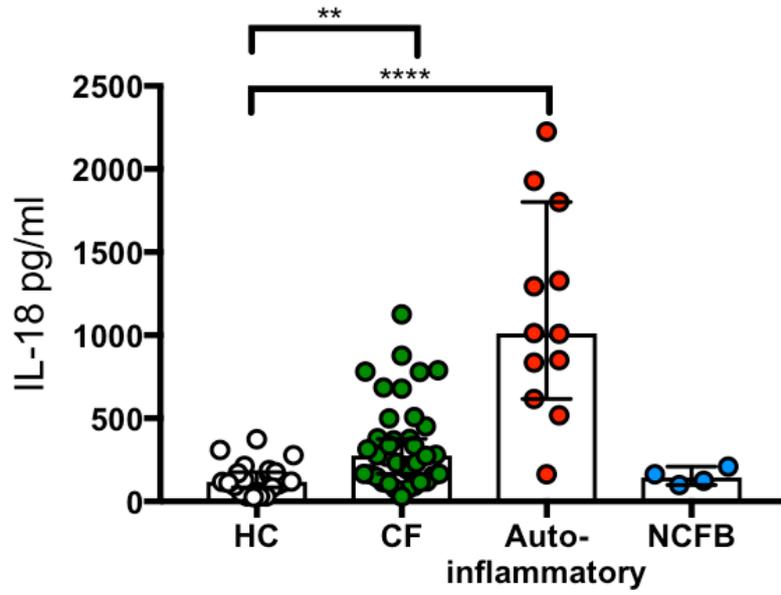
(Figure 3.3.1.1 legend on next page)

Figure 3.3.1.1: IL-18, Il-1β and IL-1Ra levels in patient sera. ELISA assays were used to detect IL-18 (HC n=21, CF n=36, Autoinflammatory n=12, NCFB=4), IL-1β (HC n=10, CF n=31, Autoinflammatory n=13, NCFB=4) and IL-1Ra (HC n=20, CF n=37, Autoinflammatory n=7, NCFB=4). The Mann-Whitney non-parametric test was performed (p values * = ≤0.05, **= ≤0.01, ***= ≤0.001 and ****= ≤0.0001).

Levels of IL-18 was observed to be significantly elevated in sera from patients with CF (all Δf508/Δf508) and SAID compared to that of HC individuals (p=0.0128 and p=0.0042 respectively). Both IL-1β and IL-1Ra were also significantly increased compared to HC sera in both CF (0.0002 and <0.0001 respectively) and SAID (0.0039 and 0.0006 respectively) cohorts. There was no significant difference between HC and NCFB for any of the measured cytokines in this study. The ratio of IL-1β in serum from patients with SAID was not as high, relative to HC, CF or NCFB compared to that of the levels IL-18. IL-1β serum concentrations were comparatively low compared to other cytokine measurements.

3.3.2 Serum ASC Specks
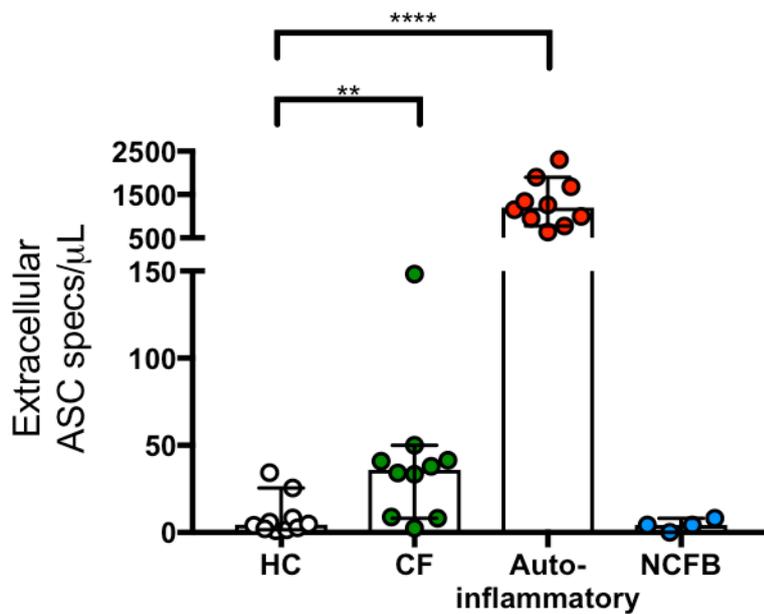
Figure 3.3.2.1: Extracellular ASC specks in patient sera. Flow cytometry was used to detect ASC specks in sera of patients with CF and HCs (d) (HC n=10, CF n=10, Autoinflammatory n=10, NCFB=4). The gating of ASC specks using flow cytometry is detailed in appendix figure 7. The Mann-Whitney non-parametric test was performed (no comparisons reached statistically significance p>0.05).

Low amounts of ASC specks were detected in sera from HC or NCFB individuals. Sera from patients with CF had significantly elevated serum ASC specks compared to HC and NCFB sera. Autoinflammatory patient sera had around 10-fold greater ASC speck levels than that of CF sera.

3.3.3 Serum Caspase-1 activity
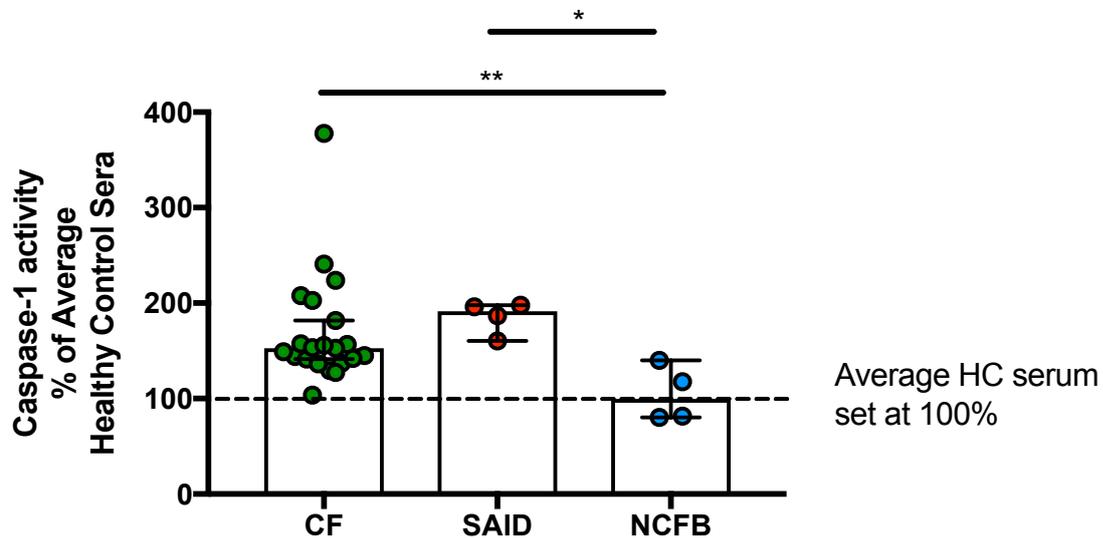
Figure 3.3.3.1: Caspase-1 activity in patient sera. A colorimetric assay to detect caspase-1 activity in sera of patients with CF, NCFB and SAID as a percentage of the average caspase-1 activity from HC (n=10) with a mean absorbance of 0.20845 nm (HC n=10, CF n=21, Autoinflammatory n=4, NCFB=4). The Mann-Whitney non-parametric test was performed (no comparisons reached statistically significance p>0.05).

Caspase-1 activity in serum samples from patients with CF, NCFB and SAID was measured and compared to a mean average of caspase-1 activity in a set of HC serum samples (n=10). Sera from patients with CF had elevated serum caspase-1 activity, with an average of around 50% increase. This elevated serum caspase-1 activity in patients with CF was significantly increased compared to patients with NCFB (p=0.0043), as was serum from patients with SAID (p=0.0286).

3.3.4 Other proinflammatory serum cytokines

In order to understand the significance of elevated serum IL-1 family cytokines, as well as the presence of serum ASC specks in patients with CF, it is important to compare the inflammasome-related cytokines and macromolecules with other proinflammatory cytokines in serum. This will allow further interpretation of the data, in respect to whether these phenomena are due to hyper-activation of the inflammasome pathways or because of a general proinflammatory cytokine profile. Initially tumour necrosis factor (TNF) and IL-6 were measured in the same serum samples, as in sections 3.3.1 and 3.3.2 (Fig. 3.3.4) by ELISA. Different numbers of patients were used for each figure due to sample availability.
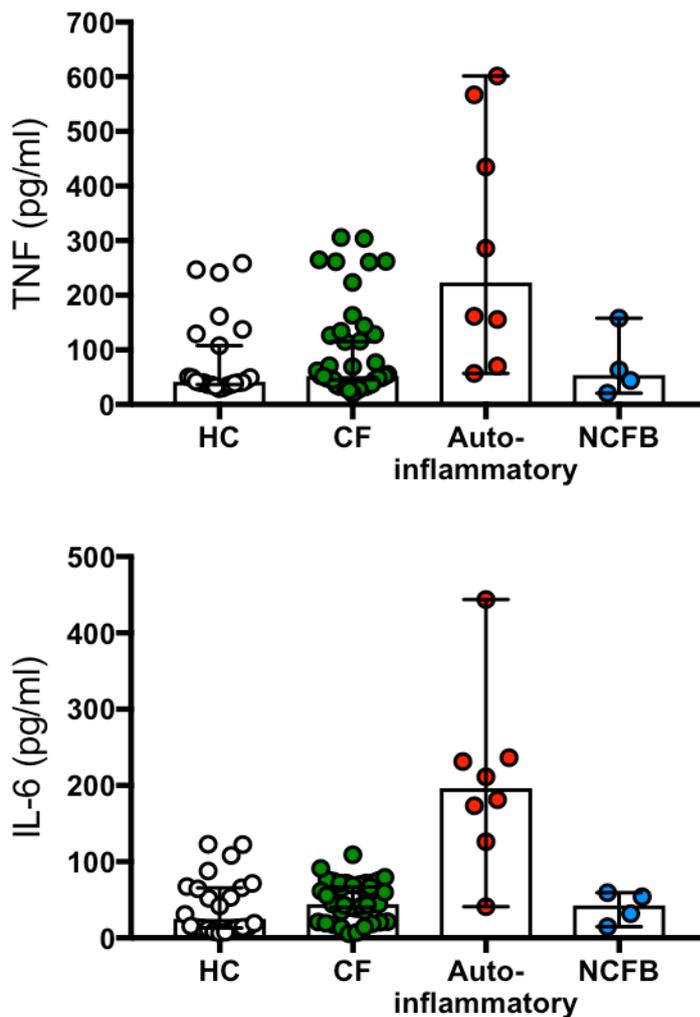
Figure 3.3.4.1: TNF and IL-6 serum concentrations. ELISA assay was used to detect TNF (a) and IL-6 in serum (b) (HC n=24, CF n=40, Autoinflammatory n=8, NCFB=4). The Mann-Whitney non-parametric test was performed (no comparisons reached statistically significance p>0.05).

3.4 *In vitro* inflammasome activation

3.4.1 In vitro NLRC4, AIM2 and Pyrin inflammasome activation

Figure 3.4.1 shows that the HBEC lines all activate the NLRC4, AIM2 and Pyrin inflammasomes in response to the appropriate stimulation (optimised in appendix Fig 1). There is little to no difference between the Beas-2b (WT) HBEC line and the HBEC lines with CF-associated mutations. The stimulation with dsDNA created a more robust IL-18 response compared with flagellin and TcdB. Figure 3.4.1b shows monocyte stimulations and also indicates that the dsDNA, and thus AIM2 inflammasome, is the more potent stimulation. Again, there is no significant difference between HC monocytes compared to monocytes from patients with CF. IL-18 secretion from the same monocytic stimulations (Fig 3.4.1) supports the IL-1β data (Fig 3.4.1b), in that there is no difference between HC monocytes compared to monocytes from patients with CF with any of the inflammasome stimulations. However, a strong flagellin/NLRC4 IL-18 response was recorded, which was slightly elevated in CF monocytes. No difference was noted for the TcdB/Pyrin IL-18 response between HC and CF monocytes. The dsDNA/AIM2 stimulation again produced the highest cytokine secretion, although with HC monocytes producing more IL-18, compared to CF monocytes.

LPS	-	+	+	+
Flagellin	-	+	-	-
TcdB	-	-	+	-
dsDNA	-	-	-	+
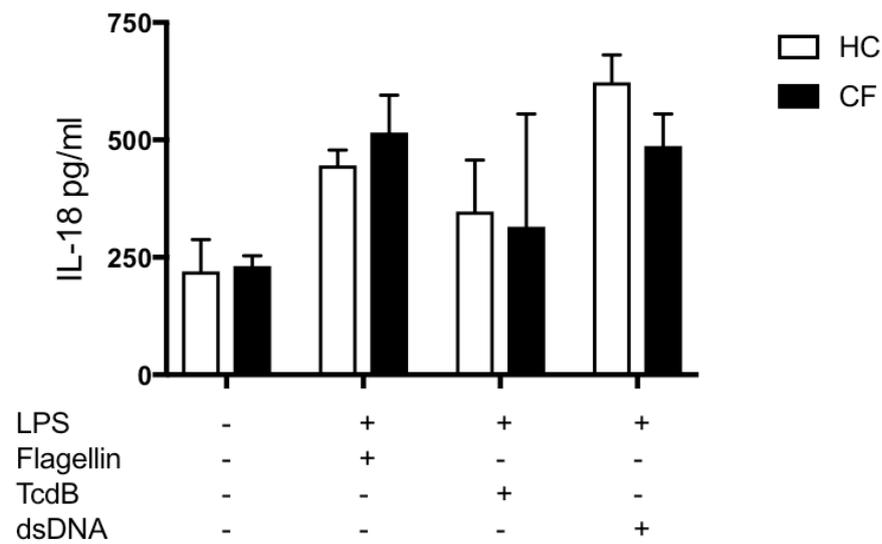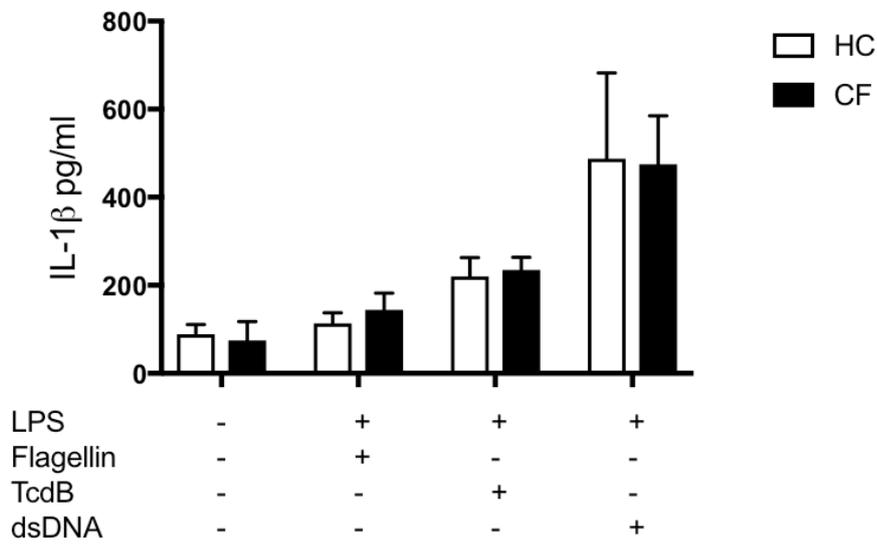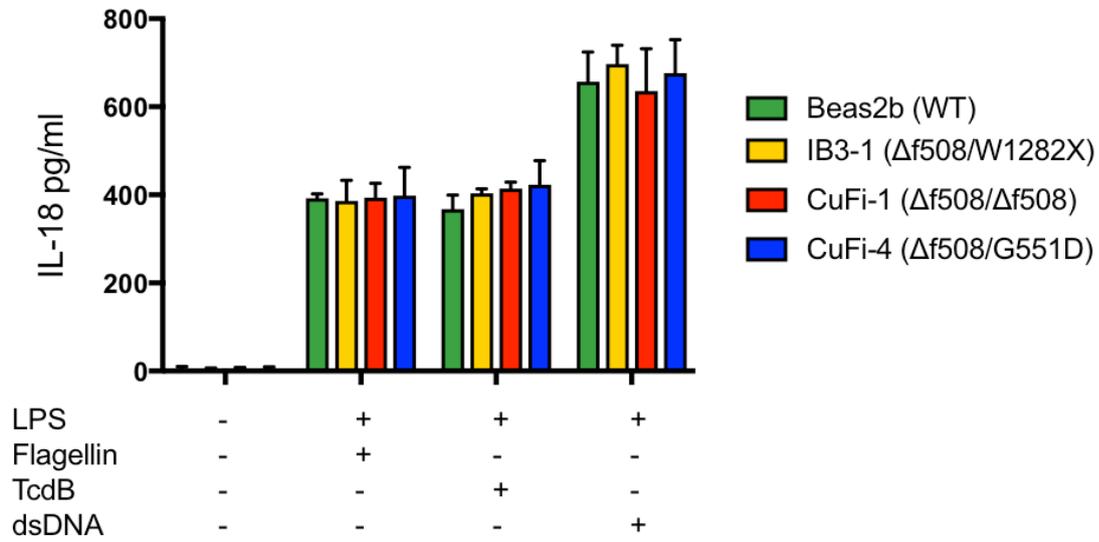
(Figure 3.4.1.1 legend on next page)

Figure 3.4.1.1: *in vitro* NLRC4, AIM2 and Pyrin Inflammasome activation. ELISA assays were used to detect IL-18 from supernatants of HBECs (a) (n=4) and monocytes (c) (n=10) as well as IL-1β from monocytes (b) (n=10). Cells were stimulated with LPS (10ng/mL) for 4 hours before being stimulated for 4 hours with Flagellin (10ng/mL with Lipofectamine 2000), TcDB (10ng/mL) or poly(dA:dT) dsDNA (1µg/mL with Lipofectamine 2000). A repeated measures 2-way ANOVA statistical test was performed with Turkey's multiple comparisons test (p values * = ≤0.05, **= ≤0.01, ***= ≤0.001 and ****= ≤0.0001).

3.4.2 In vitro NLRP3 inflammasome activation

With no statistically significant difference in NLRC4, AIM2 or Pyrin inflammasome activation between WT HBECs or HC monocytes and cells harbouring CF-associated mutations, the NLRP3 inflammasome was then assessed, with and without small molecule inhibitors, using the same stimulation protocol (Methods section 2.4).

Notably, HBEC lines harbouring CF-associated mutations hyper-responded to NLRP3 activation in both ATP and ouabain stimulation, in terms of IL-18 secretion. However, only IB3-1 (Δf508/W1282X) and CuFi-1 (Δf508/Δf508) cell lines produced a statistically significant increase in IL-18 secretion *in vitro* compared to the Beas2b (WT) HBEC line. All four inhibitors depleted IL-18 secretion in all four cell lines effectively, particularly inhibition of TLR4 by OxPAC, upstream of NF-κB priming of NLRP3 components. The two specific NLRP3 inhibitors, MCC950 and $CFTR_{172}$, sufficiently blocked downstream IL-18 secretion in all cell lines after NLRP3 stimulation. The caspase-1 inhibitor, AC-YVADD-cmv, was also able to reduce IL-18 secretion by preventing cleavage and activation of the pyrogen by inhibiting upstream caspase-1 activity. However, despite caspase-1 inhibition the HBECs with CF-associated mutations maintained a statistically significant increase in IL-18 secretion post-

stimulation with ATP for NLRP3 activation. IL-1β secretion was undetectable in HBEC line cultures.
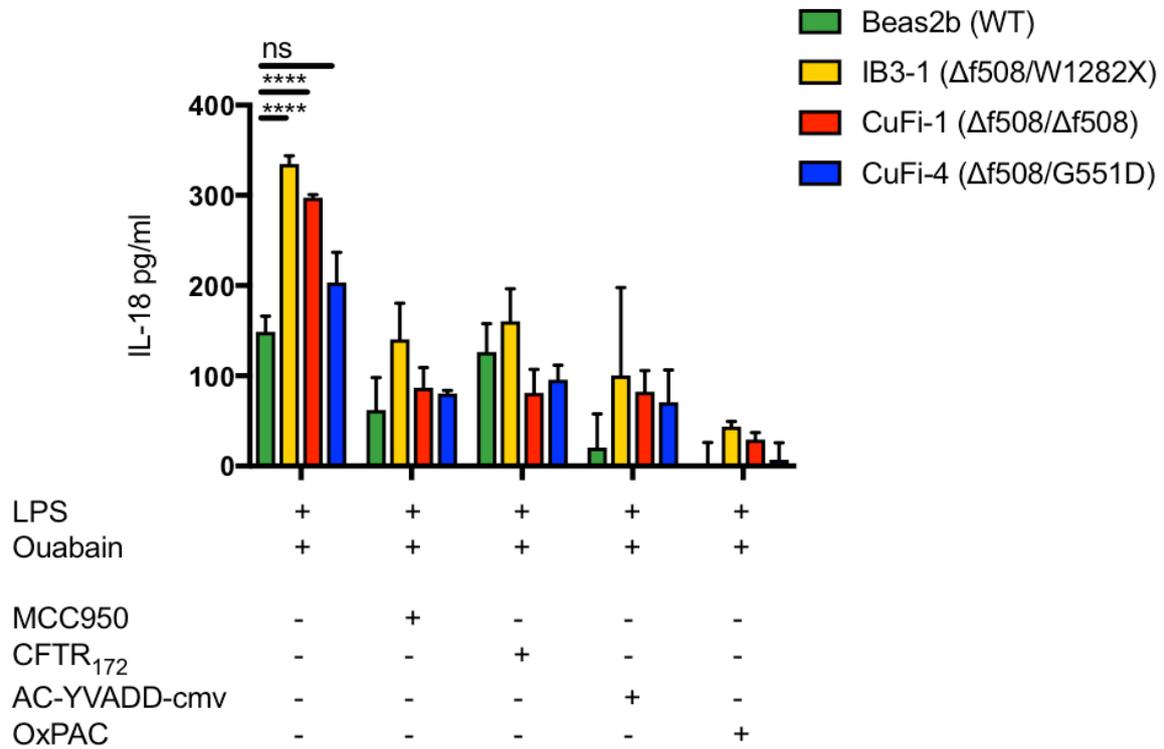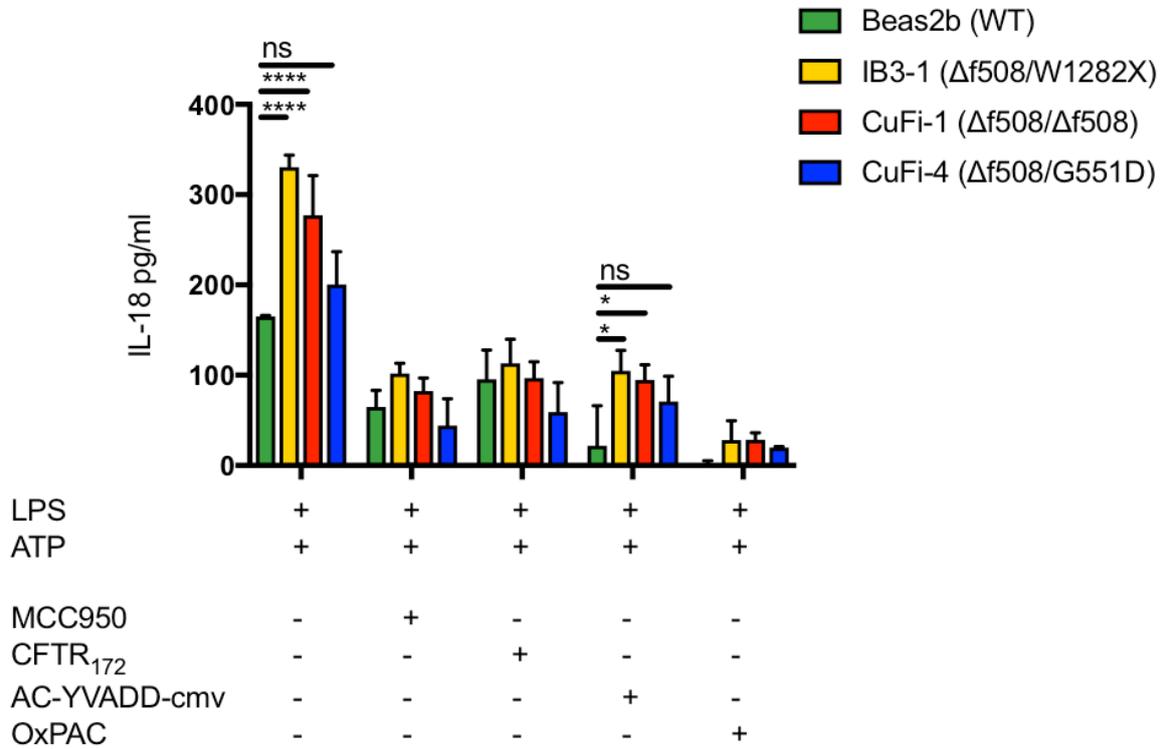
(Figure 3.4.2.1 legend on next page)

Figure 3.4.2.1: *in vitro* IL-18 secretion from NLRP3 Inflammasome activation in HBEC lines. ELISA assays were used to detect IL-18 from supernatants of HBECs using ATP (5mM, 30mins) or ouabain (100nM, 24 hours) (n=3). Cells were stimulated with LPS (10ng/mL, 4 hours) before being stimulated for 30 minutes with ATP (5mM, 30 mins) or Ouabain (100nM, 24 hours). The following inhibitors were pre-treated, before NLRP3 inflammasome activation: MCC950 (15nM, 1 hour), $CFTR_{172}$ (10µg/mL, 1 hour), AC-YVADD-cmv (2µg/mL, 1 hour) and OxPAC (30µg/mL, 1 hour). A repeated measures 2-way ANOVA statistical test was performed with Turkey's multiple comparisons test (p values * = ≤0.05, **= ≤0.01, ***= ≤0.001 and ****= ≤0.0001).
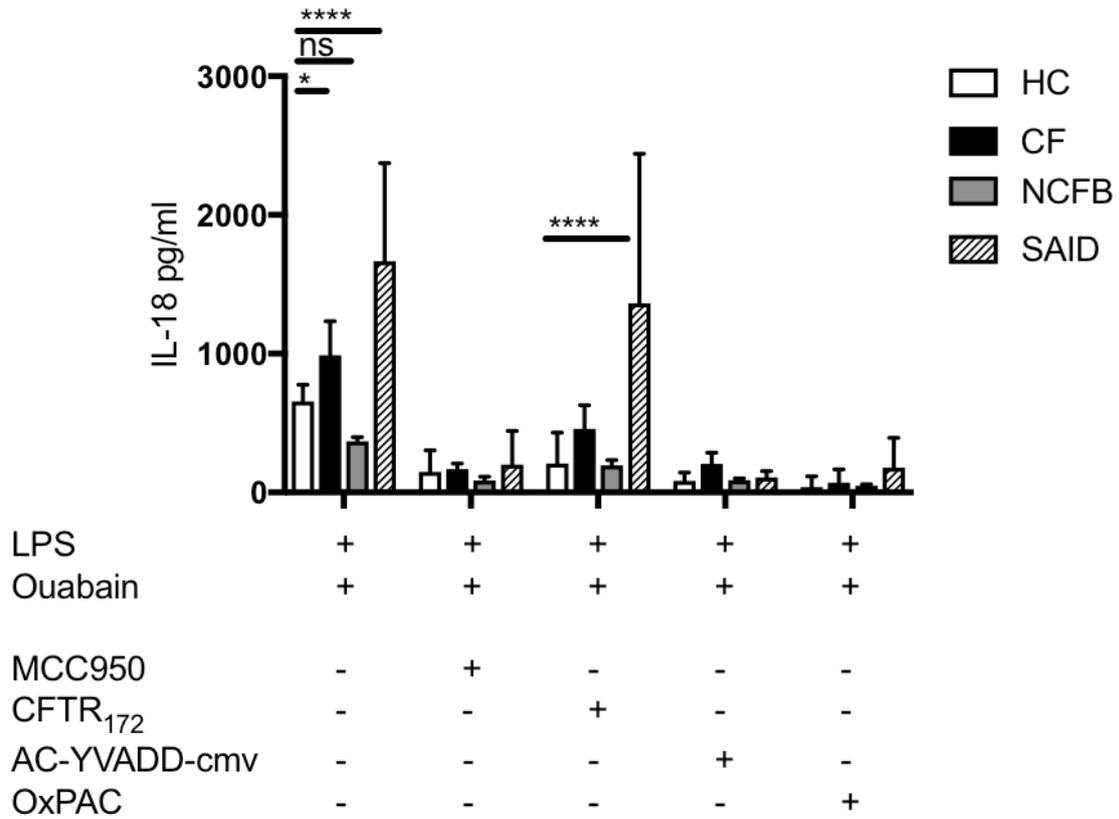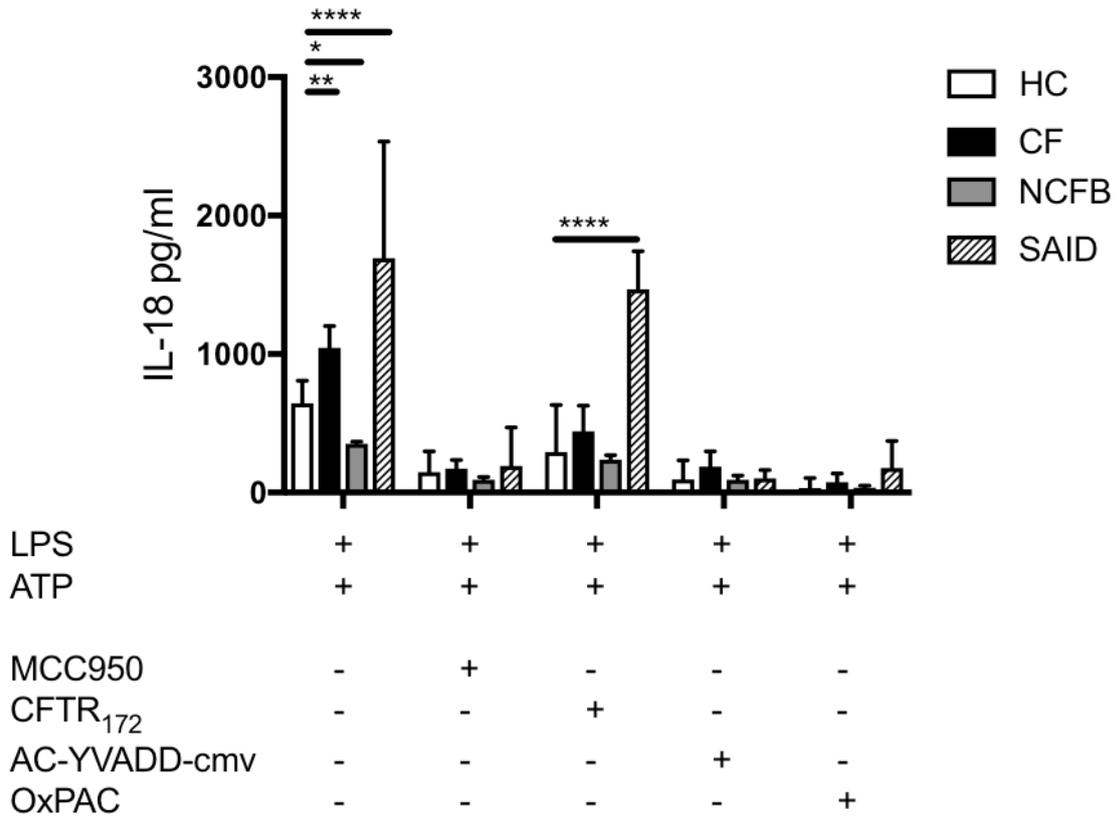
(Figure 3.4.2.2 legend on next page)

Figure 3.4.2.2: *in vitro* IL-18 secretion from NLRP3 inflammasome activation in primary monocytes. ELISA assays were used to detect IL-18 from supernatants of primary monocytes using ATP or ouabain (HC n=6; CF n=6; NCFB n=4; SAID n=4). Cells were stimulated with LPS (10ng/mL, 4 hours) before being stimulated for 30 minutes with ATP (5mM, 30 mins) or Ouabain (100nM, 24 hours). The following inhibitors were pre-treated, before NLRP3 inflammasome activation: MCC950 (15nM, 1 hour), $CFTR_{172}$ (10μg/mL, 1 hour), AC-YVADD-cmv (2μg/mL, 1 hour) and OxPAC (30μg/mL, 1 hour). A repeated measures 2-way ANOVA statistical test was performed with Turkey's multiple comparisons test (p values * = ≤0.05, **= ≤0.01, ***= ≤0.001 and ****= ≤0.0001).

(Figure 3.4.2.3 legend on next page)

Figure 3.4.2.3: *in vitro* **IL-1β secretion from NLRP3 inflammasome activation in primary monocytes.** ELISA assays were used to detect IL-1β from supernatants of primary monocytes using ATP or ouabain (HC n=6; CF n=6; NCFB n=4; SAID n=4). Cells were stimulated with LPS (10ng/mL, 4 hours) before being stimulated for 30 minutes with ATP (5mM, 30 mins) or Ouabain (100nM, 24 hours). The following inhibitors were pre-treated, before NLRP3 inflammasome activation: MCC950 (15nM, 1 hour), $CFTR_{172}$ (10μg/mL, 1 hour), AC-YVADD-cmv (2μg/mL, 1 hour) and OxPAC (30μg/mL, 1 hour). A repeated measures 2-way ANOVA statistical test was performed with Turkey's multiple comparisons test (p values * = ≤0.05, **= ≤0.01, ***= ≤0.001 and ****= ≤0.0001).

Similar observations were made when the same experiments were carried out in primary monocytes from HC individuals and patients with CF, NCFB and SAID. In terms of IL-18 secretion, monocytes from patients with CF secreted significantly increased amounts of IL-18 cytokine compared to HC and NCFB controls. Monocytes from patients with SAID secreted large amounts of IL-18 upon stimulation with either ATP or ouabain, approximately twice the amount compared to that of HC. Again, all four small molecule inhibitors were able to supress IL-18 secretion in all patient cohorts. However, $CFTR_{172}$ inhibition was not as effective in this regard, notably with monocytes from patients with SAID. IL-1β secretion was elevated in patients with CF and, to a greater extent, in SAID, compared to HC and NCFB control cohorts. All four inhibitors potently inhibited IL-1β secretion to the very lower limits of detection for this assay.

3.4.3 in vitro extracellular ASC speck release

ASC is an integral constituent of many inflammasomes, linking the NLRs with caspase-1. All of the inflammasomes in this study utilise ASC in the process of assembling an inflammasome complex. However, based on the above data indicating that the NLRP3 inflammasome was significantly activated in CF, only NLRP3 was pursued further in this study. ASC specks (section 3.1.5) are released from the cell post-inflammasome activation, particularly under chronic or strong NLRP3 stimulation or with a lack of resolution signals. The following data show the detection of extracellular ASC specks, using a flow cytometry-based assay (section 3.2.2) following NLRP3 activation *in vitro* (section 2.4).
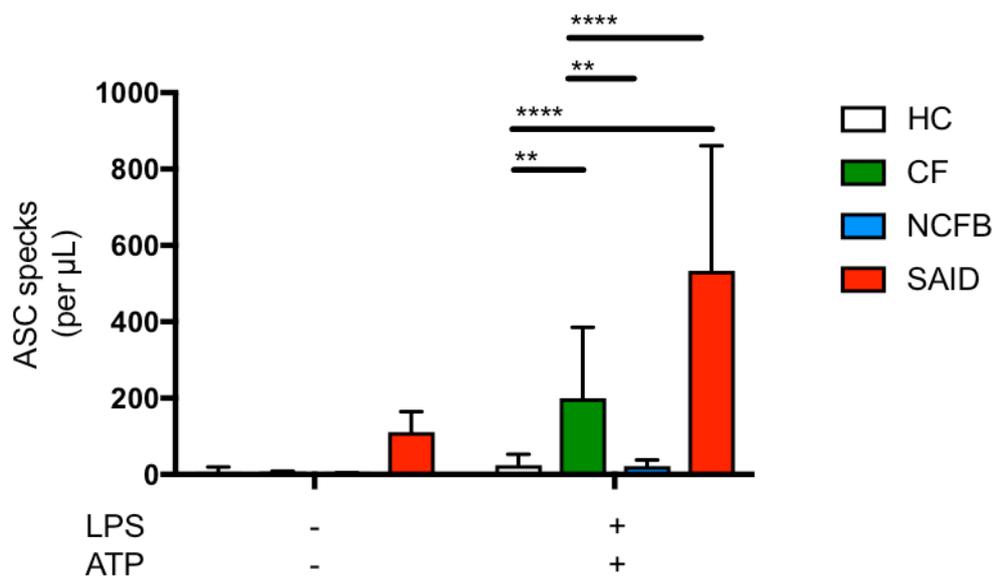
Figure 3.4.3.1: Extracellular ASC specks in *in vitro* monocyte supernatants. Flow cytometry was used to detect ASC specks in supernatant of primary monocytes from individuals with CF, NCFB, SAID and HCs (HC n=6, CF n=6, SAID n=6, NCFB=4). Cells were stimulated with LPS (10ng/mL, 4 hours) before being stimulated for 30 minutes with ATP (5mM, 30 mins). A repeated measures 2-way ANOVA statistical test was performed with Turkey's multiple comparisons test (p values * = ≤0.05, **= ≤0.01, ***= ≤0.001 and ****= ≤0.0001).

It was particularly noticeable that extracellular ASC specks were observed in unstimulated monocyte supernatants from patients with SAID. Upon NLRP3 stimulation, the number of extracellular ASC specks, in monocytes from patients with SAID, increased around five-fold. Extracellular ASC specks were also detected in monocytes from HC individuals and patients with NCFB after stimulation with ATP. In concordance with IL-18 and IL-1β secretion, significantly elevated extracellular ASC specks were observed in stimulated CF monocyte supernatant, but significantly less than that of SAID monocytes.

3.4.4 in vitro Caspase-1 activity

Caspase-1 is the active zymogen component of any inflammasome, driving GSDMD, pro-IL-1β and pro-IL-18 cleavage and activation, and is ultimately the limiting factor for IL-1β and IL-18 secretion. To measure caspase-1 activity, lysates from both HBEC lines and monocytes were used in a colorimetric enzyme activity assay. Increased caspase-1 activity was detected in all cohorts and cell types after NLRP3 stimulation with ATP or ouabain. This was enhanced in cells from patients with CF and SAID, compared to HC and NCFB controls. Again, the caspase-1 activity of a sample corroborated the corresponding pyrogen secretion and ASC speck release, from the aforementioned sample. The small molecule NLRP3 inhibitor, MCC950 potently inhibited caspase-1 activity in all LPS/ATP and LPS/ouabain stimulated samples and across all cohorts.
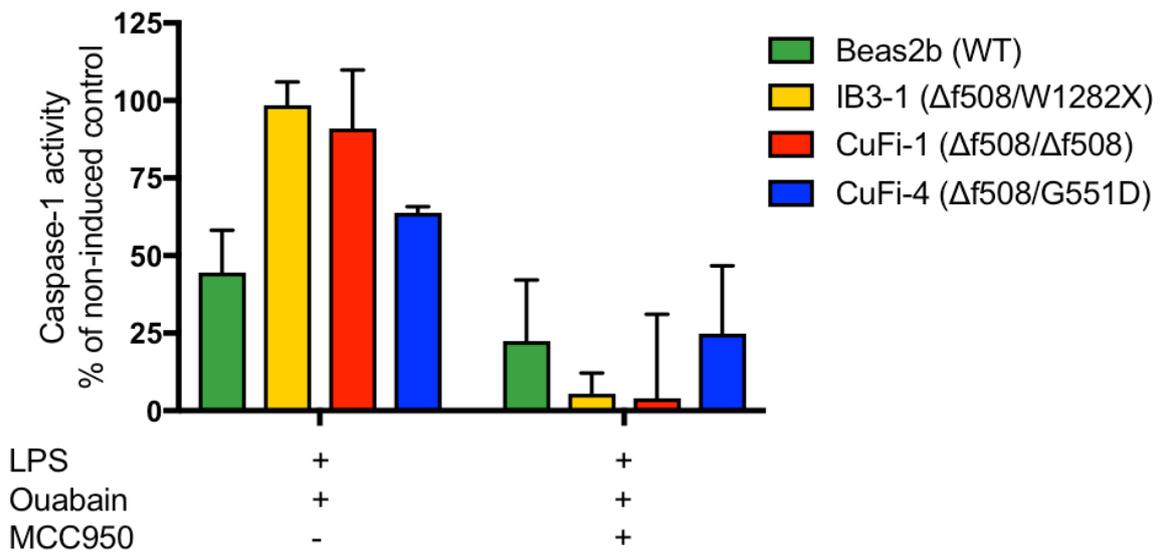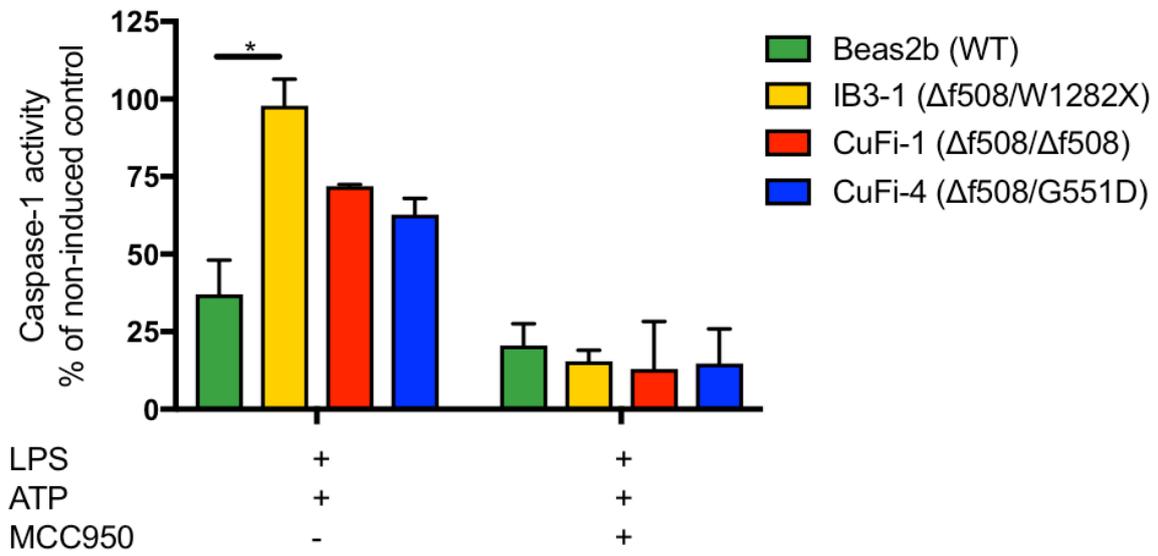
(Figure 3.4.4 legend on next page)
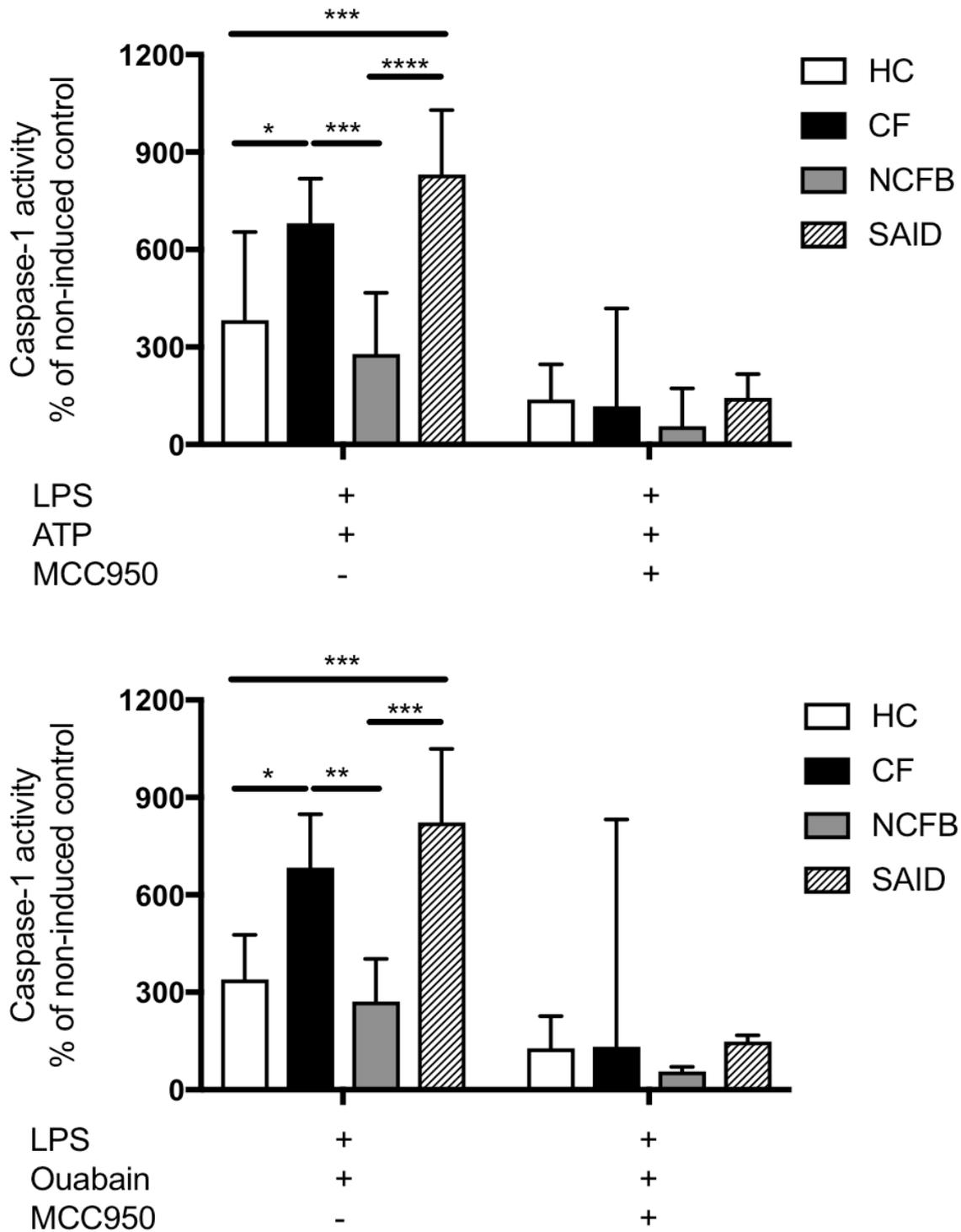
Figure 3.4.4: Caspase-1 activity in HBEC lines and monocytes. A colorimetric assay to determine caspase-1 activity via cleavage of a caspase-specific peptide conjugated to a colour reporter molecule p-nitroalinine (pNA). The assay was performed in protein lysates from primary monocytes from individuals with CF, NCFB, SAID and HCs (HC n=10, CF n=10,

SAID n=4, NCFB=4) and HBEC lines (n=3). Cells were stimulated with LPS (10ng/mL, 4 hours) before being stimulated for 30 minutes with ATP (5mM, 30 mins). A pre-treatment of MCC950 (15nM, 1 hour) was used before NLRP3 inflammasome activation. A repeated measures 2-way ANOVA statistical test was performed with Turkey's multiple comparisons test (p values * = ≤0.05, **= ≤0.01, ***= ≤0.001 and ****= ≤0.0001).

3.4.5 In vitro Pyroptosis

In order to quantify pyroptosis and discriminate it from other forms of cell death, lactose dehydrogenase (LDH) is measured with and without a caspase-1 inhibitor. LDH is released from a necrotic cell, which provides a distinguishing factor between necrosis and programmed cell death, such as apoptosis where LDH is contained within the apoptotic vesicles, or blebs. To further distinguish pyroptosis from necrosis, a caspase-1 inhibitor is used in a control sample to prevent pyroptosis. Any LDH that is detected in the presence of the caspase-1 inhibitor is then termed necrosis and is taken away from the LDH release from the experimental sample, without a caspase-1 inhibitor pre-treatment. The remaining LDH level is presented as caspase-1-dependent pyroptosis, calculated as a percentage of complete necrotic cell death using lysis buffer and water controls.

Upon stimulation with LPS and ATP, increased pyroptosis is observed in WT HBECs, with the majority of necrotic cell death measured by LDH release being caspase-1 dependent and therefore pyroptosis. HBECs harbouring CF-associated mutations had increased pyroptotic activity with the IB3-1 (Δf508/W1282X) cell line significantly increased compared to Beas-2b (WT). Monocytes from HC individuals and patients with NCFB also presented with pyroptotic cell death upon NLRP3 inflammasome activation, but with a greater level of caspase-1 independent necrosis in this cell type. The increase in pyroptosis was augmented in cells from

patients with CF and SAID, with the level of caspase-1 independent necrosis being elevated further in SAID monocytes compared to CF monocytes.
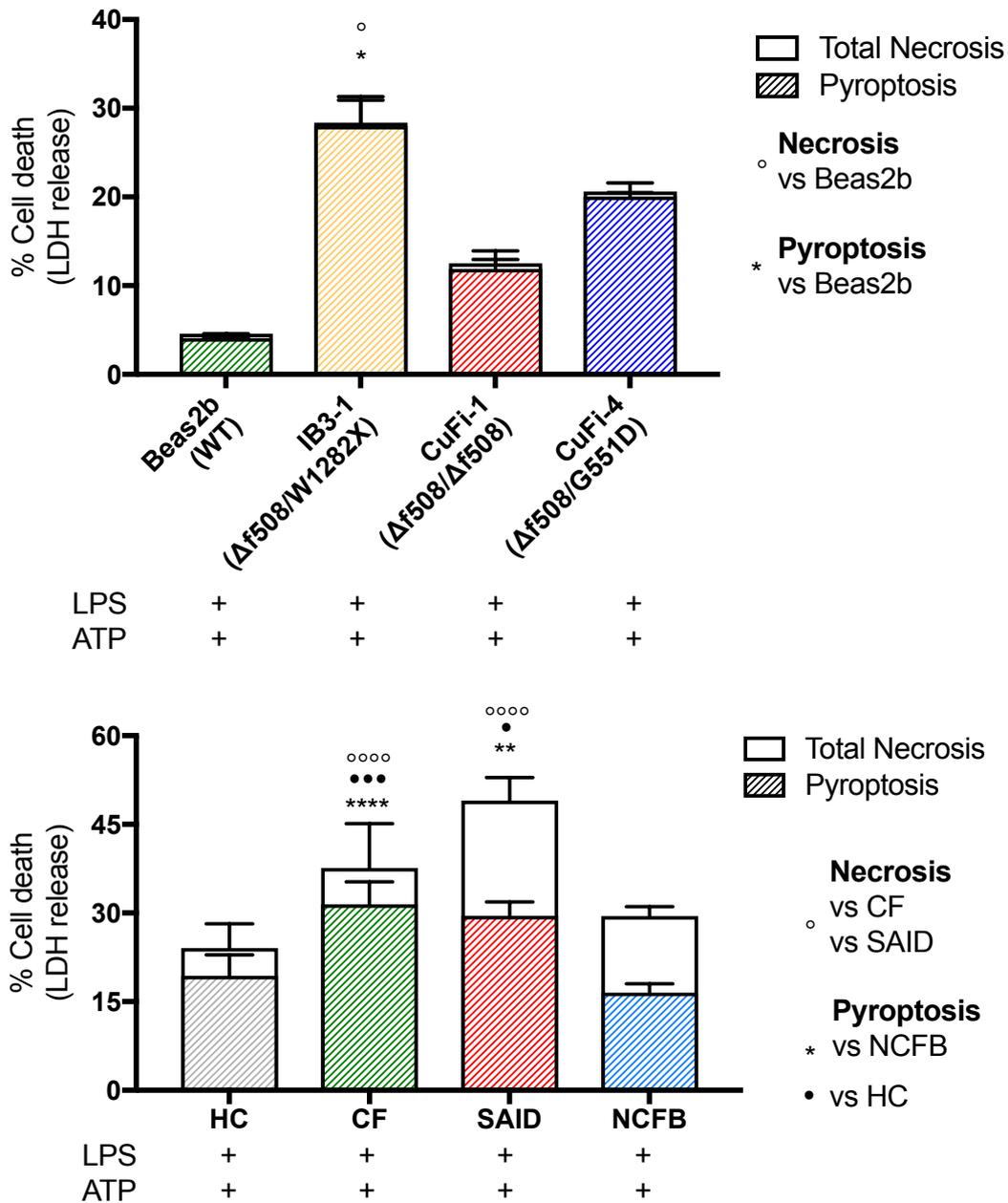
Figure 3.4.5: Pyroptosis after NLRP3 inflammasome activation in HBEC lines and primary monocytes. The figure displays necrosis and pyroptosis as superimposed bar charts, representing the percentage of total necrosis that is caspase-1 dependent, or pyroptosis. Pyroptotic cell death was calculated by measuring total necrosis via the presence of lactose dehydrogenase (LDH) from cell culture samples in a 96-well plate, colorimetric assay. Each

sample/condition was repeated in parallel with a caspase-1 inhibitor (AC-YVADD-cmv (2μg/mL, 1 hour)) pre-treatment. The total necrosis level was then taken away from the capase-1 inhibited sample, or 'caspase-1 independent' necrosis, with the remaining LDH level termed 'caspase-1 dependent necrosis' or pyroptosis. The assay was performed with primary monocytes from individuals with CF, NCFB, SAID and HCs (HC n=10, CF n=10, SAID n=4, NCFB=4) and HBEC lines (n=3). Cells were stimulated with LPS (10ng/mL, 4 hours), followed by ATP (5mM, 30 minutes). A repeated measures 2-way ANOVA statistical test was performed with Turkey's multiple comparisons test (p values •, o, * = ≤0.05, ••, o o ,**= ≤0.01, •••, o o o ,***= ≤0.001 and ••••, o o o o, ****= ≤0.0001).

3.5 Monocyte and macrophage phenotypes in CF

3.5.1 M1 and M2 macrophage polarisation

To determine if elevated IL-1β and IL-18 levels correlate with a sustained, chronic inflammatory response, as seen in CF, the capacity of human CF monocytes to differentiate into M1-type and M2-type macrophages was analysed. M1-type macrophages are considered to have a proinflammatory role in peripheral tissues and are characterised by an inherent ability to produce proinflammatory IL-6 and TNF cytokines, whilst M2-type macrophages are archetypically associated with production of the anti-inflammatory cytokine, IL-10. Peripheral monocytes were differentiated and activated into either M1-type or M2-type macrophages. Macrophage cell surface markers and intracellular cytokines were measured, using flow cytometry and ELISA and characterised, as described in section 3.2.3 and Figure 3.5.1.1, with details of the gating in appendix figure 3.
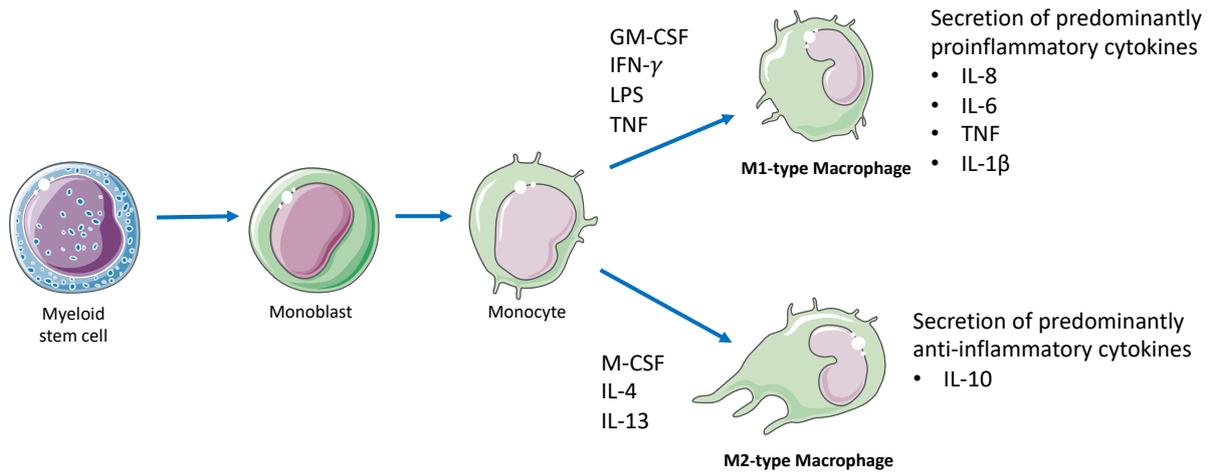
Figure 3.5.1.1: Monocyte to macrophage *in vitro* polarisation. Surface markers for M1-type (CD14+ CD16+ HLA-DR+ CD274+ CD86+) and M2-type (CD14+ CD16+ CD206+) were analysed using flow cytometry. M1-type macrophage activation was achieved by supplementing growth media with 100ng/mL human IFN-γ, 100ng/mL TNF and 50ng/mL LPS. M2-type macrophage activation was achieved by supplementing growth media with 20ng/mL IL-13 and 20ng/mL IL-4. M1 macrophages display a rounded morphology, whilst M2 macrophages display a tortuous, dendritic morphology (appendix figure 4).
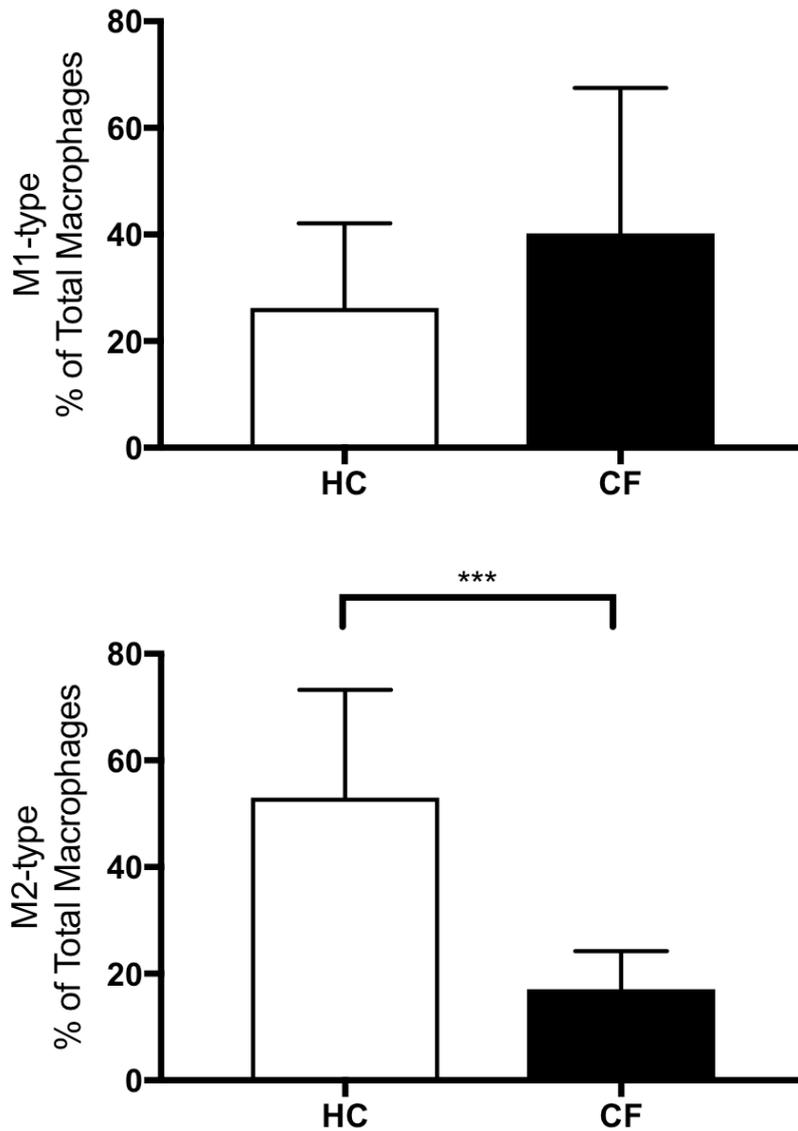
Figure 3.5.1.2: M1/M2-type macrophage polarisation. Monocytes from whole blood were differentiated into macrophages and characterised as M1-type (markers- CD14$^+$ CD16$^+$ HLA-DR$^+$ CD274$^+$ CD86$^+$ TNF^{HI}) or M2-type (markers- CD14$^+$ CD16$^+$ CD206$^+$ IL-10^{HI}). Numbers of polarised macrophages are presented as percentage of total macrophages in samples (n=7). The Mann-Whitney non-parametric test was performed (p values * = ≤0.05, **= ≤0.01, ***= ≤0.001 and ****= ≤0.0001).

Following *ex vivo* monocyte differentiation, we observed no significant difference in M1-type macrophages, although there is an elevated proportion of M1-type macrophages in patients with CF, compared to HCs. There was a significantly decreased number of M2-type macrophages from patients with CF compared to HC macrophages. Furthermore, these changes were associated with significantly increased production of IL-6 by M1-type macrophages, originating from CF patients, and also reduced IL-10 release by CF-derived M2-type macrophages compared to HC.
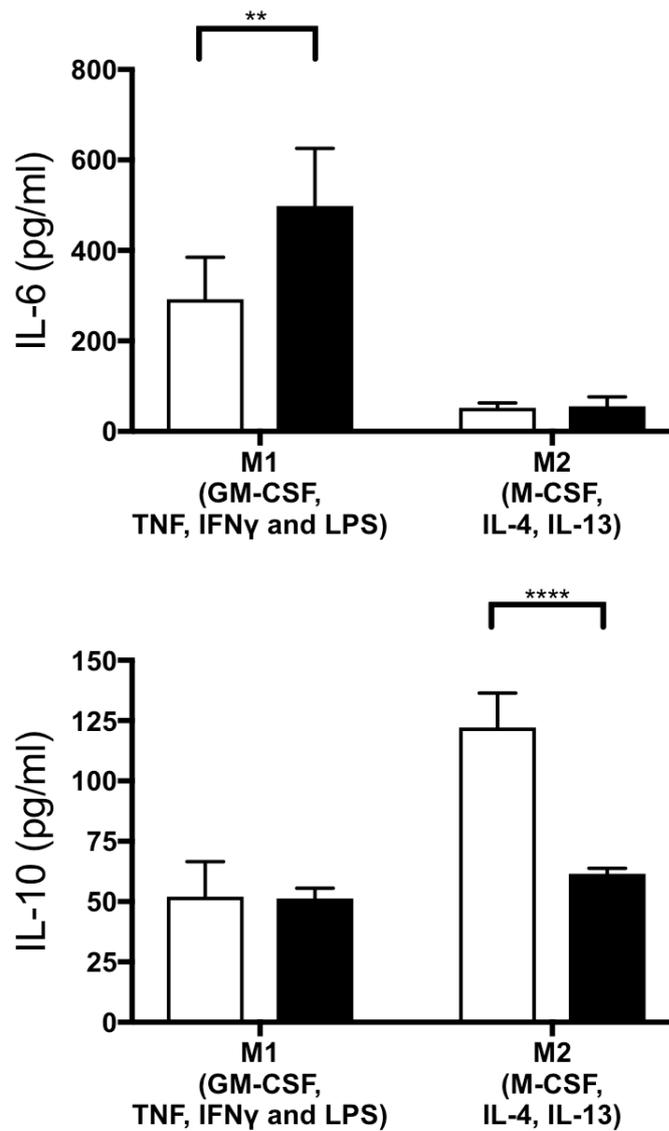
(Figure 3.5.1.3 legend on next page)

Figure 3.5.1.3: M1/M2 macrophage cytokine secretion. IL-6 and IL-10 levels were measured by ELISA from macrophage supernatant (n=7). A repeated measures 2-way ANOVA statistical test was performed with Turkey's multiple comparisons test (p values * = ≤0.05, **= ≤0.01, ***= ≤0.001 and ****= ≤0.0001).

3.5.2 Monocyte populations

In addition to the above differences in M1-type and M2-type macrophage phenotype, there was some expansion of peripheral monocytes of intermediate and non-classical phenotype, known to be associated with other chronic inflammatory conditions, such as atherosclerosis and rheumatoid arthritis, and a related significant decrease in numbers of classical monocytes. Details of the gating in appendix figure 3.
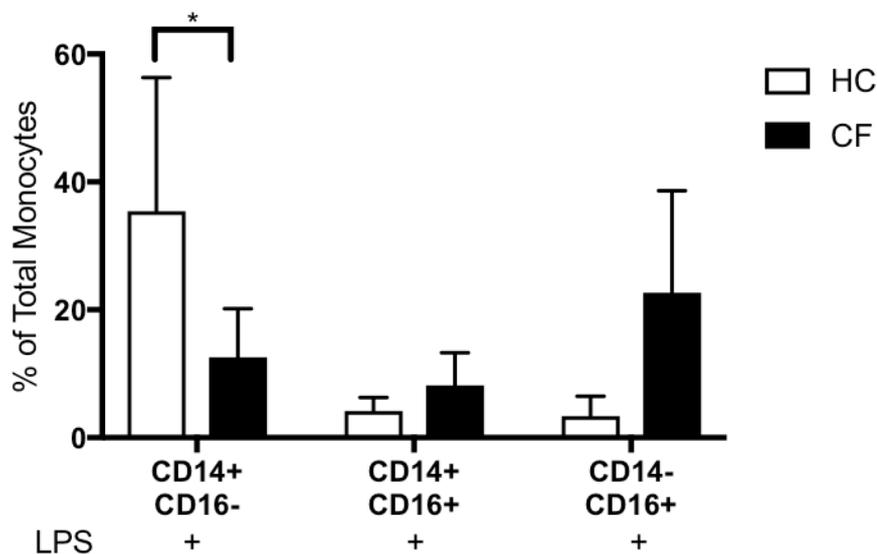
Figure 3.5.2.1: Peripheral monocyte populations. Monocytes were gated on based on forward and side scatter and then based on CD14 and CD16 expression as follows: classical (CD14++CD16−), non-classical (CD14dimCD16++), and intermediate (CD14++CD16+). Cells were stimulated with LPS (10ng/mL, 4 hours). The Mann-Whitney non-parametric test was performed (p values * = ≤0.05, **= ≤0.01, ***= ≤0.001 and ****= ≤0.0001).

3.6 Hypoxia

Hypoxia was included as an experimental condition in this study as the lower lung is often observed as being hypoxic due to mucous plugging, with anaerobic P. aeruginosa present in the CF lung (Hassett et al., 2009, Legendre et al., 2011, Fritzsching et al., 2015, Montgomery et al., 2017). Under hypoxic conditions all HBEC lines secreted significantly increased IL-18, despite the absence of stimulation with LPS or ATP. Upon stimulation with LPS and ATP under hypoxic conditions, all HBEC lines secreted significantly increased IL-18 compared to the same stimulation at normoxia. Notably the HBEC lines, with CF-associated mutations, had significantly increased IL-18 secretion in normoxia and hypoxia compared to WT Beas-2b HBEC lines under the same conditions and stimulations; however, IL-18 secretion was around 2-fold in all cell lines and MCC950 blocked all IL-18 secretion under both normoxic and hypoxic conditions.

Similar observations were made with IL-18 and IL-1β, using monocytes from HC and CF cohorts, with significantly higher amounts of both cytokines being secreted by CF monocytes, and this being exacerbated around 2-fold under hypoxic conditions. Notably, HC monocytes did not increase IL-18 secretion under hypoxia after stimulation compared to the same stimulations at normoxia.
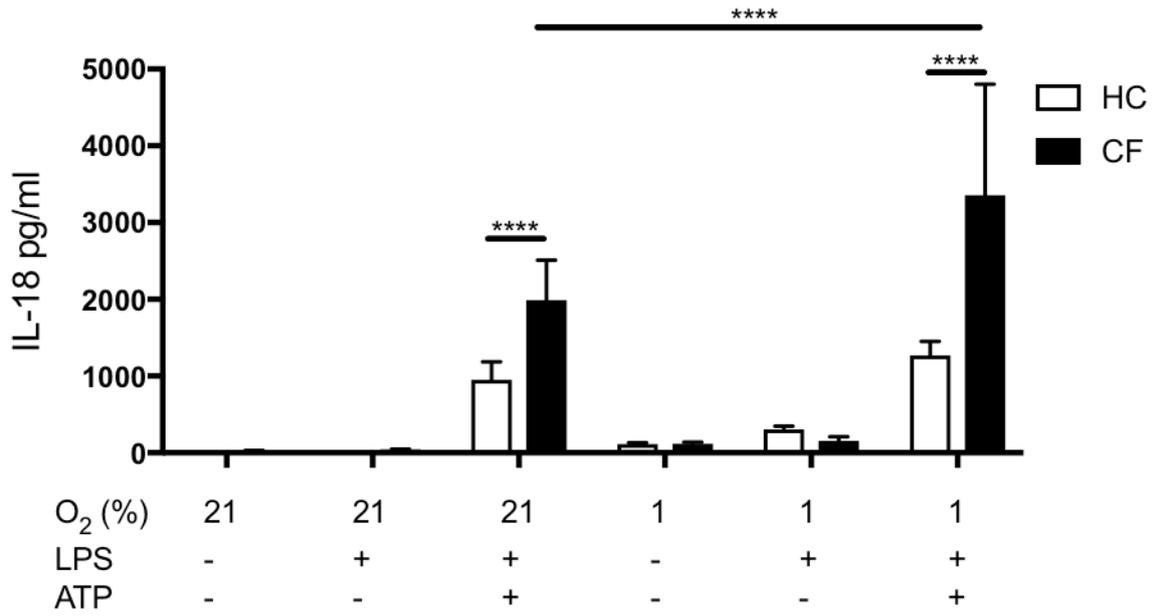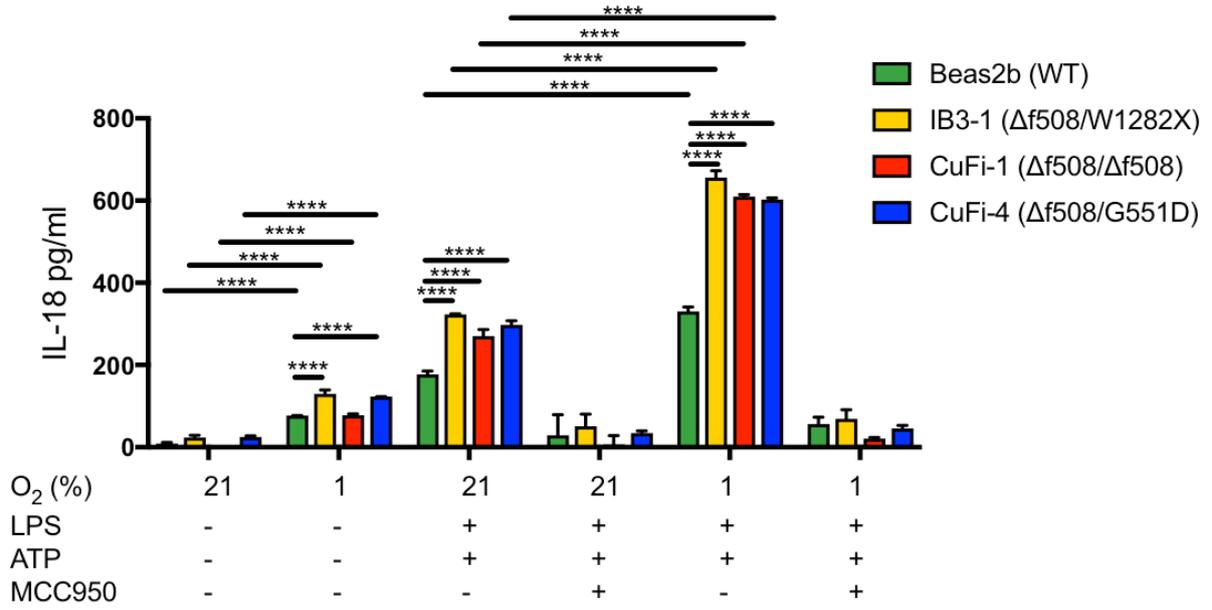
(Figure 3.6.1 legend on next page)
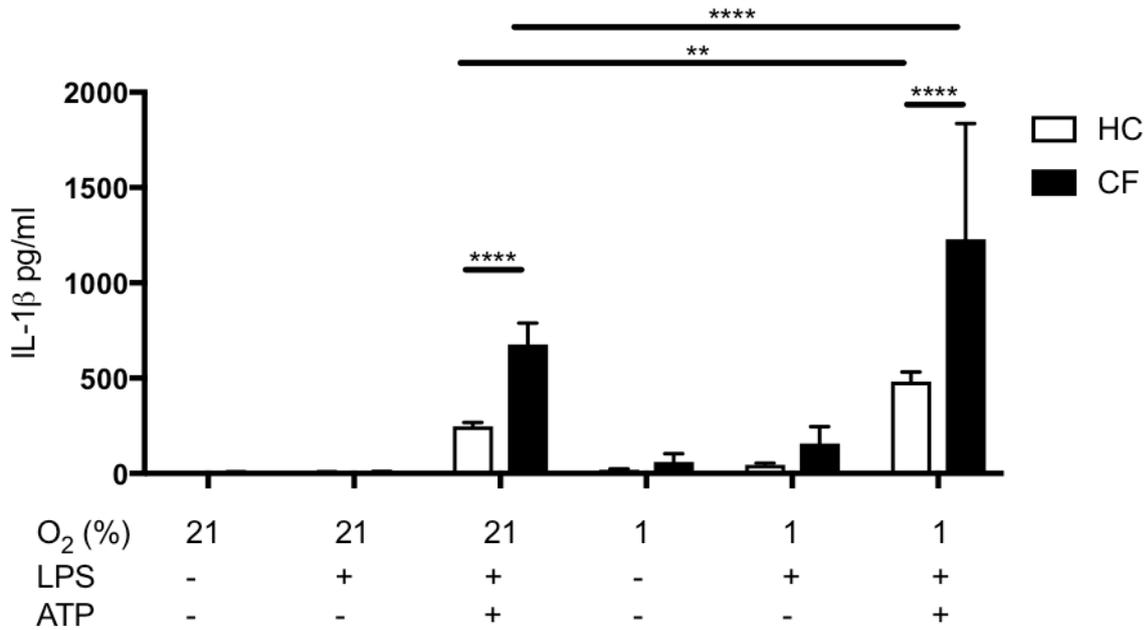
Figure 3.6.1: *in vitro* **IL-1β and IL-18 secretion in HBEC lines and primary monocytes**

under either normoxic or hypoxic conditions. ELISA assays were used to detect IL-1β and

IL-18 from supernatants of primary monocytes (HC n=6; CF n=6) and HBEC lines (n=3). Cells

were cultured overnight in the Don Whitley H35 Hypoxystation at 1% O_2 for hypoxic

conditions and at 21% O_2 5% CO_2 in a SANYO MC0 20A1C incubator for normoxia. After

the overnight incubation, cells were stimulated with LPS (10ng/mL) for 4 hours before being

stimulated for 30 minutes with ATP (5mM). A repeated measures 2-way ANOVA statistical

test was performed with Turkey's multiple comparisons test (p values * = ≤0.05, **= ≤0.01,

= ≤0.001 and *= ≤0.0001).

TNF was also measured in the same supernatants. Interestingly, no elevation in TNF

secretion was observed under hypoxia in any of the HBEC lines. However, CF monocytes

increased TNF secretion by around 2-fold under hypoxic conditions compared to normoxia

with the same stimulations, whereas HC monocytes did not, with no significant difference

observed between normoxia and hypoxia as with the HBEC lines. MCC950 did not inhibit

TNF secretion.
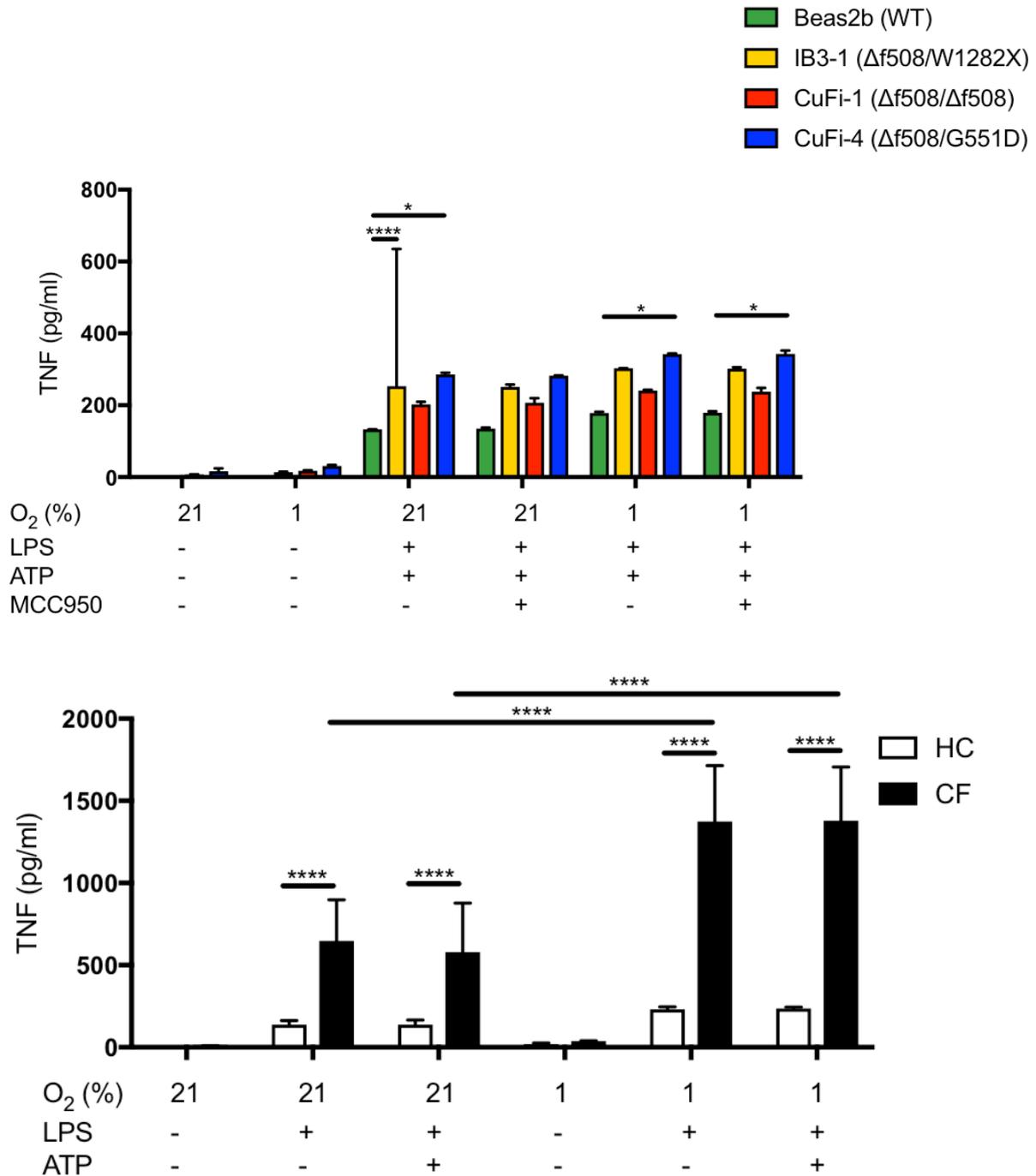
Figure 3.6.2: *In vitro* TNF secretion from in HBEC lines and primary monocytes in either normoxic or hypoxic conditions. ELISA assay was used to detect TNF from supernatants of primary monocytes (HC n=6; CF n=6) and HBEC lines (n=3). Cells were cultured overnight in the Don Whitley H35 Hypoxystation at 1% O_2 for hypoxic conditions and at 21% O_2 5% CO_2 in a SANYO MC0 20A1C incubator for normoxia. After the overnight incubation, cells were stimulated with LPS (10ng/mL) for 4 hours before being stimulated for 30 minutes with

ATP (5mM). A repeated measures 2-way ANOVA statistical test was performed with Turkey's multiple comparisons test (p values * = ≤0.05, **= ≤0.01, ***= ≤0.001 and ****= ≤0.0001).

3.7 Modulation of IFNγ responses by NLRP3 activation
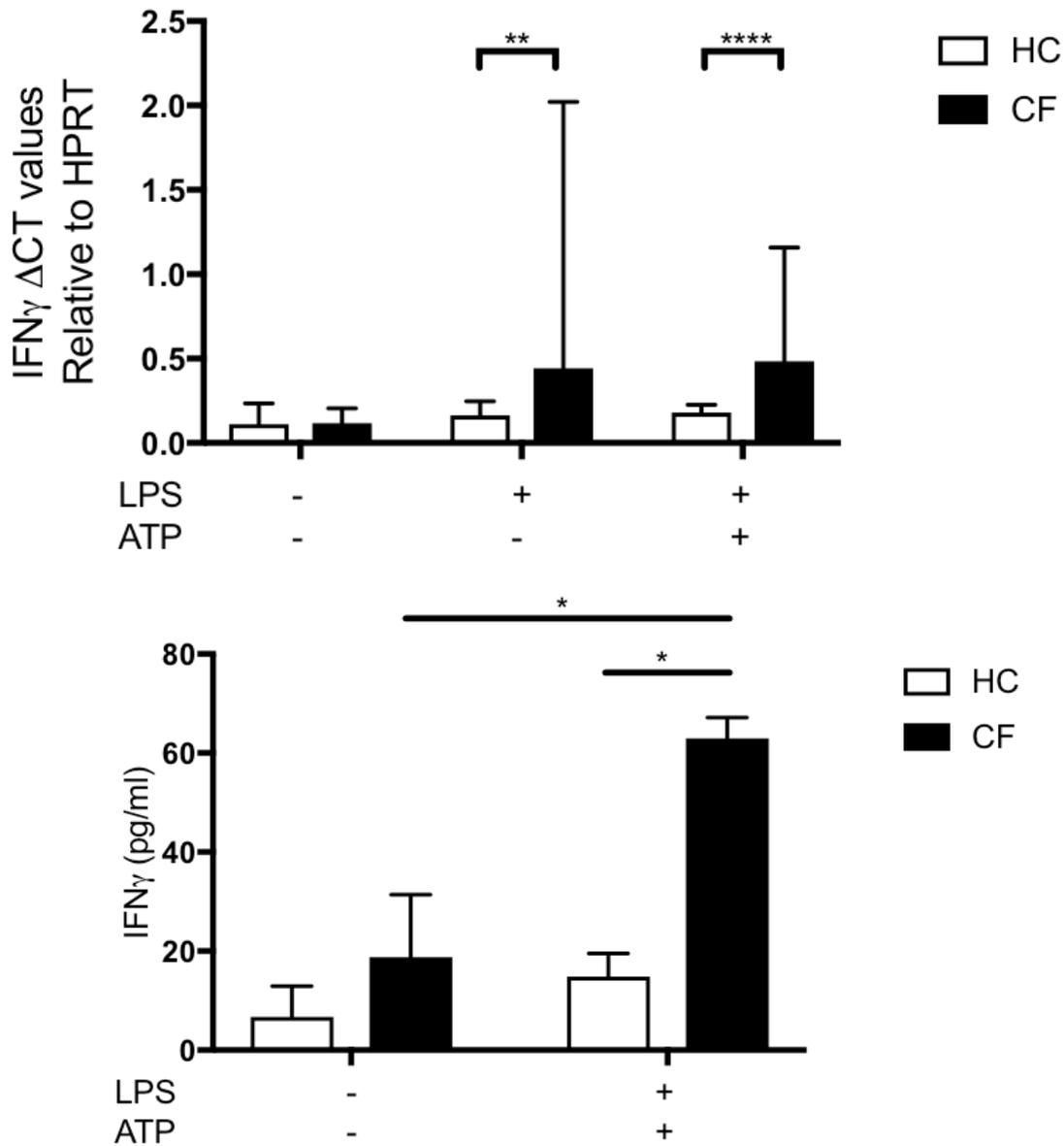
Figure 3.7.1.1: *IFNγ gene expression and secretion in peripheral blood mononuclear cells.* Taqman® RT-qPCR was used to measure *IFNγ* gene expression and Luminex was used to measure IFNγ secretion from peripheral blood mononuclear cells (PBMC) populations from

HCs and patients with CF-associated mutations (n=10). Cell stimulation was as follows: LPS (10ng/mL) 4-hours with an ATP (5mM) stimulation for the final 30 minutes. A repeated measures 2-way ANOVA statistical test was performed with Turkey's multiple comparisons test (p values $* = \leq0.05$, $** = \leq0.01$, $*** = \leq0.001$ and $**** = \leq0.0001$).

In order to understand the consequences of elevated IL-1β and IL-18 on the adaptive immune system, PBMCs were stimulated with LPS and ATP in order to activate the NLRP3 inflammasome within monocytes. Monocytes express TLR4/2, which detect LPS. It has been previously described that IL-18 and IL-1β are able to activate and cause proliferation and activation of natural killer (NK) cells, T-helper 1 (T$_H$1) and T$_H$17 cells. The hypothesis of this experiment is that the subsequent IL-18 and IL-1β secreted by the activated monocytes within the PBMC population, will then activate NK cells. *IFNγ* gene expression and secretion were measured in LPS/ATP stimulated PBMCs to detect activated NK cells. Post-NLRP3 inflammasome activation, *IFNγ* gene expression and secretion in PBMCs were significantly increased in the PBMCs from patients with CF.

3.8 Ionic fluxes

3.8.1 Sodium flux

Having established that the priming and activation of the NLRP3 inflammasome is exacerbated and hyper-responsive in HBECs and monocytes with CF-associated mutations through stimulation with LPS and ATP or ouabain, it was important to establish the precise mechanism behind this exaggerated response. NLRP3 was of interest, primarily due to its known activating event being K$^+$ efflux in combination with the primary CF-causing mutation

being within an ion channel. Investigating ion channel flux and intracellular ion concentration was carried out by using fluorescent molecular probes, which bind to free, intracellular Na^+ and K^+ ions. Cells were cultured in 96-well plates and stimulated, as in previous experiments, for NLRP3 inflammasome activation, but with the addition of pre-treatments of key ion channel inhibitors in order to elucidate changes in intracellular ion concentration and NLRP3 inflammasome activation. The hypotheses in these experiments are centred around the relationship between Na^+ and K^+ ion fluxes. As previously discussed (Section 1.1), Na^+ influx is elevated in many CF genotypes, due to loss of control of ENaC activity owing to loss of functional CFTR surface protein. Dysregulated Na^+ influx will produce various molecular consequences that cells with CF-associated mutations are required to adapt to in order to maintain cellular homeostasis. An important adaptation required to address the restoration of ionic or electrochemical homeostasis is the balance of ionic gradients. Na^+ and K^+ exist as an ionic gradient with a low intracellular Na^+ concentration and a high K^+ intracellular concentration. This gradient is maintained by the Na^+/K^+ ATP-gated channel, which will pump the aforementioned ions across the plasma membrane against the electrochemical gradient; this process requires energy in the form of ATP. With excess Na^+ influx, the natural electrochemical gradient is disturbed, requiring the Na^+/K^+ ATP-gated pump to increase its activity in order to maintain this homeostasis. A consequence of this will be influx of K^+. As K^+ efflux is the common NLRP3 inflammasome activator it is of interest to probe this molecular adaptation, to further understand the role uninhibited Na^+ influx has on the efflux of K^+ upon stimulation.

To understand the extent of Na^+ influx in cells with CF-associated mutations, HBECs and monocytes from HC individuals and patients with CF were stimulated with amiloride, a potent Na^+ channel inhibitor. When cells from all cohorts are treated with amiloride, the intracellular Na^+ concentration is significantly reduced. Notably, the increase in intracellular

Na$^+$ concentration after ATP stimulation was significantly higher in both HBECs and monocytes, possessing CF-associated mutations, compared with their WT equivalents. A significant decrease in Na$^+$ concentration also occurred in response to pre-treatment with EIPA and the SPLUNC1-derived peptide S18, to a similar extent to that seen with amiloride across both cell types and WT or CF. Ouabain increased Na$^+$ concentration within the cells as expected. Due to the nature of the assay, changes in intracellular ion concentrations from baseline or untreated control samples, basal levels of intracellular Na$^+$ or K$^+$ concentration cannot be compared across cell line or patients with confidence, as the quantification is arbitrary.
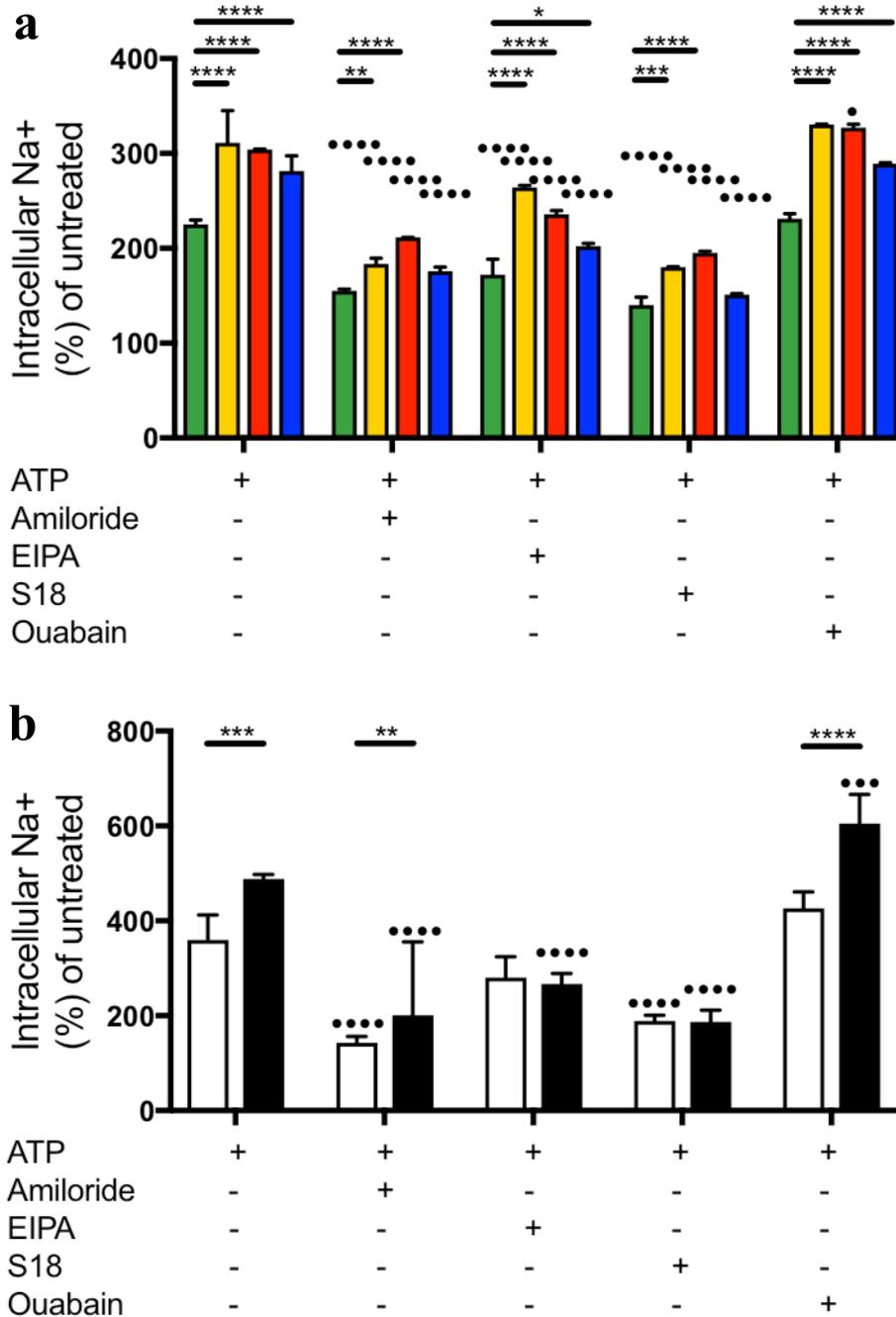
Figure 3.8.1.1: Intracellular Na⁺ flux in HBEC lines and primary monocytes. Intracellular

Na⁺ was detected using an AM ester of sodium indictor SBFI (S-1263); changes in fluorescence

were measured by fluorimeter post-stimulation in monocytes from patients with CF (a) (n=7)

as well as HBECs (b) (n=3). Cell stimulation was as follows: amiloride (100mM, 1hour), EIPA

(10μM, 1 hour), S18 derived peptide (25μM, 4 hours) and ouabain (100nM, 24 hours) were

pre-treated before a stimulation with LPS (10ng/mL) for 4-hours with an ATP (5mM)

stimulation for the final 30 minutes. A repeated measures 2-way ANOVA statistical test was performed with Turkey's multiple comparisons test (p values •, * = ≤0.05, ••, **= ≤0.01, •••, ***= ≤0.001 and ••••, ****= ≤0.0001) where the symbol • refers to the relevant level of significance between the indicated bar with that of the ATP alone stimulation for that bar's cohort.

3.8.2 Potassium flux

Stimulation of both HBECs and monocytes with ATP will activate and open the P2X7 purinoceptor. This is observed in Figure 3.8.2.1, with a 60% decrease in intracellular K^+ concentration after stimulation. Interestingly, this efflux of K^+ is greater in HBECs with CF-associated mutations. Whether the amount of K^+ efflux corresponds with the level of NLRP3 activation and thus IL-1β and IL-18 secretion is not clear, but in these experiments the two observations seem to be strongly associated. A similar interpretation is made with monocyte stimulations, with greater ATP-driven K^+ efflux in monocytes from patients with CF. When amiloride or the SPLUNC1-derived S18 peptide was used to inhibit ENaC Na^+ influx, a notable reduction in K^+ efflux was observed, indicating a relationship between amiloride-sensitive Na^+ influx and ATP-dependent K^+ efflux. The EIPA pre-treatment, which targeted all Na^+ channels except for ENaC, where its inhibition is minimal, did not significantly modulate K^+ efflux upon stimulation, compared to cells with no pre-treatment with ion channel inhibition. Ouabain increased K^+ efflux within the cells, as expected.
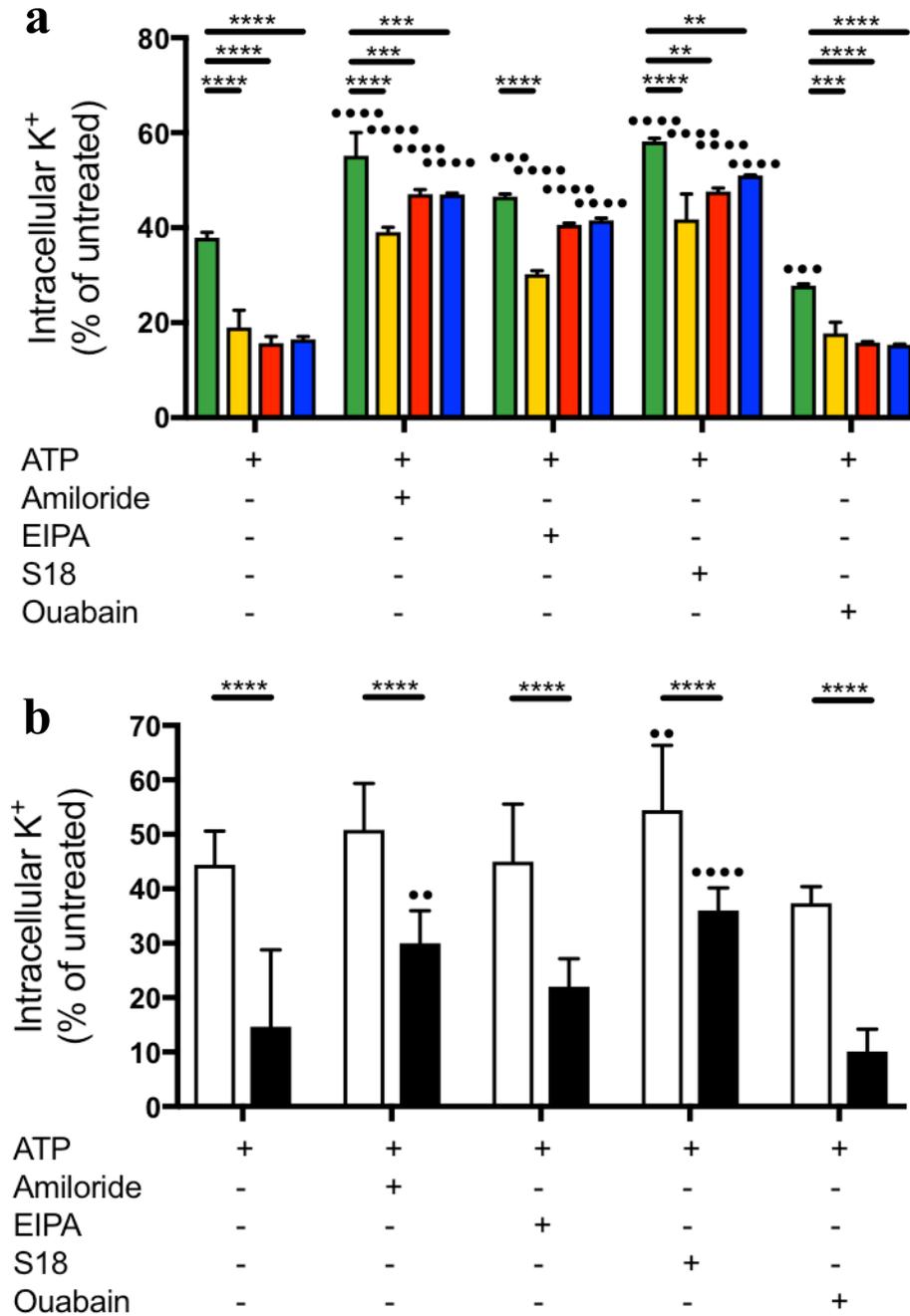
Figure 3.8.2.1: Intracellular K$^+$ flux in HBEC lines and primary monocytes. Intracellular

K$^+$ was detected using an AM ester of potassium indictor PBFI (P-1266); changes in

fluorescence were measured by fluorimeter post-stimulation in monocytes from patients with

CF (a) (n=7) as well as HBECs (b) (n=3). Cell stimulation was as follows: amiloride (100mM,

1hour), EIPA (10µM, 1 hour), S18 derived peptide (25µM, 4 hours) and ouabain (100nM, 24

hours) were pre-treated before a stimulation with LPS (10ng/mL) for 4-hours with an ATP

(5mM) stimulation for the final 30 minutes. A repeated measures 2-way ANOVA statistical test was performed with Turkey's multiple comparisons test (p values •, * = ≤0.05, ••, **= ≤0.01, •••, ***= ≤0.001 and ••••, ****= ≤0.0001) where the symbol • refers to the relevant level of significance between the indicated bar with that of the ATP alone stimulation for that bar's cohort.

3.9 Effects of ion channel inhibition on NLRP3 inflammasome activation

3.9.1 Sodium Channel inhibition

In order to study whether Na^+ influx predisposes K^+ efflux upon ATP stimulation in the context of inflammation, in particular NLRP3 activation, cytokine secretion, caspase-1 activity and pyroptosis were all measured in the presence of various channel inhibitors. The hypothesis that Na^+ flux modulates K^+ flux and, therefore, NLRP3 inflammasome has been previously tested (Munoz-Planillo et al., 2013, Yaron et al., 2015); however, in this study the hypothesis was tested in the context of a channelopathy (CF) wherein ENaC-driven Na^+ influx is pathologically overactive. The following data describe how these ion channel inhibitors modulate NLRP3 inflammasome activation upstream, in cells with CF-associated mutations.

To elucidate the role of Na^+ influx in cells with CFTR mutations, selected Na^+ channel inhibitors, with a range of potencies and specificities, were used to better understand which channel activities are pathogenic in CF and how modulating these channels may have anti-inflammatory benefits *in vitro* in terms of NLRP3 inflammasome activation. n-amidino-3,5 diamino-6-chloropyrazine carboxamide (amiloride), 5-(N-Ethyl-N-isopropyl) amiloride (EIPA) and SPLUNC1-peptide 18 (S18) were used to treat cells in order to diminish Na^+ flux in both HBECs and monocytes. Amiloride targets ENaC with high potency, but is nonspecific,

and has been shown to inhibit a variety of other Na$^+$ channels at higher doses. EIPA is a broad-spectrum Na$^+$ channel inhibitor but has poor inhibition of ENaC.
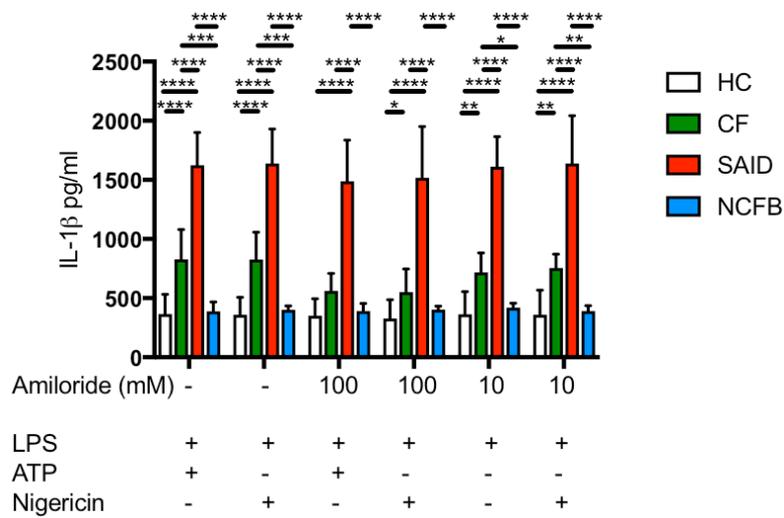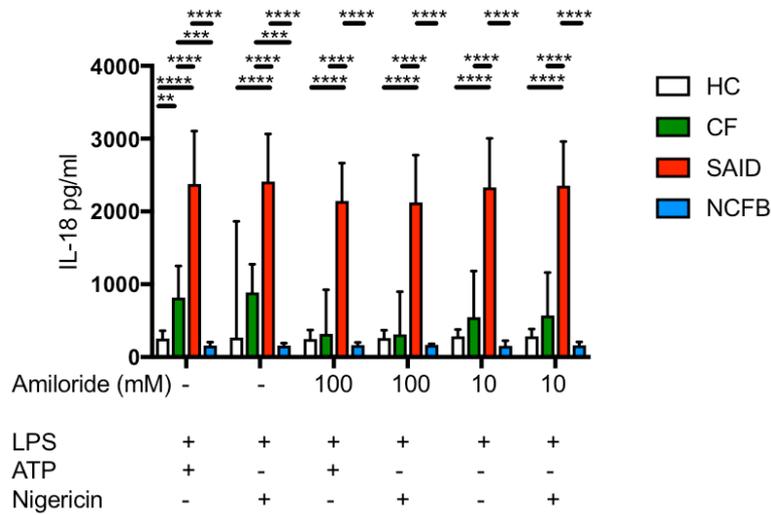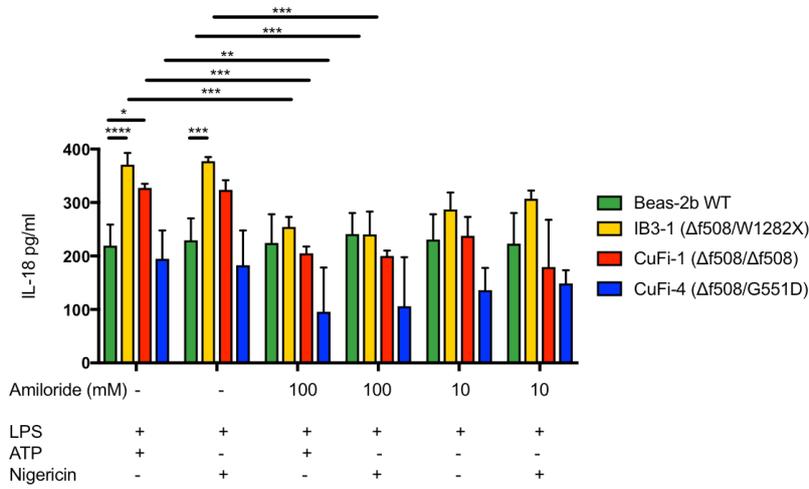
(Figure 3.9.1.1 legend on next page)

Figure 3.9.1.1: The effects of amiloride on cytokine secretion in HBEC lines and primary monocytes. ELISA assays were used to detect IL-18 and IL-1β in monocytes from HC (n=10), patients with CF (n=10), SAID (n=4) and NCFB (n=4) as well as HBECs (n=3). Cell stimulation was as follows: Amiloride (100mM or 10mM, 1hour) was used as a pre-treatment before a stimulation with LPS (10ng/mL) for 4-hours with an ATP (5mM) stimulation for the final 30 minutes. A repeated measures 2-way ANOVA statistical test was performed with Turkey's multiple comparisons test (p values * = ≤0.05, **= ≤0.01, ***= ≤0.001 and ****= ≤0.0001).

Finally, S18 is an experimental compound, kindly gifted by Spyryx Biosciences, Inc ®, which is highly specific for ENaC and has been demonstrated to have no off-target ion channel inhibition. S18 is a compound derived on the endogenous SPLUNC1 protein, described earlier. With the above compounds, the precise contribution of ENaC dependent Na^+ influx on downstream NLRP3 priming and assembly can be assessed. The relationship between Na^+ and K^+ signalling is complex, with several channels with a multitude of activating signals and feedback mechanisms controlling the flux of both ions. The following experiments were designed to elucidate the role of the ENaC Na^+ channel in modulating K^+ and thus NLRP3 inflammasome activation.

In order to activate the NLRP3 inflamamsome, K^+ efflux is required for assembly of the protein complex, decribed previously (Section 1.3). There are multiple molecules that are able to induce a strong enough K^+ efflux for NLRP3 activation (optimised in appendix figure 1). Previously ATP and ouabain were used to this end, however as ouabain is itself an ion channel inhibitor and ATP is capable of opening various ion channels, the pore forming toxin nigericin is used throughout sections 3.9.1-3 to ensure that the effects any ion channel inhibitor has on inflammation are not clouded by off-target ATP activity.

Figure 3.9.1.1 investigates the anti-inflammatory effects of amiloride at two concentrations commonly used in the literature (Rolfe et al., 1992). At 100mM, amiloride inhibited IL-18 secretion in all ATP stimulated HBEC lines with CF-associated mutations, which was statistically significant (Figure 3.9.1.1 A). CuFi-4 (Δf508/G551D) did not produce an increased IL-18 without amiloride pre-treatment. At the lower 10mM concentration, amiloride was unable to effect IL-18 secretion in any HBEC line. Amiloride, at either concentration, did not affect IL-18 secretion in the Beas-2b (WT) HBEC line. Without amiloride, CF and SAID monocytes secreted statistically significant IL-18 and IL-1β levels, upon stimulation with either LPS and ATP or nigericin, compared to HC and NCFB monocytes. When amiloride at 100mM is pre-treated before NLRP3 inflammasome activation, IL-18 and IL-1β secretion is no longer statistically significant compared to HC or NCFB monocytes under the same conditions. This reduction in IL-18 and IL-1β secretion does not occur in SAID, NCFB or HC monocytes, indicating a CF specific phenomenon. At 10mM, amiloride is able to reduce IL-18 but not IL-1β under the same conditions.
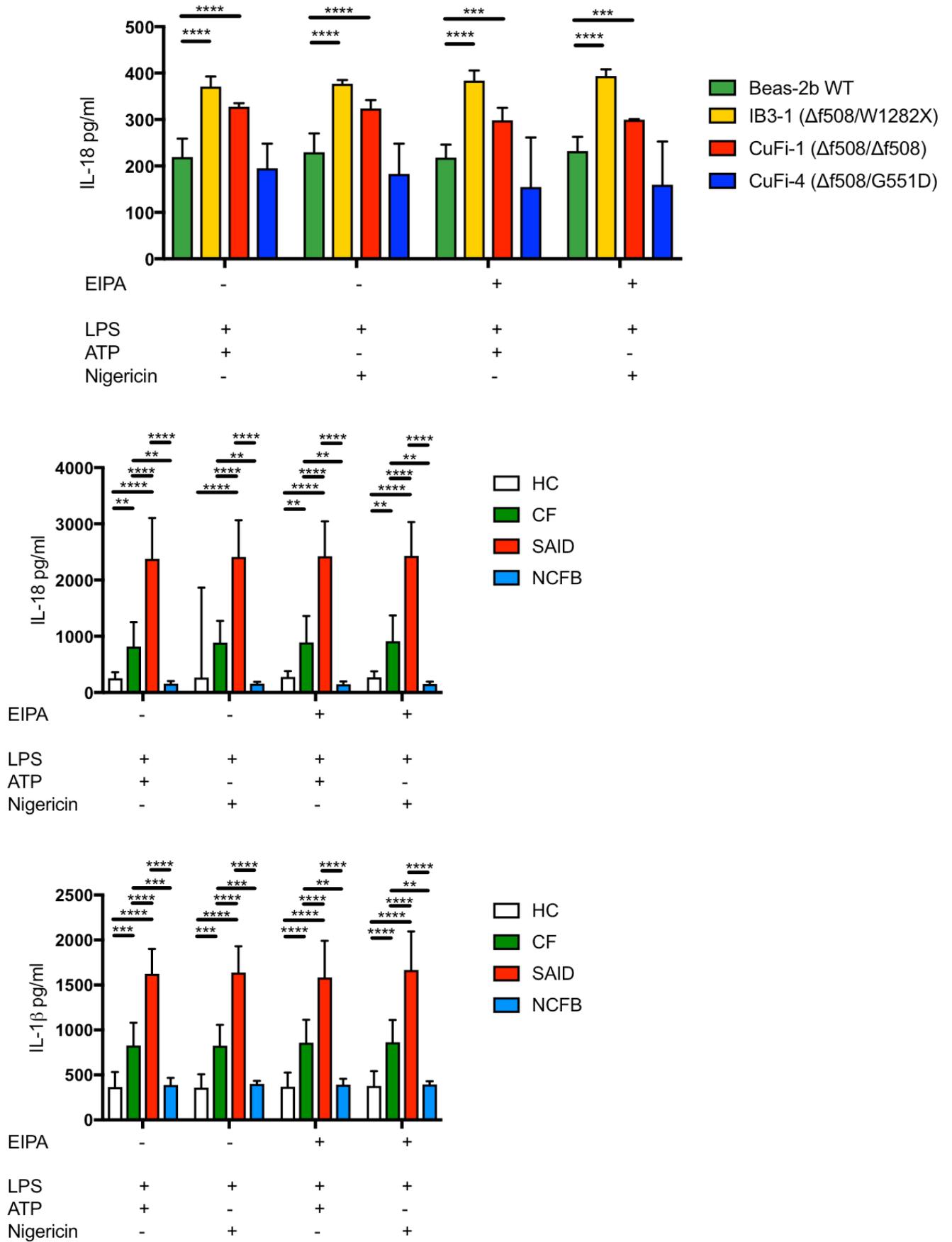
(Figure 3.9.1.2 legend on next page)

Figure 3.9.1.2: The effects of EIPA on cytokine secretion in HBEC lines and primary monocytes. ELISA assays were used to detect IL-18 and IL-1β in monocytes from HC (n=10), patients with CF (n=10), SAID (n=4) and NCFB (n=4) as well as HBECs (n=3). Cell stimulation was as follows: EIPA (10μM, 1 hour) was used as a pre-treatment before a stimulation with LPS (10ng/mL) for 4-hours with an ATP (5mM) stimulation for the final 30 minutes. A repeated measures 2-way ANOVA statistical test was performed with Turkey's multiple comparisons test (p values * = ≤0.05, **= ≤0.01, ***= ≤0.001 and ****= ≤0.0001).

EIPA is a broad-spectrum Na$^+$ channel inhibitor but has been shown to inhibit ENaC with low potency. The data in figure 3.9.1.2 show the effects of an EIPA pre-treatment on the secretion of IL-18 and IL-1β after NLRP3 inflammasome activation. The amount of IL-18 secretion did not change with EIPA pre-treatment in any of the HBEC cell lines. The absence of any anti-inflammatory effects of EIPA are also observed in stimulation of primary monocytes with neither IL-18 or IL-1β secretion being inhibited by EIPA in any of the patient cohorts.
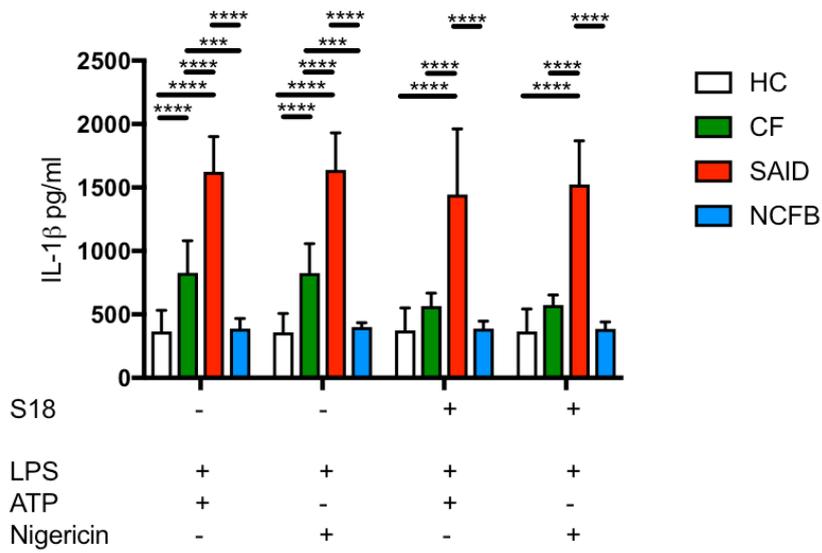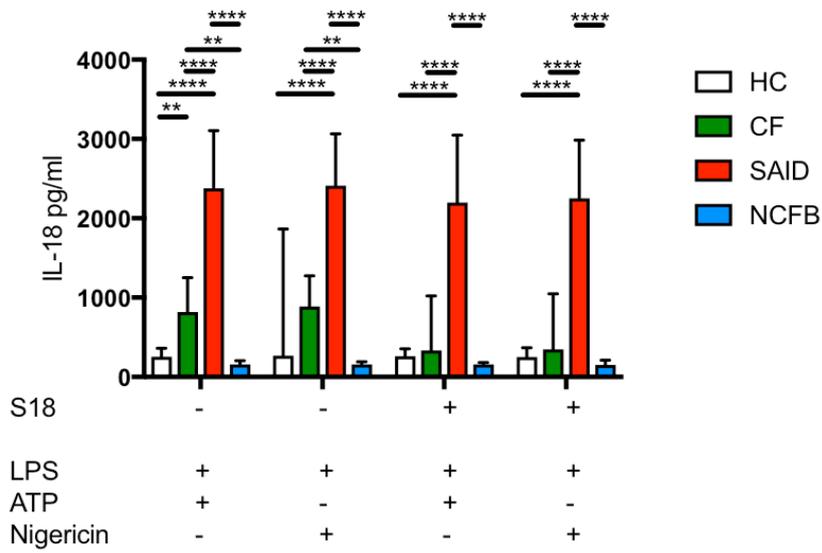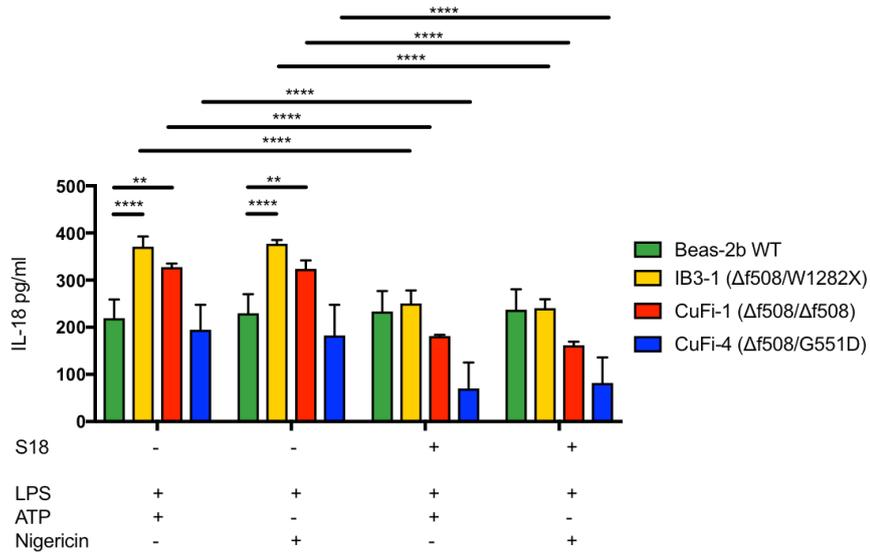
(Figure 3.9.1.3 legend on next page)

Figure 3.9.1.3: The effects of S18 peptide on cytokine secretion in HBEC lines and primary monocytes. ELISA assays were used to detect IL-18 and IL-1β in monocytes from HC (n=10), patients with CF (n=10), SAID (n=4) and NCFB (n=4) as well as HBECs (n=3). Cell stimulation was as follows: S18 derived peptide (25μM, 4 hours) was used as a pre-treatment before a stimulation with LPS (10ng/mL) for 4-hours with an ATP (5mM) stimulation for the final 30 minutes. A repeated measures 2-way ANOVA statistical test was performed with Turkey's multiple comparisons test (p values * = ≤0.05, **= ≤0.01, ***= ≤0.001 and ****= ≤0.0001).

The observation that a pre-treatment of amiloride (specifically at 100mM) is able to potently inhibit the secretion of the cytokines IL-18 and IL-1β, processed by the NLRP3 inflammasome, in cells with CF-associated mutations suggests that overactive ENaC is regulating NLRP3 activation via modulating Na^+ and K^+ efflux. This potential mechanism is further corroborated by the failure of EIPA to replicate the anti-inflammatory effects of amiloride. In order to further confirm this hypothesis S18, a highly potent and specific inhibitory peptide based on the endogenous ENaC inhibitor SPLUNC1, was used to confirm that inhibition of ENaC modulates NLRP3 activation in cells with CF-associated mutations.

The peptide S18 was able to inhibit IL-18 and IL-1β secretion from both ATP or nigericin stimulated monocytes and HBECs with CF-associated mutations (Figure 3.9.1.3), to a similar extent to that of amiloride at 100mM (Figure 3.9.1.1). S18 had no effect on IL-18 and IL-1β secretion from monocytes and HBECs from HC, NCFB or SAID cohorts.

To understand the point at which inhibition of ENaC activity modulates IL-18 and IL-1β secretion from monocytes and HBECs with CF-associated mutations, caspase-1 activity was measured using a colorimetric assay using cell lysates. These experiments are aimed at

deciphering whether it is the secretion of IL-18 and IL-1β that is being inhibited or the processing of the zymogens by active caspase-1 and, therefore, NLRP3 assembly.

Figure 3.9.1.4 displays data measuring caspase-1 activity as a percentage of non-induced, or unstimulated sample. Upon stimulation with LPS and ATP, caspase-1 activity increases compared to the non-induced sample by around 30% in the Beas-2b (WT) HBEC line. This increase in caspase-1 activity is not altered by pre-treatment with amiloride (100mM or 10mM), EIPA or S18 peptide. Amiloride (100mM) was able significantly reduce caspase-1 activity in IB3-1 (Δf508/W1282X) and CuFi-1 (Δf508/Δf508) HBEC lines, with S18 peptide able to do so in all three HBEC lines with CF-associated mutations. The reduction in caspase-1 activity with amiloride (100mM) and S18 peptide also occurred in primary monocyte cultures, with the significant increase in caspase-1 in CF monocytes compared to HC monocytes diminishing to non-significant levels.
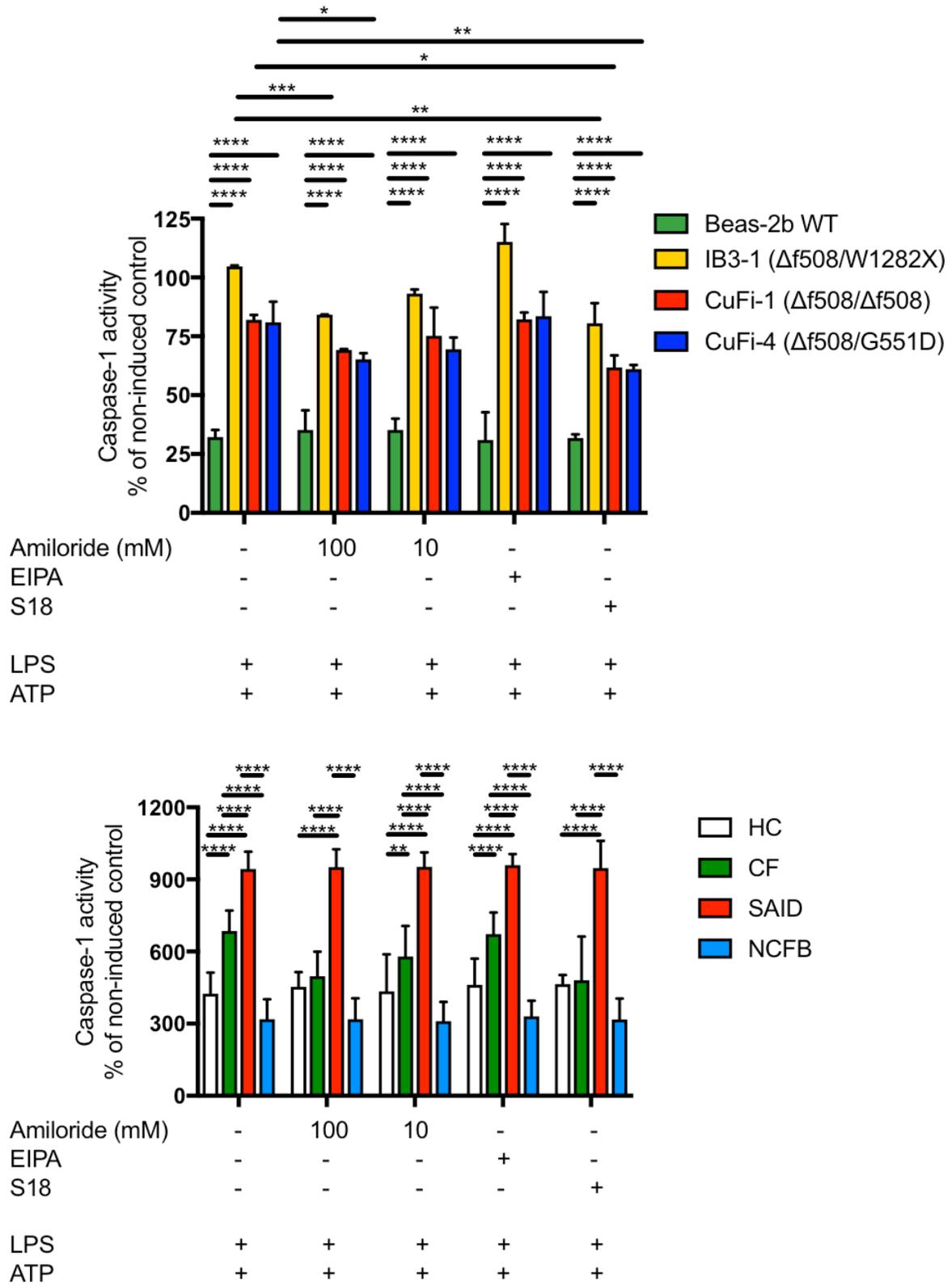
Figure 3.9.1.4: Caspase-1 activity in HBEC lines and monocytes. A colorimetric assay to determine caspase-1 activity via cleavage of a caspase-specific peptide conjugated to a colour reporter molecule p-nitroalinine (pNA). The assay was performed in protein lysates from

primary monocytes from individuals with CF, NCFB, SAID and HCs (HC n=10, CF n=10, SAID n=4, NCFB=4) and HBEC lines (n=3). Cell stimulation was as follows: Amiloride (100mM, 1hour), EIPA (10μM, 1 hour) or S18 derived peptide (25μM, 4 hours) were used as a pre-treatment before a stimulation with LPS (10ng/mL) for 4-hours with an ATP (5mM) stimulation for the final 30 minutes. A repeated measures 2-way ANOVA statistical test was performed with Turkey's multiple comparisons test (p values * = ≤ 0.05, **= ≤ 0.01, ***= ≤ 0.001 and ****= ≤ 0.0001).
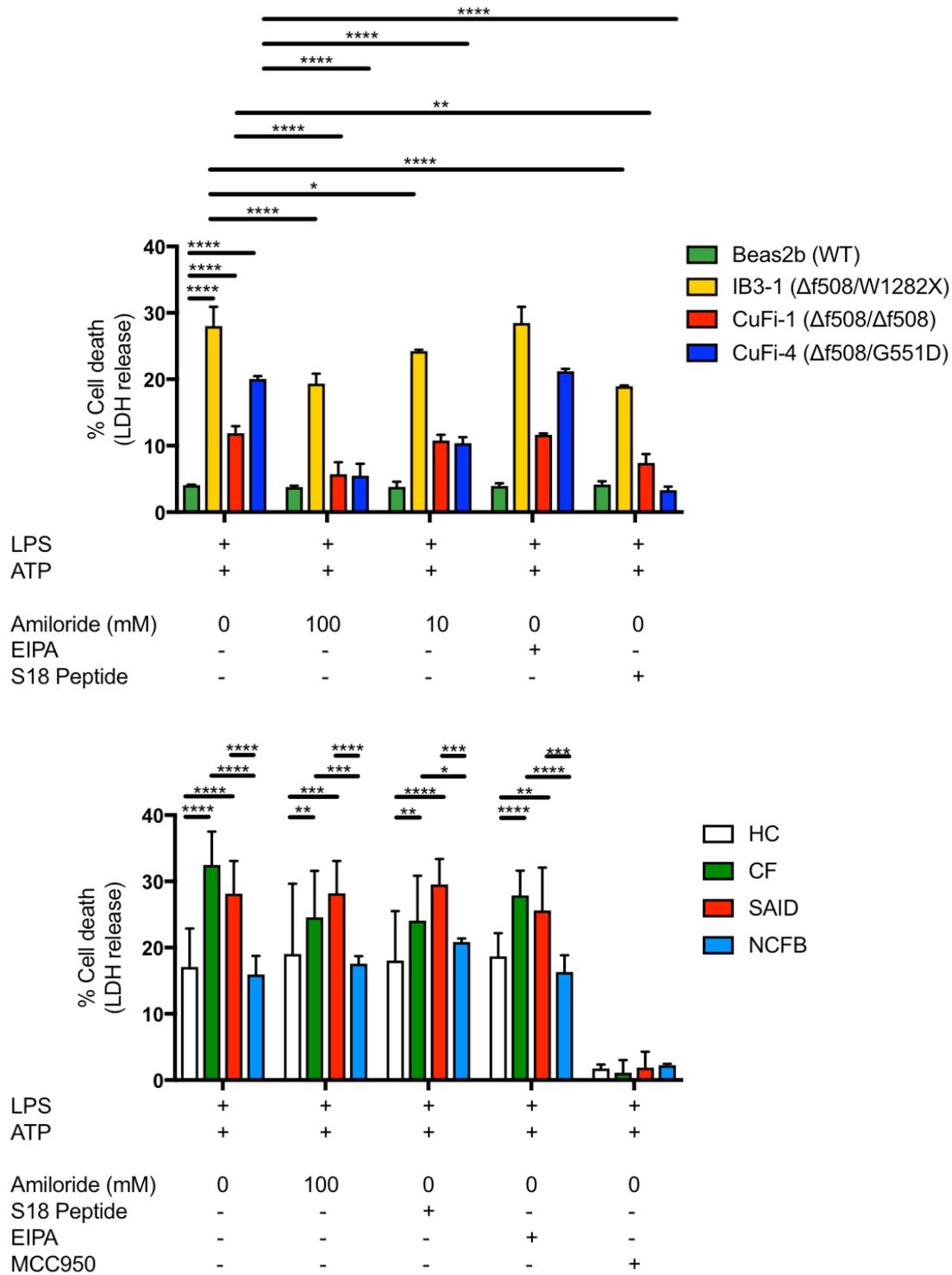
Figure 3.9.1.5: The effects of sodium channel and NLRP3 inhibition on pyroptosis after NLRP3 inflammasome activation in HBEC lines and primary monocytes. The figure displays pyroptosis representing the percentage of total necrosis that is caspase-1 dependent, or pyroptosis. Pyroptotic cell death was calculated by measuring total necrosis via the presence

of lactose dehydrogenase (LDH) from cell culture samples in a 96-well plate, colorimetric assay. Each sample/condition was repeated in parallel with a caspase-1 inhibitor (AC-YVADD-cmv, 2μg/mL, 1 hour) pre-treatment. The total necrosis level was then taken away from the capase-1 inhibited sample, or 'caspase-1 independent' necrosis, with the remaining LDH level termed 'caspase-1 dependent necrosis' or pyroptosis. The assay was performed with primary monocytes from individuals with CF, NCFB, SAID and HCs (HC n=10, CF n=10, SAID n=4, NCFB=4) and HBEC lines (n=3). Cell stimulation was as follows: Amiloride (100mM, 1hour), EIPA (10μM, 1 hour), S18 derived peptide (25μM, 4 hours) or MCC950 (15nM, 1 hour) were used as a pre-treatment before a stimulation with LPS (10ng/mL) for 4-hours with an ATP (5mM) stimulation for the final 30 minutes. A repeated measures 2-way ANOVA statistical test was performed with Turkey's multiple comparisons test (p values $*$ = ≤ 0.05, $**$= ≤ 0.01, $***$= ≤ 0.001 and $****$= ≤ 0.0001).

In order to assess the downstream significance of ENaC-driven NLRP3 inflammasome activation and elevated IL-18 and IL-1β secretion, pyroptosis was measured, as in section 3.4.5. In Figure 3.9.1.5, pyroptotic cell death (caspase-1 dependent necrosis) is shown to be increased in HBEC lines with CF-associated mutations after NLRP3 inflammasome activation. The percentage of pyroptosis after NLRP3 inflammasome activation decreased when either amiloride (100mM) or S18 peptide was added to the cell culture before NLRP3 inflammasome activation. Amiloride at 10mM was also able to significantly inhibit pyroptosis in IB3-1 (Δf508/W1282X) and CuFi-4 (Δf508/G551D) HBEC lines. EIPA had no effect on pyroptosis in any of the HBEC lines.

A similar set of stimulations was used in primary monocyte cultures, with a similar outcome. Amiloride at 100mM and S18 peptide reduced pyroptosis in primary monocytes with CF-associated mutations but not in HC, NCFB or SAID cohorts. Pre-treatment with MCC950

almost completely abrogated pyroptotic cell death in primary monocytes from all patient cohorts.

3.9.2 Chloride Channel inhibition

By using small molecules and peptides to inhibit Na^+ channels, an increased intracellular Na^+ concentration and enhanced K+ efflux has been diminished in cells with CF-associated mutations. Furthermore, the ENaC specific Na^+ channel inhibitors were able to modulate and decrease caspase-1 activity, IL-18 and IL-1β secretion and pyroptosis in cells with CF-associated mutations. Next, Cl^- channel inhibitors were used to understand whether the exacerbated NLRP3 inflammasome activation was in fact due to aberrant Na^+ channel, specifically ENaC, activity or due to deregulation of Cl^- flux, as is the case with mutations in the CFTR. 5-Nitro-2-(3-phenylpropylamino) benzoic acid (NPPB) inhibits calcium-sensitive chloride currents and the $CFTR_{172}$ small molecule inhibits the conductance of chloride currents by the CFTR. Therefore, NPPB was used to inhibit global Cl^- channels and $CFTR_{172}$ to inhibit the activity of the CFTR specifically.

As previously shown, HBECs with CF-associated mutations secreted increased IL-18 and primary monocytes harvested from individuals with CF-associated mutations secreted increased IL-18 and IL-1β upon *in vitro* NLRP3 inflammasome activation. NPPB did not alter IL-18 secretion (Figure 3.6.2.1) in HBEC lines, except of IB3-1(Δf508/W1282X), where IL-18 secretion significantly increased. NPPB was also ineffective and modulating IL-18 or IL-1β in any of the primary monocyte cohorts. Notably, the $CFTR_{172}$ small molecule decreased IL-18 in all HBEC lines and both IL-18 and IL-1β, particularly the latter in all primary monocyte cohorts.
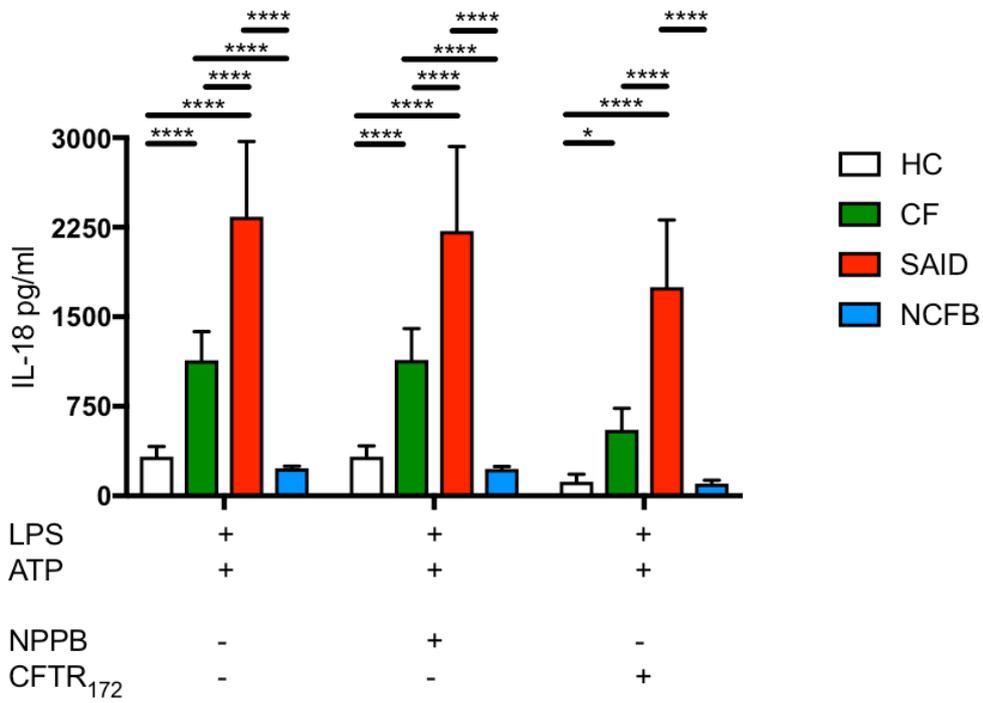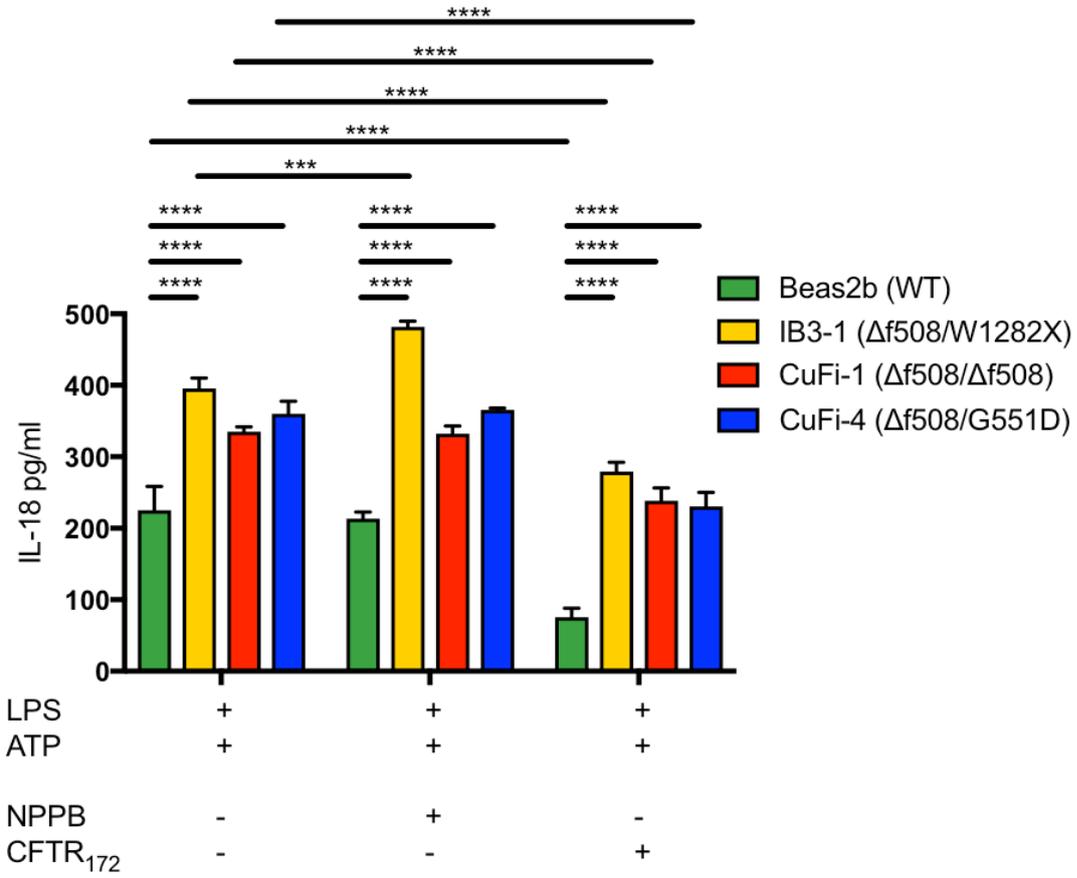
(Figure 3.9.2.1 legend on next page)
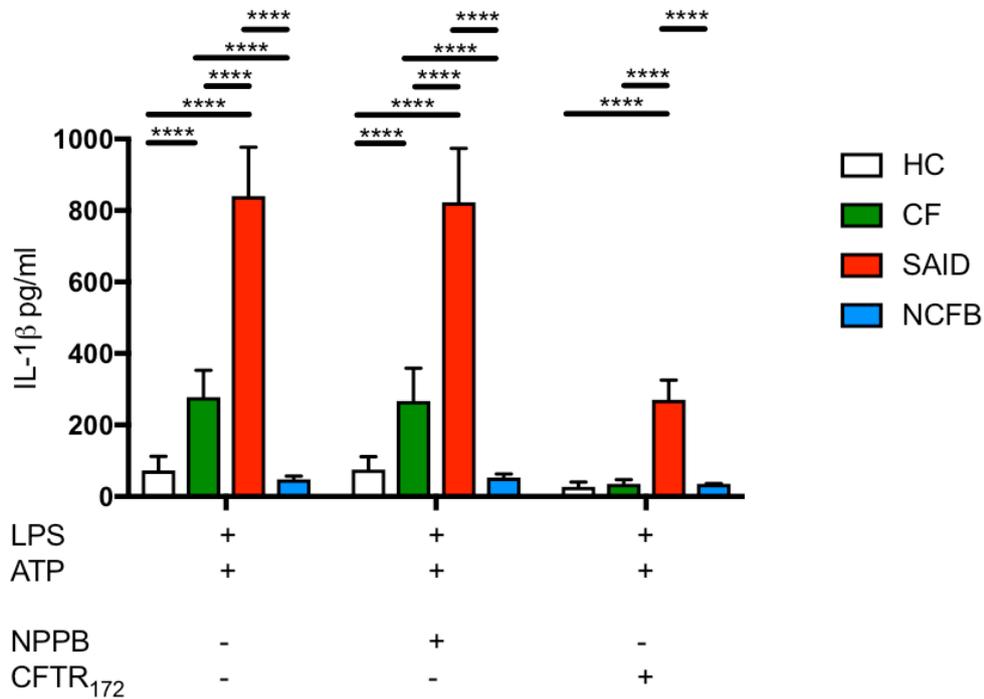
Figure 3.9.2.1: The effects of NPPB on cytokine secretion in HBEC lines and primary monocytes. ELISA assays were used to detect IL-18 and IL-1β in monocytes from HC (n=10), patients with CF (n=10), SAID (n=4) and NCFB (n=4) as well as HBECs (n=3). Cell stimulation was as follows: NPPB (100μM, 1 hour) or CFTR$_{172}$ (10μg/mL, 1 hour) were pre-treated for 4-hours before a stimulation with LPS (10ng/mL) for 4-hours with an ATP (5mM) stimulation for the final 30 minutes. A repeated measures 2-way ANOVA statistical test was performed with Turkey's multiple comparisons test (p values * = ≤0.05, **= ≤0.01, ***= ≤0.001 and ****= ≤0.0001).

Again, in order to understand the role reduced Cl⁻ flux has on NLRP3 inflammasome activation, caspase-1 activity was measured under the same conditions. NPBB did not change caspase-1 activity, upon LPS and ATP stimulation, in either HBEC lines or primary monocytes in any cohort or genotype. However, CFTR$_{172}$ was able to reduce caspase-1 activity

significantly in all HBEC lines and primary monocytes in all cohort or genotypes.
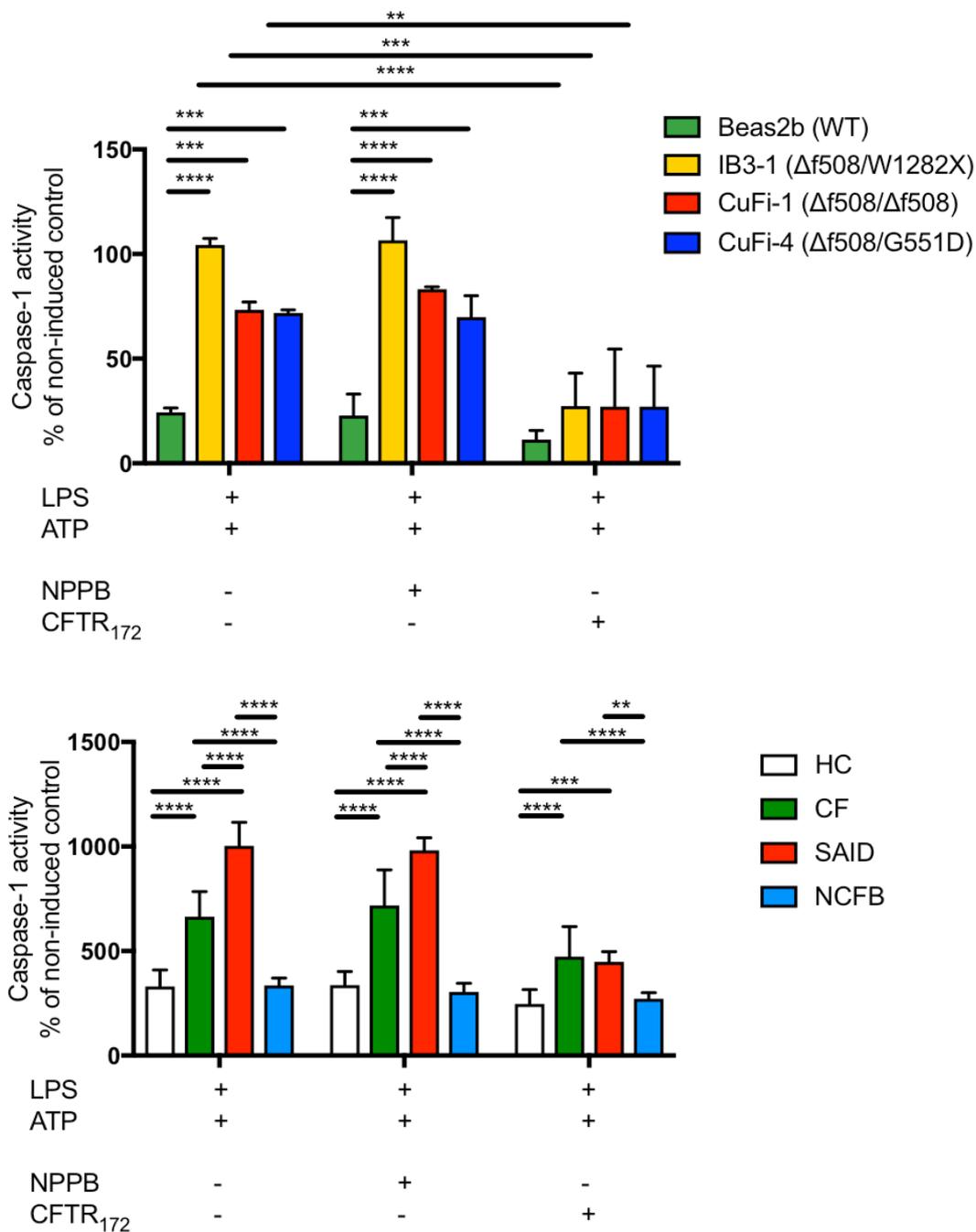
Figure 3.9.2.2: The effect of NLRP3 inhibition on caspase-1 activity in HBEC lines and monocytes. A colorimetric assay to determine caspase-1 activity via cleavage of a caspase-specific peptide conjugated to a colour reporter molecule p-nitroalinine (pNA). The assay was performed in protein lysates from primary monocytes from individuals with CF, NCFB, SAID and HCs (HC n=10, CF n=10, SAID n=4, NCFB=4) and HBEC lines (n=3). Cell stimulation

was as follows: NPPB (100μM, 1 hour) or CFTR$_{172}$ (10μg/mL, 1 hour) were pre-treated for 1-hour before a stimulation with LPS (10ng/mL) for 4-hours with an ATP (5mM) stimulation for the final 30 minutes. A repeated measures 2-way ANOVA statistical test was performed with Turkey's multiple comparisons test (p values * = ≤0.05, **= ≤0.01, ***= ≤0.001 and ****= ≤0.0001).

Figure 3.9.2.3: The effects of CFTR and NLRP3 inhibition on pyroptosis after NLRP3 inflammasome activation in HBEC lines and primary monocytes. The figure displays pyroptosis representing the percentage of total necrosis that is caspase-1 dependent, or pyroptosis. Pyroptotic cell death was calculated by measuring total necrosis via the presence of lactose dehydrogenase (LDH) from cell culture samples in a 96-well plate, colorimetric assay. Each sample/condition was repeated in parallel with a caspase-1 inhibitor (AC-YVADD-cmv) pre-treatment. The total necrosis level was then taken away from the capase-1 inhibited sample, or 'caspase-1 independent' necrosis, with the remaining LDH level termed 'caspase-1 dependent necrosis' or pyroptosis. The assay was performed with primary monocytes from individuals with CF, NCFB, SAID and HCs (HC n=10, CF n=10, SAID n=4,

NCFB=4) and HBEC lines (n=3). Cell stimulation was as follows: MCC950 (15nM, 1 hour) or CFTR$_{172}$ (10μg/mL, 1 hour) were pre-treated for 1-hour before a stimulation with LPS (10ng/mL) for 4-hours with an ATP (5mM) stimulation for the final 30 minutes. A repeated measures 2-way ANOVA statistical test was performed with Turkey's multiple comparisons test (p values * = ≤0.05, **= ≤0.01, ***= ≤0.001 and ****= ≤0.0001).

Pyroptotic cell death was then analysed using CFTR$_{172}$ and MCC950, the NLRP3 inflammasome inhibitor. Both small molecules almost completely inhibited pyroptotic cell death in all HBEC lines, with MCC950 displaying slightly increased effectiveness.

3.9.3 Sodium Potassium ATP gated Channels inhibition

Finally, Na^+/K^+ ATP gated channel inhibition was tested for its ability to modulate NLRP3 inflammasome activation. Both ouabain and digoxin have been shown to inhibit the activity of the Na^+/K^+ ATP gated channel, with high efficacy. The Na^+/K^+ ATP gated channel has been shown to be highly active in CF epithelia. In the context of the hypotheses tested in this study, Na^+/K^+ ATP gated channel activity is thought to be increased as a compensatory mechanism to efflux excess intracellular Na^+ concentration, in exchange for K^+ hence the increased propensity, or decreased threshold for NLRP3 inflammasome activation. However, ouabain is a known NLRP3 inflammasome activator, due to its role in replenishing and maintaining intracellular K^+.
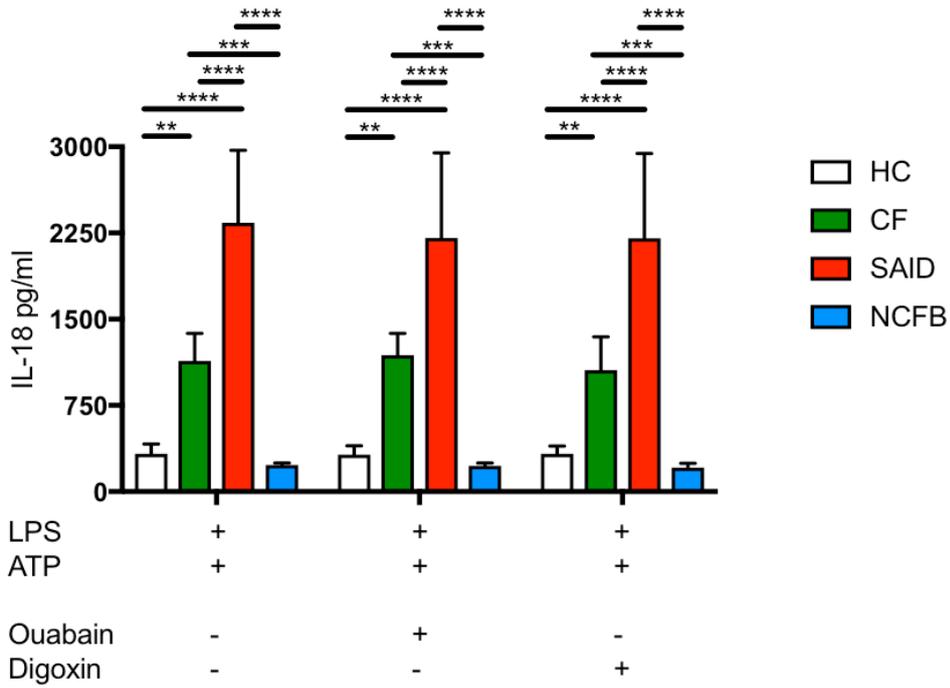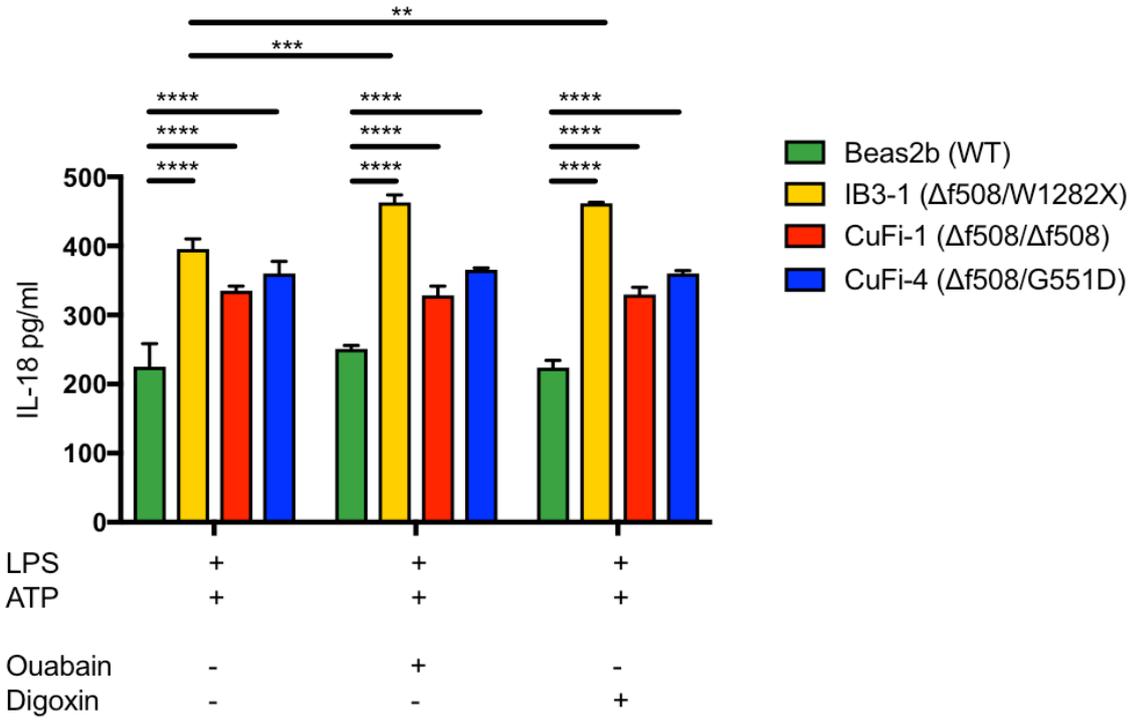
(Figure 3.9.3.1 legend on next page)
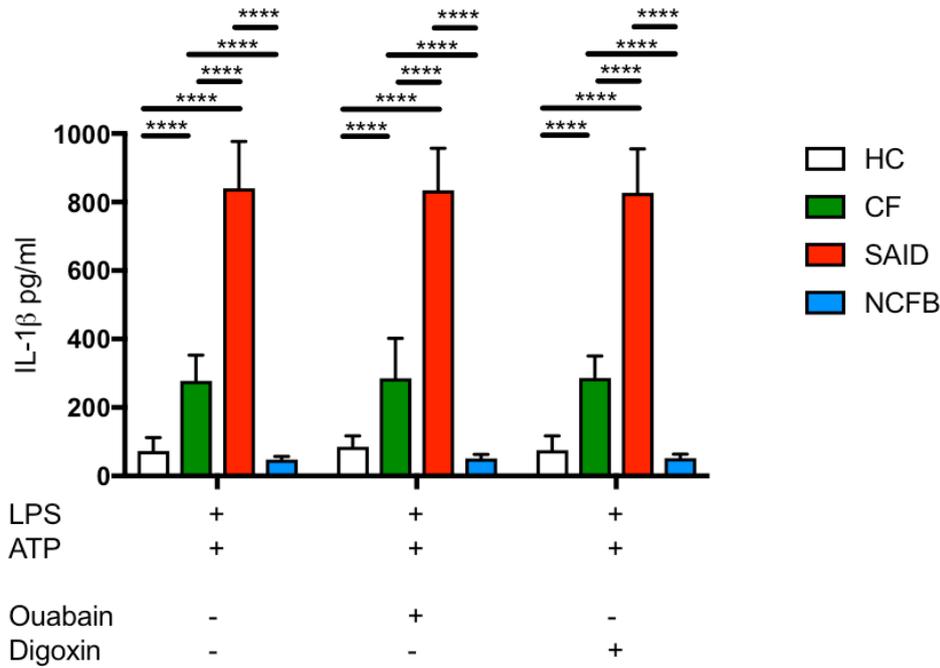
Figure 3.9.3.1: The effects of sodium/potassium ATP gated channel inhibition on cytokine secretion in HBEC lines and primary monocytes. ELISA assays were used to detect IL-18 and IL-1β in monocytes from HC (n=10), patients with CF (n=10), SAID (n=4) and NCFB (n=4) as well as HBECs (n=3). Cell stimulation was as follows: ouabain (100nM, 24 hours) or digoxin (100nM, 24 hours) were pre-treated before a stimulation with LPS (10ng/mL) for 4-hours with an ATP (5mM) stimulation for the final 30 minutes. A repeated measures 2-way ANOVA statistical test was performed with Turkey's multiple comparisons test (p values * = ≤0.05, **= ≤0.01, ***= ≤0.001 and ****= ≤0.0001).

Pre-treatment of either ouabain or digoxin increased IL-18 secretion in the IB3-1 (Δf508/W1282X) HBEC line, although they had little effect in CuFi-1 (Δf508/Δf508) and CuFi-4 (Δf508/G551D) HBEC lines. IL-18 and IL-1β secretion did not change with incubation of ouabain or digoxin in any of the primary monocyte cohorts. Caspase-1 activity also remained unchanged with incubation of ouabain or digoxin in any of the HBEC lines or primary monocyte cohorts.
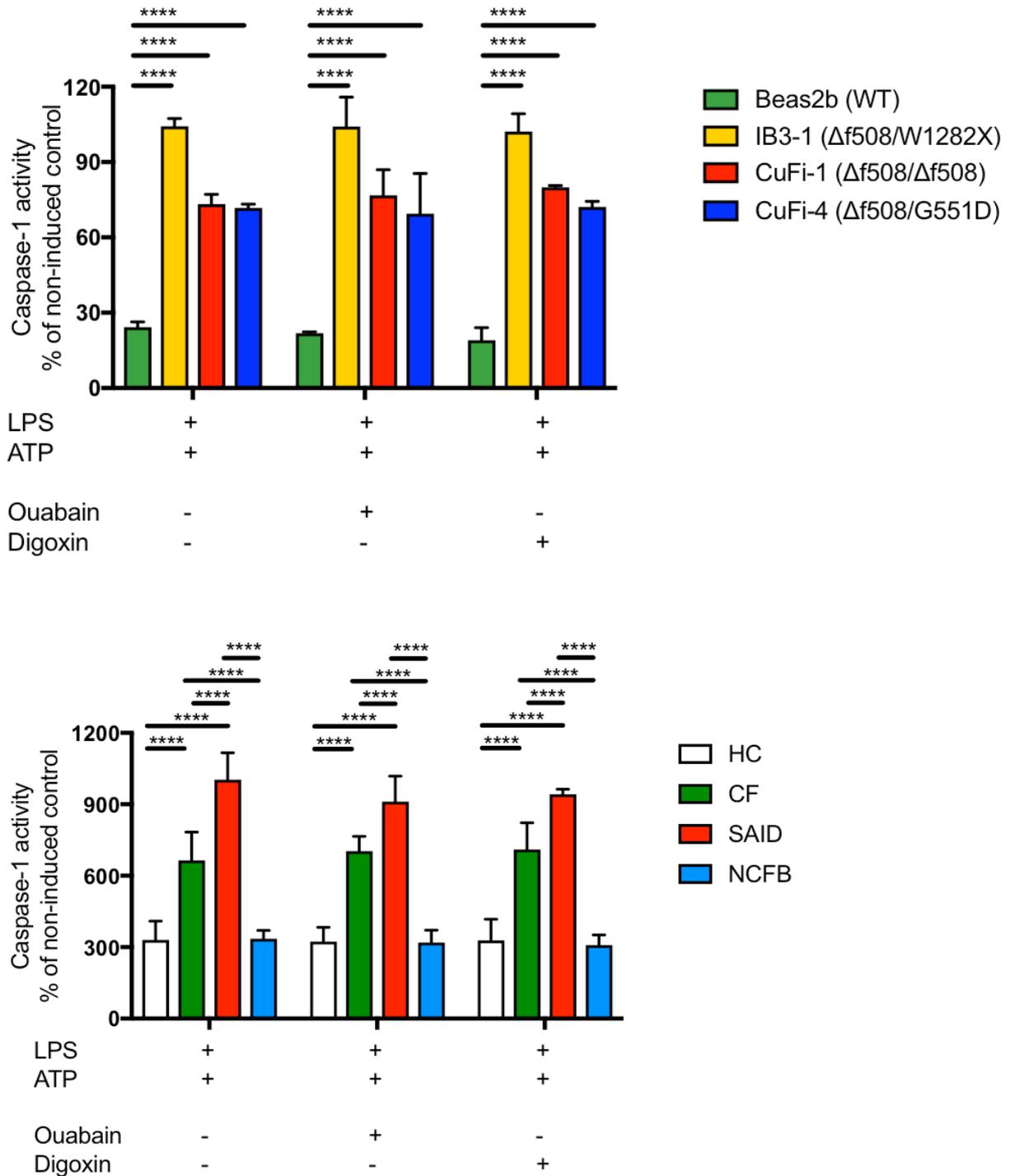
Figure 3.9.3.2: The effects of sodium/potassium ATP gated channel inhibition on caspase-1 activity in HBEC lines and monocytes. A colorimetric assay to determine caspase-1 activity via cleavage of a caspase-specific peptide conjugated to a colour reporter molecule p-nitroalinine (pNA). The assay was performed in protein lysates from primary monocytes from individuals with CF, NCFB, SAID and HCs (HC n=10, CF n=10, SAID n=4, NCFB=4) and

HBEC lines (n=3). Cell stimulation was as follows: ouabain (100nM, 24 hours) or digoxin (100nM, 24 hours) were pre-treated for 1-hour before a stimulation with LPS (10ng/mL) for 4-hours with an ATP (5mM) stimulation for the final 30 minutes. A repeated measures 2-way ANOVA statistical test was performed with Turkey's multiple comparisons test (p values * = ≤0.05, **= ≤0.01, ***= ≤0.001 and ****= ≤0.0001).

3.10 Discussion

3.10.1 Systemic autoinflammation in CF

IL-1 was first described by Auron *et al* as a protein with several biological activities regulating host defence and immune responses, which requires post-translational processing into its active form (Auron et al., 1984, Dinarello, 1998). This processing is predominantly achieved via assembly of inflammasomes and subsequent caspase-1 cleavage. It is now known that IL-1 is just one (IL-1β) of a family of related cytokines with both pro- and anti-inflammatory effects. IL-1β is a highly potent cytokine that, despite being at low or undetectable levels in the circulation, mediates a systemic immune response (McDermott, 2004, Church et al., 2008, Dinarello Charles, 2017). The predominant sources of IL-1β at sites of inflammation are myeloid and epithelial innate immune cells (Lei-Leston et al., 2017, Dinarello, 1996, Dinarello, 1998). It has been established that pulmonary inflammation in CF is driven by the innate immune system, with increased numbers of neutrophilic infiltrations, the presence of neutrophil extracellular traps (NETs) as well as myeloid cell recruitment (Law and Gray, 2017, Mall et al., 2004, Machen, 2006, Bruscia et al., 2009, Cohen and Prince, 2012, Gao and Su, 2015, Montgomery et al., 2017).

To address the importance of IL-1 cytokines in CF, serum levels of IL-1β, IL-18 and IL-1Ra were measured in the serum of patients with either CF, NCFB, or diagnosed autoinflammatory disease in addition to healthy controls (HC). Consistent with previous studies, members of this cytokine family are significantly elevated in sera from patients with CF, with levels comparable to that of individuals with functional mutations in the IL-1-inflammasome pathway (Rimessi et al., 2015, Fritzsching et al., 2015, Iannitti et al., 2016, Montgomery et al., 2017).

With increased levels of IL-1β and IL-18 in the periphery, the hypothesis that these systemic cytokines contribute to the inflammatory phenotype observed in CF is supported. The fact the IL-1Ra is also elevated can be evaluated in two ways: firstly, it may be postulated that there is a potent anti-inflammatory response in CF that is specific to the inflammasome and IL-1 cytokine pathway, and secondly that the presence of IL-1Ra further indicates the activation of the aforementioned pathway. Other serum inflammatory cytokines associated with innate immune activation and immunological pathologies, such as TNF and IL-6, were not elevated in CF to the same extent as members of the IL-1 cytokine family. These data suggest that IL-1 cytokines are prevalent and play an essential role in CF disease pathology. Interestingly, the same CF patients with the higher IL-18 serum levels within the CF population, also had elevated TNF, caspase-1 activity, IL-1 and IL-1Ra serum levels. However, no associated with anti-inflammatory medication, exacerbation or genotype could be made to differentiate this group.

Further evidence to support the hypothesis that the heightened, systemic inflammation in CF is autoinflammatory in nature comes from the fact that the cellular infiltrations into the lungs are innate immune cells (Veltman et al., 2016), and also the elevated caspase-1 activity and ASC speck release in serum from patients with CF. Using a flow cytometry-based assay, extracellular ASC specks were detected in sera from patients with CF, NCFB, SAID and HCs.

ASC is released from the cell when chronic inflammasome activation is sustained, leading to gasdermin D-dependent plasma membrane perforations and pyroptotic cell death. The presence of ASC in the serum indicates prolonged and elevated inflammasome-mediated inflammation and pyroptosis. In addition, increased caspase-1 activity in serum supports the hypothesis that increased pyroptotic cell death is a signature of systemic inflammation in CF. The case for autoinflammation in CF is further supported by data from the control cohorts in this study. The SAID cohort of patients have all confirmed diagnoses of mutations in well-characterised genes associated with sterile innate immune-driven inflammation. In addition, their disease is well controlled by biological therapies targeting established innate immune cytokines, such as anakinra for IL-1β. When analysing the serum data, comparing the CF and SAID cohorts allows for the conclusion that the nature and type of cytokine systemic cytokine response, particularly IL-18, is comparable across the two patient cohorts. Patients within the NCFB cohort have severe lung disease and bronchiectasis but have been confirmed not to have CF-associated CFTR mutations. The serum cytokine levels, within the NCFB cohort, as well as the ASC speck and caspase-1 activity assays were analogous to that of HC, rather than CF or SAID. These observations provide evidence that the elevated serum cytokine levels, presence of ASC specks and increased caspase-1 activity in CF is due to an intrinsic molecular defect downstream from the CFTR mutation, rather than a symptom of respiratory infection, inflammation or scarring (bronchiectasis).

These data also have implications beyond CF lung disease. As previously described (section 1.1), CF is a genetic disease that manifests as a multi-system, multi-organ disease. Many of the manifestations of CF are diseases in their own right, such as diabetes, arthritis, Crohn's disease and liver disease. Interestingly, the individual pathologies and progression of all of these manifestations can be associated with IL-1 cytokine signalling. It is known that

there is a plethora of inflammasome priming and activating stimuli in the CF lung and there may be evidence for a sterile priming of NLRP3 and IL-1β.

Therefore, based on these data there is a good reason to hypothesise that CF shares pathology with, or is in fact, an autoinflammatory disease. A further testable hypothesis is that excessive and inappropriate inflammasome activation in the CF lung causes elevated levels of systemic IL-1β and IL-18 secretion, which then drive secondary inflammatory complications in individuals with CF.

This hypothesis, if accepted, justifies the use anti-inflammatory IL-1 targeted biologic therapy in CF to target systemic inflammation that stems from lung inflammation. This approach should proceed on the side of caution, as anti-inflammatory therapy in CF must be controlled so as not to compromise the individual's immune response to infection.

3.10.2 NLRP3 activation in CF

To understand the cellular and molecular source of IL-1β, IL-18, IL-1Ra (and to a lesser extent IL-6 and TNF) in the sera of patients with CF, ASC specks and caspase-1 activity, *in vitro* assays were used to test monocytes and HBEC lines for inflammasome activation. Many inflammasomes from innate immune and epithelial cells utilise ASC as a component of the structural signalling platform, with IL-1β and IL-18 secretion and capsase-1 activity common to all inflammasomes, with only small variations in the preferential processing and secretion of IL-1β to IL-18. The next task was to identify the specific inflammasome responsible for the autoinflammatory-like state in CF. The experimental *in vitro* assay to distinguish inflammasomes is based on the unique and specific activating signals of each inflammasome. AIM2, NLRC4, Pyrin and NLRP3 inflammasomes were tested by priming expression of inflammasome components by activating the LPS/TLR4/NFκB signalling cascade (Figure

3.1.2). The second, activation or assembly signal is then administered (section 2.4). When testing AIM2, NLRC4 and pyrin inflammasomes, successful secretion of IL-1β and IL-18 was detected in HC and CF monocytes and the latter in HBECs from all genotypes. However, no significant difference was observed in terms of IL-1β or IL-18 secretion between HC and CF monocytes, or in IL-18 secretion between WT HBECs and HBECs with CF-associated mutations upon activation of AIM2, NLRC4 or pyrin inflammasomes. These data suggested that the elevated systemic inflammation observed in serum from patients with CF did not derive from AIM2, NLRC4 or pyrin inflammasomes. However, the case must be made that if there are excessive amounts of stimuli for the aforementioned inflammasomes then the observation that there is no intrinsic defect or difference in their activation compared to WT cells may not be relevant. These data do however fit the hypothesis that the link between CFTR mutation and inflammasome-driven autoinflammation in CF was centred around a disruption in ion flux. NLRP3 was an obvious candidate inflammasome for contributing to the pathogenic inflammatory state in CF, as its primary activating event is itself an ion flux- K^+ efflux. In order to activate the NLRP3 inflammasome *in vitro*, specific stimuli that induce K^+ efflux are used in combination with a selection of small molecule inhibitors, to elucidate the pathway in detail. Again, the LPS/TLR4/NF-κB signalling cascade was used to prime inflammasome expression, with ATP or ouabain being used as the K^+ efflux inducing assembly/activating signal. Under these conditions IL-18 secretion was significantly increased in IB3-1 (Δf508/W1282X) and CuFi-1 (Δf508/Δf508) HBEC lines compared to Beas-2b (WT).

Notably, the CuFi-4 (Δf508/G551D) HBEC line did not secrete significantly increased IL-18 upon NLRP3 inflammasome activation with either ATP or ouabain stimulation. This highlights an important phenomenon- there are genotypic differences in disease severity and progression in CF. In fact, there are often differences in disease severity and progression within CF-associated genotypes (Geborek and Hjelte, 2011, Najafi et al., 2015). For example, class I

mutations (of which W1282X is an example) are characterised by a lack of CFTR protein expression and are considered by many CF specialists to be one of the more clinically severe disease classes, whereas class IV mutations, characterised by poor CFTR channel conductance on the plasma membrane (of which R347H and R117H are examples), are less severe clinically with greater life expectancy (Marson et al., 2016). Each class of CF mutation may have differential downstream molecular mechanisms, in terms of inducing sterile inflammation, due to a disparity in surface CFTR expression, CFTR stability, CFTR conductance and CFTR folding within the ER. Clarifying the inflammatory mechanisms and consequences associated with these discrepancies is relevant but beyond the scope of this study.

When HBEC lines are stimulated for NLRP3 inflammasome activation, as described above, in combination with a pre-treatment by small molecule inhibitors of NLRP3, caspase-1 or TLR4, then subsequent IL-18, caspase-1 activity and pyroptosis are significantly inhibited. These data confirm that not only does the LPS and ATP/ouabain stimulate NLRP3 inflammasome activation specifically, but that HBECs with CF-associated mutations inappropriately activate this pathway compared to WT HBECs. The most potent small molecule inhibitor for preventing IL-18 secretion in HBECs was the TLR4 inhibitor, indicating that the priming of the NLRP3 inflammasome was a crucial process in the secretion of IL-18.

Similar data was generated when the NLRP3 inflammasome was stimulated under the same conditions, with the same inhibitors, in primary monocytes. Both IL-1β and IL-18 were secreted to a greater extent in primary monocytes from patients with SAID and CF than that of patients with NCFB or HC individuals. Again, TLR4 inhibition potently inhibited IL-1β and IL-18 secretion, as did MCC950 NLRP3 inhibitor. This suggests that inflammasome priming is essential and that inhibiting NLRP3, the PRR and initiator of ASC oligomerisation is crucial for downstream IL-18 and IL-1β secretion. The further upstream a small molecule targets, along the NLRP3 inflammasome pathway, the more effective the inhibitory effects on cytokine

secretion. This has implications for modern therapeutics, as current biologics act on the active, secreted cytokine (anakinra and canakinumab target IL-1β) rather than preventing its secretion upstream. Based on these data, targeting the upstream priming or assembly of aforementioned inflammasomes will be a more potent and successful approach for IL-1 mediated disease.

To further validate the above data, suggesting that the NLRP3 inflammasome is 'inappropriately' activated upon stimulation in CF comparable to that of SAID, caspase-1 activity and pyroptosis were examined *in vitro* in HBEC lines and primary monocytes. Caspase-1 activity was elevated in NLRP3 stimulated (LPS and ATP) HBECs and monocytes with CF-associated mutations and primary monocytes from patients with SAID. This implies that more NLRP3 inflammasome complexes are being formed within cells with CF-associated mutations and primary monocytes from patients with SAID, with increased caspase-1 expression and thus activity. When necrotic cell death was measured under the same conditions, elevated caspase-1 dependent pyroptosis cell death was increased in IB3-1 (Δf508/W1282X) HBECs and primary monocytes from patients with CF and SAID. This confirms that chronic and inappropriate inflammasome activation is present in these cell types, leading to an increase in an inflammatory form of cell death. This was also supported by increased detection of extracellular ASC specks in primary monocyte cultures from patients with CF and SAID. Pyroptosis is, arguably, the most inflammatory form of cell death; with all the inflammatory consequences of necrosis but with active, assembled inflammasomes and the related cytokines also being released into the extracellular space. This this form of cell death heightened in cell with CF-associated mutations, one can conclude that the inflammatory response in CF is both excessive and pathogenic.

3.10.3 Monocyte and macrophage polarisation in CF

An important aspect to consider regarding chronic NLRP3 inflammasome activation is the inflammatory phenotype of monocytes and macrophages, in the context of the CF lung, in combination with the potential intrinsic defects downstream of CFTR mutation. As previously discussed, monocytes differentiate into macrophages *in vivo* when entering tissues from the periphery and migrating to the site of inflammation. Macrophages can be put onto a spectrum of inflammatory phenotypes, with proinflammatory M1-type macrophages at one pole, and anti-inflammatory M2-type macrophages at the diametric opposite end of the spectrum (Italiani and Boraschi, 2014). These phenotypes are determined based on characterised cell surface markers and cytokine secretions. With a significant decrease in the ability of primary monocytes from patients with CF to differentiate *in vitro* into anti-inflammatory M2-type macrophages indicates that, due to intrinsic defects concomitant with CF-associated mutations, there is an autoinflammatory signature in CF. There is was more M1-type macrophage differentiation in monocytes from patients with CF, but the difference between HC M1-type macrophage differentiation was not statistically significant. The functionality of the differentiated macrophages was then analysed with CF macrophages producing significantly increased levels of IL-6 and significantly decreased IL-10. The observation that primary peripheral monocytes from patients with CF are predisposed to NLRP3 inflammasome activation and have a deficiency in the propensity for M2-type macrophage differentiation suggest that there autoinflammation is present in CF and is a major part of the pathology of chronic systemic inflammation in CF. Whether or not NLRP3 activation and/or priming is able to predispose a macrophage towards the M1-type, or rather away from the M2-type is an interesting hypothesis. There is evidence, in the literature, that this may be the case, but investigating this basic biological question is beyond the scope of this study.

3.10.4 Hypoxia exacerbates NLRP3 activation in CF

Hypoxia is an important factor in many disease states, including tumour microenvironments, rheumatoid arthritis joints and IBD (Mapp et al., 1995, Taylor and Sivakumar, 2005, Fearon et al., 2016, Montgomery et al., 2017). In CF, the lower airways have been described as being in a hypoxic environment due to an accumulation of viscous, dehydrated mucous with the presence of anaerobic *P. aeruginosa* (Hassett et al., 2009, Legendre et al., 2011, Fritzsching et al., 2015, Montgomery et al., 2017). Hypoxia has been described as a confounding factor in many inflammatory diseases, with the inflammatory transcription factor, HIF1α, a driving force behind the response to hypoxia in terms of cell adaptation, cell death, metabolism and inflammation (Tannahill et al., 2013a). Studying hypoxia *in vitro* was achieved by using a hypoxic cell culture chamber, in which cell cultures were exposed to various levels of O_2. At 1% O_2, NLRP3 inflammasome activation is exacerbated in Beas-2b (WT) HBECs and primary monocytes from HC individuals by around 2-fold. However, when HBECs and primary monocytes with CF-associated mutations are cultured under the same conditions the increase in IL-18 and IL-1β secretion is exacerbated. When TNF was measured under the same conditions, it too was elevated but to a lesser extent. In combination with hypoxic environments, CF-associated mutations can cause vastly inappropriate and exaggerated responses to NLRP3 inflammasome activating stimuli. These data further support the hypothesis that there are multiple factors capable of stimulating various steps in inflammasome priming and assembly. A hypothesis to be discussed further in chapter 4 (section 4.6.4) is that the hypoxia observed in the CF lower airways may be due to increased cellular metabolism in cells with CF-associated mutations, specifically oxidative phosphorylation and, thus, oxygen consumption, leading to reduced extracellular oxygen

concentrations and hypoxia. This hypothesis, if proven, would suggest that the hypoxia in CF may be druggable, if specific metabolic pathways are targeted.

3.10.5 NLRP3 activation activates the adaptive immune response

To understand the implications of hyperbolic NLRP3 inflammasome activation, its downstream effects were analysed by measuring IFNγ expression and secretion in response to monocytic NLRP3 activation, and subsequent IL-18 and IL-1β secretion, by other cells of the innate and adaptive immune systems. IFNγ is crucial to the inhibition of virus replication. As well as its immunomodulatory effects, IFN-γ is also a potent proinflammatory cytokine produced predominantly by natural killer (NK) and natural killer T (NKT) cells, as part of the innate immune response (Srivastava et al., 2013, Chaix et al., 2008). It is also secreted by T_H1 and cytotoxic T-lymphocyte (CTL) cells as part of antigen-specific, adaptive immunity but to a lesser extent. IL-18 and IL-1β have been implicated in the differentiation and activation of NK cells and effector T-cells (Srivastava et al., 2013, Chaix et al., 2008). In a sample of PBMCs, an LPS and ATP stimulation will activate the NLRP3 inflammasome in the monocyte population within that sample. The secreted IL-18 and IL-1β will then be capable of inducing IFNγ secretion, predominantly by NK cells. When the mRNA from the PBMC sample was analysed for *IFNγ* gene expression, increased transcripts were observed in samples stimulated with LPS as well as LPS plus ATP. These IFNγ levels were confirmed at the secreted protein level by ELISA.

These data suggest that IFNγ secretion (derived from NK cell and T-cell) is enhanced in the CF PBMC population due to excessive NLRP3 inflammasome activation from myeloid cell types. The subsequent IL-18 and IL-1β secretion may be potentially inducing the IFNγ secretion.

3.10.6 Sodium-mediated NLRP3 inflammasome activation in CF

Having shown an autoinflammatory cytokine signature *in vivo* from CF patient serum and corroborated this finding *in vitro* with NLRP3 inflammasome activation in HBECs and monocytes, it was important to attempt to establish a link between CF-associated mutations and NLRP3 inflammasome activation. It has been well described that CFTR protein expression on the plasma membrane has inhibitory effects on the activity of the ENaC Na^+ channel (König et al., 2001, König et al., 2002, Donaldson et al., 2002, Konstas et al., 2003, Mall et al., 2004, Berdiev et al., 2009). With the CFTR absent, misfolded, unstable or non-functional, control over ENaC activity has been described as being compromised. When βENaC is overexpressed in murine models, a CF-like lung disease develops from birth, characterised by innate immune cell infiltrations and an IL-1 cytokine signature (Keiser et al., 2015, Fritzsching et al., 2015, Montgomery et al., 2017). The hypothesis is therefore that increased Na^+ influx via ENaC modulates NLRP3 activation in monocytes and HBEC lines with CF-associated mutations, via downstream modulation of K^+ efflux. The relationship between ion fluxes and ion channels is complex and not fully understood. A seminal paper by Gabriel Nunez's group, describing K^+ efflux as the common activator of the NLRP3 inflammasome, also addressed the roles of Na^+ and Cl^- in modulating this pathway (Munoz-Planillo et al., 2013, Yaron et al., 2015). Without directly activating NLRP3 alone, Na^+ influx was able to modulate the amount of K^+ efflux and, thus, NLRP3 activation.

With these baseline studies in mind, the intracellular Na^+ and K^+ concentrations of monocytes and HBECs were measured, upon NLRP3 stimulation and with the inhibition of Na^+ channels. Notably elevated levels of intracellular Na^+ in HBEC lines and monocytes from patients with CF were reduced, upon inhibition of Na^+ channels with EIPA, and, more

specifically, by ENaC inhibition using amiloride and SPLUNC1-derived S18 peptide. Ouabain inhibition of Na^+/K^+ ATP-gated channels increased intracellular Na^+ significantly in CuFi-1 ($\Delta f508/\Delta f508$) HBECs and monocytes from patients with CF. By inhibiting Na^+/K^+ ATP-gated channels, elevated intracellular Na^+ is less able to efflux from the HBEC lines and monocytes from patients with CF. These observations fit with the conclusions of previous studies that ENaC activity is elevated in CF lung. This is the first time these results have been replicated in human monocytes. Inhibition of ENaC by the SPLUNC1-derived S18 peptide achieved the greatest reduction in intracellular Na^+, with statistically significant decreases observed in monocytes and HBEC lines regardless of CF-associated mutations.

Intracellular K^+ concentrations were analysed, under the same conditions of Na^+ channel inhibition, in testing the hypothesis that upstream Na^+ modulates K^+ efflux and, thus, NLRP3 inhibition. When LPS primed WT HBEC lines and HC monocytes were stimulated with ATP, intracellular K^+ concentration decreased by approximately 60% due to the opening of the P2X purinoceptor 7 (P2X7) K^+ channel and efflux of K^+. This known NLRP3 activation event was also shown to be present in HBEC lines with CF-associated mutations and monocytes from patients with CF. However, a significantly greater K^+ efflux was observed in HBEC lines with CF-associated mutations of around 80% and monocytes from patients with CF experiencing an average K^+ efflux of 85% under the same conditions. Whether the amount of K^+ efflux effects the strength or amount of NLRP3 activation and assembly is not fully understood, but the two measurements in this study are correlated. With pre-treatment of amiloride or the SPLUNC1-derived S18 peptide, K^+ efflux was significantly lessened, in both HBEC lines and monocytes with CF-associated mutations. This observation supports the hypothesis that modulating ENaC-dependent Na^+ influx in cells with CF-associated mutations will modulate downstream K^+ efflux and NLRP3 inflammasome activation, upon stimulation. When ouabain is used as a pre-treatment, K^+ efflux is greater in all HBEC lines and monocytes

compared to with ATP alone. With inhibition of Na^+/K^+ ATP-gated channels, ouabain prevents the influx of K^+, via these channels that would normally replenish the loss of K^+ experienced upon ATP stimulation.

The greater intracellular Na^+ concentration present in cells with CF-associated mutations supports the fact that ENaC activity is elevated in CF, particularly as this intracellular Na^+ concentration is modulated *in vitro* by small molecule and peptide inhibitors of the ENaC channel. The outstanding data in this section showed how inhibition of ENaC activity modulated downstream intracellular K^+ concentration. When ENaC was inhibited by amiloride or S18 peptide, the intracellular K^+ concentration was higher after ATP stimulation. These data support the hypothesis that ENaC activity primes NLRP3 inflammasome activation. A greater efflux of K^+ in cells with CF-associated mutations suggests that a lower threshold of K^+ efflux will induce potent NLRP3 inflammasome activation in CF cells (Figure 3.10.6).
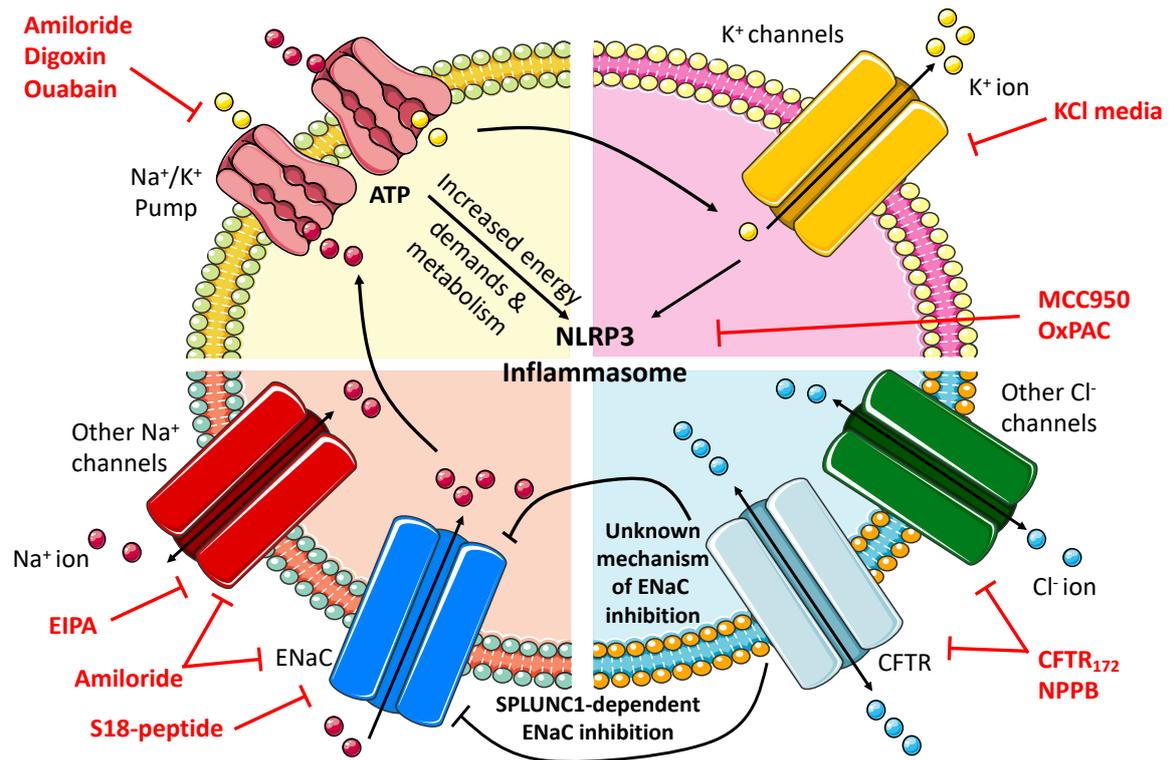
Figure 3.10.6: Dysregulated ion channel activity modulates NLRP3 inflammasome priming and activation. Mutated CFTR (light blue) is unable to modulate ENaC (dark blue) activity via SPLUNC1 or any other means. Overactive ENaC induces an increased Na^+ influx and subsequently increases the activity of the Na^+/K^+ ATP-gated pump (pink) in order to efflux the excessive Na^+, in exchange for K^+. The increased energy demands and K^+ influx produced by the Na^+/K^+ ATP-gated pump, may induce NLRP3 inflammasome activation through metabolic reprogramming and a reduced threshold for K^+ efflux, via the P2X7 ATP-gated channel, respectively. Na^+- sodium; K^+- potassium; Cl^-- chloride; CFTR- Cystic fibrosis transmembrane conductance regulator; ENaC- epithelial sodium channel; ATP- Adenosine triphosphate; KCL- potassium chloride.

3.10.7 Anti-inflammatory effects of sodium channel inhibition

The hypothesis that inhibition of ENaC Na^+ channel activity will negatively regulate NLRP3 inflammasome activation, by limiting K^+ efflux, was tested by the treatment of HBEC lines and monocytes with various ion channel inhibitors before an NLRP3 inflammasome stimulation *in vitro*. Secretion of IL-18 and IL-1β, caspase-1 activity and pyroptotic cell death were measured under the above conditions. As previously described, two concentrations of amiloride were used, in these experiments, due to its known off-target effects (ubiquitous Na+ channel inhibition) at higher concentrations. In addition to amiloride, EIPA and S18 peptide were used to inhibit ENaC with low and high specificity respectively. Amiloride at 100mM significantly reduced IL-18 secretion in HBEC lines with CF-associated mutations. At the lower dose of 10mM, the reduction in IL-18 was not significant. This was also the case for IL-18 and IL-1β secretion from primary monocytes with CF-associated mutations. Amiloride did not reduce IL-18 or IL-1β secretion by monocytes from patients with SAID, NCFB or HC individuals. These results imply that by inhibiting the amiloride-sensitive channel, NLRP3 inflammasome activation is specifically reduced in cells from patients with CF. EIPA treatment had no effect on IL-18 secretion by any HBEC line, or IL-18 or IL-1β secretion by primary monocytes across all cohorts, despite being able to modulate intracellular Na+ concentrations under the same conditions. However, EIPA was unable to modulate K+ efflux and the decrease in intracellular Na+ with EIPA treatment was modest. The SPLUNC1-derived peptide S18 potently and significantly reduced IL-18 secretion in HBEC lines with CF-associated mutations. S18 also significantly inhibited IL-18 and IL-1β secretion from primary monocytes with CF-associated mutations. S18 did not reduce IL-18 or IL-1β secretion in monocytes from patients with SAID, NCFB or HC individuals. These data support the hypothesis that inhibiting ENaC activity specifically, has anti-inflammatory effects restricted, specifically in cells with

CF-associated mutations. To understand whether these anti-inflammatory effects are NLRP3 inflammasome-specific, caspase-1 activity and caspase-1 dependent cell death, pyroptosis, was analysed. As expected, amiloride and S18 peptide successfully inhibited caspase-1 activity and pyroptosis upon ATP stimulation in HBECs and monocytes with CF-associated mutations, with EIPA unable to replicate this inhibition. The NLRP3 inhibitor MCC950 potently abrogated caspase-1 activity and pyroptotic necrosis. Notably, secretion of TNF was not modulated by amiloride, suggesting that the inhibition of sodium channels modulates NLRP3-driven inflammation specifically (appendix figure 5).

To investigate the role of chloride ion channels in the NRPR3 inflammasome assay, both the $CFTR_{172}$ inhibitor and NPPB, a global chloride ion channel inhibitor to test the role of chloride signalling upstream of K^+ efflux and NLRP3 inflammasome priming and assembly. NPPB pre-treatment was unable to modulate IL-1β, IL-18, caspase-1 activity or pyroptosis in any cell type, cohort or genotype. As previously mentioned (section 1.1.3) and described (Jiang et al., 2017) by others, the $CFTR_{172}$ inhibitor inhibits NLRP3 activity as well as CFTR activity and so the observed reduction in IL-1β, IL-18, caspase-1 activity and pyroptosis in HC and disease cohorts as well as all HBEC lines indicated the validity of $CFTR_{172}$ inhibitory action on NLRP3.

Finally, ouabain and digoxin were tested as a pre-treatment to inhibit Na^+/K^+ ATP-gated pump activity. These stimulations were used to test the hypothesis that the link between the Na+ influx through ENaC and the K^+ efflux through P2X7 are linked by the Na^+/K^+ ATP-gated pump and by inhibiting this intermediate then the pathogenic effects of high Na+ influx are diminished. However, neither ouabain or digoxin had any anti-inflammatory effect and, actually, ouabain alone induced increased intracellular Na^+ concentration and a greater K^+ efflux, with consequential NLRP3 activation and secretion of IL-1β and IL-18 and increased caspase-1 activity and pyroptosis. The conclusion of these data is that the Na^+/K^+ ATP-gated

pump is not the pathogenic facilitator of downstream K^+ efflux and NLRP3 activation but is the guardian of ion homeostasis within the CF cell and that an increased propensity for K^+ efflux and NLRP3 activation is merely a consequence of this.

Chapter 4

4.0 Mitochondrial Metabolism in Cystic Fibrosis

4.1 Introduction

4.1.1 Metabolism in CF

Individuals with CF often have pancreatic insufficiency with malabsorption (Gibson-Corley et al., 2016), and, therefore, have unique dietary requirements. Many patients with CF are given high-calorie, high-fat diets in order to compensate for this lack of nutrient absorption (Schindler et al., 2015). There is also evidence for metabolic alkalosis and increased metabolic rate (Lerman-Sagie et al., 1986, Bates et al., 1997, Baird et al., 2002). High-fat, high-glucose diets have been shown to induce obesity and have been associated with the development of diabetes, IBD and colitis (Gulhane et al., 2016, van der Heijden et al., 2015, Kim et al., 2012). However, the aforementioned diets do not typically induce weight gain among patients with CF, who are, in fact, more often characterised as being malnourished, due to their increased energy usage, increased energy demand and failure to consume enough daily calories (Culhane et al., 2013).

It was these observations, in the clinic and literature, that led to the hypothesis that perturbed metabolism is a feature of CF, systemically, and this perturbation is a marker of, and contributing factor towards the inflammatory phenotype, described in chapter 3, at the cellular and molecular level. An alternative hypothesis is that the high-fat, high-glucose diet may alter the gut microbiome and nutrient availability, causing systemic metabolism to have an influence

on cellular metabolism, and, in particular, immune cell metabolism, which may be referred to as immunometabolism (Norata et al., 2015).

Acidification of the airway surface liquid (ASL) in CF is a well-studied, yet frequently debated and poorly understood phenomenon. As previously mentioned (section 1.1), the highly proteolytic and 'acidic' ASL causes degradation and denaturation of SPLUNC1, the glycoprotein which is highly expressed in the respiratory epithelium (Garland et al., 2013, Jiang et al., 2013). Recent studies have shown that the pH of ASL, from children with CF was neutral and not acidic and was, therefore, not significantly different from HC ASL (Schultz et al., 2017), contradicting other groups that have reported the contrary (Tang et al., 2016). The hypothesis regarding the reduced pH in the CF lung is based on the fact that the CFTR is a HCO_3^- bicarbonate transporter, a basic (rather than acidic) molecule that will buffer an acidic solution. With CFTR absent or dysfunctional, the loss of HCO_3^- bicarbonate transport will allow ASL to become acidic. However, dysregulation of metabolism is another potential hypothesis to address in relation to the observed acidic nature of ASL in CF (Garnett et al., 2016). Garnett *et al* reported that the hyperglycaemia observed in CF and CF-related diabetes (CFRD) was elevated compared to HC and was associated with bacterial infection. The authors went on to examine the metabolic consequences of hyperglycaemia in CF and CFRD, and demonstrated an increased metabolic rate, with elevated glycolysis and lactate production through monocarboxylate transporter (MCT) 2, which was glucose dependent; the authors designated these observations as a metabolic shift (Garnett et al., 2016). By inhibiting MCT2, they observed decreased lactate concentration and increased pH in CF ASL. In addition, the MCT transporters efflux H^+ with lactate, further contributing to the acidic state of the ASL, particularly with the loss of HCO_3^- bicarbonate transport via the CFTR. Finally, the authors describe how *P. aeruginosa* stimulates a metabolic shift towards glycolysis during hyperglycaemia, potentially through LPS/TLR4 signalling and they propose that the acidity of

CF ASL may, in part, be due to glycolysis-dependent lactate and H^+ secretion. With elevated glycolysis, fuelled by hyperglycaemic conditions, particularly in those individuals with CFRD, immune responses can also be 'shifted' towards a proinflammatory phenotype, in response to increased glycolysis.

4.1.2 Cellular metabolism

The mitochondria are intracellular organelles that share ancestry with that of early primordial aerobic bacteria (McInerney et al., 2015, Mills et al., 2017). It is often considered that the first instance of endosymbiosis began with the fusion, or phagocytosis, and subsequent mutualistic relationship of primitive bacteria and their eukaryotic hosts (a mutualistic relationship exists when two organisms of different species "collaborate together," to their mutual benefit). This relationship enabled elevated levels of energy expenditure, production and metabolism. Oxygen is a toxic molecule as it may cause oxidative processes. In the presence of a mutualistic relationship between aerobic bacterium and the eukaryote, oxygen could not only be scavenged but also converted to the desirable "molecular unit of currency" of intracellular energy transfer, ATP. In addition to ATP, the 'bacterium' provided macromolecules for essential intracellular processes, as well as reactive oxygen species (ROS), which are fundamental requirements for the killing of any phagocytosed pathogens. The bacterium, or mitochondria, benefited from a protected structure in which to survive and proliferate. Important evidence for the theory of endosymbiosis is that mitochondrial DNA (mtDNA) is near identical in structure to prokaryotic DNA as is highly immunogenic, activating the NLRP3 inflammasome and type I IFN responses (Zhang et al., 2010, Zhang et al., 2014, Rodríguez-Nuevo et al., 2018).

Mitochondrial metabolism utilises fuels, such as glucose, to produce ATP molecules by exchange of protons, across the inner mitochondrial membrane via the electron transport chain (ETC), composed of a series of multiheteromeric enzyme complexes (Mills et al., 2017). Briefly, these complexes include NADH-dehydrogenase (complex 1), succinate dehydrogenase (complex 2), ubiquinone bc1 complex (complex 3), cytochrome c and cytochrome c oxidase (complex 4) and ATP synthase (complex 5). This metabolic pathway, occurring in the mitochondria, is termed oxidative phosphorylation (OXPHOS). In this biochemical process protons are pumped across the inner mitochondrial membrane to generate a membrane potential, which culminates in interactions with oxygen. ATP synthase (complex 5) is driven by the proton gradient to produce ATP molecules from ADP. Upstream of OXPHOS, the Krebs cycle or the citric acid (TCA) converts acetyl CoA into six NADH and two $FADH_2$ molecules through substrate-level phosphorylation, fuelling the ETC. Acetyl CoA is generated from pyruvate, the product of glycolysis. Generally, OXPHOS is a highly efficient (34 ATP per glucose per one molecule of glucose) but a relatively slow pathway, involving multiple enzymatic reactions required for energy production. Glycolysis is a rapid yet inefficient pathway occurring in the cytoplasm, producing just two ATP per glucose molecule (TCA also produces two ATP per glucose, bringing the total ATP per glucose to ~38 for the full glycolysis/TCA/OXPHOS pathway).

4.1.2 Immunometabolism

Immune cells utilise OXPHOS under resting or quiescent states (Mills et al., 2017). This mitochondrial metabolic pathway is, as previously stated, highly efficient but time consuming, culminating in abundant ATP production through a single glucose substrate. When an immune cell is then activated and, depending on the cell type, it proliferates and becomes an effector

cell from its naïve state, cellular metabolism is switched to upregulate glycolysis and bypass OXPHOS, for rapid ATP production, despite the relatively low yield. An example of this metabolic switch in immune cells is the activation of naïve T-cells into T_H1 and T_H2 effector cells (Roos and Loos, 1973, Loos and Roos, 1973). This adaptive immune cell type specifically defends the host against bacterial/viral and helminth infection respectively. Both T-cell effectors, when stimulated and activated *in vitro,* proliferate and induce well characterised transcription factors, cell surface markers and cytokine secretion profiles, specific for their function. In addition, activation of thymocytes induces a metabolic switch towards glycolysis and lactate production (Brand, 1985, Brand et al., 1989, Greiner et al., 1994, Chen et al., 2015, Macintyre et al., 2014). This exploitation of metabolism, depending on activation state, is characteristic of T-cells, with naïve cells utilising glucose, lipids and amino acids for TCA and OXPHOS pathways. Activation of T-cells is a unique process of T-cell receptor (TCR) signalling, along with costimulatory signals and Ca^{2+} store release. TCR activation is accompanied by increased levels of glycolysis, for rapid ATP production (Sena et al., 2013, Ron-Harel et al., 2016).

Store-operated Ca^{2+} entry (SOCE) is a fundamental component of TCR activation and T-cell signalling; it is a process in which stromal interaction molecule (STIM) 1 and STIM2 activate Ca^{2+} release-activated Ca^{2+} (CRAC) channels (Vaeth et al., 2015). It has been shown that the switch to glycolysis in quiescent or naïve T-cells, upon TCR activation and differentiation into T-effector cells, is controlled by SOCE and its regulation of calcineurin (Vaeth et al., 2017). SOCE regulates the expression various glycolytic enzymes via nuclear factor of activated T cells (NFAT) and mTOR. The process of T-cell activation and the metabolic reprogramming of T-effector cells is controlled by ionic fluxes, in this case Ca^{2+}. This is of particular interest, as pathogenic dysregulation of ion fluxes is central to CF

pathology, and can be hypothesised to influence metabolism, cell activation, cell phenotype and cell function, as observed in chapter 3.

After TCR activation there is an increase in cell size and proliferation, which is complemented with an increase in mitochondrial size and number, to support T-cell effector cell functions (Rathmell et al., 2000). There are also differences in mitochondrial structure and function between T-effectors (as mentioned above) and T-memory cells (Liesa and Shirihai, 2016). Fused, extended mitochondria are present in T-memory cells, for greater mitochondrial OXPHOS for prolonged cell survival in the T-memory cell pool (Buck et al., 2016). Mitochondria with loose cristae and increased fission are characteristic of T-effector cells, aiding mROS and decreased respiratory capacity, or OXPHOS, and therefore preferential glycolytic metabolism. A further characteristic of mitochondria that may be adapted, depending on cell function or activation state, is the presence of ETC super-complexes. ETC super-complexes are present in naïve and memory T-cells to support OXPHOS (Cogliati et al., 2013, Mishra et al., 2014). T-cells in RA have been described as being hypo-glycolytic, with impairment in the function of glycolytic enzyme 6-phosphofructo-2-kinase/fructose-2,6-bisphosphatase 3 (PFKFB3) (Yang et al., 2013b). RA T-cells have been shown to be susceptible to apoptosis, due to insufficient ATP levels and being metabolically reprogrammed. With a switch to OXPHOS, RA T-cells became quiescent due to the association of OXPHOS with a resting state and the impairment of glycolysis and thus effector function. Overall, it is clear that metabolism is switched depending on the function and activation state of an immune cell.

4.1.3 Immunometabolism in macrophages

The NLRP3 inflammasome is an integral component of macrophage and monocyte function, to a much greater extent than other cells of the immune system, and these are also the major cell type present in CF lung infiltrates. Macrophage metabolism is a well-studied area and the links between OXPHOS and glycolysis and macrophage phenotype and function have been substantiated by various groups (Tannahill et al., 2013a, Baseler et al., 2016, Fleetwood et al., 2017, Kelly and O'Neill, 2015, Van den Bossche et al., 2015, Bertaux et al., 2018). Mitochondrial collapse is a phenomenon associated with M1-type macrophage activation with PAMPs (such as LPS), and describes the nitrosylating effects of nitric oxide (NO) on complexes 1, 2 and 4 of the ETC (Everts et al., 2012). This nitrosylation inhibits the activity of the ETC and therefore reduces mitochondrial ATP production via OXPHOS and redeploys the ETC for mROS production via complex 1, to aid innate immune responses. Therefore, M1-type macrophages preferentially utilise glycolysis, whereas M2-type macrophages employ mitochondrial OXPHOS for the most part.

Macrophage metabolism not only supports cell phenotype function and proliferation, but the mitochondria itself acts as a signalling platform for innate immune cells. NLRP3 inflammasome oligomerisation occurs on the outer membrane of mitochondria (Franchi et al., 2014, Park et al., 2013, Subramanian et al., 2013). Cardiolipin translocates to the surface of the mitochondria upon mitochondrial membrane depolarisation. Once at the surface, cardiolipin acts as a signalling platform for NLRP3 inflammasome assembly, where they interact and induce the recruitment of ASC and pro-caspase-1. This is an interesting interaction as NLRP3 is known to be potently activated by both mtDNA and mROS, supposedly independent of K^+ efflux (Groß et al., 2016). Another key interaction that occurs on the surface of the outer mitochondrial membrane is interaction of the mitochondrial antiviral-signalling protein (MAVS), a protein activated as part of the anti-viral immunity and interferon regulatory factor (IRF) induction (Loo and Gale, 2011). This induction may be due to the direct interaction

between mROS and MAVS, independent of viral RNA (Seth et al., 2005). MAVS has also been shown to interact and recruit NLRP3 to the mitochondrial membrane. Therefore, the size, activity and integrity of the mitochondria influences NLRP3 signalling, particularly the presence of mtDNA and mROS.

4.1.4 Succinate, itaconate, HIF1α and IL-1β

A key pathway recently elucidated by Mills *et al.* describes an important link between the metabolic switch from mitochondrial metabolism to glycolysis and innate immune responses, particularly *IL1β* expression (Mills et al., 2017, Mills et al., 2016). When an M1-type macrophage is stimulated with LPS, the switch to glycolytic metabolism is associated with breaks in the TCA cycle, causing an accumulation of certain metabolites specific to these break-points. One of these metabolites is succinate. The breakpoint at complex 2 (SDH), which converts succinate to fumarate, as part of the TCA cycle, begins to oxidise succinate and induces reverse electron transport (RET). With electrons passing from complex 2 to complex 1, RET increases mROS production by complex 1, which then activates the transcription factor, HIF1α. *IL1β* is a known transcriptional target of HIF1α; in fact, inhibition of SDH, complex 1 or RET inhibits this process of HIF1α-induced *IL1B*. Studies using HIF1α knockout-mouse models have elegantly shown that the glycolytic switch within myeloid cells under anaerobic conditions is HIF1α-dependent and that HIF1α knockout-macrophages have reduced ATP and impaired function in anaerobic environments (Cramer et al., 2003). These investigations also elucidated the LPS/TLR4/SDH/RET/mROS axis, providing new detail into how LPS can induce M1-type macrophage activation, NLRP3 inflammasome assembly and mROS production (Chouchani et al., 2014, Littlewood-Evans et al., 2016, Mills et al., 2016, Tannahill et al., 2013a).

However, a control mechanism exists that involves another break in the TCA cycle at isocitrate dehydrogenase, which converts citrate into succinate, rather than itaconate. However, in an M1-type induced macrophage, itaconate accumulates and has been shown to block RET and SDH-dependent succinate oxidation. Itaconate was shown to inhibit mROS-driven *IL1B* expression, when cells were pre-treated with itaconate *in vitro* and *in vivo* (Cordes et al., 2016, Lampropoulou et al., 2016). This anti-inflammatory aspect of itaconate is necessary for cell survival, as prolonged succinate accumulation and the associated downstream inflammation will cause chronic oxidative stress and autoinflammation. Interestingly, the metabolite-inflammation association described above seems to be specific for IL-1β, suggesting that immunometabolism, and glycolysis in particular, has a large role to play in NLRP3 inflammasome activity and the consequential macrophage phenotype.

4.2 Methods

4.2.1 Seahorse extracellular flux assay

As in section 2.9.

Briefly, live analysis of ECAR and OCR using the cell energy phenotype kit was performed, using the Seahorse XF-96 Extracellular Flux Analyser (Agilent Seahorse Bioscience), as per the manufacturer's instructions. Details of seahorse OCR and ECAR traces are described in appendix figure 8 and 9.

4.2.2 Intracellular fluorometric assay

As in section 2.8.

Briefly, ATP and succinate (Assay kits, Abcam) were measured, as per the manufacturer's instructions.

4.2.3 Extracellular fluorometric assay

As in section 2.8.

Briefly, Extracellular glucose and L-lactate (Assay kits, Abcam) were measured, as per the manufacturer's instructions.

4.2.4 mitoSOX

MitoSox was used with Flow cytometry to detect mROS intracellularly. 5 mM MitoSOX™ reagent stock solution was prepared by dissolving the contents (50 μg) of one vial of MitoSOX™ mitochondrial superoxide indicator (Component A) in 13 μL of dimethylsulfoxide (DMSO) to make a 5 mM MitoSOX™ reagent stock solution. The 5 mM MitoSOX™ reagent stock solution (prepared above) was diluted in HBSS/Ca/Mg or suitable buffer to make a 5 μM MitoSOX™ reagent working solution. Note: The concentration of the MitoSOX™ reagent working solution should not exceed 5 μM. Concentrations exceeding 5 μM can produce cytotoxic effects, including altered mitochondrial morphology and redistribution of fluorescence to nuclei and the cytosol. Sterile DMSO is incorporated in one vial of MitoSOX™ (to make 5 mM MitoSOX™) and dissolved to the required amount to 1/1000 in PBS to final concertation of 5 μM MitoSOX™ reagent working solution. Cells are loaded into FACS tubes at 0.5×10^6 per tube. Cells are stimulated and washed with PBS. 5 μM MitoSOX™ reagent working solution is added to cover entirely the cells ~500 ul of the mix

and incubated at 37°C for 10 minutes. Cells are washed 2x with PBS supplemented with 2% FBS. Cells are then resuspended in 200ul FACS buffer and passed through a flow cytometer.

4.3 Basal metabolic phenotype

4.3.1 Oxidative phosphorylation

It is important to measure the activity of metabolic reactions or pathways rather than merely the presence or expression of protein or gene. This is because the broad presence of a metabolic enzyme or series of enzymes is not enough to be confident in stating that said metabolic pathway is active. This is particularly relevant in acute, *in vitro* experiments particularly with short stimulations with LPS, as is the case in this study. OXPHOS activity can be measured by oxygen consumption (see methods). This measure of OXPHOS activity is reliable as OXPHOS cannot take place without extracellular oxygen consumption as there are no 'oxygen stores' within a cell. Measuring this rate-limiting substrate is an accurate and precise measurement of OXPHOS.

Figure 4.3.1 shows data from experiments performed measuring OXPHOS *in vitro*, using HBEC lines and primary monocytes and T-cells from HC individuals and patients with CF. The hypothesis being tested in these experiments was that cells with CF-associated mutations, particularly immune cells, are more metabolically active with higher levels of glycolysis due to an inflammatory phenotype, as characterised in the previous chapter. Not only is glycolysis a read-out of inflammation and inflammatory phenotypes in immune cells but elevated metabolism may be satisfying an elevated energy demand in cells with CF-associated mutations. The potential molecular reasons behind this hypothesised increase in energy demands are discussed later in this chapter (section 4.6).
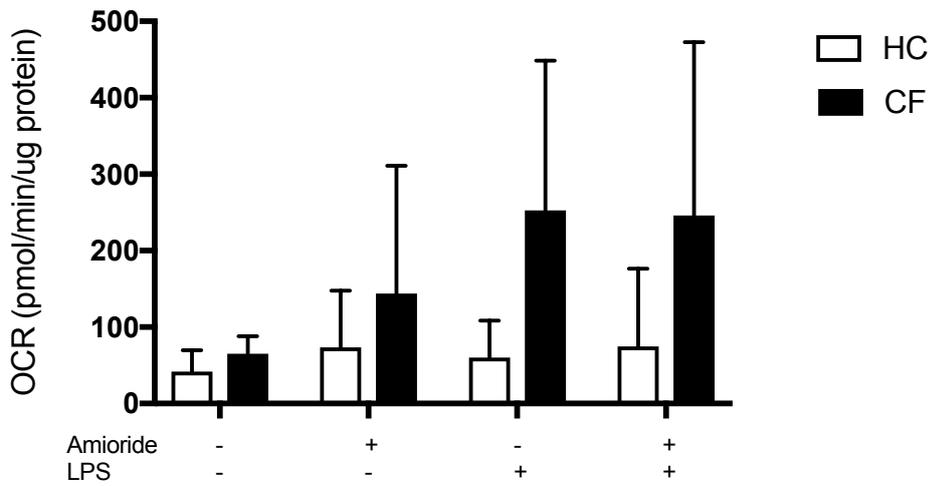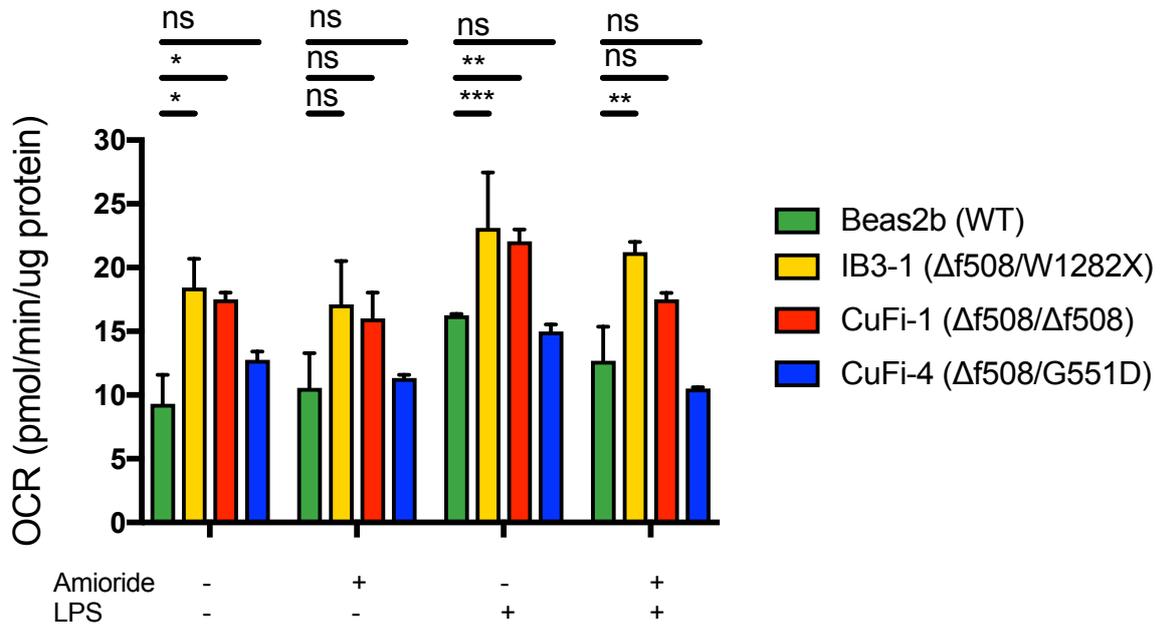
(Figure 4.3.1 legend on next page)
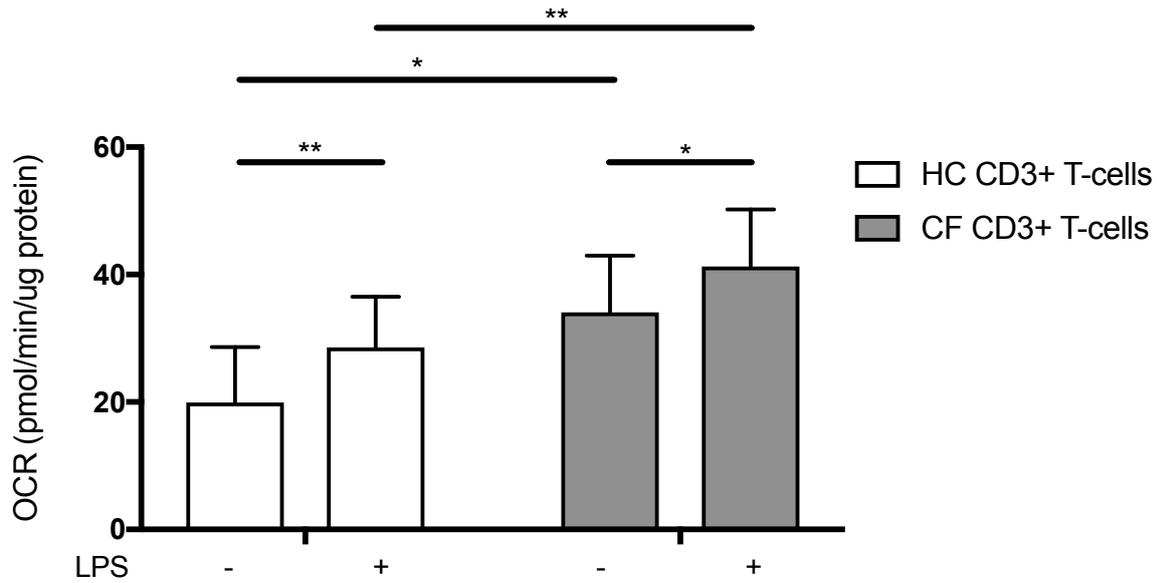
Figure 4.3.1: Oxygen consumption in HBEC lines, monocytes and T-cells. A Seahorse extracellular flux analyser measured the oxygen consumption rate (OCR) in HBECs (n=3), monocytes (n=4) and T-cells (n=4). Oligomycin (10μM), an inhibitor of ATP synthase, and the uncoupling agent, Carbonyl cyanide-4-(trifluoromethoxy) phenylhydrazone (FCCP) (5μM), were used to metabolically stress and depolarise cellular mitochondrial membranes. Cell were pre-treated with amiloride (100mM, 1 hour) before an LPS (10ng/mL, 4 hours) stimulation. A 2-way ANOVA was performed (p values * = ≤0.05, **= ≤0.01, ***= ≤0.001 and ****= ≤0.0001).

Under basal conditions, oxygen consumption was significantly elevated in both IB3-1 (Δf508/W1282X) and CuFi-1 (Δf508/Δf508) compared to Beas2b (WT) HBECs. This increase in oxygen consumption was not statistically significant in the CuFi-4 (Δf508/G551D) HBECs compared to Beas2b (WT) HBECs. After LPS stimulation, oxygen consumption was again significantly elevated in both IB3-1 (Δf508/W1282X) and CuFi-1 (Δf508/Δf508) compared to Beas2b (WT) HBECs. Pre-treatment with amiloride did not significantly decrease oxygen

consumption in any of the cell lines, although the significant difference found between IB3-1 (Δf508/W1282X) and CuFi-1 (Δf508/Δf508) compared to Beas2b (WT) was lost, indicating that oxygen consumption across WT cells and cells with CF-associated mutations was similar with the amiloride pre-treatment.

No statistical difference was observed when oxygen consumption was measured in primary monocytes from HC and patients with CF-associated mutations. There were a few outlying data points in the CF monocyte cohort that indicate a potential trend towards increased oxygen consumption in CF monocytes, but there was not sufficient evidence to conclude this unequivocally.

CD3+ T-cells were also used to test for oxygen consumption, with and without LPS. There was increased oxygen consumption upon LPS stimulation in both HC and CF T-cells, which was an unexpected result as T-cells are not known for their efficient LPS responses. Notably, there was an elevated, statistically significant level of oxygen consumption present in CF monocytes with both unstimulated and LPS conditions compared to HC T-cells.

4.3.2 Extracellular acidification
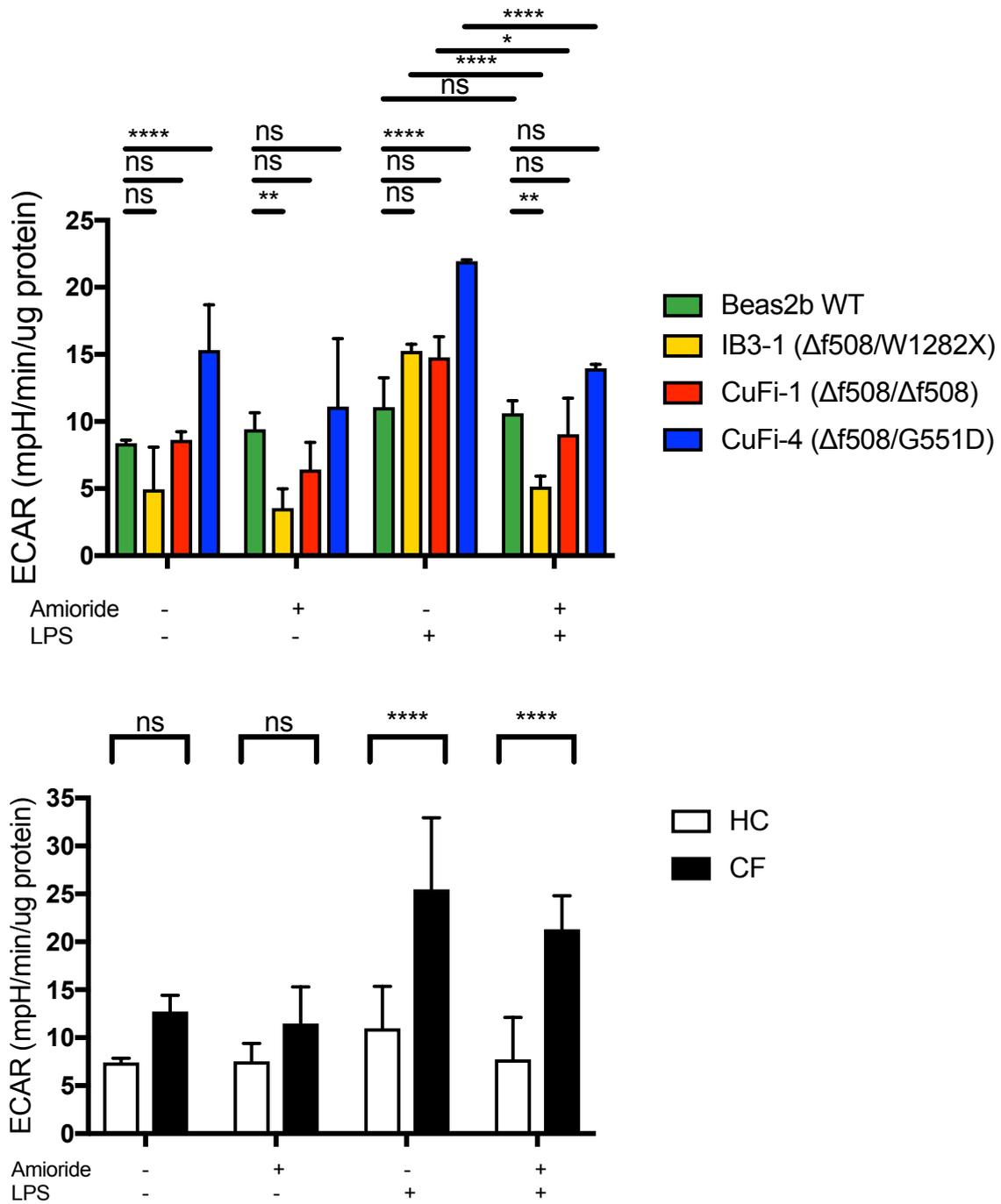
(Figure 4.3.2 legend on next page)
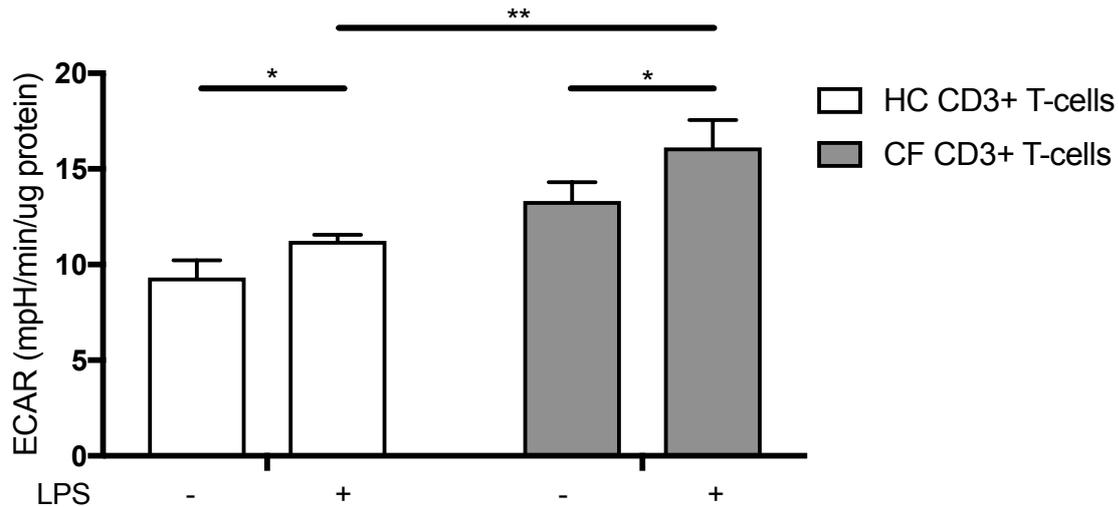
Figure 4.3.2: Extracellular acidification rate (ECAR) in HBEC lines, monocytes and T-cells. A Seahorse extracellular flux analyser measured the extracellular acidification rate (ECAR) in HBECs (n=3), monocytes (n=4) and T-cells (n=4). Oligomycin (10μM), an inhibitor of ATP synthase, and the uncoupling agent, Carbonyl cyanide-4-(trifluoromethoxy) phenylhydrazone (FCCP) (5μM), were used to metabolically stress and depolarise cellular mitochondrial membranes. Cell were pre-treated with amiloride (100mM, 1 hour) before an LPS (10ng/mL, 4 hours) stimulation. A 2-way ANOVA was performed (p values * = ≤0.05, **= ≤0.01, ***= ≤0.001 and ****= ≤0.0001).

The extracellular acidification rate (ECAR) was used as a measure of glycolysis, as this metabolic pathway produces lactic acid and H^+ as a by-product, that then can be detected extracellularly (Figure 4.3.2). When ECAR was measured in HBECs, as a measure of glycolysis, only CuFi-4 (Δf508/G551D) HBEC lines were significantly increased compared to Beas2b (WT) at both unstimulated and during LPS stimulation. Interestingly, amiloride was able to decrease ECAR in IB3-1 (Δf508/W1282X) HBECs compared to Beas2b (WT), as well

as decreasing ECAR when amiloride was used as a pre-treatment to LPS stimulation in all HBEC lines with CF-associated mutations.

Primary monocytes from patients with CF-associated mutations had increased ECAR and, therefore, glycolysis upon LPS stimulation, compared to monocytes from HC individuals, and this difference was statistically significant (p=<0.0001). Pre-treatment with amiloride had little effect on ECAR in either patient cohort.

Again, both HC and CF T-cells responded with increased glycolysis upon LPS treatment, measured by ECAR. However, there was a heightened ECAR response in LPS-activated T-cells from patients with CF-associated mutations compared to those isolated from HC individuals.

4.3.3 ATP concentration

ATP is a measure of the final product produced by both glycolysis, TCA cycle and OXPHOS. In this study it is used as a general measure of the metabolic rate of a cell and provides an insight into the energy demands the cell is trying to meet, in terms of ATP production.
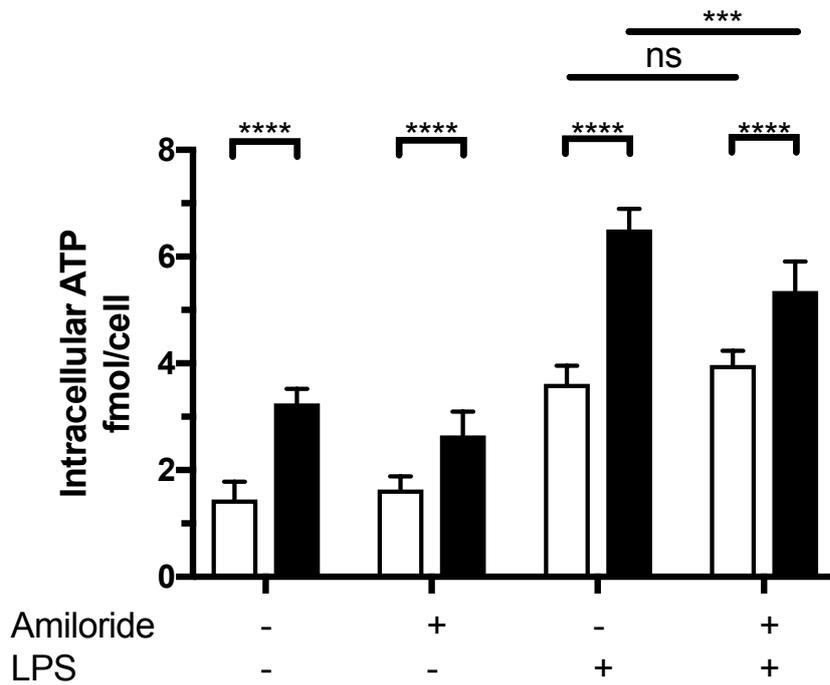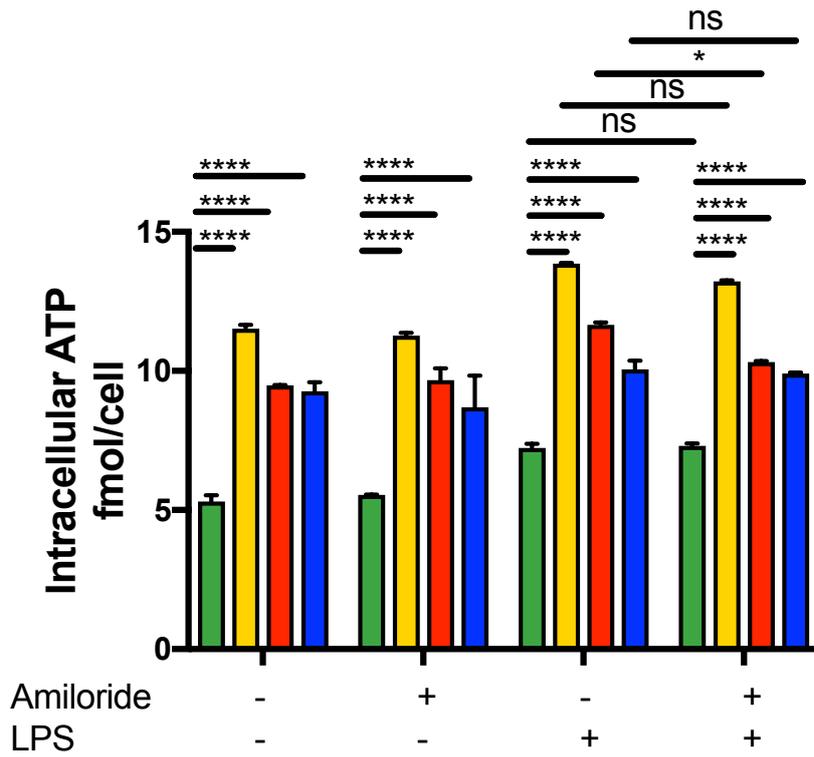
Figure 4.3.3: Intracellular ATP concentration in HBECs and primary monocytes.
Colorimetric assays were used to detect intracellular ATP in HBECs (n=3) and primary monocytes (n=7). Cell were pre-treated with amiloride (100mM, 1 hour) before an LPS

(10ng/mL, 4 hours) stimulation. A 2-way ANOVA was performed (p values * = ≤0.05, **= ≤0.01, ***= ≤0.001 and ****= ≤0.0001).

ATP production is significantly higher than Beas2b (WT) in HBECs with CF-associated mutations, at baseline (Figure 4.3.3). This correlates with the ECAR and OXPHOS readouts where at least one metabolic pathway was shown to be increased in activity in HBECs with CF-associated mutations compared to Beas2b (WT). This increased ATP concentration remained elevated when amiloride was added to the untreated cultures. ATP production increased in all HBEC lines upon LPS stimulation and then decreased in CuFi-1 (Δf508/Δf508) HBECs with a pre-treatment of amiloride before LPS stimulation.

Interestingly, ATP concentrations were, overall, less compared to that of epithelial cell lines. However, the increase in ATP concentration was also significantly increased in monocytes from patients with CF-associated mutations compared to monocytes from HC individuals. Upon LPS stimulation, both HC and CF monocytes increased ATP production by approximately 2-fold, although CF monocytes maintained their significantly elevated levels of intracellular ATP. Notably, pre-treatment with amiloride before LPS stimulation significantly decreased ATP production in CF monocytes but not HC monocytes.

4.4 Glycolysis

4.4.1 L-Lactate production

L-lactate is the most abundant and biologically relevant isometric from of lactate and is produced during anaerobic glycolytic processes, in which pyruvate is reduced to lactate (typically the L-lactate isomer). By measuring L-lactate (referred to as lactate) in the

extracellular fluid of *in vitro* cultures, inferences can be made regarding the amount of glycolysis, particularly anaerobic glycolysis.
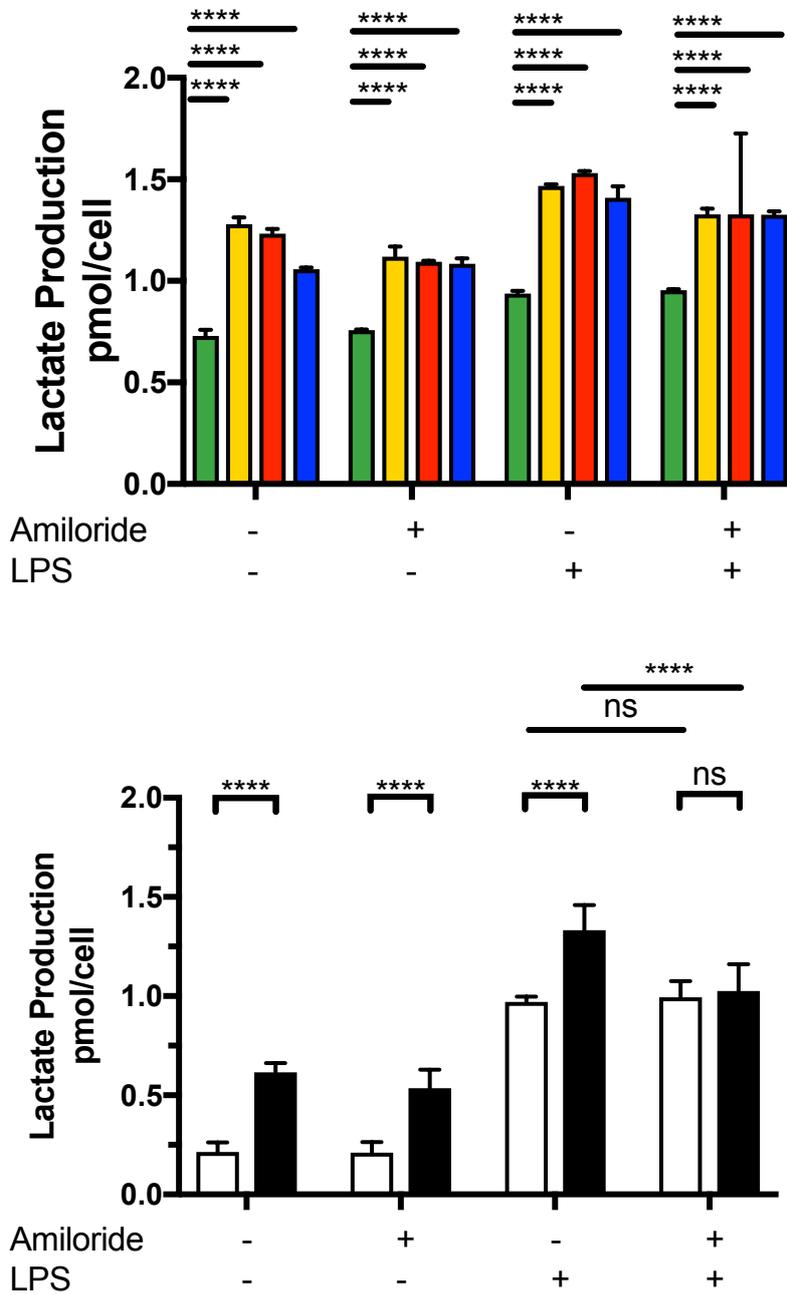
Figure 4.4.1: Extracellular L-lactate secretion in HBECs and primary monocytes. Colorimetric assays were used to detect intracellular L-lactate production in HBECs (n=3) and primary monocytes (n=7). Cell were pre-treated with amiloride (100mM, 1 hour) before an

LPS (10ng/mL, 4 hours) stimulation. A 2-way ANOVA was performed (p values * = ≤0.05, **= ≤0.01, ***= ≤0.001 and ****= ≤0.0001).

Significantly elevated levels of lactate were observed in all of the HBEC lines with CF-associated mutations (Figure 4.4.1). Amiloride did not significantly decrease lactate secretion in any of the cell lines. LPS stimulation increased lactate production in all cell lines with HBECs with CF-associated mutations remaining significantly elevated compared to Beas2b (WT).

The increase in lactate secretion was also significantly increased in monocytes from patients with CF-associated mutations compared to monocytes from HC individuals. Upon LPS stimulation, both HC and CF monocytes increased lactate secretion although CF monocytes maintained their significantly elevated levels of lactate secretion. Notably, pre-treatment with amiloride before LPS stimulation significantly decreased lactate secretion in CF monocytes but not in HC monocytes.

4.4.2 Glucose consumption

Glucose is an important substrate for ATP production for both glycolysis and OXPHOS, so distinguishing between these pathways using glucose alone is not sufficient. However, before OXPHOS is able to utilise glucose it must first be converted to pyruvate and acetyl CoA by glycolysis and then the TCA cycle. Therefore, as glucose molecules feed directly into the glycolytic pathway, glucose consumption is a measurement of the consumption of the substrate for glycolysis specifically. Glucose consumption, therefore, cannot infer what happens to the metabolites of aforementioned glucose. A cell's consumption of glucose is strictly a measure of metabolism and glycolysis.

Figure 4.4.2: Glucose consumption in HBECs and primary monocytes. Colorimetric assays were used to detect intracellular glucose consumption in HBECs (n=3) and primary monocytes (n=7). Cell were pre-treated with amiloride (100mM, 1 hour) before an LPS (10ng/mL, 4 hours) stimulation. A 2-way ANOVA was performed (p values * = ≤0.05, **= ≤0.01, ***= ≤0.001 and ****= ≤0.0001).

The consumption of glucose is elevated in the HBEC lines with CF-associated mutations compared to the Beas2b (WT) line (Figure 4.4.2). Amiloride had a modest effect on reducing glucose consumption in any of the HBEC lines. Upon stimulation with LPS, all of the HBEC lines increased their consumption of glucose, although this increase was still statistically elevated in the HBEC lines with CF-associated mutations compared to Beas2b (WT). Pre-treatment with amiloride was able to decrease glucose consumption significantly in IB3-1 (Δf508/W1282X) and CuFi-1 (Δf508/Δf508) lines.

4.4.3 Succinate accumulation

Succinate was discussed earlier in this chapter (section 4.1.4) with regard to its influence on myeloid inflammation. Briefly, accumulation of succinate occurs when the TCA cycle activity reduces with multiple break points at key enzymatic reactions causing accumulation of substrates for aforementioned reactions. One such substrate is succinate, which has inflammatory signalling effects on the activation of inflammatory transcription factors and expression of inflammatory cytokine gene expression such as *IL1β*. Therefore, measurement of succinate is an excellent readout for not only the switch of cellular metabolism from OXPHOS to glycolysis, but also the potential downstream inflammatory effects of this metabolic switch.
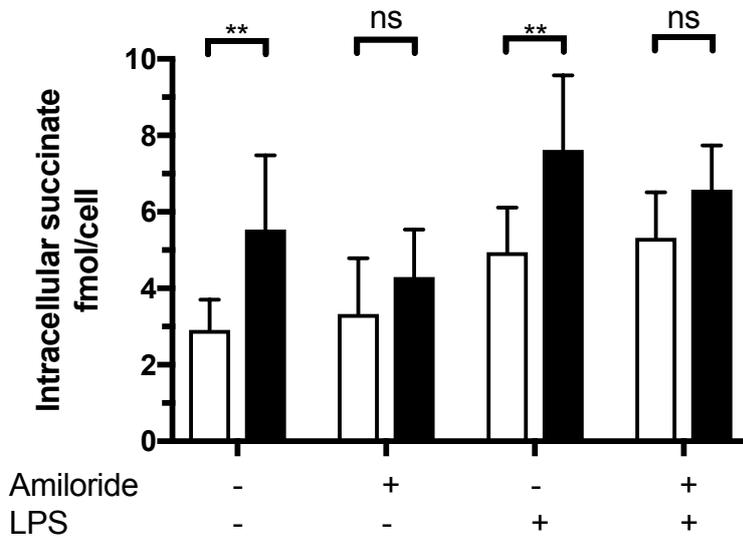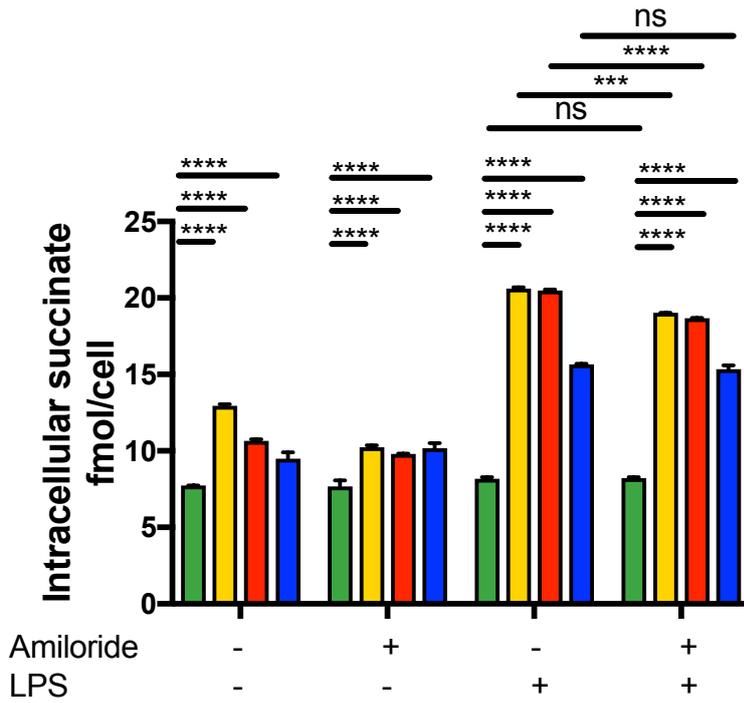
Figure 4.4.3: Intracellular succinate concentration in HBECs and primary monocytes.

Colorimetric assays were used to detect intracellular succinate in HBECs (n=3) and primary monocytes (n=7). Cell were pre-treated with amiloride (100mM, 1 hour) before an LPS (10ng/mL, 4 hours) stimulation. A 2-way ANOVA was performed (p values * = $\leq$0.05, **= $\leq$0.01, ***= $\leq$0.001 and ****= $\leq$0.0001).

Succinate accumulation was significantly increased in HBEC lines with CF-associated mutations compared to Beas2b (WT) (p=<0.0001) (Figure 4.4.3). Amiloride was able to reduce the succinate accumulation but did not alter the statistically significant elevation in succinate in HBEC lines with CF-associated mutations compared to Beas2b (WT). Upon LPS treatment, succinate levels approximately doubled in both IB3-1 (Δf508/W1282X) and CuFi-1 (Δf508/Δf508) HBEC lines compared to unstimulated, and CuFi-4 (Δf508/G551D) increased by around 50%. The Beas2b (WT) cell line did not increase succinate levels upon LPS treatment. Amiloride significant decreased succinate accumulation in both IB3-1 (Δf508/W1282X) and CuFi-1 (Δf508/Δf508) HBEC lines.

Succinate accumulation was significantly increased in monocytes from patients with CF at both unstimulated and with LPS stimulation compared to HC monocytes (p=0.0003 and p=0.0003 respectively). Increased succinate accumulation was observed in both HC and CF monocytes with LPS stimulation compared to the relative unstimulated control. Amiloride was able to modulate succinate accumulation in CF monocytes when it was used to pre-treat cells, prior to LPS stimulation.

4.4.4 Glycolytic flux assay

The glycolytic flux assay measures ECAR, as with the basal metabolic phenotype data (section 4.3), but probes further into the key parameters of glycolytic flux (Figure 4.4.4). This assay is described in detail in the methods section of this chapter (section 2.9) but briefly, glucose is injected into the *in vitro* assay plate to measure the rate of glycolysis under basal conditions, then oligomycin (10μM) is injected to induce pyruvate production as well as ATP, NADH, H_2O and H^+ and the final injection of 2-deoxy-glucose (2-DG) is then injected onto

the cells to inhibit glycolysis, through competitive-binding to glucose hexokinase. By using the above injection strategy, the glycolysis stress test can determine the following parameters (Details of seahorse OCR and ECAR traces are described in appendix figure 8 and 9):

Glycolysis- The amounts of glycolysis taking place in response to glucose.

Glycolytic Capacity- the maximum amount of glycolysis that can take place in a cell in response to oligomycin (OXPHOS inhibitor), which drives the cell to use glycolysis to its theoretical maximum capacity.

Glycolytic Reserve- how close a cell is to using its theoretical glycolytic capacity or the difference between glycolysis and glycolytic capacity.

Non-Glycolytic acidification- at baseline, how much ECAR is taking place before glucose is added, indicating other sources of ECAR that are not due to glycolysis. This ECAR measurement is in addition, rather than a component part of, the above parameters.
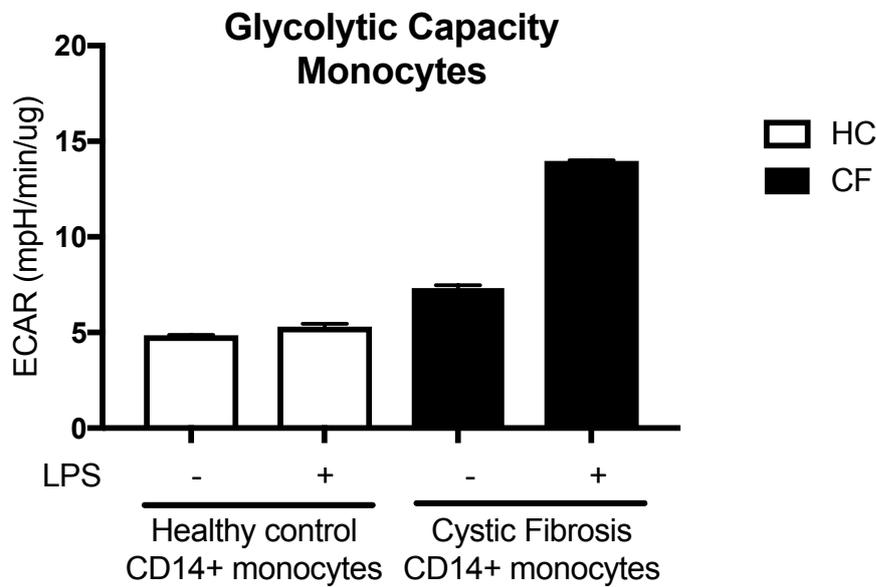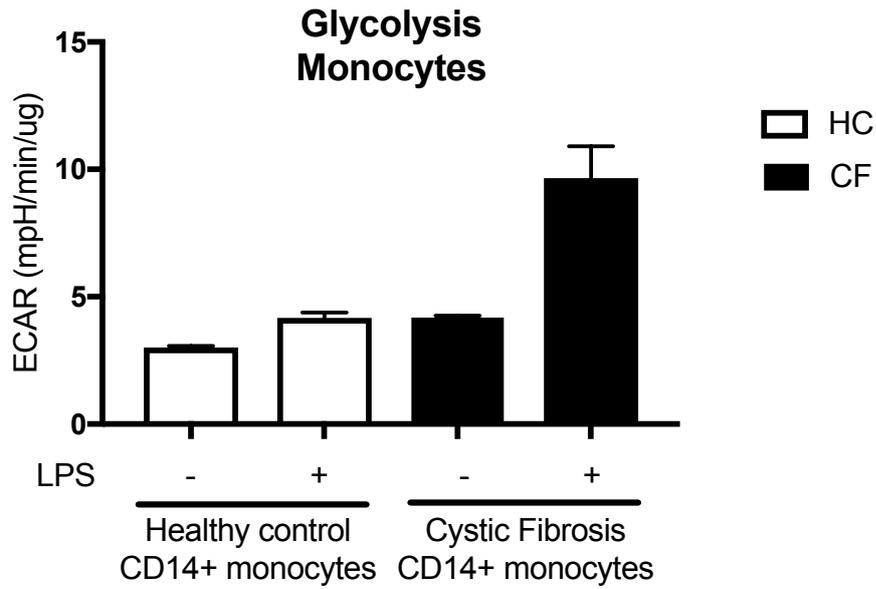
(Figure 4.4.4 legend on next page)
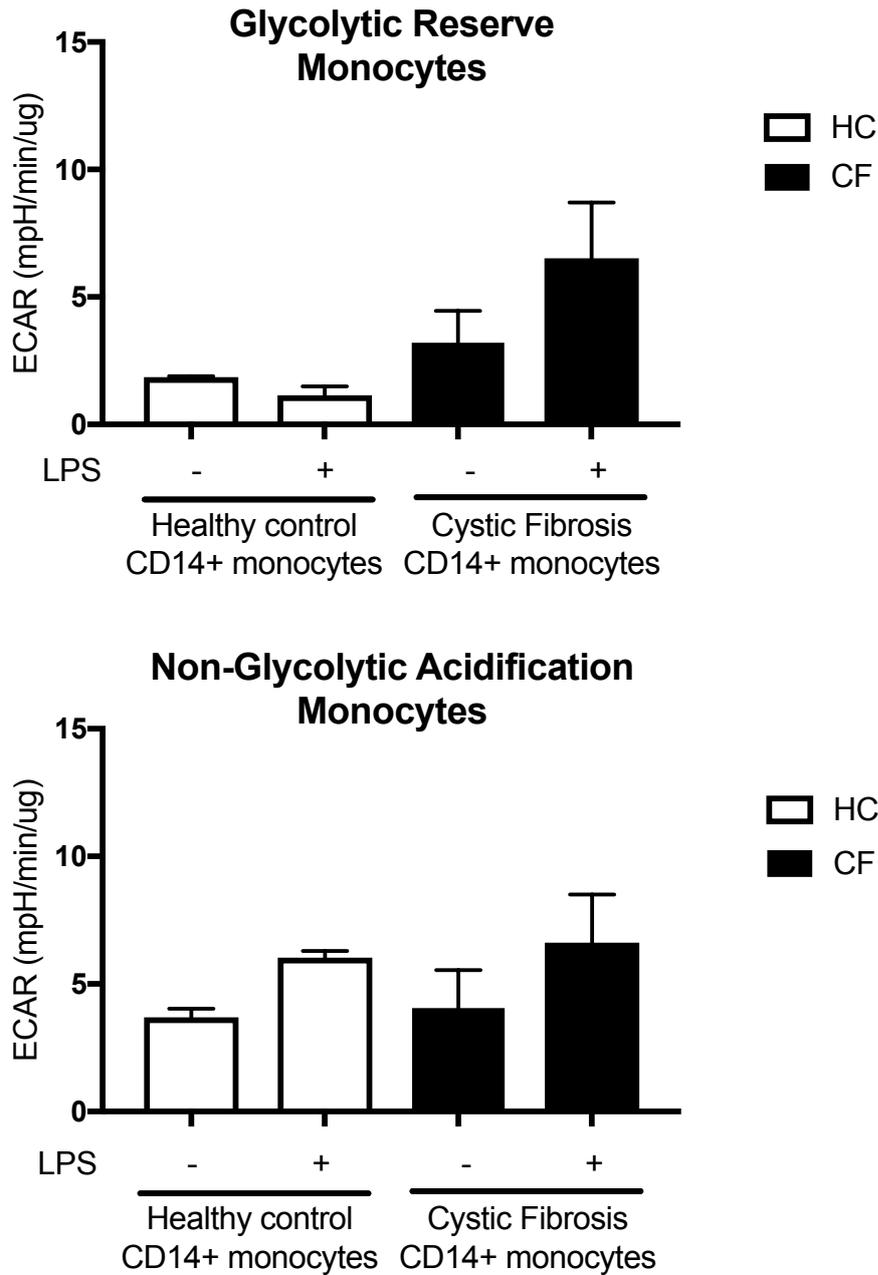
Figure 4.4.4: Glycolytic flux in monocytes from HC individuals and patients with CF. A

Seahorse extracellular flux analyser measured the extracellular acidification rate (ECAR) in

HBECs (n=3) and monocytes (n=3). Oligomycin (10μM), an inhibitor of ATP synthase, and

the uncoupling agent, Carbonyl cyanide-4-(trifluoromethoxy) phenylhydrazone (FCCP)

(5μM), were used to metabolically stress and depolarise cellular mitochondrial membranes.
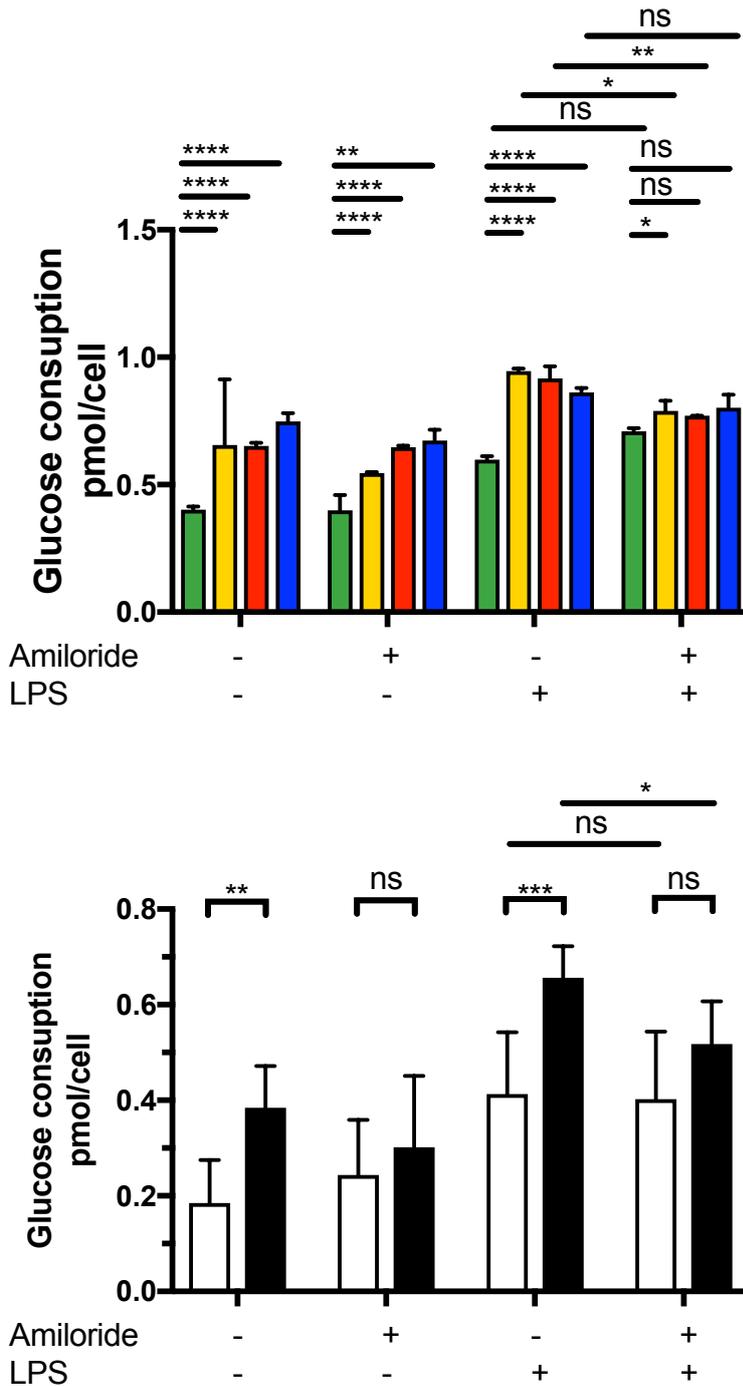
Cell were pre-treated with amiloride (100mM, 1 hour) before an LPS (10ng/mL, 4 hours)

stimulation. A 2-way ANOVA was performed (p values * = ≤0.05, **= ≤0.01, ***= ≤0.001 and ****= ≤0.0001).

Glycolysis is elevated upon LPS stimulation in both HC and CF monocytes, but more so in CF monocytes (Figure 4.4.4). There was no statistical significance due to large 95% confidence interval in the CF monocytes upon stimulation data. The median glycolytic capacity is higher in CF monocytes upon stimulation with LPS compared to HC monocytes under the same conditions. There was no statistical significance due to large 95% confidence interval in the CF monocytes upon stimulation data. There was no real difference observed between LPS stimulated or unstimulated conditions within either HC or CF cohorts. However, the median glycolytic reserve is higher in CF monocytes compared to HC monocytes. There was no statistical significance due to large 95% confidence interval in the CF monocytes upon stimulation data. There was no real difference between HC or CF cohorts in terms of non-glycolytic acidification. However, the median non-glycolytic acidification is higher in the LPS stimulated or unstimulated conditions within either HC or CF cohorts. There was no statistical significance due to large 95% confidence interval in the CF monocytes upon stimulation data.

4.4.5 HIF1α and IL-1β

As glycolysis and the subsequent succinate accumulation are associated with downstream *IL1β* gene expression, a RT-qPCR was performed on monocytes from HC, CF and a SAID patient with Pyrin-Associated Autoinflammation with Neutrophilic Dermatosis (PAAND) (a control cohort for elevated *IL1β* gene expression responses to LPS stimulation) after LPS stimulation (Figure 4.4.5). The hypothesis is based on the data shown in this chapter, suggesting metabolism is heightened (or energetic) in cells with CF-associated mutations,

particularly when challenged with LPS and that there is a metabolic switch to glycolysis, where glycolysis in the form of ECAR, lactate production, glucose consumption and succinate accumulation was shown to be elevated to a statistically significant level.
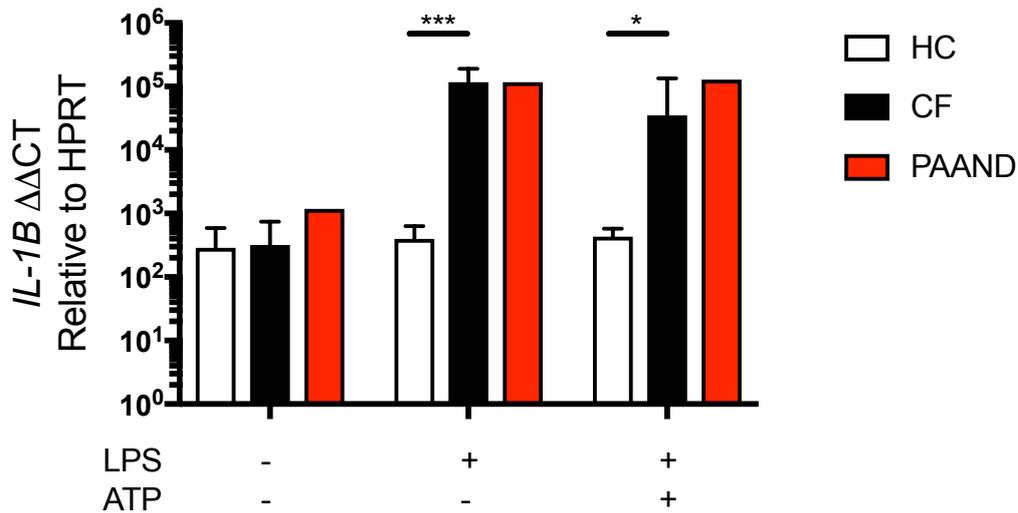
Figure 4.4.5: Gene expression of *IL1B* in monocytes: Gene expression of *IL1B* was measured using RT-qPCR and a SYBR green detection assay in monocytes from HC (n=10), patients with CF (n=12) and PAAND (n=1). Cell stimulation was as follows: stimulation with LPS (10ng/mL) for 4-hours with an ATP (5mM) stimulation for the final 30 minutes. Data are presented on a logarithmic scale with A repeated measures 2-way ANOVA statistical test was performed with Turkey's multiple comparisons test (p values * = ≤0.05, **= ≤0.01, ***= ≤0.001 and ****= ≤0.0001).

Both CF and PAAND monocytes increased *IL1β* transcript levels upon stimulation with LPS or LPS and ATP in combination, in comparison to monocytes from HC individuals. Statistically significant levels of *IL1β* were observed in the CF cohort, but not in the PAAND monocytes due to there being an n=1 for this rare condition.

4.5 Mitochondrial ROS

Mitochondrial ROS (mROS) was investigated because, as previously discussed in Chapter 3 (section 3.1.1 and figure 3.1.2), the link between metabolism and NLRP3 inflammasome activation may be due to the fact that a metabolic switch towards glycolysis causes RET and mROS production by complex I of the ETC. This mROS is a known activator of NLRP3. Therefore, the hypothesis to be tested here is that the increased glycolytic metabolism, described in this chapter, primes the inflammasome through mROS and perhaps even mitochondrial damage and mtDNA release, rather than TCA cycle break points inducing succinate-driven NLRP3 inflammasome priming. Details of mitosox flow cytometry gating are described in appendix figure 10.

4.5.1 mitoSOX
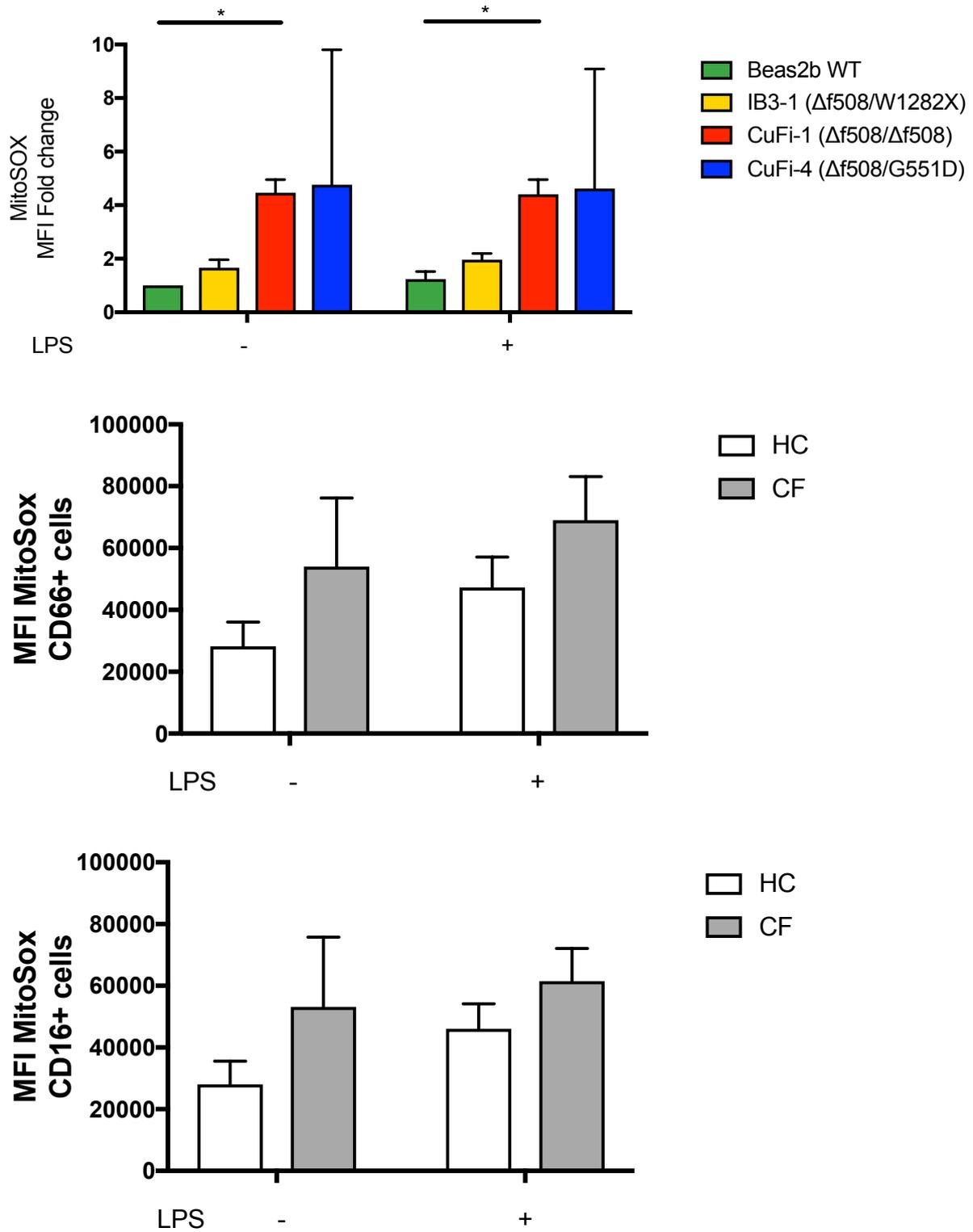
Figure 4.5.1: Mitochondrial reactive oxygen species (mROS) levels in HBECs and immune cells from whole blood. Peripheral blood mononuclear cells (PBMCs) (n=3) were

isolated from whole blood and analysed using flow cytometry based on CD16 and CD66 cell surface marker expression, forward and side scatter (size and granularity) as well as mitoSOX, a fluorescent stain for mROS. Data is expressed as median fluorescence intensity (MFI). Cell stimulation was with LPS (10ng/mL) for 4-hours. A repeated measures 2-way ANOVA statistical test was performed with Turkey's multiple comparisons test (p values $* = \leq 0.05$, $** = \leq 0.01$, $*** = \leq 0.001$ and $**** = \leq 0.0001$).

Using a specific fluorescent, intracellular probe for the presence of mROS, both HBEC lines and whole blood samples from patients with CF and healthy control individuals were examined for this form of ROS, using flow cytometry in order to quantify the amount of ROS in different populations (Figure 4.5.1). Elevated levels of mROS were detected in all three HBEC lines with CF-associated mutations, however only CuFi-1 (Δf508/Δf508) HBECs were significantly increased. There was no difference in mROS production between unstimulated and LPS-stimulated cells.

When CD66$^+$ cells and CD16$^+$ were gated on using whole blood, there was no significant difference between HC or CF cells or between unstimulated and LPS-stimulated cells in terms of mROS production.

4.6 Glycolysis and NLRP3 inflammasome activation

4.6.1 Inhibition of glycolysis modulates NLRP3 inflammasome activation

With the data in this chapter thus far indicating a glycolytic metabolic shift in HBECs and immune cells with CF-associated mutations, the next hypothesis to be tested was that this

glycolysis is both a marker of and a contributing element to the proinflammatory phenotype and function of both these cell types, as observed in chapter 3. 2-DG was used to inhibit glycolysis and cytokine secretion was then measured from these *in vitro* cell cultures, to determine whether glycolysis is modulating the secretion of these cytokines.
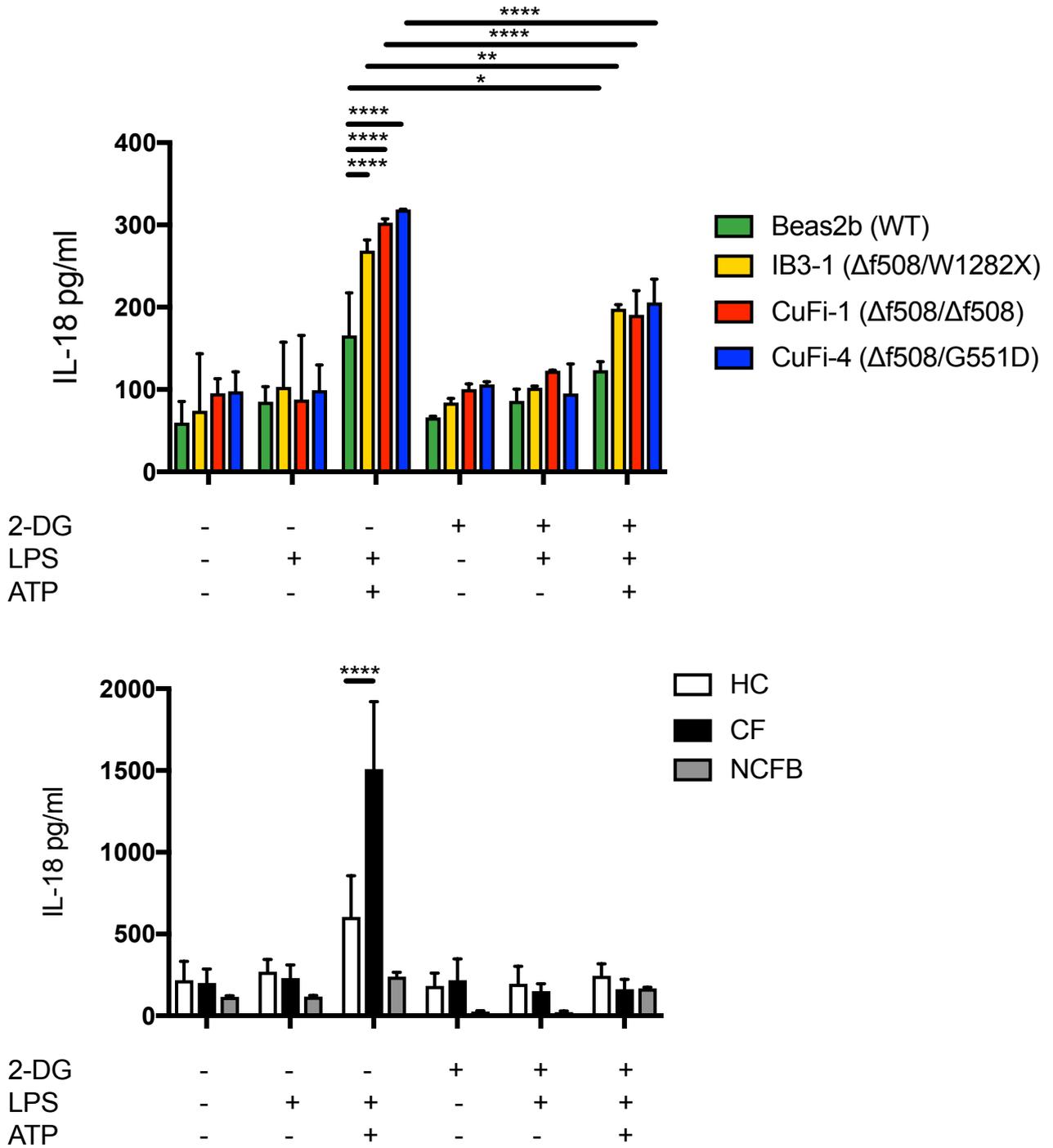
(Figure 4.6.1 legend on next page)
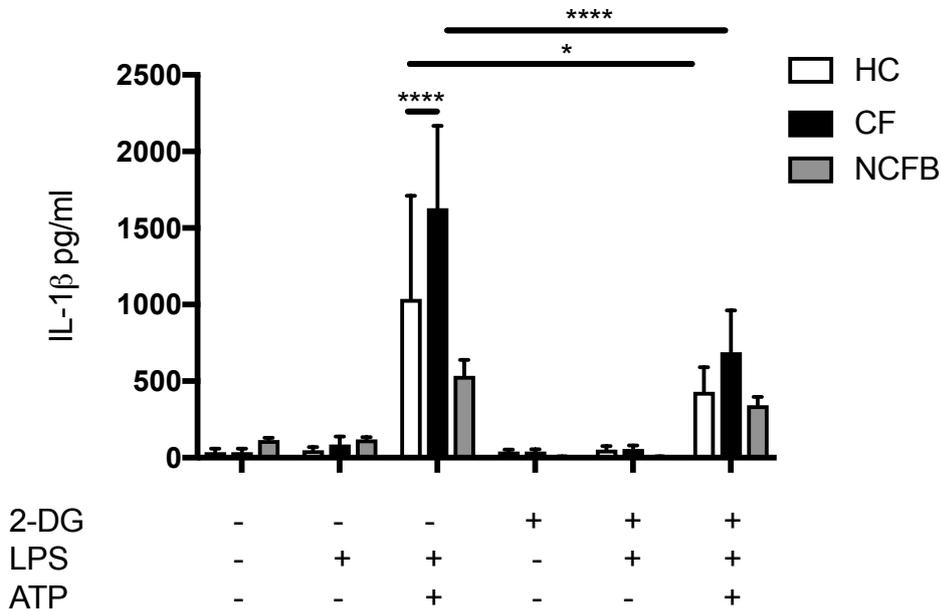
Figure 4.6.1: Effects of glycolysis inhibition on IL-18 and IL-1β secretion in HBECs and monocytes. ELISA assays were used to detect IL-18 and IL-1β in monocytes from HC (n=6), patients with CF (n=6) and NCFB (n=4) as well as HBECs (n=3). Cell stimulation was as follows: 2-DG (0.5mM) was pre-treated for 2-hours before a stimulation with LPS (10ng/mL) for 4-hours with an ATP (5mM) stimulation for the final 30 minutes. A repeated measures 2-way ANOVA statistical test was performed with Turkey's multiple comparisons test (p values * = ≤0.05, **= ≤0.01, ***= ≤0.001 and ****= ≤0.0001).

As demonstrated before (Section 3.4.2, Figure 3.4.2.1), HBEC lines with CF-associated mutations had increased levels of IL-18 secretion to a statistically significant level after LPS-driven priming and ATP-driven assembly of the NLRP3 inflammasome. When HBECs were pre-treated with the small molecule 2-DG to inhibit glycolysis, IL-18 secretion was

significantly inhibited in all HBEC lines with CF-associated mutations as well as the Beas2b (WT) cell line (Figure 4.6.1).

IL-18 and IL-1β secretion was, as previously observed (Section 3.4.2; Figure 3.4.2.2) significantly elevated in monocytes from patients with CF-associated mutations compared to HC and NCFB monocytes. The pre-treatment of 2-DG significantly inhibited the secretion of both IL-18 and IL-β in monocytes from all cohorts, with no significant difference between HC, CF and NCFB monocytes with 2-DG pre-treatment and subsequent NLRP3 inflammasome activation (figure 4.6.1).

4.6.2 Inhibition of glycolysis does not modulate TNF
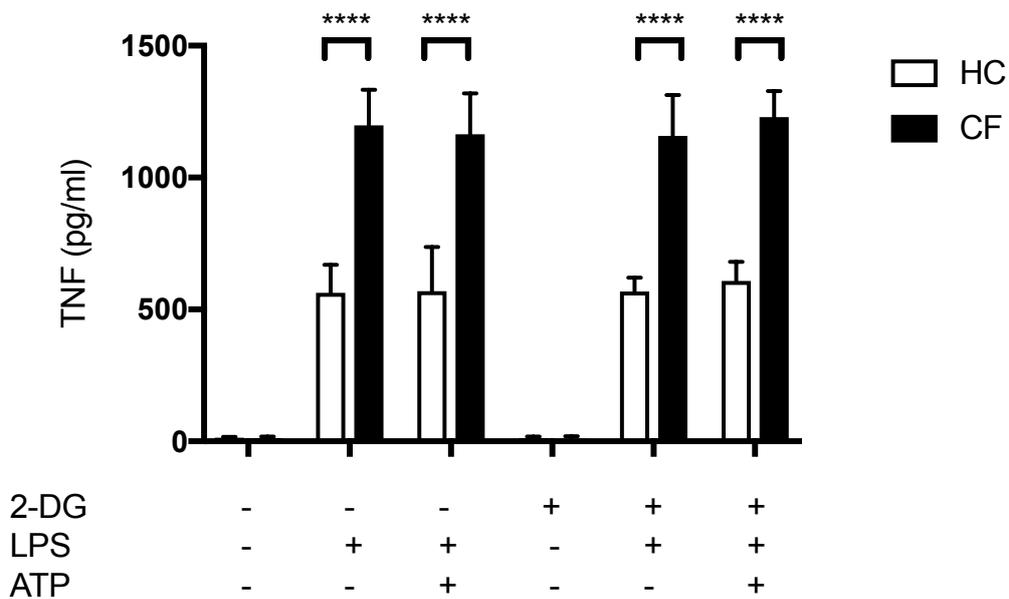
Figure 4.6.2: Effects of glycolysis inhibition on TNF secretion in HBECs and monocytes. ELISA assays were used to detect TNF in monocytes from HC (n=6), patients with CF (n=6) and NCFB (n=4) as well as HBECs (n=3). Cell stimulation was as follows: 2-DG (0.5mM) was pre-treated for 2-hours before a stimulation with LPS (10ng/mL) for 4-hours with an ATP

(5mM) stimulation for the final 30 minutes. A repeated measures 2-way ANOVA statistical test was performed with Turkey's multiple comparisons test (p values * = ≤0.05, **= ≤0.01, ***= ≤0.001 and ****= ≤0.0001).

To ensure that inhibition of glycolysis was indeed inhibiting the glycolysis/succinate/IL-1β axis, rather than inhibiting another inflammatory pathway or preventing secretion or inducing cell death through off-target effects of 2-DG, the proinflammatory cytokine, TNF was analysed under the same conditions as in section 2.6.1 (Figure 4.6.2). TNF secretion was elevated in monocytes from patents with CF to a statistically significant level. Notably, inhibition of glycolysis with a 2-DG pre-treatment had no effect on TNF secretion in either patient cohort.

4.6 Discussion

4.6.1 Energetic metabolic phenotype in CF

Based on the data presented in this chapter, it can be confidently stated that both HBEC lines and immune cells with CF-associated mutations not only have an energetic metabolic phenotype, perhaps due to an increased energy demand, but they also have an enhanced predisposition for a glycolytic metabolic switch, particularly when challenged with stimuli, such as LPS, to induce a proinflammatory immune response. Both OXPHOS and glycolysis are elevated in HBEC lines, monocytes and T-cells with CF-associated mutations, particularly upon stimulation. ECAR levels, as a readout of glycolysis, were notably upregulated in HBEC lines, monocytes and T-cells with CF-associated mutations. Further data to suggest that HBEC lines and monocytes with CF-associated mutations were upregulating metabolic pathways,

particularly glycolysis in response to LPS, was that intracellular ATP levels were also significantly increased, especially upon LPS stimulation. Notably, inhibition of Na^+ channels with a pre-treatment of amiloride was able to modulate ECAR and ATP, but not oxygen consumption. These data suggest that inhibition of Na^+ channels upstream have the following effects:

1. Direct modulation of the proinflammatory phenotype (through modulation of NLRP3 inflammasome activation) and, therefore, less glycolysis is observed, as a marker of such inflammatory phenotypes.
   and/or;

2. Lessening of the cell's energy demands by reducing the effects of overactive Na^+ channels and the consequential energy consuming compensatory mechanisms a cell may employ to re-establish electrochemical homeostasis and therefore reducing the need for enhanced metabolism to fuel such mechanisms, causing the downstream inflammatory effects of glycolysis to also reduce.

The first of these hypotheses has been shown to be true in the previous chapter, with data describing the anti-inflammatory effect that inhibiting Na^+ channels, particularly ENaC, has on NLRP3 inflammasome activation. If one considers the glycolytic metabolic switch to be a marker of a cell's decision to move into a proinflammatory state or phenotype and that upregulating glycolysis is perhaps downstream of other inflammatory pathways and decisions, then there is good evidence of this throughout this and the previous chapter. Therefore, HBEC lines and monocytes (and T-cells) with CF-associated mutations are predisposed and possess an inflammatory phenotype, particularly post-LPS challenge, and this inflammatory phenotype is characterised by enhanced NLRP3 inflammasome activation, IL-18 and IL-1β secretion and a metabolic switch towards glycolysis. Furthermore, by modulating Na^+ channels in HBEC

lines and monocytes, this inflammatory state can be diminished in terms of glycolytic metabolic shift, NLRP3 inflammasome activation and IL-18 and IL-1β secretion.

The latter hypothesis regards the metabolic switch towards glycolysis as a driving force behind NLRP3 inflammasome activation and subsequent IL-18 and IL-1β secretion. A possible cause for an increased energy demand in CF in terms of disruption of ion flux concerns the increased activity of the Na^+/K^+ ATP-activated channel in CF; an important adaptation necessary to tackle the reestablishment of the balance of Na^+ and K^+. This balance is maintained by the Na^+/K^+ ATP-activated channel, which pumps Na^+ and K^+ ions across the plasma membrane against the electrochemical gradient. This process requires energy in the form of ATP. The excess Na^+ influx, in CF cells requires the Na^+/K^+ ATP-gated pump to increase its activity in order to re-establish homeostasis. A consequence of this will not only be an influx of K^+ as described in the previous chapter, but a huge energy demand to fuel this channel. The hypothesis under these circumstances is that a cell with CF-associated mutations upregulates both OXPHOS and glycolysis to fuel the increased energy demand described above. Therefore, when a cell is further challenged to produce a proinflammatory state, a predisposition to shift to glycolysis and therefore exaggerated downstream inflammatory responses, such as NLRP3 inflammasome activation occur.

A caveat with the metabolic T-cell data in figures 4.3.1 - 4.3.2 is that the existence of TLR4-expressing T-cells capable of responding to LPS is limited to $CD4^+$ T-cell populations. The data presented in figures 4.3.1 – 4.3.2 is a population of $CD3^+$ T-cells and is not purified for TLR4-expressing $CD4^+$ T-cells and therefore will be contaminated with an unknown population of $CD8^+$ T-cells, unable to respond to LPS stimulation. This limitation makes the interpretation of the increased metabolic read outs for CF T-cells in response to LPS inconclusive. A future experiment to clarify the metabolic phenotype of CF T-cells would to

be purify both $CD3^+$ $CD4^+$ and $CD3^+$ $CD8^+$ T-cells and challenge them with TLR4 and T-cell receptor (TCR) agonists.

Evidence for both of the above hypotheses exists and the reality may, in fact, be a combination of both: diminishment of the exacerbated Na^+ influx in CF cells corrects an intrinsic pathogenic defect that underlies a predisposition to an inflammatory state and therefore both glycolysis and NLRP3 inflammasome activation are controlled downstream.

4.6.2 Elevated glycolysis in CF

Although the energy phenotype assay provided data suggesting that metabolism is both energetic and glycolytic in cells with CF-associated mutations, additional markers of glycolysis were measured to probe this observation further. These included lactate production, glucose consumption, succinate accumulation, glycolytic flux and subsequent *IL1β* transcript levels. As described in section 4.4, all of these read outs suggest a highly glycolytic metabolic shift in cells with CF-associated mutations as well as heightened *IL1β* transcript levels, compared to HC cells. In addition, each of these read outs can be further interpreted to provide additional information regarding CF pathology.

Increased lactate production corroborates Garnett *et al*s' report in which the consequences of elevated hyperglycaemia, observed in CF and CFRD, involved elevated glucose-dependent glycolysis and lactate production through MCT2. This metabolic shift described by Garnett *et al* was also observed in this study. However, in contrast to Garnett *et al*s' report, the glycolysis studied in this study has been strongly linked with Na^+-induced inflammation (rather than acidity of ASL). The MCT transporters that Garnett *et al* describe efflux H^+ with lactate, a possible mechanism for the ECAR observed in this study. Garnett *et al* also describe how *P. aeruginosa* is capable of stimulating a metabolic shift towards

glycolysis during hyperglycaemia, potentially through LPS/TLR4 signalling. This is also confirmed in this chapter, with LPS stimulations directly inducing an exaggerated and somewhat inappropriate glycolytic and inflammatory state in cells with CF-associated mutations compared their WT equivalents.

Increased glucose consumption and the subsequent glycolysis may actually be exacerbated and worsened in terms of the potential inflammatory consequences, by the high-calorie, high-fat diet. During *in vitro* experiments in which glucose was added to cells to measure glycolytic flux, cells with CF-associated mutations hyper-responded. This suggests that although the diet is there to compensate for malnutrition in individuals with CF, it may also be worsening the glycolytic inflammatory state observed in cells with CF-associated mutations throughout this study. Therefore, these data indicate that the CF diet should be altered to reduce hyperglycaemia and associated glucose consumption and glycolysis.

The understanding of how glycolysis and inflammation are linked and closely related is now well-described and understood. In this study, we conclusively show that succinate and *IL1β* are elevated in cells with CF-associated mutations. However, we were unable to detect HIF1α in either cell type or cohort. The link between succinate and *IL1β* is the activation HIF1α and this criticism of the data in this chapter only allows the link between succinate and *IL1β* to be correlated rather than stated with evidence-based vigour.

4.6.3 Elevated mROS in CF

To investigate the link between metabolism and inflammation in this study, it was also important to address mROS as a product of the metabolic switch to glycolysis and as a known activator of this study's inflammatory pathway of interest, the NLRP3 inflammasome. As previously discussed, mROS is produced after RET and is dependent on complex one of the

ETC. As NLRP3 is a PRR, it will detect mitochondrial components as if they were foreign, due to the ancient origins of the mitochondrial relationship with eukaryotic cells (see section 4.1.2). In this study, both HBEC lines and immune cells from whole blood were examined for mROS production, using a flow cytometry-based assay. Elevated mROS was observed in the CuFI-1 (ΔF508/ΔF508) HBEC line compared to the Beas2b (WT) cell line, with other two HBEC lines with CF-associated mutations also producing a higher amount of mROS compared to the Beas2b (WT) cell line, but this was not statistically significant. Notably, the HBEC lines did not respond to the LPS stimulation in terms of mROS production. This experiment was repeated multiple times as this was not an expected result, but if taken to be correct, then the logical conclusion is that HBEC lines did not respond to LPS challenge by upregulating mROS. It may be that the timing of this experiment was either too short or too long to see either a delayed or acute and transient mROS response, respectively.

When immune cells were analysed for mROS production from whole blood, the CD16 and CD66 cell surface markers were used to gate on specific populations of immune cells. CD66 is a marker for granulocytes, particularly neutrophils and CD16 is a cell marker that is expressed broadly on immune cells, but particularly on monocytes, when the size and granularity are used to further select for monocytic cells. However, it must be stated that other cell types may have been selected based on flow cytometric gating for CD16 positive cells. When these cell types were analysed for mROS from both HC individuals and patients with CF, there was an observed increased mROS level in both CD16+ and CD66+ cells, when LPS was used as a stimulant for mROS production, although not statistically significant. There was also a higher level of mROS in both CD16+ and CD66+ cells from patients with CF-associated mutations, compared to cells from HC individuals, but, again, this increase did not reach significance. Notably, the LPS stimulation did not increase mROS in these cell types in this

assay, as was the case with the HBEC lines. This indicates that perhaps the LPS stimulation may not have been correct, in terms of dose or timing, as previously mentioned.

The fact that there is no real significant increase in mROS upon LPS challenge, suggests that further optimisation of this stimulation may be required. However, there are no statistically significant data to indicate whether there is more mROS present at baseline between cells with CF-associated mutations or those that have WT CFTR or from HC individuals.

4.6.4 Oxygen consumption and hypoxia

An interesting result was that both oxygen consumption and ECAR were both elevated simultaneously in HBEC lines. When a metabolic switch is described in the literature, it is often described as an exclusive, 'all-or-nothing' switch to either OXPHOS or glycolysis. However, in this study evidence for both OXPHOS and glycolysis being simultaneously active may suggest there is a large number of elongated mitochondria, so that both pathways are able to take place, although further studies are required to investigate this theory. This phenomenon has been described in the literature (Zu and Guppy, 2004) and supports the hypothesis of an increased energy demand, within cells with CF-associated mutations, which are, therefore, highly metabolic in response.

As mentioned earlier (section 4.1.1), highly metabolic HBECs and immune cells with both increased oxygen consumption and ECAR will have profound effects on the CF lung. Not only will increased glycolytic activity and subsequent H^+ and lactate acidify the CF ASL, but an increased OXPHOS and oxygen consumption will also have an overwhelming effect on the oxygen concentration. This is particularly relevant in the CF lung as oxygen consumption, in combination with dehydrated mucous, will promote hypoxia. Hypoxia in the CF lung is often contributed to the presence of dehydrated mucous alone, preventing oxygen from dispersing to

the lower airways. The data throughout this chapter suggest that the increased energy dynamics observed in cells with CF-associated mutations may also have a confounding effect on ASL oxygen concentrations, thereby contributing to hypoxia in the lower airways.

4.6.5 Metabolism modulating macrophage phenotype

It is difficult to discern the true driving force behind the reduction in anti-inflammatory M2-type macrophages in CF after *in vitro* polarisation, as described in chapter 3 and by others (Tarique et al., 2017). The question of whether the inflammatory phenotype of CF cells is first driven by the intrinsic defect in ionic flux, leading to a predisposition towards NLRP3 activation and subsequent induction of glycolytic metabolism; or the contrary, in which the intrinsic defect predisposes to glycolytic metabolism and, therefore, to an enhanced NLRP3 inflammasome response. The data in this study suggest the latter. When 2-DG is used to inhibit glycolysis, NLRP3 inflammasome activation, in terms of IL-1β and IL-18 secretion, is diminished in both CF and HC monocytes and also in HBEC lines. This indicates that glycolysis is overactive in CF and that it is upstream of NLRP3 inflammasome activation. With glycolysis being a known influencer of macrophage phenotype, it can be inferred that the switch observed in metabolism in CF predetermines the lack of M2-type anti-inflammatory macrophages with CF-associated mutations. There is also evidence that NLRP3 expression and activation supports M2-type macrophages, via IL-14 signalling (Liu et al., 2018).

4.6.6 Systemic metabolism and cellular metabolism

The hypothesis being tested in this study is that aberrant ENaC-dependent Na^+ influx drives ATP-dependent ion channels, such as the Na^+/K^+ ATP-activated channel, in cells with

CF-associated mutations, which then increases cellular energy demands, subsequent energetic metabolism and downstream inflammatory phenotype reprogramming. Metabolically configured proinflammatory CF immune cells are then prone to excessive and inappropriate inflammatory responses to stimuli, in particular via the NLRP3 inflammasome.

There is another hypothesis that may also explain some of the observations made in this study. Systemic metabolism, that is nutrient availability and peripheral metabolite concentration, is affected by the gut microbiome and an individual's diet. These factors will have a profound impact on the immune cells' own metabolic pathways and, thus, their inflammatory phenotype. The metabolic microenvironment will influence epigenetic changes within immune cells, in terms of control over metabolic gene expression and pathway activity. Hyperlipidaemia, obesity and diabetes have been studied for links between systemic metabolism and immune cell metabolism and phenotype, with inflammatory consequences. This leads to a potential opportunity to therapeutically modify both diets and gut microbiome to modulate the degree of inflammation in a variety of conditions, including CF.

Chapter 5

5.0 NLRP3 inflammasome and metabolism during Orkambi treatment

5.1 Introduction

The most successful new medicines for the treatment of CF have been the targeted small molecule drugs, which have led to the dawn of a new era of personalised, precision medicines. Vertex® Pharmaceuticals have pioneered this revolution in CF therapy, with their flagship small molecules VX-770 (ivacaftor) and VX-809 (lumacaftor), which respectively potentiate and correct specific CFTR mutations (Deeks, 2016, Wainwright et al., 2015, Zhang et al., 2016) (described in section 1.1, figure 1.1.2). In combination, ivacaftor/lumacaftor (orkambi) is used as a targeted therapy for the most common CF genotype- Δf508/Δf508. The success of these molecules, particularly ivacaftor for class II mutations (Cholon et al., 2014), has provoked several pharmaceutical companies to target multiple ion channels in order to increase the length and quality of life for patients with all CF-associated mutations. This chapter will introduce the multitude of small molecules that have been developed for treatment of CF before presenting data generated by this study that will describe how the combination of ivacaftor/lumacaftor (orkambi) not only improved lung function, but also has anti-inflammatory properties.

5.1.1 Small molecule drugs for CF therapy

Ivacaftor was the first, approved mutation-specific drug for use in CF (Accurso et al., 2010). Ivacaftor targets class III mutations (Figure 1.1.2), which are characterised by CFTR

mutations causing gating defects leading to a permanently closed channel. The most common class III mutation carried by approximately 4% of CF patients is Gly551Asp or G551D. Other class III mutations account for a further 1% of patients. Ivacaftor was discovered using high-throughput screening of over 200,000 small molecules for potentiation of CFTR, which showed increased conductance and open probability of CFTR *in vitro* (Wainwright et al., 2015). Ivacaftor improved multiple outcome measures in CF patients and is now used for various class III mutations as well as in combination with lumacaftor (Deeks, 2016).

Lumacaftor was also discovered using high-throughput screening of small molecules for improvements in chloride transport of CFTR (Van Goor et al., 2011). Lumacaftor was shown to bind CFTR directly *in vitro*, and was able to stabilise TMD1, improving folding and interactions between the domains of CFTR (Ren et al., 2013). Lumacaftor improved chloride transport to around 14% of that of WT CFTR. The next generation of correctors has led to new analogues of lumacaftor, such as VX-661, as well as double- or triple-combination small molecule therapies for CF treatment (Mijnders et al., 2017). In class I mutations, no protein is produced and, therefore, small molecule modulators that directly bind and modulate CFTR are ineffective. Other potent CFTR correctors exist, such as GLPG2222 and GLPG2851, that, in combination with secondary C2 correctors such as GLPG2737, induce elevated CFTR expression and activity (Singh et al., 2016).

Premature termination codons (PTCs) cause ribosomes to read the PTC and halt translation of the protein (Welch et al., 2007). This premature termination of translation results in an unstable and non-functional CFTR protein. PTCs can be targeted therapeutically, with aminoglycoside antibiotics that interfere with normal bacterial translation by binding to 16S ribosomal RNA and causing an accumulation of truncated proteins and bacterial cell death (Hermann, 2007). Synthetic aminoglycoside (geneticin), a read-through agent, was able to supress PTC detection by ribosomes in HeLa and IB3-1 cells, with full length CFTR being

expressed in the latter cell line (Howard et al., 1996). Ataluren (PTC124) is a systemic bioavailable read-through agent taken orally, which has been trialled for class I CFTR mutations as well as Duchenne muscular dystrophy caused by nonsense mutations (Bushby et al., 2014). Ataluren is similar to aminoglycoside in that it is able to supress PTC detection by ribosomes (Bushby et al., 2014, Kerem et al., 2014, McElroy et al., 2013, Wilschanski et al., 2011, Kerem et al., 2008, Welch et al., 2007). A significant caveat to read-through agents is that there is the potential for significant off-target effects.

Cavosonstat and Riociguat are two proteostasis regulators that act on the CFTR interactome, meaning their mechanism of action is indirect in terms of CFTR modulation (Solomon et al., 2015, Donaldson et al., 2017). Nitric oxide (NO) produces cyclic GMP (cGMP) by NO-sensitive guanylate cyclase, which then activates protein kinase G2, which is able to induce CFTR activity through phosphorylation (Bellingham and Evans, 2007). Notably, NO and cGMP are also able to inhibit amiloride-sensitive sodium channel activity, perhaps through recovery of CFTR activity (Jain et al., 1998). Riociguat increases sensitivity of soluble guanylate cyclase to NO. Cavosonstat is an inhibitor of S-nitrosoglutathione reductase, increasing NO levels and thus levels of CFTR phosphorylation and activity.

Another approach to increase CFTR expression and amplification is through small molecule amplifiers. The small-molecule HDAC7 inhibitor SAHA1 amplifies Phe508del CFTR expression (Hutt et al., 2010). There is also evidence that SAHA1 also is able to modulate other HDAC7-senstive pathways that improve Phe508del folding, stability, trafficking and activity in addition to increasing CFTR expression. The specific CFTR amplifier PTI-428 increases CFTR protein levels that then allow correctors and potentiators to act on a larger pool of CFTR protein.

5.1.2 Targeting alternative chloride and sodium channels for CF therapy

Another tactic to restore ionic homeostasis is to target alternative channels. Epithelial cells are able to secrete chloride through calcium-activated chloride transport independent of CFTR. Stimulation of epithelial cells with agonists of calcium-release from intracellular stores induces chloride transport, independent of CFTR (Knowles et al., 1991). TMEM16A, or anoctamin-1 (ANO1), is a Ca^{2+}-dependent chloride channels (CaCC) that murine knockouts for TMEM16A abrogates the above non-CFTR calcium-mediated chloride transport upon calcium agonist stimulation (Caputo et al., 2008, Schroeder et al., 2008, Yang et al., 2008). Interestingly, TMEM16A has been shown to be activated by asthma-related Th2 cytokines IL-4 and IL-13 and TMEM16A has been shown to be elevated in airways of patients with asthma (Scudieri et al., 2012). TMEM16A may be a targetable alternative chloride ion channel for CF treatment with small molecule drugs.

SLC26A9 is an anion channel transporter that selectively functions as a chloride channel, without bicarbonate transport (Loriol et al., 2008). SLC26A9 is a 12 transmembrane domain channel that forms a chloride channel pore. Again, asthma-related Th2-driven inflammation has also been shown to upregulate SLC26A9 and may be a valid targetable alternative chloride ion channel for CF treatment with small molecule drugs (Anagnostopoulou et al., 2010).

Amiloride-sensitive sodium channels have been shown to be instrumental in CF pathology in terms of mucous dehydration (Kerem et al., 1999). In this study, said channels have been shown to be implicated in hyperinflammation and proinflammatory phenotypes of immune cells. ENaC is widely expressed and is involved in apical sodium uptake by absorptive epithelial cells. ENaC activity is elevated in CF, theoretically due to WT CFTR's ability to inhibit ENaC whereas Phe508del CFTR is unable to do so, although the precise mechanisms

remain unclear (Mall et al., 1998, Boucher et al., 1986, Knowles et al., 1981). In addition, the proinflammatory environment in the airways is able to activate ENaC directly and indirectly through neutrophil elastase and proteolytic cleavage and degradation of SPLUNC1 (section 1.1) (Hobbs et al., 2013). The βENaC-Tg mouse overexpresses the β-subunit of ENaC, with subsequent increases in Na^+ absorption leads to dehydration of the ASL and a CF-like lung disease, including periodic infection and inflammation (Mall et al., 2004, Zhou et al., 2011, Zhou et al., 2008). Targeting amiloride-sensitive sodium channels such as ENaC has been attempted in the early 1990's using amiloride with little efficacy, most likely due to amiloride's modest half-life and effectiveness (Graham et al., 1993, Knowles et al., 1990). There are recent studies showing that pre-emptive amiloride may be more effective, based on studies with the βENaC-Tg mouse (Zhou et al., 2008). Developing new ENaC inhibitors is an ongoing mission of multiple academic and pharmaceutical groups: high-throughput screening of small molecules (as with ivacaftor and lumacaftor), small interfering RNAs (siRNAs) (Gianotti et al., 2013), targeting the proteases that activate ENaC (Gaillard et al., 2010) and modifying endogenous ENaC inhibitors to increase their viability in the acidic CF lung (Garcia-Caballero et al., 2009), are all approaches for *in vivo* ENaC inhibition.

Inhibitors of amiloride-sensitive sodium channels or stimulation of alternative Cl^- channels are two therapeutic strategies that not only may have disease modifying effects but also offer therapeutic potential regardless of CFTR genotype.

5.1.3 Ivacaftor and Lumacaftor combination therapy – CFTR modulation

The outstanding disease modifying effects of ivacaftor have revolutionised treatment of patients with class III CFTR mutations. Due to the nature of the drug discovery process in the case of ivacaftor and lumacaftor, the precise molecular mechanisms of action of either drug

is not fully understood. This section will summarise what is known regarding how ivacaftor and lumacaftor work at the molecular level and the clinical trials that have followed, leading to their approval and use for treatment of CF.

Ivacaftor, as previously described, was discovered using high-throughput screening of small molecules for potentiation of class III mutated CFTR, which showed increased short-circuit current (I_{sc}) in G551D CFTR FRT cells by around 4-fold and increased open probability (*Po*) of G551D CFTR by 6-fold *in vitro* (Eckford et al., 2012, Jih and Hwang, 2013). Greater effects of ivacaftor were observed in primary CF HBECs heterozygous for G551D, with an improved I_{sc} of 10-fold. Ivacaftor also decreased ENaC-dependent Na^+ absorption, rescuing cilia beating through mucous hydration (Eckford et al., 2012, Jih and Hwang, 2013). Studies investigating the *in vitro* molecular mechanisms of ivacaftor's modulatory effects on G551D CFTR observed that ivacaftor binds directly to the MSD domains of CFTR to stabilise its post-hydrolytic open state. Normally CFTR activity is controlled by phosphorylation, ATP and hydrolysis. Ivacaftor is able to activate CFTR in the absence of Mg-ATP through a nonconventional ATP-independent mechanism in which ivacaftor decouples the gating cycle and ATP hydrolysis cycle (Eckford et al., 2012, Jih and Hwang, 2013). Ivacaftor also increased the function of other class III and IV CFTR mutations. A multitude of trials have shown that ivacaftor is not only safe, but drastically improves lung function by at least 10%, reduces exacerbations by 55%, improves quality of life, increases weight gain and reduced sweat chloride by at least -48mmol/L by 48 weeks on average (Accurso et al., 2010, Cholon et al., 2014, Davies et al., 2013a, Davies et al., 2013b).

Lumacaftor, as previously described, was discovered using high-throughput screening of small molecules for correction of class II mutated CFTR (such as Δf508/Δf508), which showed an increase in CFTR maturation through the ER by around 7-fold and an increase in I_{sc} of 5-fold *in vitro (Ren et al., 2013, Van Goor et al., 2011, Wainwright et al., 2015).*

Equivalent effects of lumacaftor were observed in primary CF HBECs homozygous for Δf508, with an improved maturation of 8-fold and an increased I_{sc} of 4-fold. Click chemistry studies investigating the *in vitro* molecular mechanisms of lumacaftor's modulatory effects on Phe508del CFTR observed that lumacaftor binds directly to CFTR to induce correct folding in the ER (Sinha et al., 2015). Other studies have shown that lumacaftor's mechanism of action is through direct binding of Phe508del MSD1, correcting the defect to allow successful folding and escape from the ER (Ren et al., 2013). Clinical trials of lumacaftor did not produce improvements in lung function or patient outcome. However, when used in combination with ivacaftor (as in orkambi), there were significant improvements I_{sc} of up to 25% of that of WT CFTR HBECs as well as hydration of ASL *in vitro* (Wainwright et al., 2015, Zhang et al., 2016). In phase 2 and 3 trials of orkambi, both lung function and patient outcome, in terms of exacerbation rate and adverse events, showed significant improvements.

5.2 Methods

5.2.1 Patient cohort

The patient cohort in this study, recruited from 2015-2018, is detailed in the table below.

Baseline FEV	FEV1 (l/s)	FEV1 (%)	FVC (L)	FVC (%)	Weight (Kg)	BMI	CRP (mg/L)	Pathogen
40	0.95	23	1.69	35	48.3	16	31	PA
26	1.09	35	1.54	43	58.3	22.6	24	M ABS
51	0.82	28	1.37	41	53.2	19.4	<5	PA
34	1.5	35	3.09	59	74.1	22.6	<5	PA
39	1.04	28	2.26	60	58	20.8	<5	BCC
31	0.86	33	1.37	46	55.1	23.2	16.3	PA
30	0.74	17	2.56	49	64.45	19.9	27	PA
36	1.18	26	2.04	40	58.25	18.7	<5	PA

Median at Baseline	0.995	28	1.865	44.5	58.125	20.35	25.5
IQR	0.85	25.25	1.4975	40.75	54.625	19.225	22.075
Deaths	0						

Table 6: Available patient information form the Δf508/Phe508del CF Orkambi cohort recruited to this study. Details of baseline lung function FEV (l/s), FEV1, FEV1%, FVC (L), FVC%, weight (Kg) BMI, CRP (mg/L) and presence of infection are presented in this table from the patients enrolled onto the orkambi CF study (n=8), collected from clinical team at St James Hospital Adult CF ward, Leeds. Further details in appendix figure 12.

5.2.2 Cell culture

As in section 2.3.

Briefly, patients' blood samples were collected using Vacuette tubes (Greiner-bio-one) containing either clot activator or K3EDTA. Blood in clot activator tubes were allowed to clot for 60 min followed by centrifuging at 1000xg for 10 min. Sera were collected into 1mL tubes for storage at -80°C. Blood collected in K3EDTA tubes were used for PBMC isolation. EDTA treated blood were mixed with PBS in a 1:1 ratio, carefully layered onto 13mL of Lymphoprep® (Axis-Shield) in 50mL Falcon tubes and centrifuged at room temperature, 1100xg for 20 mins without brakes. The PBMCs 'buffy layer' on top of the Lymphoprep®

layer was extracted and washed in 3x volume PBS. Isolated PBMCs plated in 6 well plates, seeded at 1x106 cells/mL/well in 1mL RPMI medium (Sigma) supplemented with 10% FBS, 50 IU/ml penicillin, and 50 g/ml streptomycin.

5.2.3 ELISA

As in section 2.5.

Briefly, supernatants were collected from *in vitro* PBMC stimulations and serum was isolated from whole blood using clot-activating blood collection tubes that were centrifuged to separate out the sera from the whole blood. Serum was aliquoted and stored long-term at -80°C. Serum from healthy controls and patients with CF, diagnosed SAID and NCFB were collected and serum cytokines measured by ELISA, as per the manufacturer's instructions. The growth media supernatants from stimulated cell culture plates were stored at -20°C before being used to detect IL-1β and IL-18 cytokine secretion by ELISA.

5.2.4 Intracellular fluorometric assay

As in section 4.2.2. ATP and succinate (Assay kits, Abcam) were measured, as per the manufacturer's instructions.

5.2.5 Extracellular fluorometric assay

As in section 4.2.3. Extracellular glucose and L-lactate (Assay kits, Abcam) were measured, as per the manufacturer's instructions.

5.3 The effects of orkambi on serum cytokines

Serum levels of selected proinflammatory cytokines were analysed by ELISA, over the course of 3-months of compassionate orkambi treatment. The cytokines measured were the two proinflammatory, NLRP3-associated cytokines, IL1β and IL-18, as well IL-6 and TNF, two other cytokines also associated with innate immune cell activation.

5.3.1 Serum IL-18 and TNF
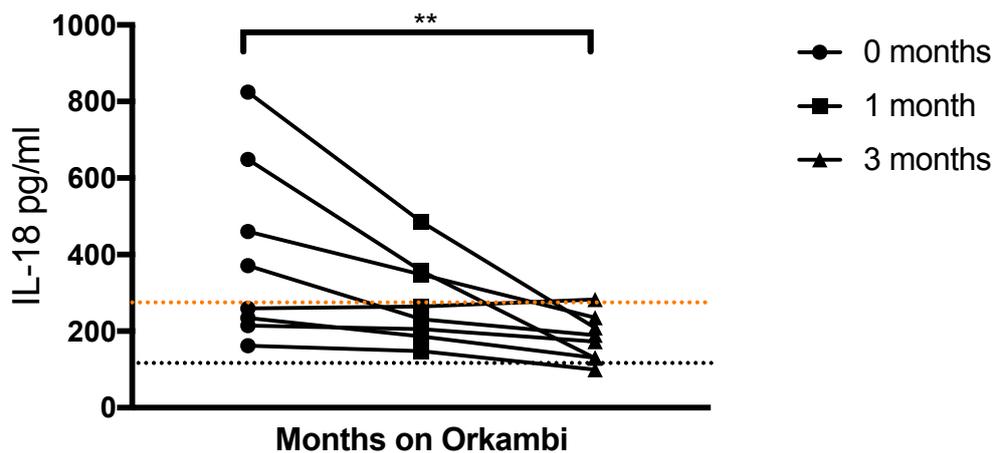
Figure 5.3.1.1: Serum IL-18 levels in patients with CF-associated mutations receiving compassionate orkambi treatment. ELISA assays were used to detect IL-18 in serum from patients (n=8) with CF-associated mutations receiving compassionate orkambi treatment. Orange and black dotted lines indicate mean average IL-18 serum levels in CF and HC serum from figure 3.3.1.1, respectively. The Friedman paired test with Dunn's multiple comparisons test was performed (p values * = ≤0.05, **= ≤0.01, ***= ≤0.001 and ****= ≤0.0001).

IL-18 is a cytokine that is constitutively expressed at the mRNA level but is only secreted upon inflammasome activation, predominantly NLRC4 and NLRP3 although this is cell type and pathogen specific. Active caspase-1 cleaves pro-IL-18 into its active form and allows its secretion through GSDMD-dependent pore formation. After 1-month of orkambi treatment, there was no statistically significant change in IL-18 serum levels. After 3-months of orkambi, there was a statistically significant reduction in serum IL-18 ($p=0.0081$).

TNF is a proinflammatory cytokine implicated in many immunological diseases, including rheumatoid arthritis and ankylosing spondylitis. TNF expression and secretion are induced by TLR activation as well as paracrine and autocrine signalling via TNF receptor binding. After 1-month of orkambi treatment, there was no statistically significant change in TNF serum levels. After 3-months of orkambi, there was a statistically significant reduction in serum TNF ($p=0.0179$).
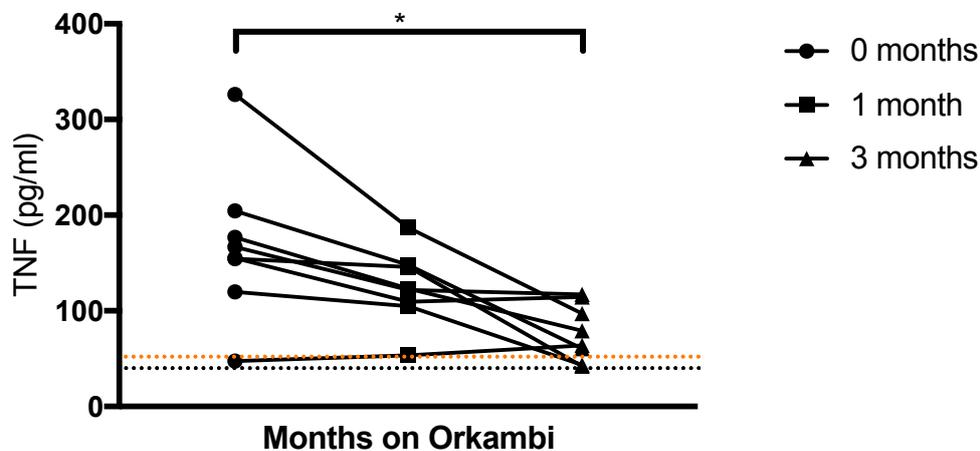
Figure 5.3.1.2: Serum TNF levels in patients with CF-associated mutations receiving compassionate orkambi treatment. ELISA assays were used to detect TNF in serum from patients (n=8) with CF-associated mutations receiving compassionate orkambi treatment. Orange and black dotted lines indicate mean average TNF serum levels in CF and HC serum

from figure 3.3.1.1, respectively. The Friedman paired test with Dunn's multiple comparisons test was performed (p values * = ≤ 0.05, **= ≤ 0.01, ***= ≤ 0.001 and ****= ≤ 0.0001).

5.3.2 Serum IL-1β and IL-6
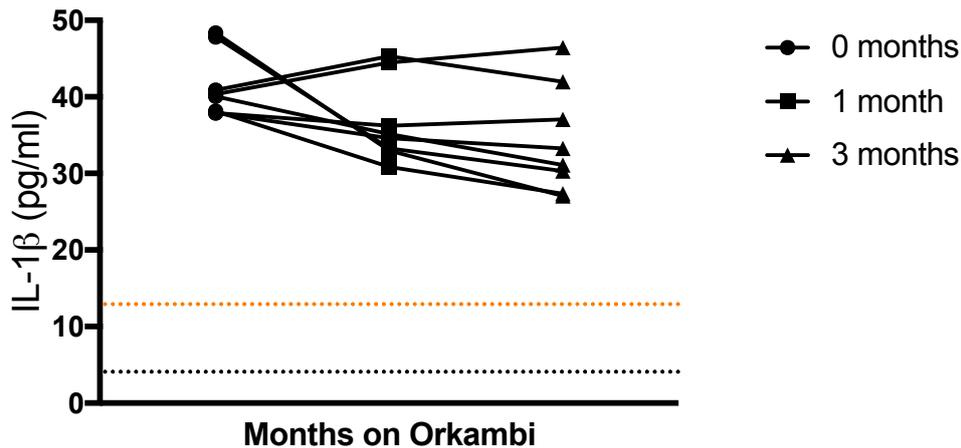
Figure 5.3.2.1: Serum IL-1β levels in patients with CF-associated mutations receiving compassionate orkambi treatment. ELISA assays were used to detect IL-1β in serum from patients (n=8) with CF-associated mutations receiving compassionate orkambi treatment. Orange and black dotted lines indicate mean average IL-1β serum levels in CF and HC serum from figure 3.3.1.1, respectively. The Friedman paired test with Dunn's multiple comparisons test was performed (p values * = ≤ 0.05, **= ≤ 0.01, ***= ≤ 0.001 and ****= ≤ 0.0001).

IL-1β is a cytokine that is expressed upon TLR activation as well as paracrine and autocrine signalling via IL-1 receptor signalling, although many other transcription factors are able to induce *IL1B* expression such as HIF1α and XBP1s. IL-1β is secreted upon inflammasome activation, predominantly NLRP3, although this is cell type and pathogen specific. Like IL-18, active caspase-1 cleaves pro-IL-1β into its active form and allows its

secretion through GSDMD-dependent pore formation. There was no statistically significant change in IL-1β serum levels after 1-month or 3-months of orkambi.

IL-6 is an atypical cytokine in that it can be both a proinflammatory and anti-inflammatory with differential roles in specific tissue-types. IL-6 is secreted by T-cells and macrophages in response to TLR activation as well as various other cytokine-mediated signalling events. IL-6 mediates fever, as does IL-1β, through facilitating the synthesis of PGE_2 in the brain. The anti-inflammatory effects of IL-6 are limited to its role as a myokine, a small molecule released by myocytes during muscle contraction with a role in repair of damaged muscle fibres post-exercise. The distinction in signalling cascades between myocytes and macrophages determines the inflammatory effects of IL-6, with macrophages predominantly utilising NF-κB as a proinflammatory transcription factor, myocytes employ Ca^{2+} driven NFAT and p38 MAPK. In this study, IL-6 is acting on a systemic level, secreted by immune cells into the peripheral blood, rather than myocyte secreted IL-6, which acts in a paracrine manner rather than systemically. There was no statistically significant change in IL-6 serum levels after 1-month or 3-months of orkambi.

Figure 5.3.2.2: Serum IL-6 levels in patients with CF-associated mutations receiving compassionate orkambi treatment. ELISA assays were used to detect IL-6 in serum from patients (n=8) with CF-associated mutations receiving compassionate orkambi treatment. Orange and black dotted lines indicate mean average IL-6 serum levels in CF and HC serum from figure 3.3.1.1, respectively. The Friedman paired test with Dunn's multiple comparisons test was performed (p values * = ≤ 0.05, **= ≤ 0.01, ***= ≤ 0.001 and ****= ≤ 0.0001).

5.4 The effects of orkambi on PBMC cytokine secretion

5.4.1 PBMC secreted IL-18 and TNF
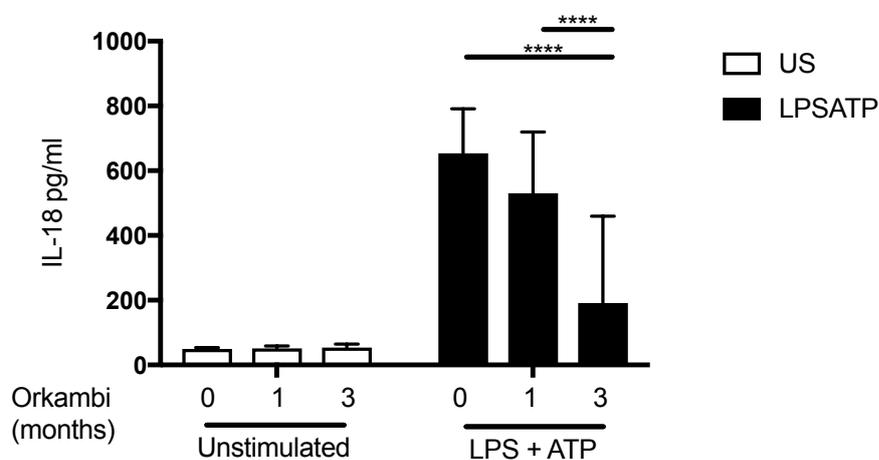
Figure 5.4.1.1: IL-18 secretion in patient PBMCs with CF-associated mutations receiving compassionate orkambi treatment. ELISA assays were used to detect IL-18 secretion in PBMCs from patients (n=8) with CF-associated mutations receiving compassionate orkambi treatment at baseline, 1-month orkambi and 3-months orkambi. PBMCs were stimulated with LPS (10ng/mL) for 4 hours before being stimulated for 30 minutes with ATP (5mM). A repeated measures 2-way ANOVA statistical test was performed with Turkey's multiple comparisons test (p values * = ≤0.05, **= ≤0.01, ***= ≤0.001 and ****= ≤0.0001).

Peripheral blood mononuclear cells (PBMC)s are immune cells isolated from whole blood with a single, round nucleus. PBMC isolation discriminates against platelets and erythrocytes (no nuclei) and granulocytes (multi-lobed nuclei). The cell types within PBMCs are predominantly monocytes and lymphocytes (B-cells, T-cells and NK cells). PBMCs were isolated from whole blood, along with serum (section 5.3), and stimulated *in vitro* with LPS and ATP for NLRP3 inflammasome priming and activation. This sample collection took place

parallel to the serum samples (section 5.3) at baseline (0-months), and after 1-month of orkambi and 3-months of orkambi therapy.

There was no change in *in vitro* IL-18 secretion at either 1-month or 3-months of orkambi treatment with unstimulated PBMCs. Upon stimulation, PBMCs from Δf508/Phe508del patients on compassionate orkambi therapy secreted large amounts of IL-18 at baseline, in a hyper-responsive reaction to NLRP3 stimulation that was also previously observed throughout chapter 3. After 1-month of orkambi treatment, PBMCs from Δf508/Phe508del patients on compassionate orkambi therapy secreted reduced IL-18 to a statistically significant level, upon stimulation with LPS and ATP. At the 3-months orkambi timepoint, IL-18 secretion *in vitro* was reduced compared to baseline and 1-month (p=<0.0001 and p=<0.0001 respectively).

There was no change in *in vitro* TNF secretion at either 1-month or 3-months of orkambi treatment with unstimulated PBMCs, with very little secreted TNF detected in any sample. Upon stimulation, PBMCs from Δf508/Phe508del patients on compassionate orkambi therapy at baseline secreted large amounts of TNF, in response to the LPS rather than ATP. After 1-month of orkambi treatment PBMCs from patients with Δf508/Phe508del mutations secreted reduced TNF but not to a statistically significant level, upon stimulation. At the 3-month orkambi timepoint, TNF secretion *in vitro* was reduced compared to baseline and 1-month (p=<0.0001 and p=<0.0001 respectively).

These observations with IL-18 and TNF correlate with the serum data (Figure 5.3.1.1) in which IL-18 and TNF levels reduced, generally, over the 3-months of orkambi treatment.
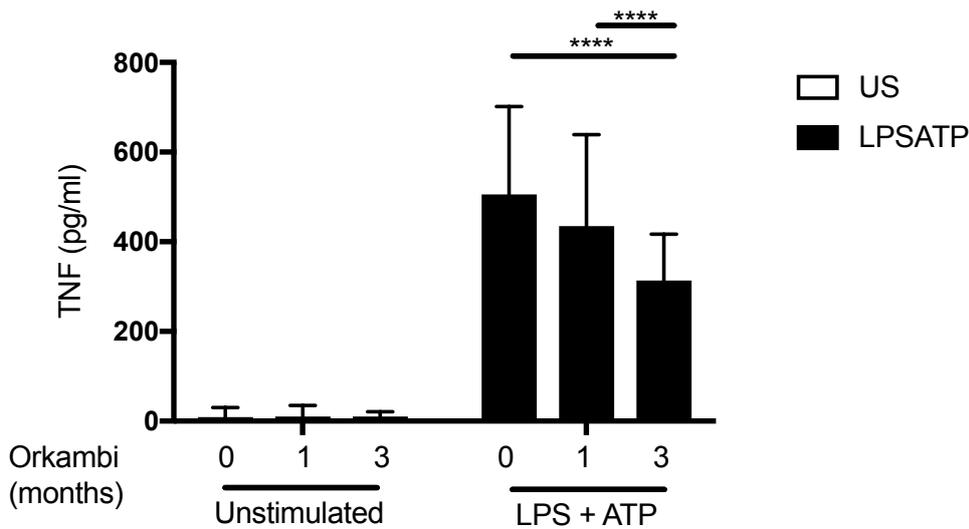
Figure 5.4.1.2: TNF secretion in patient PBMCs with CF-associated mutations receiving compassionate orkambi treatment. ELISA assays were used to detect TNF secretion in PBMCs from patients (n=8) with CF-associated mutations receiving compassionate orkambi treatment at baseline, 1-month orkambi and 3-months orkambi. PBMCs were stimulated with LPS (10ng/mL) for 4 hours before being stimulated for 30 minutes with ATP (5mM). A repeated measures 2-way ANOVA statistical test was performed with Turkey's multiple comparisons test (p values * = ≤0.05, **= ≤0.01, ***= ≤0.001 and ****= ≤0.0001).

5.4.2 PBMC secreted IL-1β and IL-6

There was no change in *in vitro* IL-1β secretion at either 1-month or 3-months of orkambi treatment with unstimulated PBMCs, with very little secreted IL-1β detected in any sample. Upon stimulation, PBMCs from Δf508/Phe508del patients on compassionate orkambi therapy at baseline secreted large amounts of IL-1β, in a hyper-responsive reaction to NLRP3 stimulation that was also previously observed with *in vitro* PBMC IL-18 and TNF secretion and throughout chapter 3. After 1-month of orkambi treatment PBMCs from Δf508/Phe508del patients on compassionate orkambi therapy secreted unchanged IL-1β levels, upon stimulation

with LPS and ATP. At the 3-month orkambi timepoint, IL-1β secretion *in vitro* was again unchanged compared to that of the other timepoints upon stimulation, with no statistically significant reduction between both 3-months and 1-month or baseline and 3-months.

There was no change in *in vitro* IL-6 secretion at either 1-month or 3-months of orkambi treatment with unstimulated PBMCs, with very little secreted IL-6 detected in any sample. Upon stimulation, PBMCs from Δf508/Phe508del patients on compassionate orkambi therapy at baseline secreted large amounts of IL-6, in response to the LPS rather than ATP. After 1-month of orkambi treatment PBMCs from Δf508/Phe508del patients on compassionate orkambi therapy secreted unchanged IL-6, upon stimulation. At the 3-month orkambi timepoint, IL-6 secretion *in vitro* was again unchanged compared to that of the other timepoints upon stimulation, with no statistically significant reduction between either 3-months and 1-month or baseline and 3-months.

These observations in IL-1β and IL-6 correlate with the serum data (Figure 5.3.1.1) in which IL-1β and IL-6 levels remained unchanged over the 3-months of orkambi treatment.
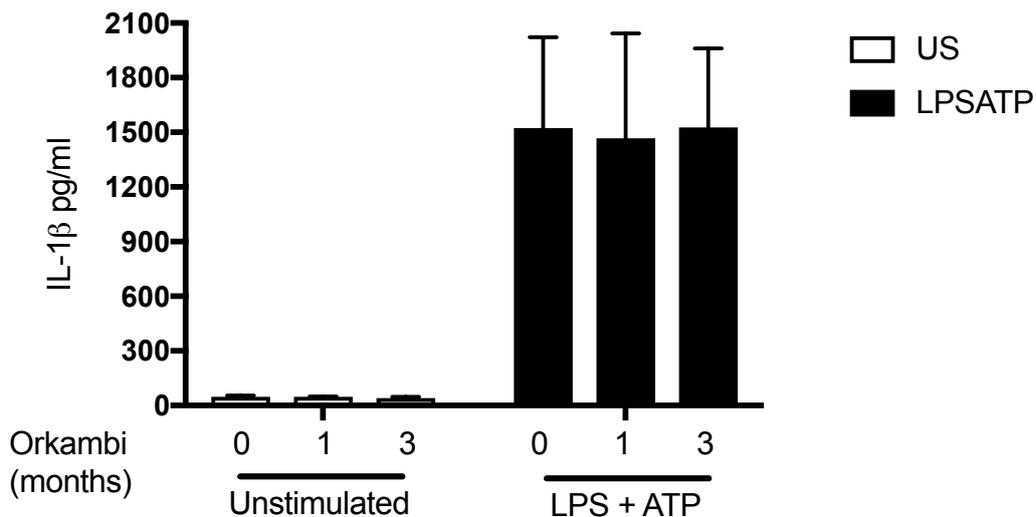
(Figure 5.4.2.1 legend on next page)
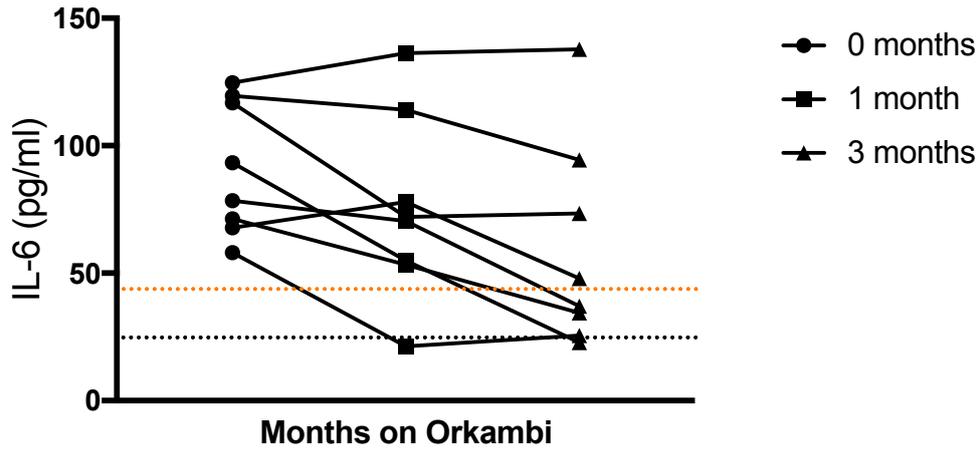
Figure 5.4.2.1: IL-1β secretion in patient PBMCs with CF-associated mutations receiving compassionate orkambi treatment. ELISA assays were used to detect IL-1β secretion in PBMCs from patients (n=8) with CF-associated mutations receiving compassionate orkambi treatment at baseline, 1-month orkambi and 3-months orkambi. PBMCs were stimulated with LPS (10ng/mL) for 4 hours before being stimulated for 30 minutes with ATP (5mM). A repeated measures 2-way ANOVA statistical test was performed with Turkey's multiple comparisons test (p values * = ≤0.05, **= ≤0.01, ***= ≤0.001 and ****= ≤0.0001).
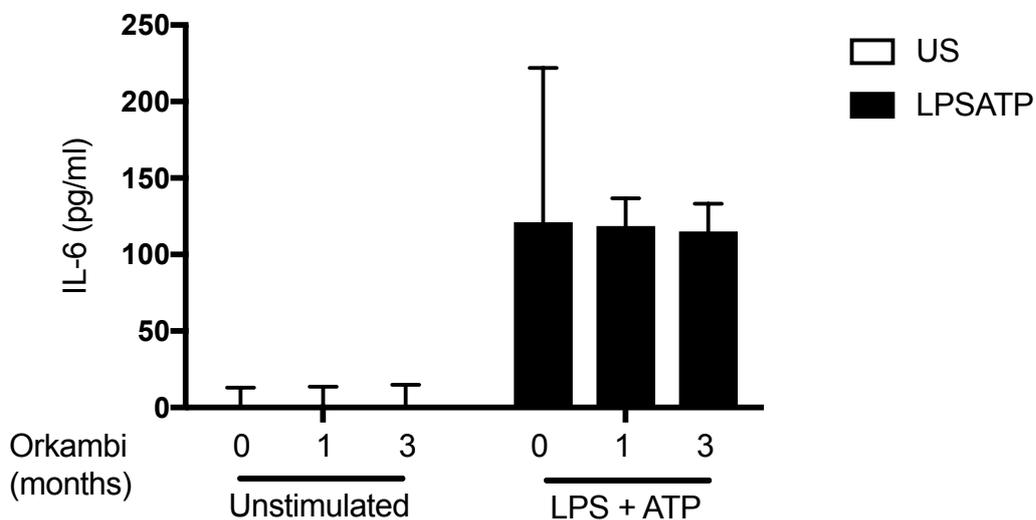
Figure 5.4.2.2: IL-6 secretion in patient PBMCs with CF-associated mutations receiving compassionate orkambi treatment. ELISA assays were used to detect IL-6 secretion in PBMCs from patients (n=8) with CF-associated mutations receiving compassionate orkambi treatment at baseline, 1-month orkambi and 3-months orkambi. PBMCs were stimulated with LPS (10ng/mL) for 4 hours before being stimulated for 30 minutes with ATP (5mM). A repeated measures 2-way ANOVA statistical test was performed with Turkey's multiple comparisons test (p values * = ≤0.05, **= ≤0.01, ***= ≤0.001 and ****= ≤0.0001).

5.4.3 PBMC secreted IL-10

The anti-inflammatory cytokine IL-10 was also detected in *in vitro* PBMC stimulations (IL-10 was undetectable in serum by ELISA). IL-10 is a potent anti-inflammatory cytokine, secreted by an array of both lymphoid and myeloid cells with anti-inflammatory or suppressive phenotypes. A lack of IL-10 secretion is an indication of pathogenic inflammation as IL-10 will induce the resolution phase of inflammation. IL-10 is known to be secreted along with TNF and IL-6 upon LPS stimulation, downstream of NF-κB.

Within the unstimulated PBMCs from Δf508/Phe508del patients on compassionate orkambi therapy, very little IL-10 was detected with a small increase in spontaneous IL-10 secretion over the 3-months of orkambi treatment, but this was not statistically significant. Upon stimulation with LPS and ATP, IL-10 secretion from *in vitro* PBMCs was detected and increased to a statistically significant level after 3-months of orkambi treatment, compared to baseline (p=0.0003). IL-10 secretion *in vitro* was significantly increased between 1-month and 3-months of orkambi treatment, upon stimulation with LPS and ATP (p=0.0071).
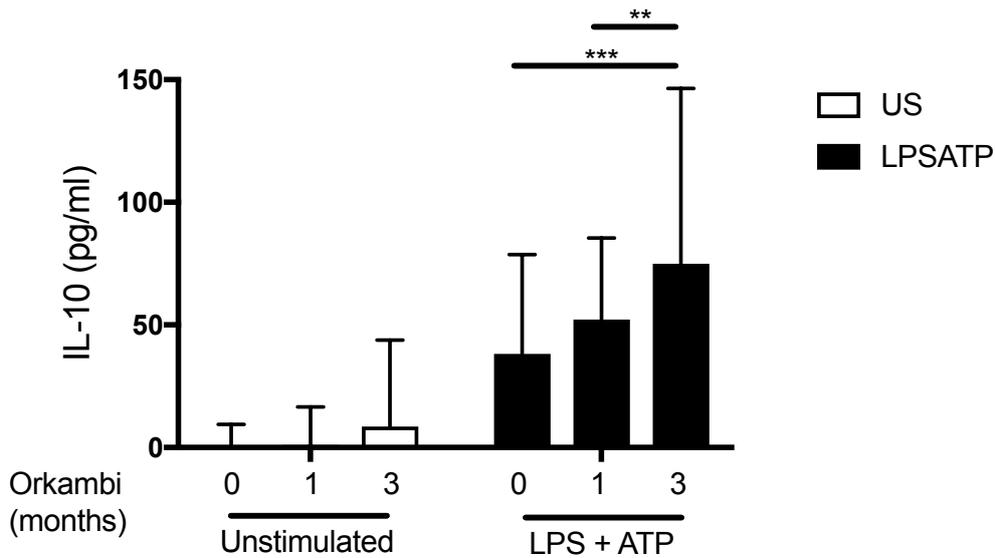
Figure 5.4.3.1: IL-10 secretion in patient PBMCs with CF-associated mutations receiving compassionate orkambi treatment. ELISA assays were used to detect IL-10 secretion in PBMCs from patients (n=8) with CF-associated mutations receiving compassionate orkambi treatment at baseline, 1-month orkambi and 3-months orkambi. PBMCs were stimulated with LPS (10ng/mL) for 4 hours before being stimulated for 30 minutes with ATP (5mM). A repeated measures 2-way ANOVA statistical test was performed with Turkey's multiple comparisons test (p values * = ≤0.05, **= ≤0.01, ***= ≤0.001 and ****= ≤0.0001).

5.5 The effect of orkambi on cellular metabolism

Cellular metabolism and control of cytokine secretion are two processes that are inextricably linked. In order to understand the effects of orkambi on cytokine secretion, specific metabolic assays were also performed in parallel. L-lactate secretion and glucose consumption were measured in PBMC supernatants from patients with the Δf508/Phe508del CFTR mutation on compassionate orkambi treatment. L-lactate secretion, glucose consumption, succinate and ATP concentrations were also measured in PBMC supernatants from HC

individuals and patients with the Δf508/Phe508del CFTR mutation (without compassionate orkambi treatment) and orkambi added as an *in vitro* pre-treatment to LPS and ATP.

5.5.1 Cellular metabolism of PBMCs from orkambi treated patients with Δf508/Δf508

A small but statistically significant increase in L-lactate secretion in PBMC supernatants from patients with the Δf508/Phe508del CFTR mutation was observed after 3-months of compassionate orkambi treatment compared to baseline measurements, before orkambi administration (p=0.0014).
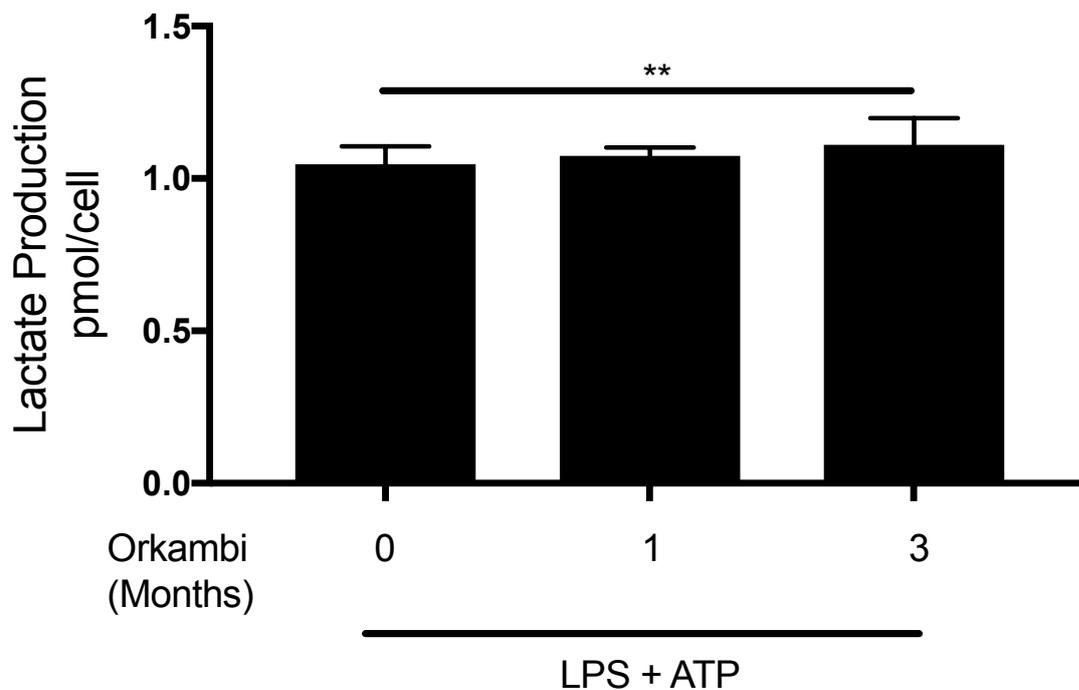
Figure 5.5.1.1: Extracellular L-lactate secretion in patient PBMCs with CF-associated mutations receiving compassionate orkambi treatment. Colorimetric assays were used to detect intracellular L-lactate production in PBMCs from patients (n=8) with CF-associated mutations receiving compassionate orkambi treatment at baseline, 1-month orkambi and 3-months orkambi. PBMCs were stimulated with LPS (10ng/mL) for 4 hours before being

stimulated for 30 minutes with ATP (5mM). A repeated measures 2-way ANOVA statistical test was performed with Turkey's multiple comparisons test (p values * = ≤0.05, **= ≤0.01, ***= ≤0.001 and ****= ≤0.0001).

There were no significant differences observed in glucose consumption in PBMC supernatants from patients with the Δf508/Phe508del CFTR mutation over the 3-months of compassionate orkambi treatment.
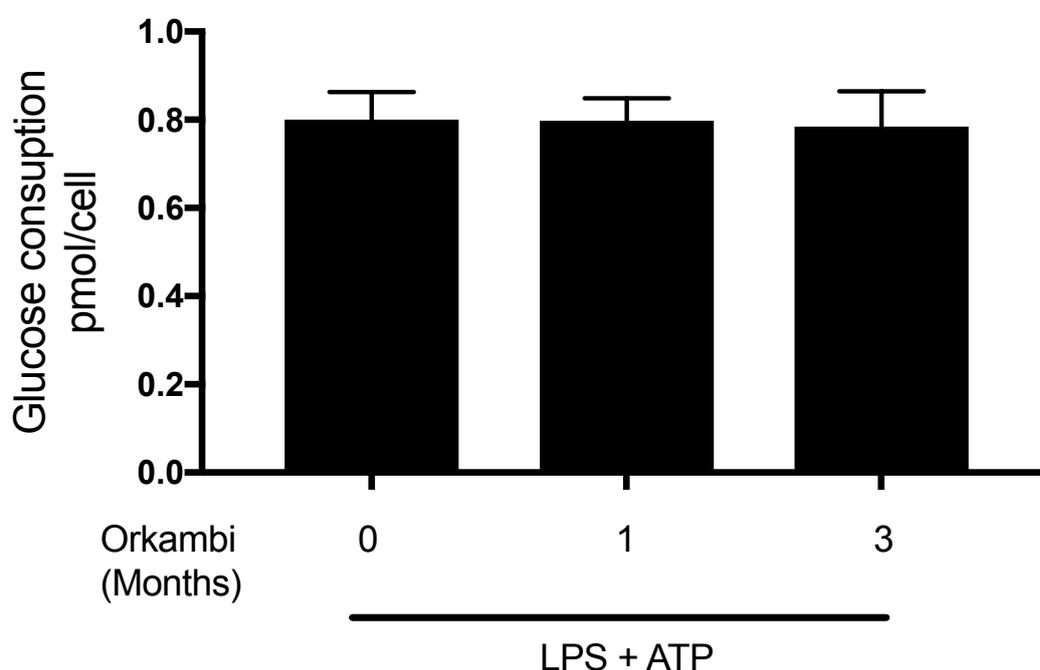
Figure 5.5.1.2: Glucose consumption in patient PBMCs with CF-associated mutations receiving compassionate orkambi treatment. Colorimetric assays were used to detect intracellular glucose consumption in PBMCs from patients (n=8) with CF-associated mutations receiving compassionate orkambi treatment at baseline, 1-month orkambi and 3-months orkambi. PBMCs were stimulated with LPS (10ng/mL) for 4 hours before being stimulated for 30 minutes with ATP (5mM). A repeated measures 2-way ANOVA statistical test was performed with Turkey's multiple comparisons test (p values * = ≤0.05, **= ≤0.01, ***= ≤0.001 and ****= ≤0.0001).

5.5.2 Cellular metabolism of Δf508/Phe508del PBMCs stimulated with orkambi in vitro

PBMCs from HC individuals and patients with the Δf508/Phe508del CFTR mutation (without compassionate orkambi treatment) were isolated and cultured *in vitro* before being treated with laboratory-grade orkambi and a stimulation with LPS and ATP. The hypotheses behind these *in vitro* experiments were two-fold: (1) Orkambi is capable of modulating cellular metabolism in PBMCs from patients with CF-associated mutations directly; and (2) Any orkambi-driven improvement in *in vivo* lung function is independent to the metabolic changes seen in orkambi-treated CF PBMCs. By recruiting patients with the Δf508/Phe508del CFTR mutation and selecting those who had never received compassionate orkambi treatment, data could be generated to determine whether the changes in immunometabolism, observed with orkambi, were due to an improvement in lung function or due to orkambi itself.
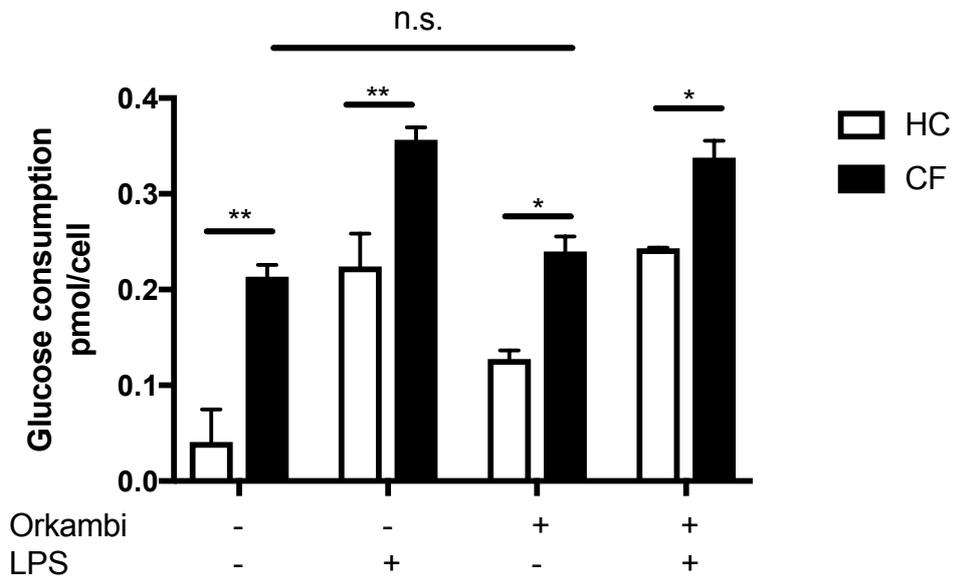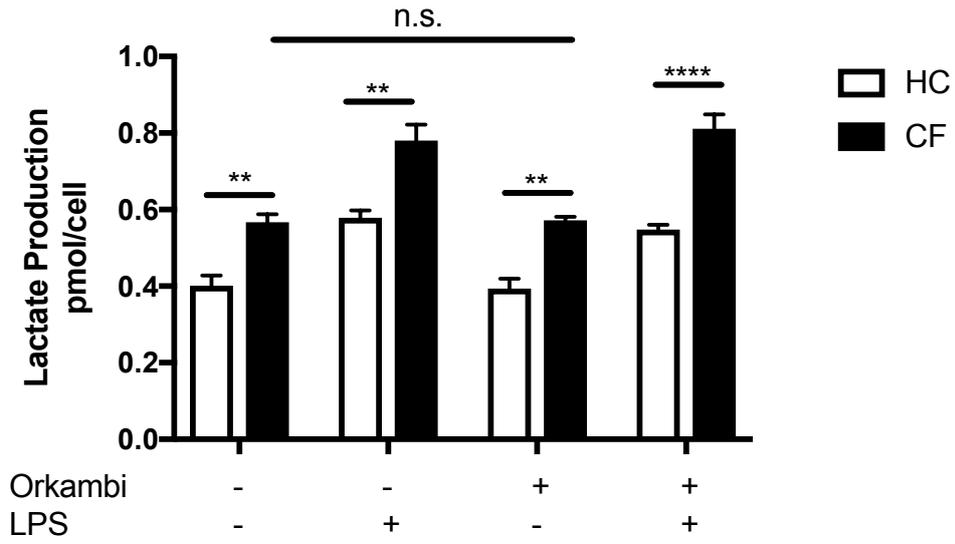
(Figure 5.5.2.1 legend on next page)
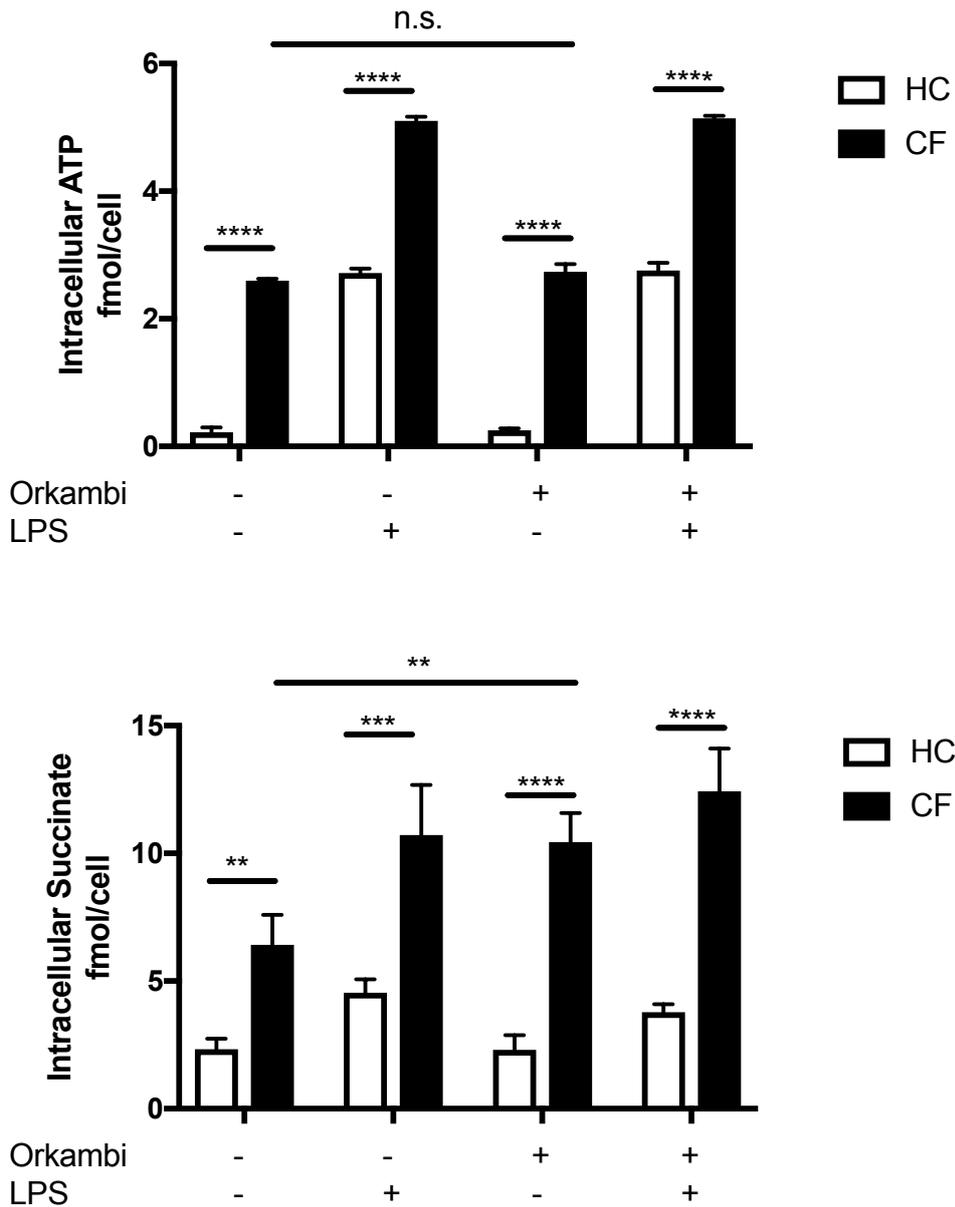
Figure 5.5.2.1: Cellular metabolism in HC and CF PBMCs with *in vitro* orkambi treatment. Colorimetric assays were used to detect intracellular L-lactate production, glucose consumption, intracellular ATP and intracellular succinate in HC and CF PBMCs with *in vitro* orkambi (VX-770 5μM; VX-809 3μM) treatment for 48 hours. PBMCs were stimulated with LPS (10ng/mL) for 4 hours before being stimulated for 30 minutes with ATP (5mM). A repeated measures 2-way ANOVA statistical test was performed with Turkey's multiple comparisons test (p values * = ≤0.05, **= ≤0.01, ***= ≤0.001 and ****= ≤0.0001).

The experiments that generated the data displayed in this figure, as well as the design of the figure itself, were carried out by Dr Heledd Jarosz-Griffiths. The author of this thesis would like to fully acknowledge Dr Jarosz-Griffiths' contribution.

L-lactate secretion was increased in PBMCs from patients with the Δf508/Phe508del CFTR mutation, as observed previously (Figure 4.4.1) to a statistically significant level, compared to PBMCs from HC individuals at baseline. Upon LPS stimulation both CF and HC PBMCs increased L-lactate secretion, with CF PBMCs maintaining their statistically significant increase in L-lactate secretion compared to PBMCs from HC individuals. A pre-treatment of orkambi for 48-hours did not affect L-lactate secretion in either CF or HC PBMCs at either baseline or their response to LPS stimulation.

Glucose consumption was increased in PBMCs from patients with the Δf508/Phe508del CFTR mutation, as observed previously (Figure 4.4.2) to a statistically significant level, compared to PBMCs from HC individuals at baseline. Upon LPS stimulation both CF and HC PBMCs increased glucose consumption, with CF PBMCs maintaining their statistically significant increase in glucose consumption compared to PBMCs from HC individuals. A pre-treatment of orkambi for 48-hours did not affect glucose consumption in either CF or HC PBMCs at either baseline or their response to LPS stimulation.

Intracellular ATP concentration was increased in PBMCs from patients with the Δf508/Phe508del CFTR mutation, as observed previously (Figure 4.3.3) to a statistically significant level, compared to PBMCs from HC individuals at baseline. Upon LPS stimulation both CF and HC PBMCs increased intracellular ATP concentration, with CF PBMCs maintaining their statistically significant increase in intracellular ATP concentration compared to PBMCs from HC individuals. A pre-treatment of orkambi for 48-hours did not affect

intracellular ATP concentration in either CF or HC PBMCs at either baseline or their response to LPS stimulation.

Intracellular succinate concentration was increased in PBMCs from patients with the Δf508/Phe508del CFTR mutation, as observed previously (Figure 4.4.3) to a statistically significant level, compared to PBMCs from HC individuals at baseline. Upon LPS stimulation both CF and HC PBMCs increased intracellular succinate concentration, with CF PBMCs maintaining their statistically significant increase in intracellular succinate concentration compared to PBMCs from HC individuals. A pre-treatment of orkambi for 48-hours increased intracellular succinate concentration in CF PBMCs at baseline, but not in HC PBMCs. Orkambi pre-treatment had no statistically significant effect on intracellular succinate concentration in LPS stimulated PBMCs.

5.6 Discussion

5.6.1 Effects of Orkambi- CFTR modulator, ENaC inhibitor or NSAID

Orkambi is a combination of two small molecule drugs: ivacaftor, a 'potentiator' to increase the open probability of the defective CFTR and; lumacaftor, a 'corrector' to chaperone CFTR protein folding through the ER and Golgi. It has been shown that orkambi is able to chaperone and potentiate the Phe508del mutated-CFTR *in vitro* and *in vivo* with modest improvements in patient lung function and outcome. The ability of orkambi to modulate inflammation is unknown. With partial restoration of functional CFTR in orkambi treated patients, ENaC inhibition is also partially restored (Cholon et al., 2014). Based on the data presented in this study, it can be hypothesised that orkambi is able to modulate inflammation in patients with CF, via restoration of ENaC-inhibition. Therefore, orkambi would be an

indirect ENaC inhibitor and the therapeutic effects observed with orkambi treatment are via controlling Na^+ influx rather than restoration of Cl^- flux. The ability of orkambi, based on the above theory, to modulate inflammation in WT cells will be limited. Based on the data presented in this study, there is increased Na^+-induced inflammation in cells with CF-associated mutations and Na^+ channel inhibition is able to modulate the excessive inflammatory response. When WT cells are treated with Na^+ channel inhibitors, cytokine secretion is not affected. Na^+ channel inhibition corrects a pathogenic consequence of the primary CFTR defect in CF, and therefore the anti-inflammatory effect in WT cells is limited. Orkambi's ability to decrease ENaC activity through restoration of CFTR then in theory would also have limited anti-inflammatory effects in WT cells.

5.6.2. Differential modulation of cytokines

Patients considered for compassionate orkambi treatment are those with a 'suitable' genotype that is compatible with the molecular mechanisms of ivacaftor and lumacaftor individually (e.g. Δf508/Δf508). All patients in the compassionate orkambi study were confirmed to be Δf508/Phe508del homozygotes. In addition to genotype, patients must be without infection but have poor lung function, due to mucous accumulation or fibrosis/bronchiectasis. Orkambi is not offered by the National Health Service (NHS) in England, with Vertex® Pharmaceuticals providing the drug to patients on compassionate grounds based on specific criteria (section sections 1.1 and 1.5, figure 1.1.2). The data in this chapter can be interpreted based on these criteria, in terms of the general health and inflammatory state of the patient cohort.

Serum IL-18 at baseline is variable within the patient population, with a range of around 200pg/mL to over 800pg/mL (HC median=117pg/mL). These data highlight that despite a

previous decline in lung function in all patients before being administered with orkambi, there is a variable inflammatory state within the overall population, in terms of serum IL-18. Serum TNF, IL-1β and IL-6 concentrations were also all above the average HC serum level for each respective cytokine. Serum IL-18 began to gradually decrease after 1-month, but this decrease was not statistically significant. This suggests that the initial period after administration with orkambi, may not yield positive results in terms of inflammatory markers. After 3-months of orkambi treatment, the decrease in IL-18 was statistically significant compared to baseline. These data indicate that orkambi is able to reduce systemic IL-18 after 3-months, with all patients ending the 3-month study period with serum IL-18 concentrations below the average for CF serum IL-18 (based on data in Figure 3.1.1). Serum TNF responded in a similar fashion, with no initial decrease after 1-month but a statistically significant decrease after 3-months. These data support a hypothesis that the beneficial anti-inflammatory effects of orkambi occur between 1-month and 3-months of treatment.

There was no notable change in serum IL-1β or IL-6 over the 3-month period of orkambi treatment in this study. However, this observation is itself noteworthy as it suggests there is a differential regulation of proinflammatory cytokines in CF with orkambi treatment. IL-1β was shown to be significantly elevated in CF serum compared to HC, NCFB and SAID cohorts (Figure 3.1.2). In this cohort, IL-1β was also elevated compared to the HC median from Figure 3.1.2 and this serum concentration remained unchanged over the 3-months of orkambi whereas IL-18, which is also processed by the NLRP3 inflammasome being significantly decreased over the same period. Differences in expression and regulation of IL-1β and IL-18 occurs at the transcriptional level, with IL-1β being induced by upstream transcription factors such as NF-κB, HIF1α and XBP1s, with IL-18 being constitutively expressed. However, TNF expression is also induced by NF-κB, HIF1α and XBP1s and serum TNF concentrations decreased to a similar extent to that of IL-18. One way that orkambi may be differentially

regulating TNF and IL-1β is through prostaglandin E$_2$ (PGE$_2$). PGE$_2$ is able to act as a pro- and anti-inflammatory mediator of inflammation, being able to inhibit TNF expression in response to LPS (Tang et al., 2017) and induce IL-1β expression (Zasłona et al., 2017). Markedly, PGE$_2$ also induces IL-6 expression and secretion (Cho et al., 2014, Ghezzi et al., 2000, Raychaudhuri et al., 2010, Kunkel et al., 1988, Hinson et al., 1996), which also remains elevated throughout the 3-months of orkambi treatment. Interestingly, data showing that dual-acting potentiator–correctors, such as the C-18 Vertex® molecule induces elevated cyclo-oxygenase (COX)-2 and the related metabolite PGE$_2$. However, investigating the exact molecular mechanisms by which orkambi differentially regulates TNF and IL-1β is beyond the scope of this study.

The cytokine data generated using *in vitro* stimulation of PBMCs from patients receiving compassionate orkambi follow the same trend to that of the serum cytokine data: IL-18 and TNF decline in concentration over 3-months of orkambi treatment, to a statistically significant level; whereas IL-16 and IL-1β are unaffected by orkambi treatment. This data supports the PGE$_2$ hypothesis mentioned above, but this was no investigated further in this study.

An interesting observation was made when IL-10 levels from *in vitro* PBMC stimulations were analysed, with secretions of this anti-inflammatory cytokine increasing over the 3-month period. IL-10 could not be detected in serum. IL-10 may explain the observed reduction in IL-18 and TNF in serum and *in vitro* PBMC secretions but IL-10 does not differentially regulate IL-6 and IL-1β and so cannot explain the discrepancy in cytokine secretion over the 3-months of orkambi treatment.

An important observation to note is that the orkambi patient cohort have higher baseline levels on average that the other CF population used in chapters 3 and 4. This can be explained by highlighting the fact that compassionate orkambi administration is considered when this subset of Phe508del/Phe508del patients' lung function is declining. Therefore, one can

correlate declining lung function and an elevated baseline serum cytokine concentration. Further details of clinical data across the 3-month study are displayed in appendix figure 12. There was no significant change in any of the parameters of lung function, inflammation or patient weight/BMI. This indicates stable clinical values across the 3-month study, with no worsening of patients on orkambi.

5.6.3. Limitations

Limitations to the data generated from this study revolve around a lack of control around dosage of orkambi. It is common practise to adjust the orkambi dose initially to a lower level that that recommended by Vertex® to then increase the dosage over the first month to prevent adverse side-effects. All patients were at maximum dose by the time of the first 1-month sample collection. The cohort was not well defined due to the small size of the study. An additional limitation to the above data regards the use of PBMCs, rather than purified immune cell populations. The ratio of cell types within the heterogenous PBMC population is not controlled for and therefore may influence the differential secretion of the measured cytokines. Future experiments would utilise flow cytometry or cell separation assays to deepen the understanding of which cell types are pathogenic in CF and how orkambi effects individual immune cell types.

5.6.4 Modulation of metabolism

Metabolism was measured within stimulated PBMC cultures over the 3-months of orkambi treatment. These data were generated in parallel with the cytokine assays to provide an insight into the inflammatory, metabolic phenotype of PBMCs over the 3-months of

orkambi treatment. With increased IL-10 and reduced IL-18 and TNF secretion, it was expected that glycolytic markers would decrease in the same samples. There was no change over the 3-months of orkambi treatment in glucose consumption after stimulation with LPS and ATP in patient PBMCs. However, L-lactate secretion significantly increased between 1-month and 3-months and between baseline and 3-months of orkambi treatment. This indicates that glycolysis may be increasing over this period, perhaps fuelling IL-1β expression through succinate accumulation. When L-lactate secretion, glucose consumption and intracellular concentration were measure in CF PBMCs treated with 48 hours of orkambi *in vitro*, there was no change in these metabolic assays. When intracellular succinate concentration was analysed, there was an increase in samples pre-treated with 48 hours of orkambi *in vitro*. These data support the hypothesis that an increase in glycolysis during orkambi treatment maintains IL-1β production, via succinate accumulation.

Chapter 6

6.0 Discussion

In the following chapter, the data and observations described in this study will be discussed, in terms of what the results mean for the understanding of CF pathophysiology, the characterisation of CF and the implications that these novel findings have on future therapies for the treatment of CF.

6.1 CF is an autoinflammatory disease

Autoinflammation is defined as an inappropriate inflammatory response, driven by dysregulated innate immune cells, without evidence of antigen-driven T cells, B-cells, or associated autoantibodies (McDermott and Aksentijevich, 2002, McDermott et al., 1999, McGonagle and McDermott, 2006, Pathak et al., 2016, Peckham et al., 2017, Kastner et al., 2010, Stoffels and Kastner, 2016). Adaptive immune cells are sometimes associated with the downstream consequences of autoinflammation, as well as increased susceptibility to infection, autoimmunity and hyperinflammation (Wekell et al., 2016). These associated adaptive immune cells are not the cause of inflammation but are merely affected bystanders. Autoinflammatory disorders range from monogenic disorders, with mutations causing dysregulation of innate immune pathways to a number of systemic immunological diseases, with significant autoinflammatory features, such as psoriasis, gout and even a subset of rheumatoid arthritis (Liang et al., 2017, Marrakchi et al., 2011, Onoufriadis et al., 2011, Sweeney et al., 2011), Aicardi-Goutières syndrome (AGS) (Crow et al., 2006) and rheumatoid arthritis (RA) (Choulaki et al., 2015, Littlewood-Evans et al., 2016, Mathews et al., 2014).

Immunodeficiencies, such as PLCG2-associated antibody deficiency and immune dysregulation (PLAID) (Chae et al., 2015) or haploinsufficiency of cytotoxic T-lymphocyte-associated protein 4 (CTLA-4) (Kuehn et al., 2014), may show increased innate immune responses to inflammatory triggers to compensate for an immunodeficient adaptive immune system (Peckham et al., 2017).

Immunological diseases lie on a spectrum, with the autoinflammatory and autoimmune diseases at the antithetical ends of a continuum (McGonagle and McDermott, 2006). Immunological diseases that incorporate features of both autoinflammation and autoimmunity exist the two absolute ends of the spectrum (sections 1.6 and 3.10.1) (Peckham et al., 2017, McGonagle and McDermott, 2006). This study proposes that CF is an immunological disease that sits towards the autoinflammatory pole of the spectrum. Evidence for CF being an autoinflammatory disease is derived from the nature of the systemic inflammation observed in patients with CF-associated mutations, in combination with the inherent characteristics of the inflammation observed at the molecular and cellular level. This study contributes towards the latter observations, providing novel insights into the basic features of the inflammatory pathways active in cells with CF-associated mutations.

A large infiltrate of myeloid immune cells is a key feature of pulmonary inflammation in patients with CF-associated mutations (Bals et al., 1999, Bruscia and Bonfield, 2016a, Hartl et al., 2012). Neutrophils dominate this immune cell influx into the lung and are described as the 'first-responders' of inflammation (Aulakh, 2018, Cohen and Prince, 2012, Hayes et al., 2011). The lung in patients with CF contains a milieu of myeloid-derived, proinflammatory cytokines and chemokines within the inflammatory environment , with significant levels of proinflammatory cytokines, including IL-8 (CXCL8), IL-6, TNF and IL-1 (IL-1α, IL-1β and IL-18), and reduced levels of anti-inflammatory IL-10 (Bals et al., 1999, Bruscia and Bonfield, 2016a, Hartl et al., 2012, Keiser et al., 2015). Many studies have described the role of IL-8 in

CF lung inflammation due to its potent chemotactic abilities, which enable further recruitment of neutrophils to the site of inflammation (Armstrong et al., 2005, Bergin et al., 2013, Grassme et al., 2014, Hubeau et al., 2004, Keiser et al., 2015). IL-8 is secreted by epithelial cells and monocytes in the CF lung to exacerbate neutrophilic inflammation. A large proportion of the above cytokines and chemokines is produced by monocytes, driving the innate immune inflammation in the CF lung. IL-1β is a pivotal cytokine in the amplification of the systemic proinflammatory cytokine response, although the increased levels of IL-1β in the lung are not correlated to patient outcome (Bals et al., 1999, Hartl et al., 2012). The fact that the dominant cell infiltrates in the CF lung are innate immune cells supports the proposed classification of CF as an autoinflammatory disease. Autoinflammation is defined as inappropriate, innate immune driven inflammation, and inflammation in CF at the systemic cellular level fits the criteria of autoinflammation.

The presence of innate immune cells and inflammatory mediators in the CF lung is associated with infection however, there is strong evidence in the literature that lung inflammation in CF is in fact sterile. Mucous dehydration and obstruction occur early-on in patients with and models of cystic fibrosis and is associated with neutrophilic inflammation in the absence of infection (Keiser et al., 2015, Fritzsching et al., 2015). One theory is that the mucous obstruction induces a hypoxic environment, and the innate immune driven inflammation is in response to hypoxic cell death (Montgomery et al., 2017). Hypoxia-driven inflammation is induced by IL-1R, which is activated under hypoxic conditions by the release of necrosis-dependent IL-1α. Pharmacological inhibition of IL-1R significant depleted airway neutrophils and fibrosis in CF. Additional evidence for sterile inflammation in CF is from the sterile (caesarean section) ferret model of CF, where mucous is found to be significantly dehydrated after birth with increased levels of IL-8 and TNF in the sterile CF ferret lung (Keiser et al., 2015). The sterile CF ferret model presents with abnormalities in various aspects of the

innate immune response, such as complement, mammalian target of rapamycin (mTOR) signalling and eukaryotic initiation factor 2 (eIF2) signalling, suggesting downstream activation of the NF-κB signalling pathway. Sterile innate immune driven inflammation is not a prerequisite of autoinflammation, but many monogenic autoinflammatory diseases have features of sterile inflammation, in that the trigger may be non-pathogenic or non-infectious (Lukens et al., 2012). For example, the cryopyrin-associated periodic syndrome (CAPS), familial cold autoinflammatory syndrome (FCAS) is an inherited autoinflammatory disorder categorised by periodic rashes, fevers, joint pain due to systemic inflammation triggered by exposure to cold (Dodé et al., 2002, Hoffman et al., 2001). The convincing evidence for sterile, hypoxia-driven innate immune driven inflammation moves CF further towards the autoinflammatory end of the immunological disease spectrum.

The NLRP3 inflammasome has been previously reported (sections 1.2 and 3.10.1) as being active in as *in vitro* cell and *in vivo* murine models of CF (Iannitti et al., 2016, Rimessi et al., 2015). Elevated levels of systemic IL-1 and activation of an inflammasome are characteristic features of autoinflammatory disease. This study has added to the growing body of evidence that the NLRP3 inflammasome is a potent inducer of IL-1 derived inflammation in CF and is hyper-responsive. In addition, the data presented throughout this study suggests the intrinsic genetic defect in CFTR contributes to the hyper-responsiveness of this pathway.

Within the definition of autoinflammation, there is the addendum that the adaptive immune system may be present and active in autoinflammatory disease, but that it is not the pathogenic source of inflammation and is merely an external, downstream factor influenced by the inappropriate innate immune driven inflammation. This is further corroborated by the lack of antigen-driven T cells, B-cells, or associated autoantibodies. In CF, the adaptive immune system plays a negligible role in the induction and progression of inflammation (Bruscia and Bonfield, 2016b). There is evidence that an adaptive immune signature occurs in late or end-

stage CF lung disease (Lammertyn et al., 2017), with the presence of tertiary lymphoid organs in the lung (Regard et al., 2018) as well as IgA autoantibodies (Aebi et al., 2000, Budding et al., 2015, Fasth and Kollberg, 1980, Hodson and Turner-Warwick, 1981, Hoiby and Wiik, 1975, Lachenal et al., 2009, Nousia-Arvanitakis et al., 2000, Rotschild et al., 2005, Schiotz et al., 1979), but this may be evidence of chronic, persistent inflammation rather that a causative effect. A further addendum to the definition of autoinflammation is that there may be a predisposition to autoimmunity, infection and hyperinflammation. There is evidence for all three of these scenarios in the CF literature, with end-stage autoantibodies (Budding et al., 2015) against components of neutrophils, in addition to characteristic and periodic lung inflammation due to infections by minor and often commensal pathogens (Filkins and O'Toole, 2015) as well as hyperinflammation (Adam et al., 2015, Cohen and Prince, 2012, Cohen-Cymberknoh et al., 2013, Montgomery et al., 2017, Peckham et al., 2017, Scambler et al., 2018), the latter being demonstrated throughout this study.

6.2 Sodium-driven inflammation in CF – ENaC inhibition

The activity of ion channels is associated with the modulation and activation of numerous inflammatory pathways in both health and disease. Disturbances in the expression or performance of an ion channel can have profound effects on the immune response. Whether CFTR has a role in immunity is debated as CFTR expression is often low in immune cells and chloride's role in immune pathways is not well described. In this study, data has been presented that suggests the disruption in sodium flux downstream of CFTR dysfunction, specifically via amiloride-sensitive channels, has a role in inducing a hyperinflammatory phenotype in epithelial and innate immune cells. There is further evidence for sodium-induced inflammation in myeloid cells in the literature. Dendritic cells (DCs) have been shown to be implicated in

hypertension when exposed to excessive extracellular sodium (Barbaro et al., 2017). Barbaro et al. describe how Na^+ influx through amiloride-sensitive channels, such as ENaC, leads to Ca^{2+} influx and activation of protein kinase C (PKC), p47[phox] and gp91[phox]. NADPH oxidase-dependent superoxides activate isolevuglandin (IsoLG)-protein adducts downstream, with subsequent IL-1β secretion and T-cell activation. Sodium transport is able to regulate inflammation through swelling, or oedema. By transporting sodium across plasma membranes, fluid also moves across cellular membranes. Sodium transport has been shown to be part of this inflammatory response and independent of the type of inflammatory trigger, with similar responses in terms of amiloride-sensitive potential difference or sodium channel activity in both allergic asthma and meningococcal septicaemia (Streb et al., 1983, Eisenhut and Southern, 2002, Eisenhut and Wallace, 2011, Eisenhut et al., 2004). In the latter study of meningococcal septicaemia, transport of sodium and chloride was shown for the first time to be disturbed in an *in vivo* human study, with the patient's sweat test at a similar level to that of a CF patient, with severe dysfunction in CFTR or ENaC (Eisenhut and Southern, 2002, Eisenhut et al., 2004). This observation confirms that ion transport of sodium and chloride is inextricably linked with inflammatory responses. Therefore, one can hypothesise that in the scenario of a genetic defect in sodium or chloride transport inflammation will be disturbed. The data in this study support this hypothesis, with evidence of ENaC-driven NLRP3 inflammasome activation and inhibition of amiloride-sensitive channels being able to modulate IL-1β and IL-18 secretion. Further data show that there is a proinflammatory phenotype of innate immune cells, in terms of reduced M2-type macrophage surface markers and glycolytic metabolism.

Interestingly, inflammation can also modulate the expression and activity of ENaC. Cytokines associated with Th1 (IFNγ) (Schmidt et al., 2007), Th2 (IL-4 and IL-13) (Danahay et al., 2002) and M1-type (IL-1β and TNF) (Schmidt et al., 2007) immune cells have all been shown to downregulate ENaC, whereas NO stimulates ENaC expression (Hardiman et al.,

2004). This feedback loop, between proinflammatory cytokines and ENaC expression, further implies that the relationship between ion channels and inflammatory responses is a close and important one.

This study has highlighted the significance of overactive ENaC as a pathogenic mediator of inflammation in CF. These data, in combination with the wealth of literature implicating ENaC as an influencer of and being influenced by inflammation, support the hypothesis that the disturbance in ion channels in CF contributes to the inflammatory phenotype characteristic of the systemic manifestations in CF. Evidence for inflammation impacting CFTR expression has also been described. The cytokines IL-2, IL-4, IL-15, IL-10 and IL-1β (O'Loughlin et al., 2001, Colgan et al., 1994, Madsen et al., 1996) as well as numerous leukotrienes, prostaglandin E_2 (PGE2) (Van Der Merwe et al., 2009) and H_2O_2 (Mayol et al., 2006) have all been shown to increase CFTR expression at the mRNA and protein level. Notably, many cytokines have also been shown to reduce CFTR expression such as TGFβ (Prulière-Escabasse et al., 2005), IFNγ and TNF. The ability of IFNγ and TNF to modulate CFTR expression involves the disruption of the stability of CFTR mRNA transcripts, reducing the overall stability of the mRNA compared to wild-type by around 65% (Nakamura et al., 1992, Besancon et al., 1994). The role of IL-1β to induce CFTR expression is concentration dependent, with higher IL-1β concentrations inhibiting, rather than inducing CFTR expression (Cafferata et al., 2000, Cafferata et al., 2001). The inhibition of CFTR by high-dose IL-1β encompasses reducing the expression of mRNA and protein rather than mRNA stability, as with IFNγ and TNF. The study investigating the role of TNF and the expression of CFTR detailed the similarity (85%) in sequence homology between CFTR regulating sequence with the TNF-regulated collagen gene sequence (Nakamura et al., 1992). This implies that the inflammatory response requires control over ion flux and thus ion channel activity.

These data suggest that therapeutic interventions targeting ion channels will beneficially have downstream anti-inflammatory effects if designed correctly for appropriate ion channel and cytokine. This is particularly relevant for channelopathies with inflammatory complications, such as CF. Targeting ENaC may be a successful anti-inflammatory therapy as well as controlling fluid absorbance and mucous dehydration. Additionally, the anti-inflammatory effects of CFTR modulation, with ivacaftor/lumacaftor demonstrated in this study, may be due to the relationship CFTR has with inflammatory mediators rather than the partial correction and potentiation of CFTR, the primary defect of CF.

6.3 Glycolytic metabolism in CF – intrinsic defect or systemic?

This study contributes to the growing amount of evidence that ion channels and ion fluxes are integral in the control and activation of inflammatory responses through the study of CF, a channelopathy with inflammatory complications. Ion channel disruption induces inflammatory phenotype in CF innate immune cells and HBEC lines. Small molecule intervention, inhibiting overactive amiloride-sensitive sodium channels is able to modulate downstream inflammatory responses. Interestingly, cells with CF-associated mutations also had metabolic disturbances, particularly in glycolysis. Whether ion channel disruption induces glycolysis directly, perhaps through an elevated energy demand, or whether the glycolysis is merely a consequence of inflammation and an indication of a proinflammatory cell phenotype is yet to be elucidated. The data in this study suggest the former, with increased energy, in the form of ATP, being required to maintain ionic homeostasis in CF, causing a metabolically stressed phenotype as inhibition of amiloride-sensitive sodium channels was able to modulate certain glycolytic read-outs thought to be upstream of inflammation. A CF cell with such

disturbances in glycolysis will then be predisposed to a proinflammatory phenotype, due to the known downstream, proinflammatory cellular responses to glycolytic metabolism.

An alternative hypothesis is that systemic metabolism, such as the alteration in the CF gut microbiome or the high-calorie, high-fat CF diet may alter inflammatory and metabolic phenotypes. Rather than an intrinsic ion channel defect causing a stressed metabolism directly and a subsequent proinflammatory phenotype, it may be that the high-fat, high-glucose diet, inducing hyperglycaemia, provides the fuel for glycolysis with successive overactivation of this pathway, particularly in innate immune cells and epithelia. This may certainly explain many of the systemic manifestations of CF such as arthritis and diabetes in which secondary sites to that of the lung experience chronic inflammation. Changes in the gut microbiome have also been associated with an alteration in the inflammatory phenotype of immune cells. Changes in the CF gut microbiome have been described and this may be due in part to the CF diet. Based on the data in this study and the deductions in the current literature, it is difficult to conclude whether metabolism and inflammation is affected by intrinsic or systemic influencers in CF. One piece of evidence that suggests the former is the successful ivacaftor therapy in patients with a G551D CFTR allele (Davies et al., 2013b). Individuals on ivacaftor begin to gain weight, a positive outcome measure in most trials. The patients do not change diet whilst on ivacaftor therapy, suggesting that correcting the intrinsic defect then alters metabolism and inflammation, with weight increasing, lung function improving and reduced number of exacerbations. Therefore, intrinsic ion channel defects in CF increase cellular energy demand, while inducing elevated metabolic activity and a glycolysis-dependent inflammatory phenotype and hyperinflammation.

6.4 Epithelia or immune cell inflammation

A debate within the CF research community exists in which the predominant cellular orchestrator of inflammation is the subject. CFTR is a channel highly expressed on epithelia in multiple organs with the majority of research in CF focussing on this cell type. The successful trials of small molecule modulators of CFTR focus on patient outcomes and epithelial CFTR function. The epithelia have a pivotal role in anti-microbial defence (Tecle et al., 2010), barrier function (LaFemina et al., 2014), mucociliary clearance (Kreda et al., 2012) as well as the detection of PAMPs and DAMPs (Lambrecht and Hammad, 2012, Armstrong et al., 2004). However, inflammation is not created by epithelial cells alone. The epithelial surfaces may orchestrate inflammation (Whitsett and Alenghat, 2015) by recruiting immune cells to sites of infection, such as the lungs in CF, but the vast majority of inflammation is carried out by leukocytes (Scambler et al., 2018). Despite the low expression of CFTR (Painter et al., 2006, Sorio et al., 2011, Johansson et al., 2014, Ettorre et al., 2014) and ENaC (Ottaviani et al., 2002, Barbaro et al., 2017, Gamper et al., 2000) channels in leukocytes many studies have shown defects in this cell type with disturbances in important cellular functions such as phagocytosis (Ng et al., 2014, Van de Weert-van Leeuwen et al., 2013, Hartl et al., 2012, Simonin-Le Jeune et al., 2013), chemotaxis (Sorio et al., 2016), cytokine secretion (Bals et al., 1999, Blohmke et al., 2012, Blohmke et al., 2008, Bonfield et al., 2012, Bruscia and Bonfield, 2016a, Bruscia et al., 2009, Cohen and Prince, 2012, Hartl et al., 2012, Keiser et al., 2015, Law and Gray, 2017, Machen, 2006, Mayer et al., 2013, Meyer et al., 2009), bacterial killing (Pezzulo et al., 2012) and cell death (Watt et al., 2005). Intrinsic defects due to CFTR mutations may be the source of these defects, as ion fluxes are known to be crucial in many inflammatory processes as previously discussed (section 6.2). Some of the mechanisms behind this may be ion-dependent cellular signalling, alterations in intracellular pH, oxidative stress, ER stress or epigenetics.

Many studies indicate that the defects in immune cell function in CF are secondary to epithelial inflammation, the environment in the lung and chronic infection. The data in this study suggest that it is in fact an intrinsic defect in ion channel expression and activity in immune cells themselves that is causing a hyperinflammatory state. This study has found ENaC expression in immune cells at the mRNA and protein level (Appendix figure 6). The function of this channel is not quite clear in immune cells however, but this is beyond the scope of this study. Therefore, it can be considered that CF epithelial cells are intrinsically hyperinflammatory and recruit excessive amounts of innate immune cells, which themselves are predisposed to proinflammatory phenotypes. This phenomenon in CF, coupled with recurrent respiratory infections, creates a chronically and inappropriately inflammatory environment resulting in bronchiectasis. This is highlighted by the fact that healthy individuals do not mount the same, aggressive inflammatory response to the pathogens common to the CF-lung.

6.5 Orkambi is an anti-inflammatory drug in patients with CF

The observations in this study suggest that disturbances in ion channel expression and activity, as is the case with the CFTR-chloride ion channel in CF contribute and modulate inflammatory pathways. Therefore, CFTR correction and potentiation with small molecules such as orkambi, although partial, modulate the primary ion channel defect in CF cells. The downstream modulation of inflammation is therefore either through correction of chloride ion flux and/or CFTR-dependent ENaC suppression. To delineate the exact mechanism by which orkambi modulates inflammation was beyond the scope of this study, but a relevant question that may lead to greater understanding of the basic defects in terms of the relationship between CFTR and ENaC channels. Based on the data in this study, it can be hypothesised that orkambi

modulates inflammation, via promoting CFTR expression and subsequent CFTR-dependent ENaC inhibition.

6.6 Concluding remarks

Based on the data generated as part of this study and the literature discussed throughout this thesis, it can be concluded that CF has many clinical and molecular similarities with autoinflammatory disease and should be treated as such. Multiple groups have postulated that biologic therapy in CF should be investigated, in particular the biological targeting of IL-1 cytokines with anakinra and canakinumab. This should be however, approached with caution and the anti-inflammatory benefits balanced with the control of infection by inflammatory mediators. Furthermore, metabolism is disturbed in cells with CF-associated mutations which may be part of the basic pathology of CF as well as a potential therapeutic target. Therapies based on metabolic pathways may be through the use of therapeutic metabolites, such as itaconate, but also through control over the high-fat, high-glucose diet. Finally, the revolutionary small molecule CFTR modulator therapies have huge therapeutic potential, but the basic mechanisms behind how the drugs not only recover CFTR expression and activity but how they modulate other channels and produce anti-inflammatory effects must also be thoroughly investigated for the benefit of future, targeted and personalised therapies.

6.7 Study limitations

The limitations in this study involve the patient cohorts recruited to this study as well as the narrow scope of the study in terms of cell types and pathways. The patient cohorts were not fully characterised, being only selected on genotype and age (Phe508del allele positive

and above the age of 18 years old). These criteria were selected based on the fact that CF is a rare genetic disease, and a large sample size was required for confidence in any differences found in terms of statistical tests therefore, the selection criteria was minimal. The orkambi patient cohort was not controlled for adherence or dosage of orkambi in the initial month of the study, due to internal clinical procedures to optimise drug dosage for a more personalised medical approach.

The immortalised cell lines are a good model for basic scientific questions, comparing cells from different individuals with different CF genotypes and a WT CFTR control (Beas2b). All the cell lines were the same cell type and has underwent the same immortalisation procedure. However, the conclusions this study makes is based on data from both HBEC lines and primary immune cells. Ideally, primary epithelia would be collected to support the HBEC line data. In addition, immortalised myeloid cell lines with various CF-associated mutations would also be a useful research tool to probe further into the basic inflammatory pathways effected by CFTR-mutation. Additionally, the cell lines are grown in different media formulations. This may have an effect on the availability of certain ions due to differential salt concentrations. However, the differential growth media formulations are optimised to ensure no significant differences in inflammation due to the growth media in appendix figure 11.

Finally, the prior expertise of the McDermott lab was focussed on innate immune mediated inflammation and autoinflammatory disease. Therefore, the research interests and questions were focussed on this research area. This study cannot comment on other immune pathways, such as lymphoid signatures or other metabolic pathways.

6.8 Future Directions

There is sufficient evidence within this study, in combination with the various seminal studies in the literature, for a comprehensive human clinical trial of anakinra as an anti-inflammatory therapy for CF. This approach may benefit from a prophylactic treatment regime rather than a specific therapy in response to infection. One can hypothesis that many so-called secondary manifestations, that is extra-pulmonary manifestations may benefit from such a regime.

The study of ENaC as a therapeutic target is advanced, with active clinical trials taking place at St James's University Hospital, Leeds and internationally for the SPLUNC1-derived peptide SPX-101. These trials, in addition to future studies using the transgenic β-ENaC-tg mouse model, should investigate immunometabolism to further understand the role of this channel in the pathology of the aggressive inflammatory phenotype in CF.

The outstanding question of how metabolism disturbed in CF and whether this is intrinsic or systemic in origin may affect the role of dietitians in CF and may support a change in dietary guidelines for patients with CF in the future, turning towards a fibre-rich diet rather than high-fat, high-glucose.

Finally, how orkambi modulates inflammation is a key question that also needs further investigation. The hypothesis suggested in section 5.6.2 should be investigated further as this may also lead to more targeted therapeutics such as PGE_2 based therapies

.

Appendix
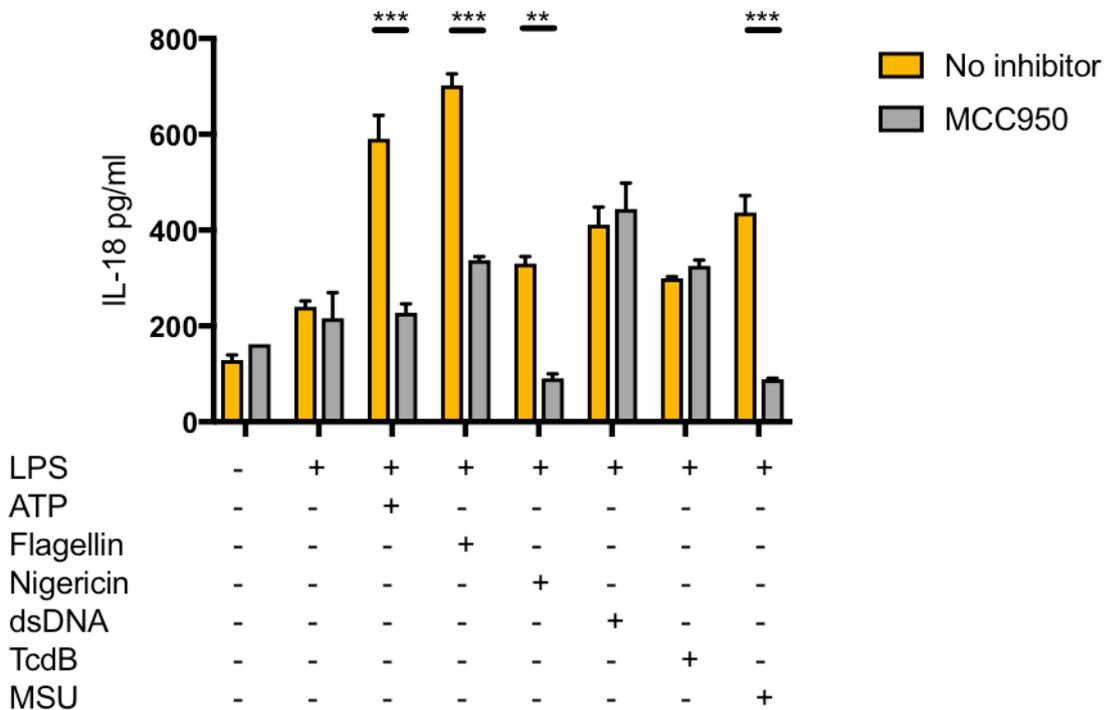
Appendix figure 1: THP-1 *in vitro* Inflammasome stimulation optimisation. ELISA assays were used to detect IL-18 from supernatants of THP-1 monocyte cell growth medium (supplemented RPMI) (n=2). THP-1s were pre-treated with MCC950 (15nM) and a priming stimulation of LPS (10ng/mL) before being stimulated for 30 minutes with ATP (5mM) or 4 hours with Flagellin (10ng/mL with Lipofectamine 2000), Nigericin (1μM), poly (dA:dT) dsDNA (1μg/mL with Lipofectamine 2000), TcdB (10ng/mL) or MSU crystals (100μg/mL). A repeated measures 2-way ANOVA statistical test was performed with Turkey's multiple comparisons test (p values $* = \leq 0.05$, $** = \leq 0.01$, $*** = \leq 0.001$ and $**** = \leq 0.0001$).
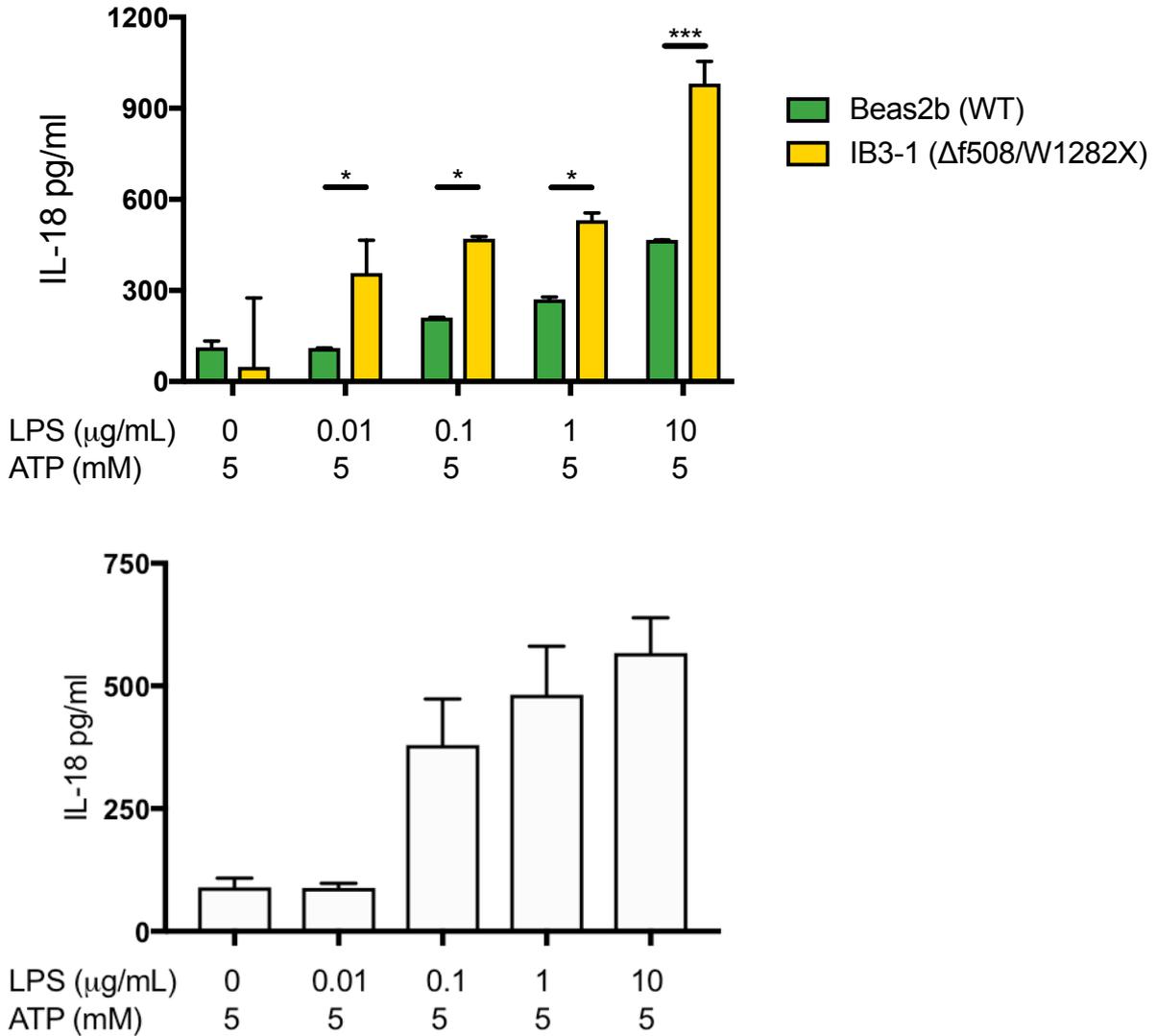
Appendix figure 2: *in vitro* NLRP3 Inflammasome stimulation optimisation. ELISA assays were used to detect IL-18 from supernatants of HBECs (a) and HC PBMCs (b) (n=2). Cells were stimulated with the indicated concentration of LPS (0-10μg/mL) before being stimulated for 30 minutes with ATP (5mM). A repeated measures 2-way ANOVA statistical test was performed with Turkey's multiple comparisons test (p values * = ≤0.05, **= ≤0.01, ***= ≤0.001 and ****= ≤0.0001).

a
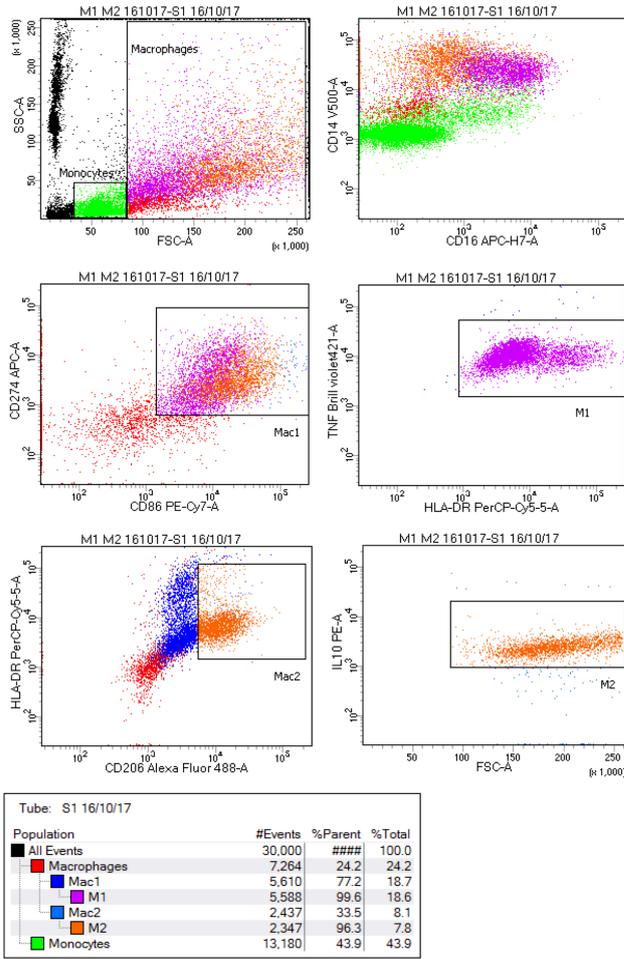
b
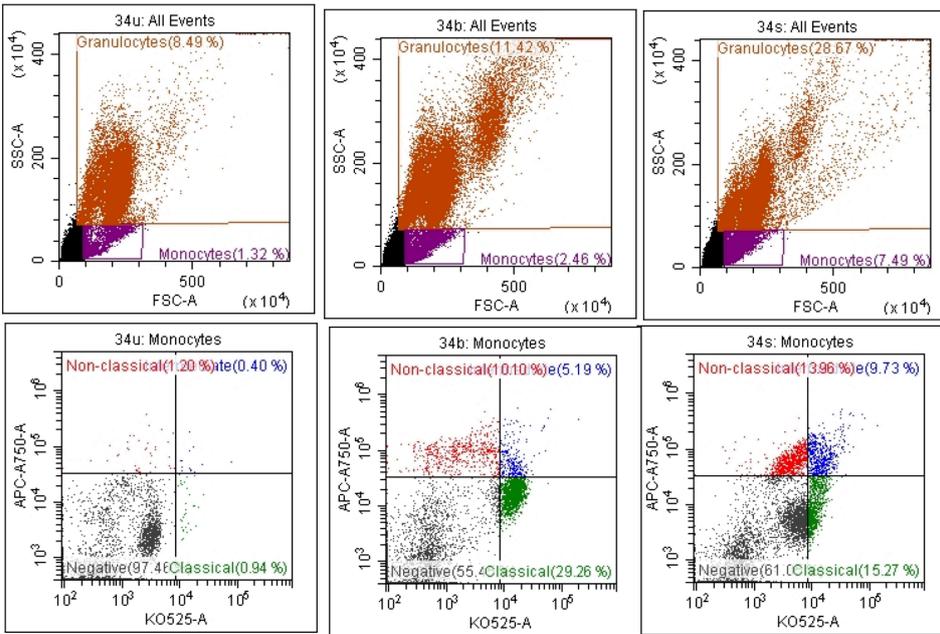
(Appendix Figure 3 legend on next page)

Appendix figure 3: Flow cytometry gating for macrophage and monocytes surface marker analysis. Monocytes from whole blood were differentiated into macrophages and gated based on forward and side scatter. M1-type (markers- CD14+ CD16+ HLA-DR+ CD274+ CD86+ TNFHI). M2-type (markers- CD14+ CD16+ CD206+ IL-10HI) (a). Monocytes were gated on based on forward and side scatter and then based on CD14 and CD16 expression as follows: classical (CD14++CD16−), non-classical (CD14dimCD16++), and intermediate (CD14++CD16+) (b).
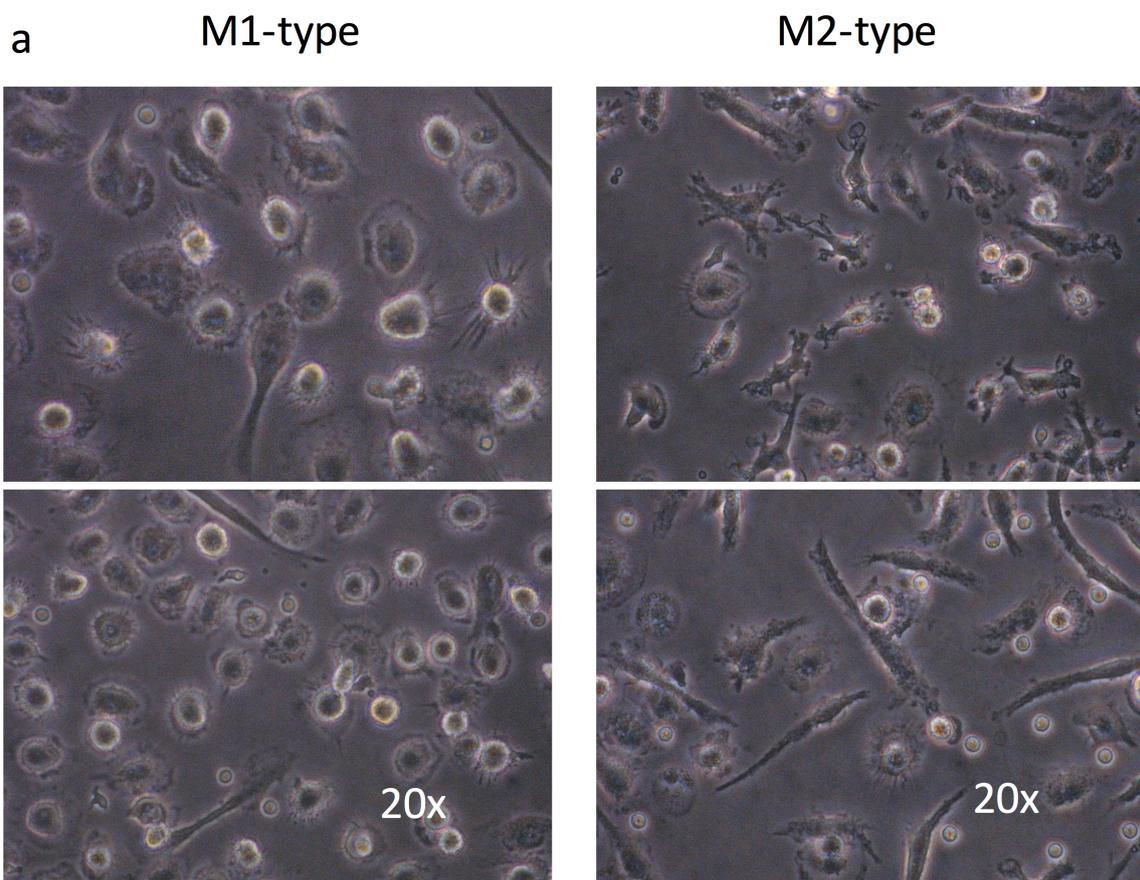
Appendix figure 4: Macrophage and monocyte populations. Phenotypic differences in M1-type and M2-type macrophages by light microscopy (n=2) from HC subjects.
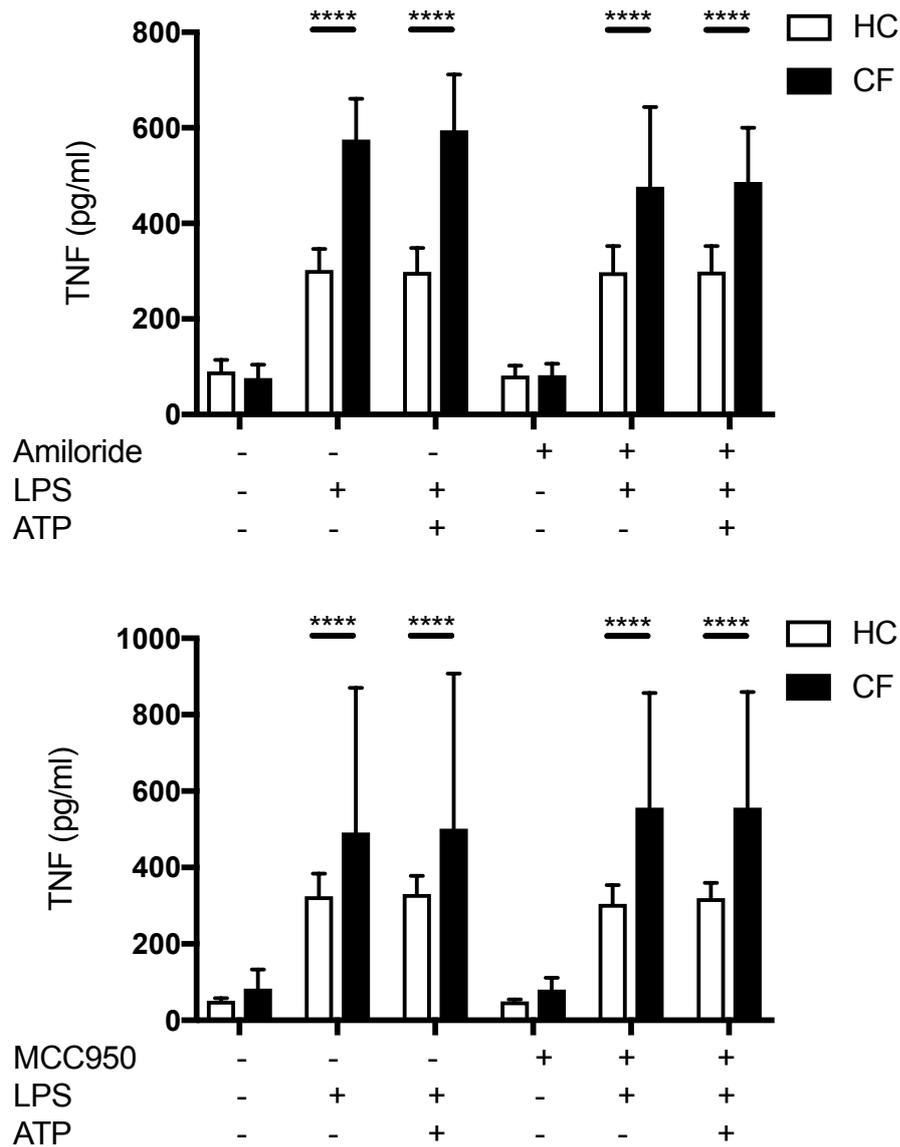
Appendix figure 5: TNF levels from stimulations of monocytes with inhibitors. Patients with CF and HC (n=6) pre-treated with amiloride (a) and MCC950 (b) were measured using ELISA. A repeated measures 2-way ANOVA statistical test was performed with Turkey's multiple comparisons test (p values * = ≤0.05, **= ≤0.01, ***= ≤0.001 and ****= ≤0.0001).

A

Band A — Complex N-glyc 110kDa (found when associated as complex)
Band B — N-glyc ENAC β subunit 96kDa (endo H sensitive)
Band C — 70kDa immature un-glycosylated

B

C
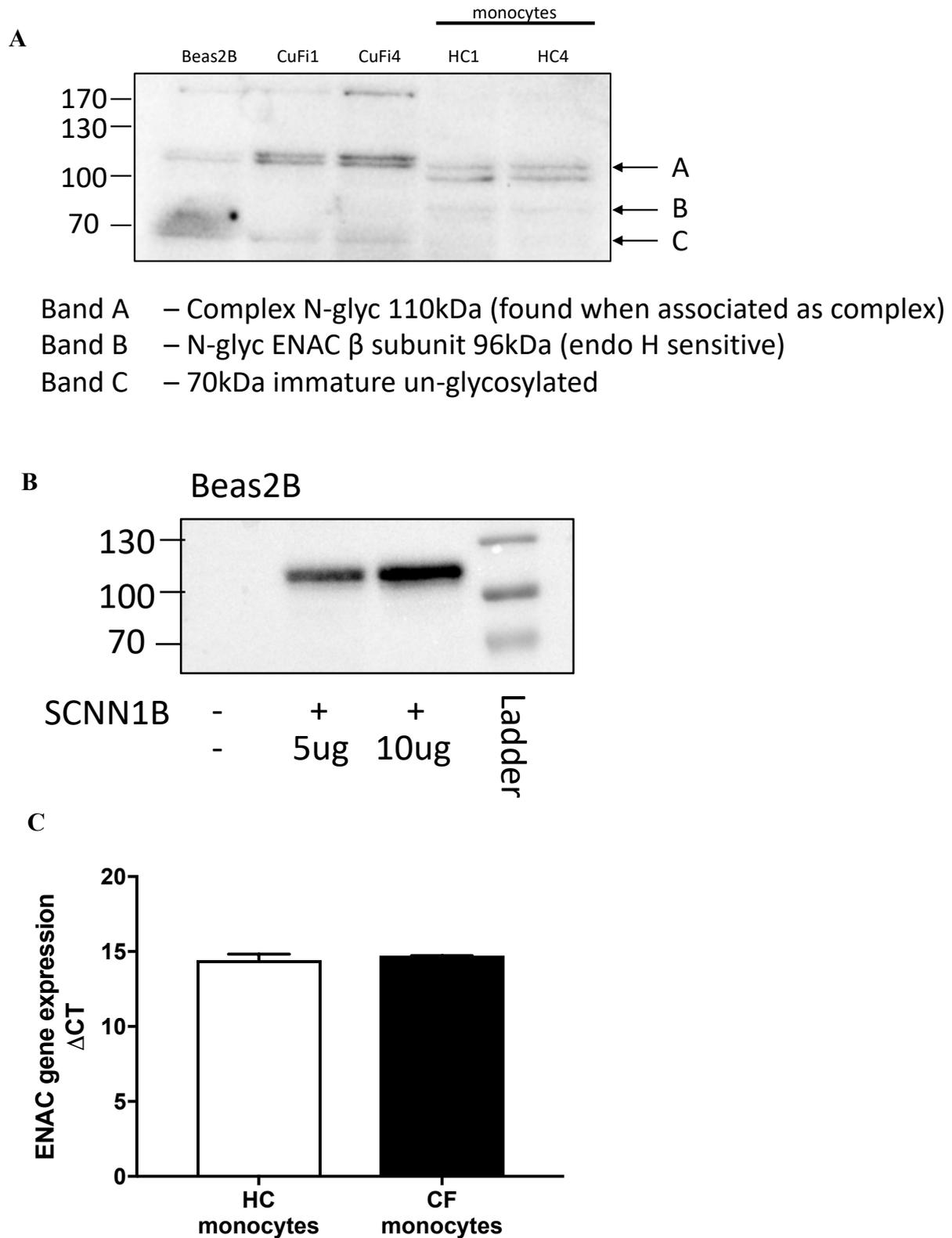
Appendix figure 6: ENaC protein and gene expression in HBEC lines and monocytes.

ENaC protein expression was detected using western blot in Beas2b, CuFi-1 and CuFi-4

HBEC lines as well as in HC monocytes (n=2) (A). To ensure that the correct band was being

interpreted, *SCNN1B* (βENaC) was overexpressed in the Beas2b (WT) HBEC line (B).

Taqman RT-qPCR was used to measure *SCNN1B* expression in HC (n=3) and CF (n=3)

monocytes (C). This figure was produced by Dr Heledd Jarosz-Griffiths and Mr Samuel Lara

Reyna.
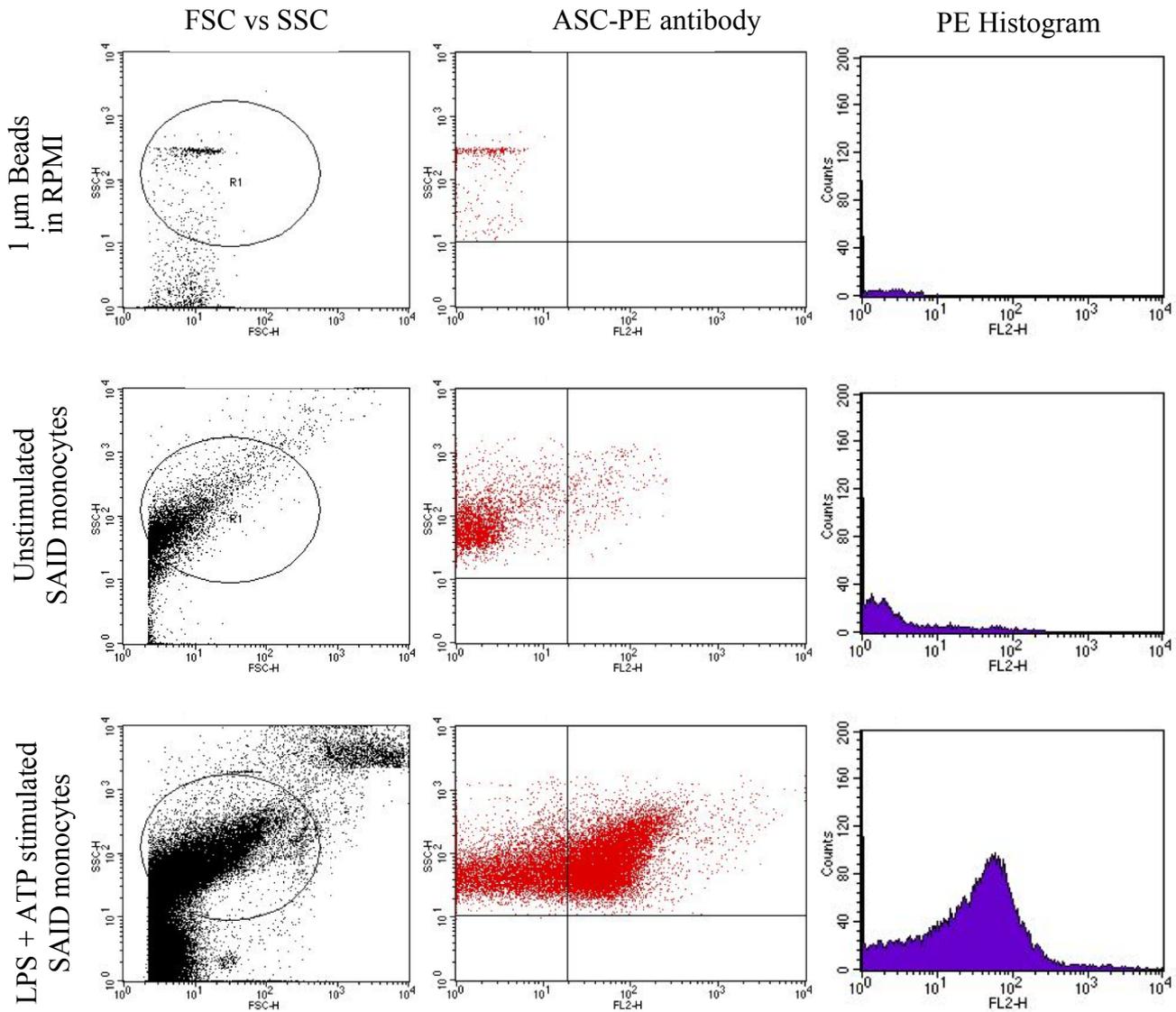
Appendix figure 7: Detection of ASC specks using flow cytometry. 1μm beads were added to uncultured complete RPMI media in order to set a gate for an approximate size and granularity of ASC specks. 1μm beads had no significant amount of background PE fluorescence. PE fluorescence was then measured within the set 1μm gate in the samples of interest. In this representative image, unstimulated and stimulated monocytes from a patient with SAID are used to display the release of extracellular ASC specks upon NLRP3 inflammasome stimulation.
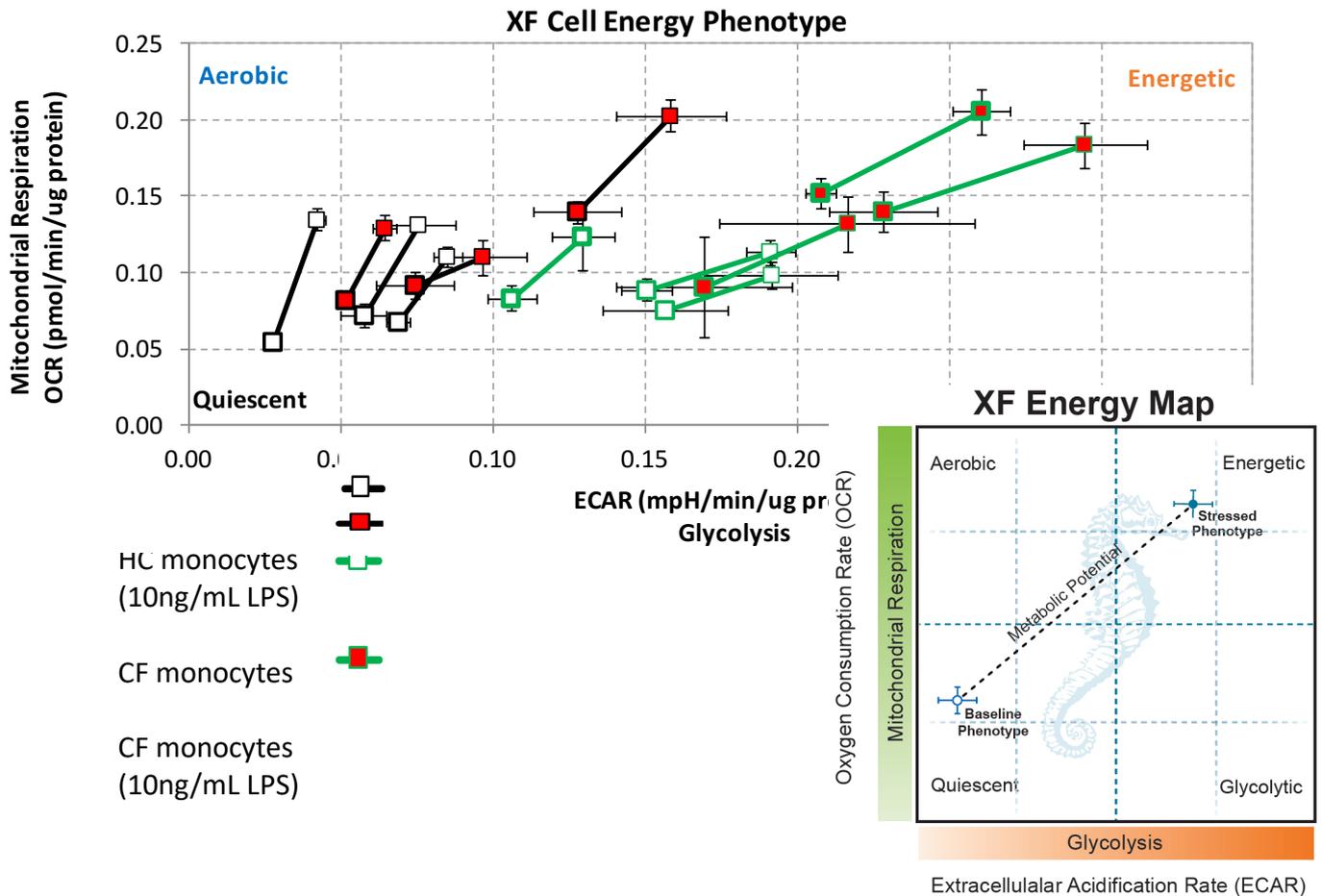
Appendix figure 8: Seahorse cell energy phenotype assay trace. Oxygen consumption rate (OCR) and extracellular acidification rate (ECAR) are used to calculate the metabolic potential and energy phenotype of a sample of interest. The relative usage of OXPHOS and glycolysis of a cell population within a sample is determined under both baseline (baseline phenotype) and stressed (stressed phenotype with oligomycin and FCCP stimulation) conditions. The response to an induced energy demand is a sample's metabolic potential.
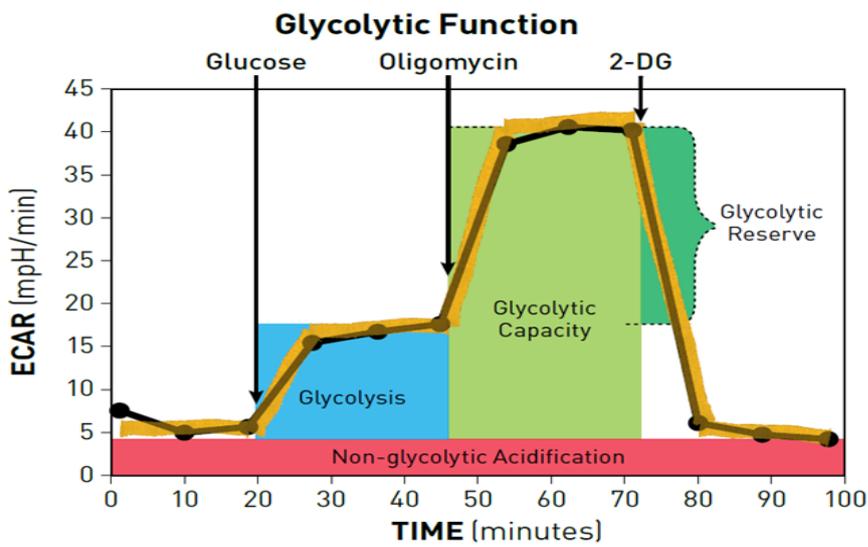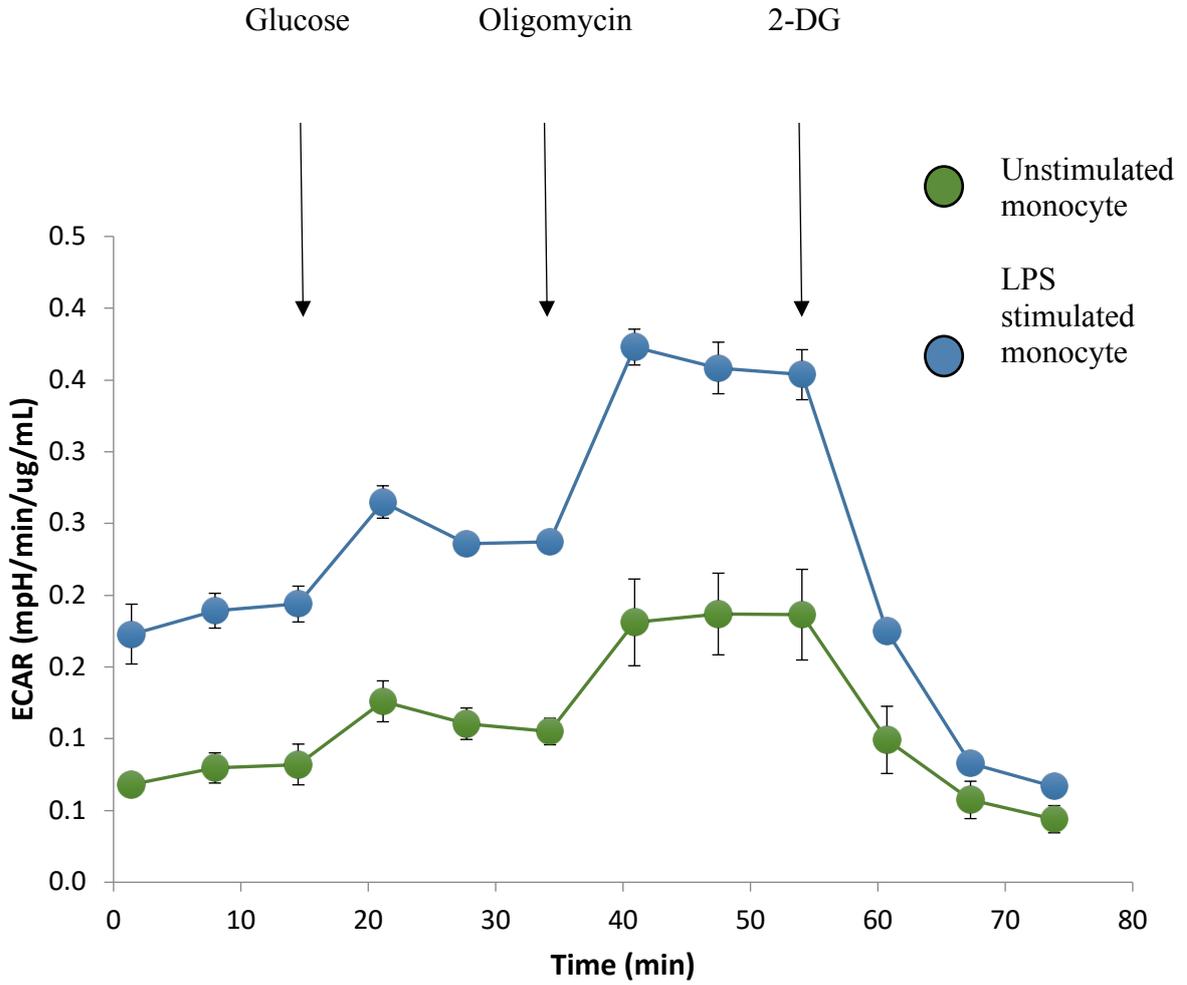
Appendix figure 9: Seahorse glycolytic function assay trace. The profile of the factors of glycolytic function detail the successive injections that allow the measurement of glycolysis, glycolytic capacity, and allow calculation of glycolytic reserve and non-glycolytic acidification.
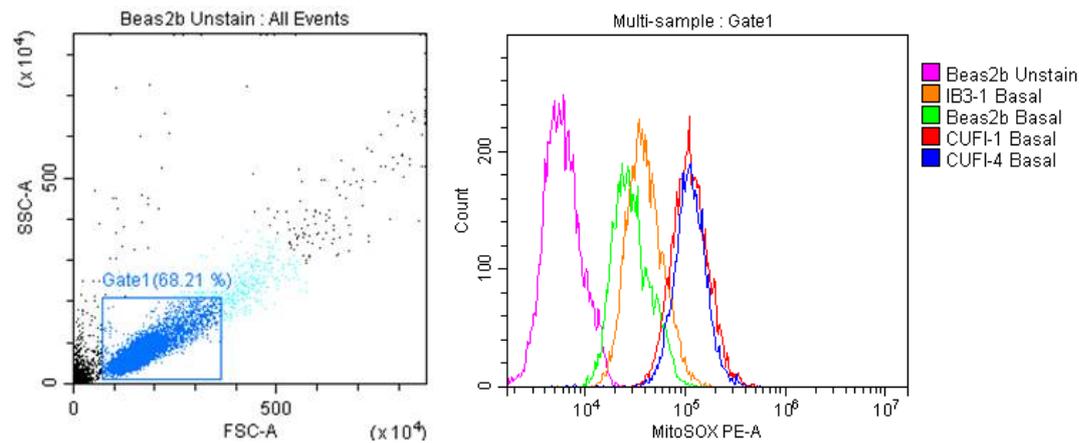
Appendix figure 10: MitoSox flow cytometry assay. Gated cells were used to measure the mean fluorescent intensity of MitoSOX (PE) of each cell line Beas-2b, IB3-1, CuFi-1, and CuFi-4 cell lines. n=3 biological replicates for each cell line. A repeated measures 2-way ANOVA statistical test was performed with Turkey's multiple comparisons test (p values * = $\leq$0.05, **= $\leq$0.01, ***= $\leq$0.001 and ****= $\leq$0.0001).
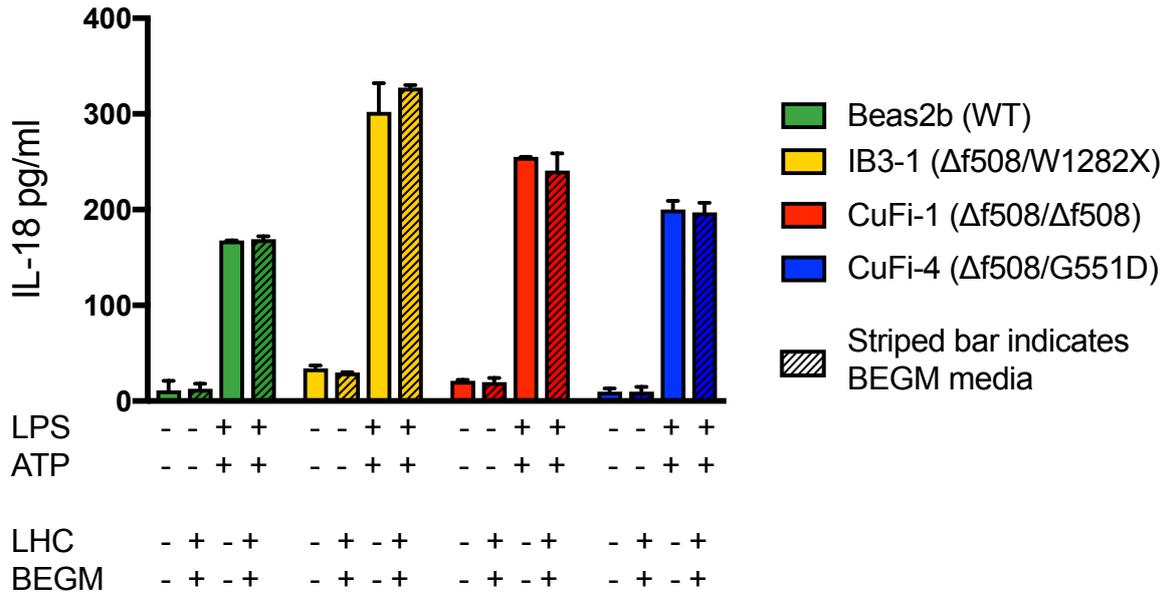
Appendix figure 11: The effect of a change in media supplementation on HBEC line NLRP3 inflammasome responses. An ELISA assay was used to detect IL-18 secretion from HBECs (n=3). Cells were cultured in the indicated media for 24-hours before being stimulated. Cell stimulation was as follows: a stimulation with LPS (10ng/mL) for 4-hours with an ATP (5mM) stimulation for the final 30 minutes. A repeated measures 2-way ANOVA statistical test was performed with Turkey's multiple comparisons test (p values * = ≤ 0.05, **= ≤ 0.01, ***= ≤ 0.001 and ****= ≤ 0.0001).
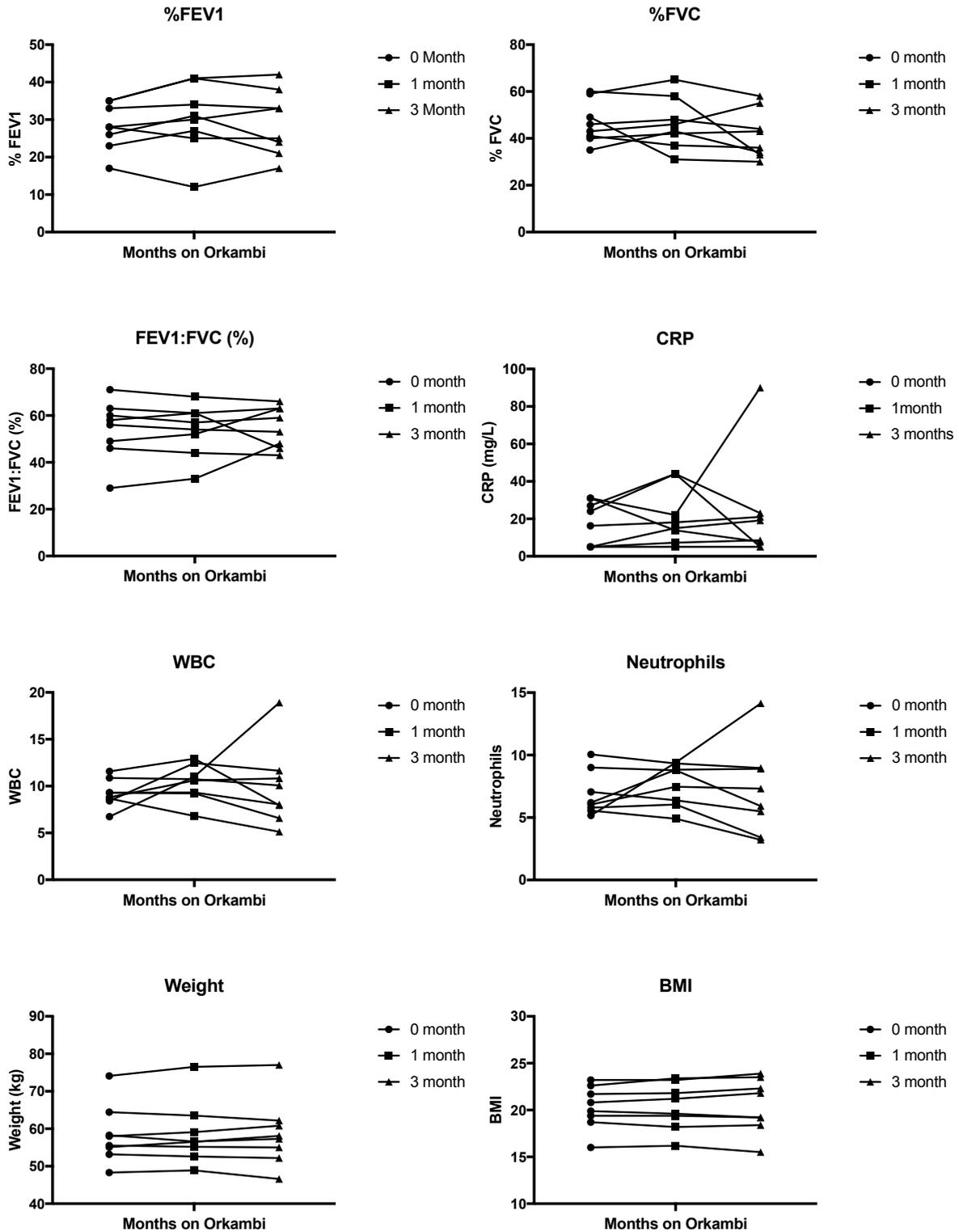
Appendix figure 12: Clinical data from orkambi patient cohort over the 3-month study.

Clinical data from patients enrolled onto the orkambi study in chapter 5 was collected

throughout. Details of baseline lung function FEV1%, FVC (L), FEV: FVC%, weight (Kg)

BMI, CRP (mg/L), white blood cell (WBC) count and neutrophil count.

Bibliography

© CYSTIC FIBROSIS TRUST REGISTERED CHARITY NO. (ENGLAND AND WALES)

1079049, R. C. N. S. S. 2018. *Cystic fibrosis treatments and medications* [Online]. What is

cystic fibrosis?: How is cystic fibrosis treated?

. Available: https://www.cysticfibrosis.org.uk/what-is-cystic-fibrosis/cystic-fibrosis-

care/treatments-and-medication# [Accessed 23/07/18 2018].

ACCURSO, F. J., ROWE, S. M., CLANCY, J. P., BOYLE, M. P., DUNITZ, J. M., DURIE,

P. R., SAGEL, S. D., HORNICK, D. B., KONSTAN, M. W., DONALDSON, S. H.,

MOSS, R. B., PILEWSKI, J. M., RUBENSTEIN, R. C., ULUER, A. Z., AITKEN,

M. L., FREEDMAN, S. D., ROSE, L. M., MAYER-HAMBLETT, N., DONG, Q.,

ZHA, J., STONE, A. J., OLSON, E. R., ORDOÑEZ, C. L., CAMPBELL, P. W.,

ASHLOCK, M. A. & RAMSEY, B. W. 2010. Effect of VX-770 in persons with

cystic fibrosis and the G551D-CFTR mutation. *New England Journal of Medicine,*

363**,** 1991-2003.

ADAM, D., ROUX-DELRIEU, J., LUCZKA, E., BONNOMET, A., LESAGE, J., MEROL,

J. C., POLETTE, M., ABELY, M. & CORAUX, C. 2015. Cystic fibrosis airway

epithelium remodelling: involvement of inflammation. *J Pathol,* 235**,** 408-19.

AEBI, C., THEILER, F., AEBISCHER, C. C. & SCHOENI, M. H. 2000. Autoantibodies

directed against bactericidal/permeability-increasing protein in patients with cystic

fibrosis: Association with microbial respiratory tract colonization. *Pediatric Infectious*

Disease Journal, 19**,** 207-212.

AGLIETTI, R. A., ESTEVEZ, A., GUPTA, A., RAMIREZ, M. G., LIU, P. S., KAYAGAKI,

N., CIFERRI, C., DIXIT, V. M. & DUEBER, E. C. 2016. GsdmD p30 elicited by

caspase-11 during pyroptosis forms pores in membranes. *Proc Natl Acad Sci U S A,*

113**,** 7858-63.

AGOSTINI, L., MARTINON, F., BURNS, K., MCDERMOTT, M. F., HAWKINS, P. N. & TSCHOPP, J. 2004. NALP3 forms an IL-1β-processing inflammasome with increased activity in Muckle-Wells autoinflammatory disorder. *Immunity,* 20**,** 319-325.

ALTHAUS, M. 2013. ENaC inhibitors and airway re-hydration in cystic fibrosis: State of the art. *Current Molecular Pharmacology,* 6**,** 3-12.

ALTON, E. W. F. W., ARMSTRONG, D. K., ASHBY, D., BAYFIELD, K. J., BILTON, D., BLOOMFIELD, E. V., BOYD, A. C., BRAND, J., BUCHAN, R., CALCEDO, R., CARVELLI, P., CHAN, M., CHENG, S. H., COLLIE, D. D. S., CUNNINGHAM, S., DAVIDSON, H. E., DAVIES, G., DAVIES, J. C., DAVIES, L. A., DEWAR, M. H., DOHERTY, A., DONOVAN, J., DWYER, N. S., ELGMATI, H. I., FEATHERSTONE, R. F., GAVINO, J., GEA-SORLI, S., GEDDES, D. M., GIBSON, J. S. R., GILL, D. R., GREENING, A. P., GRIESENBACH, U., HANSELL, D. M., HARMAN, K., HIGGINS, T. E., HODGES, S. L., HYDE, S. C., HYNDMAN, L., INNES, J. A., JACOB, J., JONES, N., KEOGH, B. F., LIMBERIS, M. P., LLOYD-EVANS, P., MACLEAN, A. W., MANVELL, M. C., MCCORMICK, D., MCGOVERN, M., MCLACHLAN, G., MENG, C., MONTERO, M. A., MILLIGAN, H., MOYCE, L. J., MURRAY, G. D., NICHOLSON, A. G., OSADOLOR, T., PARRA-LEITON, J., PORTEOUS, D. J., PRINGLE, I. A., PUNCH, E. K., PYTEL, K. M., QUITTNER, A. L., RIVELLINI, G., SAUNDERS, C. J., SCHEULE, R. K., SHEARD, S., SIMMONDS, N. J., SMITH, K., SMITH, S. N., SOUSSI, N., SOUSSI, S., SPEARING, E. J., STEVENSON, B. J., SUMNER-JONES, S. G., TURKKILA, M., URETA, R. P., WALLER, M. D., WASOWICZ, M. Y., WILSON, J. M. & WOLSTENHOLME-HOGG, P. 2015. Repeated nebulisation of non-viral CFTR gene therapy in patients with cystic fibrosis: A randomised,

double-blind, placebo-controlled, phase 2b trial. *The Lancet Respiratory Medicine,* 3**,** 684-691.

ANAGNOSTOPOULOU, P., DAI, L., SCHATTERNY, J., HIRTZ, S., DUERR, J. & MALL, M. A. 2010. Allergic airway inflammation induces a pro-secretory epithelial ion transport phenotype in mice. *European Respiratory Journal,* 36**,** 1436-1447.

ANDERSSON, B., JANSON, V., BEHNAM-MOTLAGH, P., HENRIKSSON, R. & GRANKVIST, K. 2006. Induction of apoptosis by intracellular potassium ion depletion: Using the fluorescent dye PBFI in a 96-well plate method in cultured lung cancer cells. *Toxicology in Vitro,* 20**,** 986-994.

ARMSTRONG, D. S., HOOK, S. M., JAMSEN, K. M., NIXON, G. M., CARZINO, R., CARLIN, J. B., ROBERTSON, C. F. & GRIMWOOD, K. 2005. Lower airway inflammation in infants with cystic fibrosis detected by newborn screening. *Pediatr Pulmonol,* 40**,** 500-10.

ARMSTRONG, L., MEDFORD, A. R. L., UPPINGTON, K. M., ROBERTSON, J., WITHERDEN, I. R., TETLEY, T. D. & MILLAR, A. B. 2004. Expression of functional toll-like receptor-2 and -4 on alveolar epithelial cells. *American Journal of Respiratory Cell and Molecular Biology,* 31**,** 241-245.

AUBERT, D. F., XU, H., YANG, J., SHI, X., GAO, W., LI, L., BISARO, F., CHEN, S., VALVANO, M. A. & SHAO, F. 2016. A Burkholderia Type VI Effector Deamidates Rho GTPases to Activate the Pyrin Inflammasome and Trigger Inflammation. *Cell Host Microbe,* 19**,** 664-74.

AULAKH, G. K. 2018. Neutrophils in the lung: "the first responders". *Cell and Tissue Research,* 371**,** 577-588.

AURON, P. E., WEBB, A. C., ROSENWASSER, L. J., MUCCI, S. F., RICH, A., WOLFF, S. M. & DINARELLO, C. A. 1984. Nucleotide sequence of human monocyte

interleukin 1 precursor cDNA. *Proceedings of the National Academy of Sciences of the United States of America,* 81**,** 7907-7911.

BAIRD, J. S., WALKER, P., URBAN, A. & BERDELLA, M. 2002. Metabolic alkalosis and cystic fibrosis [5]. *Chest,* 122**,** 755-756.

BALS, R., WEINER, D. J. & WILSON, J. M. 1999. The innate immune system in cystic fibrosis lung disease. *Journal of Clinical Investigation,* 103**,** 303-307.

BARBARO, N. R., FOSS, J. D., KRYSHTAL, D. O., TSYBA, N., KUMARESAN, S., XIAO, L., MERNAUGH, R. L., ITANI, H. A., LOPERENA, R., CHEN, W., DIKALOV, S., TITZE, J. M., KNOLLMANN, B. C., HARRISON, D. G. & KIRABO, A. 2017. Dendritic Cell Amiloride-Sensitive Channels Mediate Sodium-Induced Inflammation and Hypertension. *Cell Reports,* 21**,** 1009-1020.

BAROJA-MAZO, A., MARTIN-SANCHEZ, F., GOMEZ, A. I., MARTINEZ, C. M., AMORES-INIESTA, J., COMPAN, V., BARBERA-CREMADES, M., YAGUE, J., RUIZ-ORTIZ, E., ANTON, J., BUJAN, S., COUILLIN, I., BROUGH, D., AROSTEGUI, J. I. & PELEGRIN, P. 2014. The NLRP3 inflammasome is released as a particulate danger signal that amplifies the inflammatory response. *Nat Immunol,* 15**,** 738-48.

BASELER, W. A., DAVIES, L. C., QUIGLEY, L., RIDNOUR, L. A., WEISS, J. M., HUSSAIN, S. P., WINK, D. A. & MCVICAR, D. W. 2016. Autocrine IL-10 functions as a rheostat for M1 macrophage glycolytic commitment by tuning nitric oxide production. *Redox Biology,* 10**,** 12-23.

BATES, C. M., BAUM, M. & QUIGLEY, R. 1997. Cystic Fibrosis Presenting with Hypokalemia and MetabolicAlkalosis in a Previously Healthy Adolescent. *Journal of the American Society of Nephrology,* 8**,** 352-356.

BAUERNFEIND, F., NIEPMANN, S., KNOLLE, P. A. & HORNUNG, V. 2016. Aging-Associated TNF Production Primes Inflammasome Activation and NLRP3-Related Metabolic Disturbances. *The Journal of Immunology,* 197**,** 2900.

BELLINGHAM, M. & EVANS, T. J. 2007. The $\alpha_2\beta_1$ isoform of guanylyl cyclase mediates plasma membrane localized nitric oxide signalling. *Cellular Signalling,* 19**,** 2183-2193.

BERDIEV, B. K., QADRI, Y. J. & BENOS, D. J. 2009. Assessment of the CFTR and ENaC association. *Molecular BioSystems,* 5**,** 123-227.

BERGIN, D. A., HURLEY, K., MEHTA, A., COX, S., RYAN, D., O'NEILL, S. J., REEVES, E. P. & MCELVANEY, N. G. 2013. Airway inflammatory markers in individuals with cystic fibrosis and non-cystic fibrosis bronchiectasis. *J Inflamm Res,* 6**,** 1-11.

BERGSBAKEN, T., FINK, S. L. & COOKSON, B. T. 2009. Pyroptosis: host cell death and inflammation. *Nat Rev Microbiol,* 7**,** 99-109.

BERTAUX, A., CABON, L., BRUNELLE-NAVAS, M. N., BOUCHET, S., NEMAZANYY, I. & SUSIN, S. A. 2018. Mitochondrial OXPHOS influences immune cell fate: Lessons from hematopoietic AIF-deficient and NDUFS4-deficient mouse models comment. *Cell Death and Disease,* 9.

BESANCON, F., PRZEWLOCKI, G., BARO, I., HONGRE, A. S., ESCANDE, D. & EDELMAN, A. 1994. Interferon-γ downregulates CFTR gene expression in epithelial cells. *American Journal of Physiology - Cell Physiology,* 267**,** C1398-C1404.

BETTENCOURT, I. A. & POWELL, J. D. 2017. Targeting metabolism as a novel therapeutic approach to autoimmunity, inflammation, and transplantation. *Journal of Immunology,* 198**,** 999-1005.

BHALLA, V. & HALLOWS, K. R. 2008. Mechanisms of ENaC regulation and clinical implications. *J Am Soc Nephrol,* 19**,** 1845-54.

BLOHMKE, C. J., MAYER, M. L., TANG, A. C., HIRSCHFELD, A. F., FJELL, C. D., SZE, M. A., FALSAFI, R., WANG, S., HSU, K., CHILVERS, M. A., HOGG, J. C., HANCOCK, R. E. & TURVEY, S. E. 2012. Atypical activation of the unfolded protein response in cystic fibrosis airway cells contributes to p38 MAPK-mediated innate immune responses. *J Immunol,* 189**,** 5467-75.

BLOHMKE, C. J., VICTOR, R. E., HIRSCHFELD, A. F., ELIAS, I. M., HANCOCK, D. G., LANE, C. R., DAVIDSON, A. G. F., WILCOX, P. G., SMITH, K. D., OVERHAGE, J., HANCOCK, R. E. W. & TURVEY, S. E. 2008. Innate Immunity Mediated by TLR5 as a Novel Antiinflammatory Target for Cystic Fibrosis Lung Disease. *The Journal of Immunology,* 180**,** 7764-7773.

BONFIELD, T. L., HODGES, C. A., COTTON, C. U. & DRUMM, M. L. 2012. Absence of the cystic fibrosis transmembrane regulator (Cftr) from myeloid-derived cells slows resolution of inflammation and infection. *J Leukoc Biol,* 92**,** 1111-22.

BONFIELD, T. L., PANUSKA, J. R., KONSTAN, M. W., HILLIARD, K. A., HILLIARD, J. B., GHNAIM, H. & BERGER, M. 1995. Inflammatory cytokines in cystic fibrosis lungs. *Am J Respir Crit Care Med,* 152**,** 2111-8.

BOUCHER, R. C., STUTTS, M. J., KNOWLES, M. R., CANTLEY, L. & GATZY, J. T. 1986. Na+ transport in cystic fibrosis respiratory epithelia. Abnormal basal rate and response to adenylate cyclase activation. *Journal of Clinical Investigation,* 78**,** 1245-1252.

BRAND, K. 1985. Glutamine and glucose metabolism during thymocyte proliferation. Pathways of glutamine and glutamate metabolism. *Biochemical Journal,* 228**,** 353-361.

BRAND, K., FEKL, W., VON HINTZENSTERN, J., LANGER, K., LUPPA, P. & SCHOERNER, C. 1989. Metabolism of glutamine in lymphocytes. *Metabolism,* 38**,** 29-33.

BRENNAN, M. L. & SCHRIJVER, I. 2016. Cystic Fibrosis: A Review of Associated Phenotypes, Use of Molecular Diagnostic Approaches, Genetic Characteristics, Progress, and Dilemmas. *J Mol Diagn,* 18**,** 3-14.

BROZ, P. & DIXIT, V. M. 2016. Inflammasomes: Mechanism of assembly, regulation and signalling. *Nature Reviews Immunology,* 16**,** 407-420.

BRUSCIA, E. M. & BONFIELD, T. L. 2016a. Cystic Fibrosis Lung Immunity: The Role of the Macrophage. *Journal of Innate Immunity,* 8**,** 550-563.

BRUSCIA, E. M. & BONFIELD, T. L. 2016b. Innate and Adaptive Immunity in Cystic Fibrosis. *Clinics in Chest Medicine,* 37**,** 17-29.

BRUSCIA, E. M., ZHANG, P. X., FERREIRA, E., CAPUTO, C., EMERSON, J. W., TUCK, D., KRAUSE, D. S. & EGAN, M. E. 2009. Macrophages directly contribute to the exaggerated inflammatory response in cystic fibrosis transmembrane conductance regulator-/- mice. *Am J Respir Cell Mol Biol,* 40**,** 295-304.

BUCK, M. D., O'SULLIVAN, D., KLEIN GELTINK, R. I., CURTIS, J. D., CHANG, C. H., SANIN, D. E., QIU, J., KRETZ, O., BRAAS, D., VAN DER WINDT, G. J. W., CHEN, Q., HUANG, S. C. C., O'NEILL, C. M., EDELSON, B. T., PEARCE, E. J., SESAKI, H., HUBER, T. B., RAMBOLD, A. S. & PEARCE, E. L. 2016. Mitochondrial Dynamics Controls T Cell Fate through Metabolic Programming. *Cell,* 166**,** 63-76.

BUDDING, K., VAN DE GRAAF, E. A., HOEFNAGEL, T., KWAKKEL-VAN ERP, J. M., VAN KESSEL, D. A., DRAGUN, D., HACK, C. E. & OTTEN, H. G. 2015. Anti-

ET$_A$R and anti-AT$_1$R autoantibodies are elevated in patients with endstage cystic fibrosis. *Journal of Cystic Fibrosis,* 14**,** 42-45.

BUSHBY, K., FINKEL, R., WONG, B., BAROHN, R., CAMPBELL, C., COMI, G. P., CONNOLLY, A. M., DAY, J. W., FLANIGAN, K. M., GOEMANS, N., JONES, K. J., MERCURI, E., QUINLIVAN, R., RENFROE, J. B., RUSSMAN, B., RYAN, M. M., TULINIUS, M., VOIT, T., MOORE, S. A., LEE SWEENEY, H., ABRESCH, R. T., COLEMAN, K. L., EAGLE, M., FLORENCE, J., GAPPMAIER, E., GLANZMAN, A. M., HENRICSON, E., BARTH, J., ELFRING, G. L., REHA, A., SPIEGEL, R. J., O'DONNELL, M. W., PELTZ, S. W., MCDONALD, C. M., KORNBERG, A. J., WRAY, A., CARROLL, K., KENNEDY, R., VILLANO, D., DE VALLE, K., NORTH, K. N., DEXTER, M., WICKS, S., ROSE, K., BUYSE, G. M., VAN DEN HAUWE, M., VRIJSEN, B., JANMOHAMMAD, A., SCHOLTES, C., MAH, J. K., WRIGHT, C. J., CHIU, A., WALKER, L. M., SARNAT, H. B., SELBY, K., KING, C., MEISNER, L., DOPPLER, V., DE CASTRO, D., DECOSTRE, V., CHABROL, B., LEVY, N., HALBERT, C., PEREON, Y., MAGOT, A., PERRIER, J., MAHE, J. Y., PERRAU, A. S., CHASSERIEAU, R., SCHARA, U., LUTZ, S., BUSSE, M., DELLA MARINA, A., BOSBACH, T., KIRSCHNER, J., STANESCU, A., POHL, A., RENSING-ZIMMERMAN, C., EISELE, U., FETZER, I., VOGT, S., BERTINI, E., D'AMICO, A., KOFLER, A., GESU, P. B., CARLESI, A., BONETTI, A. M., GAGLIARDI, M. G., SANTECCHIA, L., EMMA, F., BERGAMI, G., VASCO, G., BIANCO, F., MAZZONE, E. S., PANE, M., DE SANCTIS, R., MAGRI, F., LUCCHINI, V., CORTI, S. P., MOGGIO, M. G., et al. 2014. Ataluren treatment of patients with nonsense mutation dystrophinopathy. *Muscle and Nerve,* 50**,** 477-487.

CAFFERATA, E. G., GONZÁLEZ-GUERRICO, A. M., GIORDANO, L., PIVETTA, O. H. & SANTA-COLOMA, T. A. 2000. Interleukin-1β regulates CFTR expression in human intestinal T84 cells. *Biochimica et Biophysica Acta - Molecular Basis of Disease,* 1500**,** 241-248.

CAFFERATA, E. G. A., GONZÁLEZ GUERRICO, A. M., PIVETTA, O. H. & SANTA-COLOMA, T. A. 2001. NF-κB Activation Is Involved in Regulation of Cystic Fibrosis Transmembrane Conductance Regulator (CFTR) by Interleukin-1β. *Journal of Biological Chemistry,* 276**,** 15441-15444.

CAI, X., CHEN, J., XU, H., LIU, S., JIANG, Q. X., HALFMANN, R. & CHEN, Z. J. 2014. Prion-like polymerization underlies signal transduction in antiviral immune defense and inflammasome activation. *Cell,* 156**,** 1207-22.

CAPUTO, A., CACI, E., FERRERA, L., PEDEMONTE, N., BARSANTI, C., SONDO, E., PFEFFER, U., RAVAZZOLO, R., ZEGARRA-MORAN, O. & GALIETTA, L. J. V. 2008. TMEM16A, a membrane protein associated with calcium-dependent chloride channel activity. *Science,* 322**,** 590-594.

CHAE, J. J., PARK, Y. H., PARK, C., HWANG, I. Y., HOFFMANN, P., KEHRL, J. H., AKSENTIJEVICH, I. & KASTNER, D. L. 2015. Connecting two pathways through Ca 2+ signaling: NLRP3 inflammasome activation induced by a hypermorphic PLCG2 mutation. *Arthritis Rheumatol,* 67**,** 563-7.

CHAIX, J., TESSMER, M. S., HOEBE, K., FUSÉRI, N., RYFFEL, B., DALOD, M., ALEXOPOULOU, L., BEUTLER, B., BROSSAY, L., VIVIER, E. & WALZER, T. 2008. Cutting edge: Priming of NK cells by IL-18. *Journal of Immunology,* 181**,** 1627-1631.

CHEN, H., YANG, T., ZHU, L. & ZHAO, Y. 2015. Cellular metabolism on T-cell development and function. *International Reviews of Immunology,* 34**,** 19-33.

CHENG, J., WANG, H. & GUGGINO, W. B. 2005. Regulation of cystic fibrosis transmembrane regulator trafficking and protein expression by a rho family small GTPase TC10. *Journal of Biological Chemistry,* 280**,** 3731-3739.

CHENG, S. H., GREGORY, R. J., MARSHALL, J., PAUL, S., SOUZA, D. W., WHITE, G. A., O'RIORDAN, C. R. & SMITH, A. E. 1990. Defective intracellular transport and processing of CFTR is the molecular basis of most cystic fibrosis. *Cell,* 63**,** 827-834.

CHO, J. S., HAN, I. H., LEE, H. R. & LEE, H. M. 2014. Prostaglandin E2 induces IL-6 and IL-8 production by the EP Receptors/Akt/NF-KB pathways in nasal polyp-derived fibroblasts. *Allergy, Asthma and Immunology Research,* 6**,** 449-457.

CHOLON, D. M., QUINNEY, N. L., FULCHER, M. L., ESTHER JR, C. R., DAS, J., DOKHOLYAN, N. V., RANDELL, S. H., BOUCHER, R. C. & GENTZSCH, M. 2014. Cystic fibrosis: Potentiator ivacaftor abrogates pharmacological correction of ΔF508 CFTR in cystic fibrosis. *Science Translational Medicine,* 6.

CHOUCHANI, E. T., PELL, V. R., GAUDE, E., AKSENTIJEVIC, D., SUNDIER, S. Y., ROBB, E. L., LOGAN, A., NADTOCHIY, S. M., ORD, E. N., SMITH, A. C., EYASSU, F., SHIRLEY, R., HU, C. H., DARE, A. J., JAMES, A. M., ROGATTI, S., HARTLEY, R. C., EATON, S., COSTA, A. S., BROOKES, P. S., DAVIDSON, S. M., DUCHEN, M. R., SAEB-PARSY, K., SHATTOCK, M. J., ROBINSON, A. J., WORK, L. M., FREZZA, C., KRIEG, T. & MURPHY, M. P. 2014. Ischaemic accumulation of succinate controls reperfusion injury through mitochondrial ROS. *Nature,* 515**,** 431-5.

CHOULAKI, C., PAPADAKI, G., REPA, A., KAMPOURAKI, E., KAMBAS, K., RITIS, K., BERTSIAS, G., BOUMPAS, D. T. & SIDIROPOULOS, P. 2015. Enhanced activity of NLRP3 inflammasome in peripheral blood cells of patients with active rheumatoid arthritis. *Arthritis Res Ther,* 17**,** 257.

CHURCH, L. D., COOK, G. P. & MCDERMOTT, M. F. 2008. Primer: inflammasomes and interleukin 1beta in inflammatory disorders. *Nat Clin Pract Rheumatol,* 4**,** 34-42.

CLAUZURE, M., VALDIVIESO, A. G., MASSIP COPIZ, M. M., SCHULMAN, G., TEIBER, M. L. & SANTA-COLOMA, T. A. 2014. Disruption of interleukin-1beta autocrine signaling rescues complex I activity and improves ROS levels in immortalized epithelial cells with impaired cystic fibrosis transmembrane conductance regulator (CFTR) function. *PLoS One,* 9**,** e99257.

COGLIATI, S., FREZZA, C., SORIANO, M. E., VARANITA, T., QUINTANA-CABRERA, R., CORRADO, M., CIPOLAT, S., COSTA, V., CASARIN, A., GOMES, L. C., PERALES-CLEMENTE, E., SALVIATI, L., FERNANDEZ-SILVA, P., ENRIQUEZ, J. A. & SCORRANO, L. 2013. Mitochondrial cristae shape determines respiratory chain supercomplexes assembly and respiratory efficiency. *Cell,* 155**,** 160-171.

COHEN, T. S. & PRINCE, A. 2012. Cystic fibrosis: a mucosal immunodeficiency syndrome. *Nat Med,* 18**,** 509-19.

COHEN-CYMBERKNOH, M., KEREM, E., FERKOL, T. & ELIZUR, A. 2013. Airway inflammation in cystic fibrosis: Molecular mechanisms and clinical implications. *Thorax,* 68**,** 1157-1162.

COLGAN, S. P., RESNICK, M. B., PARKOS, C. A., DELP-ARCHER, C., MCGUIRK, D., BACARRA, A. E., WELLER, P. F. & MADARA, J. L. 1994. IL-4 directly modulates function of a model human intestinal epithelium. *Journal of Immunology,* 153**,** 2122-2129.

COLL, R. C., ROBERTSON, A. A., CHAE, J. J., HIGGINS, S. C., MUNOZ-PLANILLO, R., INSERRA, M. C., VETTER, I., DUNGAN, L. S., MONKS, B. G., STUTZ, A., CROKER, D. E., BUTLER, M. S., HANEKLAUS, M., SUTTON, C. E., NUNEZ, G.,

LATZ, E., KASTNER, D. L., MILLS, K. H., MASTERS, S. L., SCHRODER, K., COOPER, M. A. & O'NEILL, L. A. 2015. A small-molecule inhibitor of the NLRP3 inflammasome for the treatment of inflammatory diseases. *Nat Med,* 21**,** 248-55.

COLLACO, A. M., GEIBEL, P., LEE, B. S., GEIBEL, J. P. & AMEEN, N. A. 2013. Functional vacuolar ATPase (V-ATPase) proton pumps traffic to the enterocyte brush border membrane and require CFTR. *Am J Physiol Cell Physiol,* 305**,** C981-96.

CORDES, T., WALLACE, M., MICHELUCCI, A., DIVAKARUNI, A. S., SAPCARIU, S. C., SOUSA, C., KOSEKI, H., CABRALES, P., MURPHY, A. N., HILLER, K. & METALLO, C. M. 2016. Immunoresponsive gene 1 and itaconate inhibit succinate dehydrogenase to modulate intracellular succinate levels. *Journal of Biological Chemistry,* 291**,** 14274-14284.

COUTINHO, H. D., FALCAO-SILVA, V. S. & GONCALVES, G. F. 2008. Pulmonary bacterial pathogens in cystic fibrosis patients and antibiotic therapy: a tool for the health workers. *Int Arch Med,* 1**,** 24.

CRAMER, T., YAMANISHI, Y., CLAUSEN, B. E., FÖRSTER, I., PAWLINSKI, R., MACKMAN, N., HAASE, V. H., JAENISCH, R., CORR, M., NIZET, V., FIRESTEIN, G. S., GERBER, H. P., FERRARA, N. & JOHNSON, R. S. 2003. HIF-1α is essential for myeloid cell-mediated inflammation. *Cell,* 112**,** 645-657.

CROW, Y. J., HAYWARD, B. E., PARMAR, R., ROBINS, P., LEITCH, A., ALI, M., BLACK, D. N., VAN BOKHOVEN, H., BRUNNER, H. G., HAMEL, B. C., CORRY, P. C., COWAN, F. M., FRINTS, S. G., KLEPPER, J., LIVINGSTON, J. H., LYNCH, S. A., MASSEY, R. F., MERITET, J. F., MICHAUD, J. L., PONSOT, G., VOIT, T., LEBON, P., BONTHRON, D. T., JACKSON, A. P., BARNES, D. E. & LINDAHL, T. 2006. Mutations in the gene encoding the 3'-5' DNA exonuclease

TREX1 cause Aicardi-Goutières syndrome at the AGS1 locus. *Nature Genetics,* 38**,** 917-920.

CULHANE, S., GEORGE, C., PEARO, B. & SPOEDE, E. 2013. Malnutrition in cystic fibrosis: A review. *Nutrition in Clinical Practice,* 28**,** 676-683.

D'OSUALDO, A., ANANIA, V. G., YU, K., LILL, J. R., KAUFMAN, R. J., MATSUZAWA, S. & REED, J. C. 2015. Transcription Factor ATF4 Induces NLRP1 Inflammasome Expression during Endoplasmic Reticulum Stress. *PLoS One,* 10**,** e0130635.

DANAHAY, H., ATHERTON, H., JONES, G., BRIDGES, R. J. & POLL, C. T. 2002. Interleukin-13 induces a hypersecretory ion transport phenotype in human bronchial epithelial cells. *American Journal of Physiology - Lung Cellular and Molecular Physiology,* 282**,** L226-L236.

DAVIES, J., SHERIDAN, H., BELL, N., CUNNINGHAM, S., DAVIS, S. D., ELBORN, J. S., MILLA, C. E., STARNER, T. D., WEINER, D. J., LEE, P. S. & RATJEN, F. 2013a. Assessment of clinical response to ivacaftor with lung clearance index in cystic fibrosis patients with a G551D-CFTR mutation and preserved spirometry: A randomised controlled trial. *The Lancet Respiratory Medicine,* 1**,** 630-638.

DAVIES, J. C., WAINWRIGHT, C. E., CANNY, G. J., CHILVERS, M. A., HOWENSTINE, M. S., MUNCK, A., MAINZ, J. G., RODRIGUEZ, S., LI, H., YEN, K., ORDOÑEZ, C. L. & AHRENS, R. 2013b. Efficacy and safety of ivacaftor in patients aged 6 to 11 years with cystic fibrosis with a G551D mutation. *American Journal of Respiratory and Critical Care Medicine,* 187**,** 1219-1225.

DE BOECK, K. & AMARAL, M. D. 2016. Progress in therapies for cystic fibrosis. *The Lancet Respiratory Medicine,* 4**,** 662-674.

DE GASSART, A. & MARTINON, F. 2015. Pyroptosis: Caspase-11 Unlocks the Gates of Death. *Immunity,* 43**,** 835-7.

DE NARDO, D., DE NARDO, C. M. & LATZ, E. 2014. New insights into mechanisms controlling the NLRP3 inflammasome and its role in lung disease. *Am J Pathol,* 184**,** 42-54.

DEEKS, E. D. 2016. Lumacaftor/Ivacaftor: A Review in Cystic Fibrosis. *Drugs,* 76**,** 1191-1201.

DEL PORTO, P., CIFANI, N., GUARNIERI, S., DI DOMENICO, E. G., MARIGGIO, M. A., SPADARO, F., GUGLIETTA, S., ANILE, M., VENUTA, F., QUATTRUCCI, S. & ASCENZIONI, F. 2011. Dysfunctional CFTR alters the bactericidal activity of human macrophages against Pseudomonas aeruginosa. *PLoS One,* 6**,** e19970.

DEVANEY, J. M., GREENE, C. M., TAGGART, C. C., CARROLL, T. P., O'NEILL, S. J. & MCELVANEY, N. G. 2003. Neutrophil elastase up-regulates interleukin-8 via toll-like receptor 4. *FEBS Letters,* 544**,** 129-132.

DICK, M. S., SBORGI, L., RÜHL, S., HILLER, S. & BROZ, P. 2016. ASC filament formation serves as a signal amplification mechanism for inflammasomes. *Nature Communications,* 7.

DINARELLO, C. A. 1996. Biologic basis for interleukin-1 in disease. *Blood,* 87**,** 2095-2147.

DINARELLO, C. A. 1998. Interleukin-1β, interleukin-18, and the interleukin-1β converting enzyme. *Annals of the New York Academy of Sciences.*

DINARELLO, C. A., SIMON, A. & VAN DER MEER, J. W. M. 2012. Treating inflammation by blocking interleukin-1 in a broad spectrum of diseases. *Nature Reviews Drug Discovery,* 11**,** 633-652.

DINARELLO, C. A. & VAN DER MEER, J. W. M. 2013. Treating inflammation by blocking interleukin-1 in humans. *Seminars in Immunology,* 25**,** 469-484.

DINARELLO CHARLES, A. 2017. Overview of the IL-1 family in innate inflammation and acquired immunity. *Immunological Reviews,* 281**,** 8-27.

DODÉ, C., LE DÛ, N., CUISSET, L., LETOURNEUR, F., BERTHELOT, J. M., VAUDOUR, G., MEYRIER, A., WATTS, R. A., SCOTT, D. G. I., NICHOLLS, A., GRANEL, B., FRANCES, C., GARCIER, F., EDERY, P., BOULINGUEZ, S., DOMERGUES, J. P., DELPECH, M. & GRATEAU, G. 2002. New mutations of CIAS1 that are responsible for Muckle-Wells syndrome and familial cold urticaria: A novel mutation underlies both syndromes. *American Journal of Human Genetics,* 70**,** 1498-1506.

DONALDSON, S. H. & BOUCHER, R. C. 2007. Sodium channels and cystic fibrosis. *Chest,* 132**,** 1631-1636.

DONALDSON, S. H., POLIGONE, E. G. & STUTTS, M. J. 2002. CFTR regulation of ENaC. *Methods in molecular medicine,* 70**,** 343-364.

DONALDSON, S. H., SOLOMON, G. M., ZEITLIN, P. L., FLUME, P. A., CASEY, A., MCCOY, K., ZEMANICK, E. T., MANDAGERE, A., TROHA, J. M., SHOEMAKER, S. A., CHMIEL, J. F. & TAYLOR-COUSAR, J. L. 2017. Pharmacokinetics and safety of cavosonstat (N91115) in healthy and cystic fibrosis adults homozygous for F508DEL-CFTR. *Journal of Cystic Fibrosis,* 16**,** 371-379.

DONG, Z. W., CHEN, J., RUAN, Y. C., ZHOU, T., CHEN, Y., CHEN, Y., TSANG, L. L., CHAN, H. C. & PENG, Y. Z. 2015. CFTR-regulated MAPK/NF-kappaB signaling in pulmonary inflammation in thermal inhalation injury. *Sci Rep,* 5**,** 15946.

DOWNEY, D. G., BELL, S. C. & ELBORN, J. S. 2009. Neutrophils in cystic fibrosis. *Thorax,* 64**,** 81-88.

DUBIN, P. J., MCALLISTER, F. & KOLLS, J. K. 2007. Is cystic fibrosis a TH17 disease? *Inflammation Research,* 56**,** 221-227.

DUFF, A. J. A. 2002. Psychological consequences of segregation resulting from chronic Burkholderia cepacia infection in adults with CF. *Thorax,* 57**,** 756.

ECKFORD, P. D. W., LI, C., RAMJEESINGH, M. & BEAR, C. E. 2012. Cystic fibrosis transmembrane conductance regulator (CFTR) potentiator VX-770 (ivacaftor) opens the defective channel gate of mutant CFTR in a phosphorylationdependent but ATP-independent manner. *Journal of Biological Chemistry,* 287**,** 36639-36649.

EISENHUT, M., SIDARAS, D., BARTON, P., NEWLAND, P. & SOUTHERN, K. W. 2004. Elevated sweat sodium associated with pulmonary oedema in meningococcal sepsis. *European Journal of Clinical Investigation,* 34**,** 576-579.

EISENHUT, M. & SOUTHERN, K. W. 2002. Positive sweat test following meningococcal septicaemia [2]. *Acta Paediatrica, International Journal of Paediatrics,* 91**,** 361-362.

EISENHUT, M. & WALLACE, H. 2011. Ion channels in inflammation. *Pflugers Archiv European Journal of Physiology,* 461**,** 401-421.

ELBORN, J. S. 2016. Cystic fibrosis. *Lancet*.

ETTORRE, M., VERZÈ, G., CALDRER, S., JOHANSSON, J., CALCATERRA, E., ASSAEL, B. M., MELOTTI, P., SORIO, C. & BUFFELLI, M. 2014. Electrophysiological evaluation of Cystic Fibrosis Conductance Transmembrane Regulator (CFTR) expression in human monocytes. *Biochimica et Biophysica Acta - General Subjects,* 1840**,** 3088-3095.

EVERTS, B., AMIEL, E., VAN DER WINDT, G. J. W., FREITAS, T. C., CHOTT, R., YARASHESKI, K. E., PEARCE, E. L. & PEARCE, E. J. 2012. Commitment to glycolysis sustains survival of NO-producing inflammatory dendritic cells. *Blood,* 120**,** 1422-1431.

FAJAC, I., VIEL, M., SUBLEMONTIER, S., HUBERT, D. & BIENVENU, T. 2008. Could a defective epithelial sodium channel lead to bronchiectasis. *Respir Res,* 9**,** 46.

FARINHA, C. M., MATOS, P. & AMARAL, M. D. 2013. Control of cystic fibrosis transmembrane conductance regulator membrane trafficking: not just from the endoplasmic reticulum to the Golgi. *FEBS J,* 280**,** 4396-406.

FASTH, A. & KOLLBERG, H. 1980. AUTOANTIBODIES TO TAMM-HORSFALL PROTEIN IN PATIENTS WITH CYSTIC FIBROSIS. *Acta Pædiatrica,* 69**,** 189-192.

FEARON, U., CANAVAN, M., BINIECKA, M. & VEALE, D. J. 2016. Hypoxia, mitochondrial dysfunction and synovial invasiveness in rheumatoid arthritis. *Nature Reviews Rheumatology,* 12**,** 385-397.

FERNANDES-ALNEMRI, T. & ALNEMRI, E. S. 2008. Assembly, Purification, and Assay of the Activity of the ASC Pyroptosome. *Methods in Enzymology.*

FERNANDES-ALNEMRI, T., YU, J. W., DATTA, P., WU, J. & ALNEMRI, E. S. 2009. AIM2 activates the inflammasome and cell death in response to cytoplasmic DNA. *Nature,* 458**,** 509-13.

FILKINS, L. M. & O'TOOLE, G. A. 2015. Cystic Fibrosis Lung Infections: Polymicrobial, Complex, and Hard to Treat. *PLoS Pathogens,* 11.

FLEETWOOD, A. J., LEE, M. K. S., SINGLETON, W., ACHUTHAN, A., LEE, M. C., O'BRIEN-SIMPSON, N. M., COOK, A. D., MURPHY, A. J., DASHPER, S. G., REYNOLDS, E. C. & HAMILTON, J. A. 2017. Metabolic remodeling, inflammasome activation, and pyroptosis in macrophages stimulated by Porphyromonas gingivalis and its outer membrane vesicles. *Frontiers in Cellular and Infection Microbiology,* 7.

FRANCHI, L., EIGENBROD, T., MUÑOZ-PLANILLO, R., OZKUREDE, U., KIM, Y. G., CHAKRABARTI, A., GALE, M., SILVERMAN, R. H., COLONNA, M., AKIRA, S.

& NÚÑEZ, G. 2014. Cytosolic double-stranded RNA activates the NLRP3 inflammasome via MAVS-induced membrane permeabilization and K+ efflux. *Journal of Immunology,* 193**,** 4214-4222.

FRANKLIN, B. S., BOSSALLER, L., DE NARDO, D., RATTER, J. M., STUTZ, A., ENGELS, G., BRENKER, C., NORDHOFF, M., MIRANDOLA, S. R., AL-AMOUDI, A., MANGAN, M. S., ZIMMER, S., MONKS, B. G., FRICKE, M., SCHMIDT, R. E., ESPEVIK, T., JONES, B., JARNICKI, A. G., HANSBRO, P. M., BUSTO, P., MARSHAK-ROTHSTEIN, A., HORNEMANN, S., AGUZZI, A., KASTENMÜLLER, W. & LATZ, E. 2014. The adaptor ASC has extracellular and 'prionoid' activities that propagate inflammation. *Nature Immunology,* 15**,** 727-737.

FRITZSCHING, B., ZHOU-SUCKOW, Z., TROJANEK, J. B., SCHUBERT, S. C., SCHATTERNY, J., HIRTZ, S., AGRAWAL, R., MULEY, T., KAHN, N., STICHT, C., GUNKEL, N., WELTE, T., RANDELL, S. H., LÄNGER, F., SCHNABEL, P., HERTH, F. J. F. & MALL, M. A. 2015. Hypoxic epithelial necrosis triggers neutrophilic inflammation via IL-1 receptor signaling in cystic fibrosis lung disease. *American Journal of Respiratory and Critical Care Medicine,* 191**,** 902-913.

GAILLARD, E. A., KOTA, P., GENTZSCH, M., DOKHOLYAN, N. V., STUTTS, M. J. & TARRAN, R. 2010. Regulation of the epithelial Na+ channel and airway surface liquid volume by serine proteases. *Pflugers Archiv European Journal of Physiology,* 460**,** 1-17.

GAMPER, N., HUBER, S. M., BADAWI, K. & LANG, F. 2000. Cell volume-sensitive sodium channels upregulated by glucocorticoids in U937 macrophages. *Pflugers Archiv European Journal of Physiology,* 441**,** 281-286.

GAO, Z. & SU, X. 2015. CFTR regulates acute inflammatory responses in macrophages. *QJM,* 108**,** 951-8.

GARCIA-CABALLERO, A., RASMUSSEN, J. E., GAILLARD, E., WATSON, M. J., OLSEN, J. C., DONALDSON, S. H., STUTTS, M. J. & TARRAN, R. 2009. SPLUNC1 regulates airway surface liquid volume by protecting ENaC from proteolytic cleavage. *Proceedings of the National Academy of Sciences of the United States of America,* 106**,** 11412-11417.

GARLAND, A. L., WALTON, W. G., COAKLEY, R. D., TAN, C. D., GILMORE, R. C., HOBBS, C. A., TRIPATHY, A., CLUNES, L. A., BENCHARIT, S., STUTTS, M. J., BETTS, L., REDINBO, M. R. & TARRAN, R. 2013. Molecular basis for pH-dependent mucosal dehydration in cystic fibrosis airways. *Proceedings of the National Academy of Sciences of the United States of America,* 110**,** 15973-15978.

GARNETT, J. P., KALSI, K. K., SOBOTTA, M., BEARHAM, J., CARR, G., POWELL, J., BRODLIE, M., WARD, C., TARRAN, R. & BAINES, D. L. 2016. Hyperglycaemia and Pseudomonas aeruginosa acidify cystic fibrosis airway surface liquid by elevating epithelial monocarboxylate transporter 2 dependent lactate-H + secretion. *Scientific Reports,* 6.

GEBOREK, A. & HJELTE, L. 2011. Association between genotype and pulmonary phenotype in cystic fibrosis patients with severe mutations. *Journal of Cystic Fibrosis,* 10**,** 187-192.

GHEZZI, P., SACCO, S., AGNELLO, D., MARULLO, A., CASELLI, G. & BERTINI, R. 2000. LPS induces IL-6 in the brain and in serum largely through TNF production. *Cytokine,* 12**,** 1205-1210.

GIANOTTI, A., MELANI, R., CACI, E., SONDO, E., RAVAZZOLO, R., GALIETTA, L. J. V. & ZEGARRA-MORAN, O. 2013. Epithelial sodium channel silencing as a strategy to correct the airway surface fluid deficit in cystic fibrosis. *American Journal of Respiratory Cell and Molecular Biology,* 49**,** 445-452.

GIBSON-CORLEY, K. N., MEYERHOLZ, D. K. & ENGELHARDT, J. F. 2016. Pancreatic pathophysiology in cystic fibrosis. *Journal of Pathology,* 238**,** 311-320.

GONG, T., YANG, Y., JIN, T., JIANG, W. & ZHOU, R. 2018. Orchestration of NLRP3 Inflammasome Activation by Ion Fluxes. *Trends in Immunology*.

GRAHAM, A., HASANI, A., ALTON, E. W. F. W., MARTIN, G. P., MARRIOTT, C., HODSON, M. E., CLARKE, S. W. & GEDDES, D. M. 1993. No added benefit from nebulized amiloride in patients with cystic fibrosis. *European Respiratory Journal,* 6**,** 1243-1248.

GRASSME, H., CARPINTEIRO, A., EDWARDS, M. J., GULBINS, E. & BECKER, K. A. 2014. Regulation of the inflammasome by ceramide in cystic fibrosis lungs. *Cell Physiol Biochem,* 34**,** 45-55.

GRASSMÉ, H., CARPINTEIRO, A., EDWARDS, M. J., GULBINS, E. & BECKER, K. A. 2014. Regulation of the inflammasome by ceramide in cystic fibrosis lungs. *Cell Physiol Biochem,* 34**,** 45-55.

GREALLY, P., HUSSEIN, M. J., COOK, A. J., SAMPSON, A. P., PIPER, P. J. & PRICE, J. F. 1993. Sputum tumour necrosis factor-α and leukotriene concentrations in cystic fibrosis. *Archives of Disease in Childhood,* 68**,** 389-392.

GREINER, E. F., GUPPY, M. & BRAND, K. 1994. Glucose is essential for proliferation and the glycolytic enzyme induction that provokes a transition to glycolytic energy production. *Journal of Biological Chemistry,* 269**,** 31484-31490.

GRINSTEIN, L., LUKSCH, H., ROBERTSON, A. A. B., COOPER, M. A., WINKLER, S. & RÖSEN-WOLFF, A. 2015. An optimized whole blood assay measuring expression and activity of NLRP3-, NLRC4 and AIM2-inflammasomes. *Pediatric Rheumatology,* 13**,** O51.

GROS, C. J., MISHRA, R., SCHNEIDER, K. S., MÉDARD, G., WETTMARSHAUSEN, J., DITTLEIN, D. C., SHI, H., GORKA, O., KOENIG, P. A., FROMM, S., MAGNANI, G., ĆIKOVIĆ, T., HARTJES, L., SMOLLICH, J., ROBERTSON, A. A. B., COOPER, M. A., SCHMIDT-SUPPRIAN, M., SCHUSTER, M., SCHRODER, K., BROZ, P., TRAIDL-HOFFMANN, C., BEUTLER, B., KUSTER, B., RULAND, J., SCHNEIDER, S., PEROCCHI, F. & GROS, O. 2016. K+Efflux-Independent NLRP3 Inflammasome Activation by Small Molecules Targeting Mitochondria. *Immunity,* 45**,** 761-773.

GULHANE, M., MURRAY, L., LOURIE, R., TONG, H., SHENG, Y. H., WANG, R., KANG, A., SCHREIBER, V., WONG, K. Y., MAGOR, G., DENMAN, S., BEGUN, J., FLORIN, T. H., PERKINS, A., CUÏ¿½V, P. Ï., MCGUCKIN, M. A. & HASNAIN, S. Z. 2016. High Fat Diets Induce Colonic Epithelial Cell Stress and Inflammation that is Reversed by IL-22. *Scientific Reports,* 6.

GURUNG, P., LI, B., SUBBARAO MALIREDDI, R. K., LAMKANFI, M., GEIGER, T. L. & KANNEGANTI, T. D. 2015. Chronic TLR Stimulation Controls NLRP3 Inflammasome Activation through IL-10 Mediated Regulation of NLRP3 Expression and Caspase-8 Activation. *Sci Rep,* 5**,** 14488.

GWOŹDZIŃSKA, P., BUCHBINDER, B. A., MAYER, K., HEROLD, S., MORTY, R. E., SEEGER, W. & VADÁSZ, I. 2017. Hypercapnia Impairs ENaC Cell Surface Stability by Promoting Phosphorylation, Polyubiquitination and Endocytosis of β-ENaC in a Human Alveolar Epithelial Cell Line. *Frontiers in Immunology,* 8.

HARDIMAN, K. M., MCNICHOLAS-BEVENSEE, C. M., FORTENBERRY, J., MYLES, C. T., MALIK, B., EATON, D. C. & MATALON, S. 2004. Regulation of amiloride-sensitive Na+ transport by basal nitric oxide. *American Journal of Respiratory Cell and Molecular Biology,* 30**,** 720-728.

HARRISON, S., NIZAM, S., MCDERMOT, M., MCGONAGLE, D. & SAVIC, S. 2015. Anakinra as a diagnostic challenge and treatment option for systemic autoinflammatory disorders of undefined genetic cause. *Pediatric Rheumatology*.

HARTL, D., GAGGAR, A., BRUSCIA, E., HECTOR, A., MARCOS, V., JUNG, A., GREENE, C., MCELVANEY, G., MALL, M. & DÖRING, G. 2012. Innate immunity in cystic fibrosis lung disease. *Journal of Cystic Fibrosis,* 11**,** 363-382.

HASSETT, D. J., SUTTON, M. D., SCHURR, M. J., HERR, A. B., CALDWELL, C. C. & MATU, J. O. 2009. Pseudomonas aeruginosa hypoxic or anaerobic biofilm infections within cystic fibrosis airways. *Trends Microbiol,* 17**,** 130-8.

HAWKINS, P. N., LACHMANN, H. J. & MCDERMOTT, M. F. 2003. Interleukin-1-receptor antagonist in the Muckle-Wells syndrome [8]. *New England Journal of Medicine,* 348**,** 2583-2584.

HAYES, E., POHL, K., MCELVANEY, N. G. & REEVES, E. P. 2011. The cystic fibrosis neutrophil: A specialized yet potentially defective cell. *Archivum Immunologiae et Therapiae Experimentalis,* 59**,** 97-112.

HE, W. T., WAN, H., HU, L., CHEN, P., WANG, X., HUANG, Z., YANG, Z. H., ZHONG, C. Q. & HAN, J. 2015. Gasdermin D is an executor of pyroptosis and required for interleukin-1beta secretion. *Cell Res,* 25**,** 1285-98.

HERMANN, T. 2007. Aminoglycoside antibiotics: Old drugs and new therapeutic approaches. *Cellular and Molecular Life Sciences,* 64**,** 1841-1852.

HINSON, R. M., WILLIAMS, J. A. & SHACTER, E. 1996. Elevated interleukin 6 is induced by prostaglandin E2 in a murine model of inflammation: Possible role of cyclooxygenase-2. *Proceedings of the National Academy of Sciences of the United States of America,* 93**,** 4885-4890.

HOBBS, C. A., BLANCHARD, M. G., ALIJEVIC, O., TAN, C. D., KELLENBERGER, S., BENCHARIT, S., CAO, R., KESIMER, M., WALTON, W. G., HENDERSON, A. G., REDINBO, M. R., STUTTS, M. J. & TARRAN, R. 2013. Identification of the SPLUNC1 ENaC-inhibitory domain yields novel strategies to treat sodium hyperabsorption in cystic fibrosis airway epithelial cultures. *American Journal of Physiology - Lung Cellular and Molecular Physiology,* 305**,** L990-L1001.

HODGES, K. & GILL, R. 2010. Infectious diarrhea: Cellular and molecular mechanisms. *Gut Microbes,* 1**,** 4-21.

HODSON, M. E. & TURNER-WARWICK, M. 1981. Autoantibodies in cystic fibrosis. *Clinical Allergy,* 11**,** 565-570.

HOFFMAN, H. M., MUELLER, J. L., BROIDE, D. H., WANDERER, A. A. & KOLODNER, R. D. 2001. Mutation of a new gene encoding a putative pyrin-like protein causes familial cold autoinflammatory syndrome and Muckle-Wells syndrome. *Nature Genetics,* 29**,** 301-305.

HOIBY, N. & WIIK, A. 1975. Antibacterial precipitins and autoantibodies in serum of patients with cystic fibrosis. *Scandinavian Journal of Respiratory Diseases,* 56**,** 38-46.

HORNUNG, V., ABLASSER, A., CHARREL-DENNIS, M., BAUERNFEIND, F., HORVATH, G., CAFFREY, D. R., LATZ, E. & FITZGERALD, K. A. 2009. AIM2 recognizes cytosolic dsDNA and forms a caspase-1-activating inflammasome with ASC. *Nature,* 458**,** 514-8.

HOWARD, M., FRIZZELL, R. A. & BEDWELL, D. M. 1996. Aminoglycoside antibiotics restore CFTR function by overcoming premature stop mutations. *Nature Medicine,* 2**,** 467-469.

HUBEAU, C., LE NAOUR, R., ABÉLY, M., HINNRASKY, J., GUENOUNOU, M., GAILLARD, D. & PUCHELLE, E. 2004. Dysregulation of IL-2 and IL-8 production in circulating T lymphocytes from young cystic fibrosis patients. *Clinical and Experimental Immunology,* 135**,** 528-534.

HUTT, D. M., HERMAN, D., RODRIGUES, A. P. C., NOEL, S., PILEWSKI, J. M., MATTESON, J., HOCH, B., KELLNER, W., KELLY, J. W., SCHMIDT, A., THOMAS, P. J., MATSUMURA, Y., SKACH, W. R., GENTZSCH, M., RIORDAN, J. R., SORSCHER, E. J., OKIYONEDA, T., YATES, J. R., LUKACS, G. L., FRIZZELL, R. A., MANNING, G., GOTTESFELD, J. M. & BALCH, W. E. 2010. Reduced histone deacetylase 7 activity restores function to misfolded CFTR in cystic fibrosis. *Nature Chemical Biology,* 6**,** 25-33.

IANNITTI, R. G., NAPOLIONI, V., OIKONOMOU, V., DE LUCA, A., GALOSI, C., PARIANO, M., MASSI-BENEDETTI, C., BORGHI, M., PUCCETTI, M., LUCIDI, V., COLOMBO, C., FISCARELLI, E., LASS-FLORL, C., MAJO, F., CARIANI, L., RUSSO, M., PORCARO, L., RICCIOTTI, G., ELLEMUNTER, H., RATCLIF, L., DE BENEDICTIS, F. M., TALESA, V. N., DINARELLO, C. A., VAN DE VEERDONK, F. L. & ROMANI, L. 2016. IL-1 receptor antagonist ameliorates inflammasome-dependent inflammation in murine and human cystic fibrosis. *Nat Commun,* 7**,** 10791.

IOANNIDIS, FANG YE, BETH MCNALLY, MEREDITH WILLETTE, EMILIO FLAÑO. 2013. Toll-Like Receptor Expression and Induction of Type I and Type III Interferons in Primary Airway Epithelial Cells. *Journal of Virology*, 6, 3261-3270.

ITALIANI, P. & BORASCHI, D. 2014. From Monocytes to M1/M2 Macrophages: Phenotypical vs. Functional Differentiation. *Frontiers in Immunology,* 5**,** 514.

JAIN, L., CHEN, X. J., BROWN, L. A. & EATON, D. C. 1998. Nitric oxide inhibits lung sodium transport through a cGMP-mediated inhibition of epithelial cation channels. *American Journal of Physiology - Lung Cellular and Molecular Physiology,* 274**,** L475-L484.

JEFFERY, A., CHARMAN, S., COSGRIDD, R., CARR, S. 2017. UK Cystic Fibrosis Registry Annual Data Report 2016.

JIANG, D., WENZEL, S. E., WU, Q., BOWLER, R. P., SCHNELL, C. & CHU, H. W. 2013. Human Neutrophil Elastase Degrades SPLUNC1 and Impairs Airway Epithelial Defense against Bacteria. *PLoS ONE,* 8.

JIANG, H., HE, H., CHEN, Y., HUANG, W., CHENG, J., YE, J., WANG, A., TAO, J., WANG, C., LIU, Q., JIN, T., JIANG, W., DENG, X. & ZHOU, R. 2017. Identification of a selective and direct NLRP3 inhibitor to treat inflammatory disorders. *Journal of Experimental Medicine,* 214**,** 3219-3238.

JIH, K. Y. & HWANG, T. C. 2013. Vx-770 potentiates CFTR function by promoting decoupling between the gating cycle and ATP hydrolysis cycle. *Proceedings of the National Academy of Sciences of the United States of America,* 110**,** 4404-4409.

JOHANSSON, J., VEZZALINI, M., VERZÈ, G., CALDRER, S., BOLOGNIN, S., BUFFELLI, M., BELLISOLA, G., TRIDELLO, G., ASSAEL, B. M., MELOTTI, P. & SORIO, C. 2014. Detection of CFTR protein in human leukocytes by flow cytometry. *Cytometry Part A,* 85**,** 611-620.

KASTNER, D. L., AKSENTIJEVICH, I. & GOLDBACH-MANSKY, R. 2010. Autoinflammatory Disease Reloaded: A Clinical Perspective. *Cell,* 140**,** 784-790.

KAYAGAKI, N., STOWE, I. B., LEE, B. L., O'ROURKE, K., ANDERSON, K., WARMING, S., CUELLAR, T., HALEY, B., ROOSE-GIRMA, M., PHUNG, Q. T., LIU, P. S., LILL, J. R., LI, H., WU, J., KUMMERFELD, S., ZHANG, J., LEE, W. P.,

SNIPAS, S. J., SALVESEN, G. S., MORRIS, L. X., FITZGERALD, L., ZHANG, Y., BERTRAM, E. M., GOODNOW, C. C. & DIXIT, V. M. 2015. Caspase-11 cleaves gasdermin D for non-canonical inflammasome signalling. *Nature,* 526**,** 666-71.

KEISER, N. W., BIRKET, S. E., EVANS, I. A., TYLER, S. R., CROOKE, A. K., SUN, X., ZHOU, W., NELLIS, J. R., STROEBELE, E. K., CHU, K. K., TEARNEY, G. J., STEVENS, M. J., HARRIS, J. K., ROWE, S. M. & ENGELHARDT, J. F. 2015. Defective innate immunity and hyperinflammation in newborn cystic fibrosis transmembrane conductance regulator-knockout ferret lungs. *Am J Respir Cell Mol Biol,* 52**,** 683-94.

KELLY, B. & O'NEILL, L. A. J. 2015. Metabolic reprogramming in macrophages and dendritic cells in innate immunity. *Cell Research,* 25**,** 771-784.

KEREM, B. S., ROMMENS, J. M., BUCHANAN, J. A., MARKIEWICZ, D., COX, T. K., CHAKRAVARTI, A., BUCHWALD, M. & TSUI, L. C. 1989. Identification of the cystic fibrosis gene: Genetic analysis. *Science,* 245**,** 1073-1080.

KEREM, E., BISTRITZER, T., HANUKOGLU, A., HOFMANN, T., ZHOU, Z., BENNETT, W., MACLAUGHLIN, E., BARKER, P., NASH, M., QUITTELL, L., BOUCHER, R., KNOWLES, M. R., HOMOLYA, V. & KEENAN, B. 1999. Pulmonary epithelial sodium-channel dysfunction and excess airway liquid in pseudohypoaldosteronism. *New England Journal of Medicine,* 341**,** 156-162.

KEREM, E., HIRAWAT, S., ARMONI, S., YAAKOV, Y., SHOSEYOV, D., COHEN, M., NISSIM-RAFINIA, M., BLAU, H., RIVLIN, J., AVIRAM, M., ELFRING, G. L., NORTHCUTT, V. J., MILLER, L. L., KEREM, B. & WILSCHANSKI, M. 2008. Effectiveness of PTC124 treatment of cystic fibrosis caused by nonsense mutations: a prospective phase II trial. *The Lancet,* 372**,** 719-727.

KEREM, E., KONSTAN, M. W., DE BOECK, K., ACCURSO, F. J., SERMET-GAUDELUS, I., WILSCHANSKI, M., ELBORN, J. S., MELOTTI, P., BRONSVELD, I., FAJAC, I., MALFROOT, A., ROSENBLUTH, D. B., WALKER, P. A., MCCOLLEY, S. A., KNOOP, C., QUATTRUCCI, S., RIETSCHEL, E., ZEITLIN, P. L., BARTH, J., ELFRING, G. L., WELCH, E. M., BRANSTROM, A., SPIEGEL, R. J., PELTZ, S. W., AJAYI, T. & ROWE, S. M. 2014. Ataluren for the treatment of nonsense-mutation cystic fibrosis: A randomised, double-blind, placebo-controlled phase 3 trial. *The Lancet Respiratory Medicine,* 2**,** 539-547.

KHALID, O. A., CLAUDIU, T. S. & LAURENT, S. 2017. The Warburg Effect and the Hallmarks of Cancer. *Anti-Cancer Agents in Medicinal Chemistry,* 17**,** 164-170.

KILLICK, K. E., NI CHEALLAIGH, C., O'FARRELLY, C., HOKAMP, K., MACHUGH, D. E. & HARRIS, J. 2013. Receptor-mediated recognition of mycobacterial pathogens. *Cell Microbiol,* 15**,** 1484-95.

KIM, C. S., AHMAD, S., WU, T., WALTON, W. G., REDINBO, M. R. & TARRAN, R. 2018. SPLUNC1 is an allosteric modulator of the epithelial sodium channel. *FASEB Journal,* 32**,** 2478-2491.

KIM, K. A., GU, W., LEE, I. A., JOH, E. H. & KIM, D. H. 2012. High Fat Diet-Induced Gut Microbiota Exacerbates Inflammation and Obesity in Mice via the TLR4 Signaling Pathway. *PLoS ONE,* 7.

KIM, S. & SKACH, W. 2012. Mechanisms of CFTR Folding at the Endoplasmic Reticulum. *Frontiers in Pharmacology,* 3**,** 201.

KIM, T. H. & LEE, H. K. 2014. Innate immune recognition of respiratory syncytial virus infection. *BMB Reports,* 47**,** 184-191.

KNOWLES, M., GATZY, J. & BOUCHER, R. 1981. Increased Bioelectric Potential Difference across Respiratory Epithelia in Cystic Fibrosis. *New England Journal of Medicine,* 305**,** 1489-1495.

KNOWLES, M. R., CHURCH, N. L., WALTNER, W. E., YANKASKAS, J. R., GILLIGAN, P., KING, M., EDWARDS, L. J., HELMS, R. W. & BOUCHER, R. C. 1990. A Pilot Study of Aerosolized Amiloride for the Treatment of Lung Disease in Cystic Fibrosis. *New England Journal of Medicine,* 322**,** 1189-1194.

KNOWLES, M. R., CLARKE, L. L. & BOUCHER, R. C. 1991. Activation by Extracellular Nucleotides of Chloride Secretion in the Airway Epithelia of Patients with Cystic Fibrosis. *New England Journal of Medicine,* 325**,** 533-538.

KOEHLER, D. R., DOWNEY, G. P., SWEEZEY, N. B., TANSWELL, A. K. & HU, J. 2004. Lung inflammation as a therapeutic target in cystic fibrosis. *Am J Respir Cell Mol Biol,* 31**,** 377-81.

KOFAHI, H. M., TAYLOR, N. G. A., HIRASAWA, K., GRANT, M. D. & RUSSELL, R. S. 2016. Hepatitis C Virus Infection of Cultured Human Hepatoma Cells Causes Apoptosis and Pyroptosis in Both Infected and Bystander Cells. *Scientific Reports,* 6.

KÖNIG, J., SCHREIBER, R., MALL, M. & KUNZELMANN, K. 2002. No evidence for inhibition of ENaC through CFTR-mediated release of ATP. *Biochimica et Biophysica Acta - Biomembranes,* 1565**,** 17-28.

KÖNIG, J., SCHREIBER, R., VOELCKER, T., MALL, M. & KUNZELMANN, K. 2001. The cystic fibrosis transmembrane conductance regulator (CFTR) inhibits ENaC through an increase in the intracellular C1- concentration. *EMBO Reports,* 2**,** 1047-1051.

KONSTAS, A. A., KOCH, J. P. & KORBMACHER, C. 2003. cAMP-dependent activation of CFTR inhibits the epithelial sodium channel (ENaC) without affecting its surface expression. *Pflugers Archiv European Journal of Physiology,* 445**,** 513-521.

KOZUTSUMI, Y., SEGAL, M., NORMINGTON, K., GETHING, M. J. & SAMBROOK, J. 1988. The presence of malfolded proteins in the endoplasmic reticulum signals the induction of glucose-regulated proteins. *Nature,* 332**,** 462-464.

KREDA, S. M., DAVIS, C. W. & ROSE, M. C. 2012. CFTR, mucins, and mucus obstruction in cystic fibrosis. *Cold Spring Harbor Perspectives in Medicine,* 2.

KUEHN, H. S., OUYANG, W., LO, B., DEENICK, E. K., NIEMELA, J. E., AVERY, D. T., SCHICKEL, J. N., TRAN, D. Q., STODDARD, J., ZHANG, Y., FRUCHT, D., DUMITRIU, B., SCHEINBERG, P., FOLIO, L. R., FREIN, C. A., PRICE, S., KOH, C., HELLER, T., SEROOGY, C., HUTTENLOCHER, A., RAO, V. K., SU, H. C., KLEINER, D., NOTARANGELO, L. D., RAMPERTAAP, Y., OLIVIER, K. N., MCELWEE, J., HUGHES, J., PITTALUGA, S., OLIVEIRA, J. B., MEFFRE, E., FLEISHER, T. A., HOLLAND, S. M., LENARDO, M. J., TANGYE, S. G. & UZEL, G. 2014. Immune dysregulation in human subjects with heterozygous germline mutations in CTLA4. *Science,* 345**,** 1623-1627.

KULKA, M., GILCHRIST, M., DUSZYK, M. & BEFUS, A. D. 2002. Expression and functional characterization of CFTR in mast cells. *Journal of Leukocyte Biology,* 71**,** 54-64.

KUNKEL, S. L., SPENGLER, M., MAY, M. A., SPENGLER, R., LARRICK, J. & REMICK, D. 1988. Prostaglandin E2 regulates macrophage-derived tumor necrosis factor gene expression. *Journal of Biological Chemistry,* 263**,** 5380-5384.

KUNZELMANN, K. 2003. ENaC is inhibited by an increase in the intracellular Cl-concentration mediated through activation of Cl- channels. *Pflugers Archiv European Journal of Physiology,* 445**,** 504-512.

KURI, P., SCHIEBER, N. L., THUMBERGER, T., WITTBRODT, J., SCHWAB, Y. & LEPTIN, M. 2017. Dynamics of in vivo ASC speck formation. *Journal of Cell Biology,* 216**,** 2891-2909.

LACHENAL, F., NKANA, K., NOVE-JOSSERAND, R., FABIEN, N. & DURIEU, I. 2009. Prevalence and clinical significance of autoantibodies in adults with cystic fibrosis. *European Respiratory Journal,* 34**,** 1079-1085.

LAFEMINA, M. J., SUTHERLAND, K. M., BENTLEY, T., GONZALES, L. W., ALLEN, L., CHAPIN, C. J., ROKKAM, D., SWEERUS, K. A., DOBBS, L. G., BALLARD, P. L. & FRANK, J. A. 2014. Claudin-18 deficiency results in alveolar barrier dysfunction and impaired alveologenesis in mice. *American Journal of Respiratory Cell and Molecular Biology,* 51**,** 550-558.

LAMBRECHT, B. N. & HAMMAD, H. 2012. The airway epithelium in asthma. *Nature Medicine,* 18**,** 684-692.

LAMKANFI, M. 2011. Emerging inflammasome effector mechanisms. *Nat Rev Immunol,* 11**,** 213-20.

LAMKANFI, M. & DIXIT, V. M. 2014. Mechanisms and functions of inflammasomes. *Cell,* 157**,** 1013-22.

LAMMERTYN, E. J., VANDERMEULEN, E., BELLON, H., EVERAERTS, S., VERLEDEN, S. E., VAN DEN EYNDE, K., BRACKE, K. R., BRUSSELLE, G. G., GOEMINNE, P. C., VERBEKEN, E. K., VANAUDENAERDE, B. M. & DUPONT, L. J. 2017. End-stage cystic fibrosis lung disease is characterised by a diverse inflammatory pattern: An immunohistochemical analysis. *Respiratory Research,* 18.

LAMPROPOULOU, V., SERGUSHICHEV, A., BAMBOUSKOVA, M., NAIR, S., VINCENT, E. E., LOGINICHEVA, E., CERVANTES-BARRAGAN, L., MA, X., HUANG, S. C. C., GRISS, T., WEINHEIMER, C. J., KHADER, S., RANDOLPH, G. J., PEARCE, E. J., JONES, R. G., DIWAN, A., DIAMOND, M. S. & ARTYOMOV, M. N. 2016. Itaconate Links Inhibition of Succinate Dehydrogenase with Macrophage Metabolic Remodeling and Regulation of Inflammation. *Cell Metabolism,* 24**,** 158-166.

LAW, S. M. & GRAY, R. D. 2017. Neutrophil extracellular traps and the dysfunctional innate immune response of cystic fibrosis lung disease: A review. *Journal of Inflammation (United Kingdom),* 14.

LEE, T. W. R., MATTHEWS, D. A. & BLAIR, G. E. 2005. Novel molecular approaches to cystic fibrosis gene therapy. *Biochemical Journal,* 387**,** 1-15.

LEGENDRE, C., MOOIJ, M. J., ADAMS, C. & O'GARA, F. 2011. Impaired expression of hypoxia-inducible factor-1α in cystic fibrosis airway epithelial cells - A role for HIF-1 in the pathophysiology of CF? *Journal of Cystic Fibrosis,* 10**,** 286-290.

LEI-LESTON, A. C., MURPHY, A. G. & MALOY, K. J. 2017. Epithelial cell inflammasomes in intestinal immunity and inflammation. *Frontiers in Immunology,* 8.

LERMAN-SAGIE, R., DAVIDOVICH, M., LEVI, Y., LEVI, I. & NITZAN, M. 1986. Hypo-electrolytemia with metabolic alkalosis as a presenting symptom of cystic fibrosis. *Harefuah,* 111**,** 175-176.

LEVY, H., MURPHY, A., ZOU, F., GERARD, C., KLANDERMAN, B., SCHUEMANN, B., LAZARUS, R., GARCIA, K. C., CELEDON, J. C., DRUMM, M., DAHMER, M., QUASNEY, M., SCHNECK, K., RESKE, M., KNOWLES, M. R., PIER, G. B., LANGE, C. & WEISS, S. T. 2009. IL1B polymorphisms modulate cystic fibrosis lung disease. *Pediatr Pulmonol,* 44**,** 580-93.

LIANG, Y., SARKAR, M. K., TSOI, L. C. & GUDJONSSON, J. E. 2017. Psoriasis: a mixed autoimmune and autoinflammatory disease. *Current Opinion in Immunology,* 49**,** 1-8.

LIESA, M. & SHIRIHAI, O. S. 2016. Mitochondrial Networking in T Cell Memory. *Cell,* 166**,** 9-10.

LISTON, A. & MASTERS, S. L. 2017. Homeostasis-altering molecular processes as mechanisms of inflammasome activation. *Nature Reviews Immunology,* 17**,** 208-214.

LITTLEWOOD-EVANS, A., SARRET, S., APFEL, V., LOESLE, P., DAWSON, J., ZHANG, J., MULLER, A., TIGANI, B., KNEUER, R., PATEL, S., VALEAUX, S., GOMMERMANN, N., RUBIC-SCHNEIDER, T., JUNT, T. & CARBALLIDO, J. M. 2016. GPR91 senses extracellular succinate released from inflammatory macrophages and exacerbates rheumatoid arthritis. *Journal of Experimental Medicine,* 213**,** 1655-1662.

LIU, Y., GAO, X., MIAO, Y., WANG, Y., WANG, H., CHENG, Z., WANG, X., JING, X., JIA, L., DAI, L., LIU, M. & AN, L. 2018. NLRP3 regulates macrophage M2 polarization through up-regulation of IL-4 in asthma. *Biochemical Journal,* 475**,** 1995.

LOO, Y. M. & GALE, M. 2011. Immune Signaling by RIG-I-like Receptors. *Immunity,* 34**,** 680-692.

LOOS, J. A. & ROOS, D. 1973. Changes in the carbohydrate metabolism of mitogenically stimulated human peripheral lymphocytes. III. Stimulation by tuberculin and allogeneic cells. *Experimental Cell Research,* 79**,** 136-142.

LORIOL, C., DULONG, S., AVELLA, M., GABILLAT, N., BOULUKOS, K., BORGESE, F. & EHRENFELD, J. 2008. Characterization of SLC26A9, facilitation of Cl-transport by bicarbonate. *Cellular Physiology and Biochemistry,* 22**,** 15-30.

LUBAMBA, B. A., JONES, L. C., O'NEAL, W. K., BOUCHER, R. C. & RIBEIRO, C. M. P. 2015. X-box-binding protein 1 and innate immune responses of human cystic fibrosis alveolar macrophages. *American Journal of Respiratory and Critical Care Medicine,* 192**,** 1449-1461.

LUKENS, J. R., GROSS, J. M. & KANNEGANTI, T. D. 2012. IL-1 family cytokines trigger sterile inflammatory disease. *Frontiers in Immunology,* 3.

MACHEN, T. E. 2006. Innate immune response in CF airway epithelia: hyperinflammatory? *Am J Physiol Cell Physiol,* 291**,** C218-30.

MACINTYRE, A. N., GERRIETS, V. A., NICHOLS, A. G., MICHALEK, R. D., RUDOLPH, M. C., DEOLIVEIRA, D., ANDERSON, S. M., ABEL, E. D., CHEN, B. J., HALE, L. P. & RATHMELL, J. C. 2014. The glucose transporter Glut1 is selectively essential for CD4 T cell activation and effector function. *Cell Metabolism,* 20**,** 61-72.

MADSEN, K. L., TAVERNINI, M. M., MOSMANN, T. R. & FEDORAK, R. N. 1996. Interleukin 10 modulates ion transport in rat small intestine. *Gastroenterology,* 111**,** 936-944.

MALL, M., BLEICH, M., GREGER, R., SCHREIBER, R. & KUNZELMANN, K. 1998. The amiloride-inhibitable Na+ conductance is reduced by the cystic fibrosis transmembrane conductance regulator in normal but not in cystic fibrosis airways. *Journal of Clinical Investigation,* 102**,** 15-21.

MALL, M., GRUBB, B. R., HARKEMA, J. R., O'NEAL, W. K. & BOUCHER, R. C. 2004. Increased airway epithelial Na+ absorption produces cystic fibrosis-like lung disease in mice. *Nat Med,* 10**,** 487-93.

MAPP, P. I., GROOTVELD, M. C. & BLAKE, D. R. 1995. Hypoxia, oxidative stress and rheumatoid arthritis. *British Medical Bulletin,* 51**,** 419-436.

MARCOS, V., ZHOU-SUCKOW, Z., ONDER YILDIRIM, A., BOHLA, A., HECTOR, A., VITKOV, L., KRAUTGARTNER, W. D., STOIBER, W., GRIESE, M., EICKELBERG, O., MALL, M. A. & HARTL, D. 2015. Free DNA in cystic fibrosis airway fluids correlates with airflow obstruction. *Mediators Inflamm,* 2015**,** 408935.

MARRAKCHI, S., GUIGUE, P., RENSHAW, B. R., PUEL, A., PEI, X. Y., FRAITAG, S., ZRIBI, J., BAL, E., CLUZEAU, C., CHRABIEH, M., TOWNE, J. E., DOUANGPANYA, J., PONS, C., MANSOUR, S., SERRE, V., MAKNI, H., MAHFOUDH, N., FAKHFAKH, F., BODEMER, C., FEINGOLD, J., HADJ-RABIA, S., FAVRE, M., GENIN, E., SAHBATOU, M., MUNNICH, A., CASANOVA, J. L., SIMS, J. E., TURKI, H., BACHELEZ, H. & SMAHI, A. 2011. Interleukin-36-receptor antagonist deficiency and generalized pustular psoriasis. *New England Journal of Medicine,* 365**,** 620-628.

MARSHALL, J. D., ASTE-AMÉZAGA, M., CHEHIMI, S. S., MURPHY, M., OLSEN, H. & TRINCHIERI, G. 1999. Regulation of human IL-18 mRNA expression. *Clinical Immunology,* 90**,** 15-21.

MARSON, F. A. L., BERTUZZO, C. S. & RIBEIRO, J. D. 2016. Classification of CFTR mutation classes. *The Lancet Respiratory Medicine,* 4**,** e37-e38.

MARTINON, F., BURNS, K. & TSCHOPP, J. 2002. The Inflammasome: A molecular platform triggering activation of inflammatory caspases and processing of proIL-β. *Molecular Cell,* 10**,** 417-426.

MATHEWS, R. J., ROBINSON, J. I., BATTELLINO, M., WONG, C., TAYLOR, J. C., BIOLOGICS IN RHEUMATOID ARTHRITIS, G., GENOMICS STUDY, S., EYRE, S., CHURCHMAN, S. M., WILSON, A. G., ISAACS, J. D., HYRICH, K., BARTON, A., PLANT, D., SAVIC, S., COOK, G. P., SARZI-PUTTINI, P., EMERY, P., BARRETT, J. H., MORGAN, A. W. & MCDERMOTT, M. F. 2014.

Evidence of NLRP3-inflammasome activation in rheumatoid arthritis (RA); genetic variants within the NLRP3-inflammasome complex in relation to susceptibility to RA and response to anti-TNF treatment. *Ann Rheum Dis,* 73**,** 1202-10.

MAYER, M. L., BLOHMKE, C. J., FALSAFI, R., FJELL, C. D., MADERA, L., TURVEY, S. E. & HANCOCK, R. E. 2013. Rescue of dysfunctional autophagy attenuates hyperinflammatory responses from cystic fibrosis cells. *J Immunol,* 190**,** 1227-38.

MAYOL, J. M., ADAME-NAVARRETE, Y., ALARMA-ESTRANY, P., MOLINA-ROLDAN, E., HUETE-TORAL, F. & FERNANDEZ-REPRESA, J. A. 2006. Luminal oxidants selectively modulate electrogenic ion transport in rat colon. *World Journal of Gastroenterology,* 12**,** 5523-5527.

MCDERMOTT, M. F. 2004. A common pathway in periodic fever syndromes. *Trends in Immunology,* 25**,** 457-460.

MCDERMOTT, M. F. & AKSENTIJEVICH, I. 2002. The autoinflammatory syndromes. *Current Opinion in Allergy and Clinical Immunology,* 2**,** 511-516.

MCDERMOTT, M. F., AKSENTIJEVICH, I., GALON, J., MCDERMOTT, E. M., WILLIAM OGUNKOLADE, B., CENTOLA, M., MANSFIELD, E., GADINA, M., KARENKO, L., PETTERSSON, T., MCCARTHY, J., FRUCHT, D. M., ARINGER, M., TOROSYAN, Y., TEPPO, A. M., WILSON, M., MEHMET KARAARSLAN, H., WAN, Y., TODD, L., WOOD, G., SCHLIMGEN, R., KUMARAJEEWA, T. R., COOPER, S. M., VELLA, J. P., AMOS, C. I., MULLEY, J., QUANE, K. A., MOLLOY, M. G., RANKI, A., POWELL, R. J., HITMAN, G. A., O'SHEA, J. J. & KASTNER, D. L. 1999. Germline mutations in the extracellular domains of the 55 kDa TNF receptor, TNFR1, define a family of dominantly inherited autoinflammatory syndromes. *Cell,* 97**,** 133-144.

MCELROY, S. P., NOMURA, T., TORRIE, L. S., WARBRICK, E., GARTNER, U., WOOD, G. & MCLEAN, W. H. I. 2013. A Lack of Premature Termination Codon Read-Through Efficacy of PTC124 (Ataluren) in a Diverse Array of Reporter Assays. *PLoS Biology,* 11.

MCGONAGLE, D. & MCDERMOTT, M. F. 2006. A proposed classification of the immunological diseases. *PLoS Medicine,* 3**,** 1242-1248.

MCINERNEY, J., PISANI, D. & O'CONNELL, M. J. 2015. The ring of life hypothesis for eukaryote origins is supported by multiple kinds of data. *Philosophical Transactions of the Royal Society B: Biological Sciences,* 370.

MEDICINE, I. O. 1997. *Emerging Technologies for Nutrition Research: Potential for Assessing Military Performance Capability,* Washington, DC, The National Academies Press.

MEHTA, A. 2005. CFTR: more than just a chloride channel. *Pediatr Pulmonol,* 39**,** 292-8.

MEINDL, R. S. 1987. Hypothesis: A selective advantage for cystic fibrosis heterozygotes. *American Journal of Physical Anthropology,* 74**,** 39-45.

MEYER, M., HUAUX, F., GAVILANES, X., VAN DEN BRULE, S., LEBECQUE, P., LO RE, S., LISON, D., SCHOLTE, B., WALLEMACQ, P. & LEAL, T. 2009. Azithromycin reduces exaggerated cytokine production by M1 alveolar macrophages in cystic fibrosis. *Am J Respir Cell Mol Biol,* 41**,** 590-602.

MIA, S., WARNECKE, A., ZHANG, X. M., MALMSTRÖM, V. & HARRIS, R. A. 2014. An optimized Protocol for Human M2 Macrophages using M-CSF and IL-4/IL-10/TGF-β Yields a Dominant Immunosuppressive Phenotype. *Scandinavian Journal of Immunology,* 79**,** 305-314.

MIAO, E. A., LEAF, I. A., TREUTING, P. M., MAO, D. P., DORS, M., SARKAR, A., WARREN, S. E., WEWERS, M. D. & ADEREM, A. 2010. Caspase-1-induced

pyroptosis is an innate immune effector mechanism against intracellular bacteria. *Nat Immunol,* 11**,** 1136-42.

MIJNDERS, M., KLEIZEN, B. & BRAAKMAN, I. 2017. Correcting CFTR folding defects by small-molecule correctors to cure cystic fibrosis. *Current Opinion in Pharmacology,* 34**,** 83-90.

MILLS, C. D., KINCAID, K., ALT, J. M., HEILMAN, M. J. & HILL, A. M. 2000. M-1/M-2 macrophages and the Th1/Th2 paradigm. *Journal of Immunology,* 164**,** 6166-6173.

MILLS, E. L., KELLY, B., LOGAN, A., COSTA, A. S. H., VARMA, M., BRYANT, C. E., TOURLOMOUSIS, P., DÄBRITZ, J. H. M., GOTTLIEB, E., LATORRE, I., CORR, S. C., MCMANUS, G., RYAN, D., JACOBS, H. T., SZIBOR, M., XAVIER, R. J., BRAUN, T., FREZZA, C., MURPHY, M. P. & O'NEILL, L. A. 2016. Succinate Dehydrogenase Supports Metabolic Repurposing of Mitochondria to Drive Inflammatory Macrophages. *Cell,* 167**,** 457-470.e13.

MILLS, E. L., KELLY, B. & O'NEILL, L. A. J. 2017. Mitochondria are the powerhouses of immunity. *Nature Immunology,* 18**,** 488-498.

MILLS, E. L. & O'NEILL, L. A. 2016. Reprogramming mitochondrial metabolism in macrophages as an anti-inflammatory signal. *European Journal of Immunology,* 46**,** 13-21.

MILLS, E. L., RYAN, D. G., PRAG, H. A., DIKOVSKAYA, D., MENON, D., ZASLONA, Z., JEDRYCHOWSKI, M. P., COSTA, A. S. H., HIGGINS, M., HAMS, E., SZPYT, J., RUNTSCH, M. C., KING, M. S., MCGOURAN, J. F., FISCHER, R., KESSLER, B. M., MCGETTRICK, A. F., HUGHES, M. M., CARROLL, R. G., BOOTY, L. M., KNATKO, E. V., MEAKIN, P. J., ASHFORD, M. L. J., MODIS, L. K., BRUNORI, G., SÉVIN, D. C., FALLON, P. G., CALDWELL, S. T., KUNJI, E. R. S., CHOUCHANI, E. T., FREZZA, C., DINKOVA-KOSTOVA, A. T., HARTLEY, R.

C., MURPHY, M. P. & O'NEILL, L. A. 2018. Itaconate is an anti-inflammatory metabolite that activates Nrf2 via alkylation of KEAP1. *Nature,* 556**,** 113-117.

MISHRA, P., CARELLI, V., MANFREDI, G. & CHAN, D. C. 2014. Proteolytic cleavage of Opa1 stimulates mitochondrial inner membrane fusion and couples fusion to oxidative phosphorylation. *Cell Metabolism,* 19**,** 630-641.

MONTGOMERY, S. T., MALL, M. A., KICIC, A. & STICK, S. M. 2017. Hypoxia and sterile inflammation in cystic fibrosis airways: Mechanisms and potential therapies. *European Respiratory Journal,* 49.

MUÑOZ-ARIAS, I., DOITSH, G., YANG, Z., SOWINSKI, S., RUELAS, D. & GREENE, W. C. 2015. Blood-Derived CD4 T Cells Naturally Resist Pyroptosis during Abortive HIV-1 Infection. *Cell Host and Microbe,* 18**,** 463-470.

MUNOZ-PLANILLO, R., FRANCHI, L., MILLER, L. S. & NUNEZ, G. 2009. A critical role for hemolysins and bacterial lipoproteins in Staphylococcus aureus-induced activation of the Nlrp3 inflammasome. *J Immunol,* 183**,** 3942-8.

MUNOZ-PLANILLO, R., KUFFA, P., MARTINEZ-COLON, G., SMITH, B. L., RAJENDIRAN, T. M. & NUNEZ, G. 2013. K(+) efflux is the common trigger of NLRP3 inflammasome activation by bacterial toxins and particulate matter. *Immunity,* 38**,** 1142-53.

MURUVE, D. A., PETRILLI, V., ZAISS, A. K., WHITE, L. R., CLARK, S. A., ROSS, P. J., PARKS, R. J. & TSCHOPP, J. 2008. The inflammasome recognizes cytosolic microbial and host DNA and triggers an innate immune response. *Nature,* 452**,** 103-7.

NAJAFI, M., ALIMADADI, H., ROUHANI, P., KIANI, M. A., KHODADAD, A., MOTAMED, F., MORAVEJI, A., HOOSHMAND, M., ASHTIANI, M. T. H. & REZAEI, N. 2015. Genotype-phenotype relationship in Iranian patients with cystic fibrosis. *Turkish Journal of Gastroenterology,* 26**,** 241-243.

NAKAMURA, H., YOSHIMURA, K., BAJOCCHI, G., TRAPNELL, B. C., PAVIRANI, A. & CRYSTAL, R. G. 1992. Tumor necrosis factor modulation of expression of the cystic fibrosis transmembrane conductance regulator gene. *FEBS Letters,* 314**,** 366-370.

NG, H. P., ZHOU, Y., SONG, K., HODGES, C. A., DRUMM, M. L. & WANG, G. 2014. Neutrophil-mediated phagocytic host defense defect in myeloid Cftr-inactivated mice. *PLoS One,* 9**,** e106813.

NORATA, G. D., CALIGIURI, G., CHAVAKIS, T., MATARESE, G., NETEA, M. G., NICOLETTI, A., O'NEILL, L. A. J. & MARELLI-BERG, F. M. 2015. The Cellular and Molecular Basis of Translational Immunometabolism. *Immunity,* 43**,** 421-434.

NOUSIA-ARVANITAKIS, S., GALLI-TSINOPOULOU, A., DRACOULACOS, D., KARAMOUZIS, M. & DEMITRIADOU, A. 2000. Islet autoantibodies and insulin dependent diabetes mellitus in cystic fibrosis. *Journal of Pediatric Endocrinology and Metabolism,* 13**,** 319-324.

O'LOUGHLIN, E. V., PANG, G. P., NOLTORP, R., KOINA, C., BATEY, R. & CLANCY, R. 2001. Interleukin 2 modulates ion secretion and cell proliferation in cultured human small intestinal enterocytes. *Gut,* 49**,** 636-643.

O'NEILL, L. A. J. 2015. A Broken Krebs Cycle in Macrophages. *Immunity,* 42**,** 393-394.

O'NEILL, L. A. J. 2016. A Metabolic Roadblock in Inflammatory Macrophages. *Cell Reports,* 17**,** 625-626.

ONOUFRIADIS, A., SIMPSON, M. A., PINK, A. E., DI MEGLIO, P., SMITH, C. H., PULLABHATLA, V., KNIGHT, J., SPAIN, S. L., NESTLE, F. O., BURDEN, A. D., CAPON, F., TREMBATH, R. C. & BARKER, J. N. 2011. Mutations in IL36RN/IL1F5 are associated with the severe episodic inflammatory skin disease

known as generalized pustular psoriasis. *American Journal of Human Genetics,* 89**,** 432-437.

OTTAVIANI, E., FRANCHINI, A., MANDRIOLI, M., SAXENA, A., HANUKOGLU, A. & HANUKOGLU, I. 2002. Amiloride-sensitive epithelial sodium channel subunits are expressed in human and mussel immunocytes. *Developmental and Comparative Immunology,* 26**,** 395-402.

PAINTER, R. G., VALENTINE, V. G., LANSON, N. A., LEIDAL, K., ZHANG, Q., LOMBARD, G., THOMPSON, C., VISWANATHAN, A., NAUSEEF, W. M., WANG, G. & WANG, G. 2006. CFTR Expression in Human Neutrophils and the Phagolysosomal Chlorination Defect in Cystic Fibrosis. *Biochemistry,* 45**,** 10260-10269.

PALOMO, J., DIETRICH, D., MARTIN, P., PALMER, G. & GABAY, C. 2015. The interleukin (IL)-1 cytokine family--Balance between agonists and antagonists in inflammatory diseases. *Cytokine,* 76**,** 25-37.

PANKOW, S., BAMBERGER, C., CALZOLARI, D., MARTINEZ-BARTOLOME, S., LAVALLEE-ADAM, M., BALCH, W. E. & YATES, J. R., 3RD 2015. F508 CFTR interactome remodelling promotes rescue of cystic fibrosis. *Nature,* 528**,** 510-6.

PARK, S., JULIANA, C., HONG, S., DATTA, P., HWANG, I., FERNANDES-ALNEMRI, T., YU, J. W. & ALNEMRI, E. S. 2013. The mitochondrial antiviral protein MAVS associates with NLRP3 and regulates its inflammasome activity. *Journal of Immunology,* 191**,** 4358-4366.

PARK, Y. H., WOOD, G., KASTNER, D. L. & CHAE, J. J. 2016. Pyrin inflammasome activation and RhoA signaling in the autoinflammatory diseases FMF and HIDS. *Nature Immunology.*

PATHAK, S., MCDERMOTT, M. & SAVIC, S. 2016. Autoinflammatory diseases: update on classificationn diagnosis and management. *Journal of Clinical Pathology,* IN PRESS.

PECKHAM, D., SCAMBLER, T., SAVIC, S. & MCDERMOTT, M. F. 2017. The burgeoning field of innate immune-mediated disease and autoinflammation. *Journal of Pathology,* 241**,** 123-139.

PEZZULO, A. A., TANG, X. X., HOEGGER, M. J., ABOU ALAIWA, M. H., RAMACHANDRAN, S., MONINGER, T. O., KARP, P. H., WOHLFORD-LENANE, C. L., HAAGSMAN, H. P., EIJK, M. V., BÁNFI, B., HORSWILL, A. R., STOLTZ, D. A., MC CRAY, P. B., WELSH, M. J. & ZABNER, J. 2012. Reduced airway surface pH impairs bacterial killing in the porcine cystic fibrosis lung. *Nature,* 487**,** 109-113.

PICCOLO, F., TAI, A. S., EE, H., MULRENNAN, S., BELL, S. & RYAN, G. 2017. Clostridium difficile infection in cystic fibrosis: An uncommon but life-threatening complication. *Respirology Case Reports,* 5.

PIER, G. B., GROUT, M., ZAIDI, T., MELULENI, G., MUESCHENBORN, S. S., BANTING, G., RATCLIFF, R., EVANS, M. J. & COLLEDGE, W. H. 1998. Salmonella typhi uses CFTR to enter intestinal epithelial cells. *Nature,* 393**,** 79-82.

POHL, K., HAYES, E., KEENAN, J., HENRY, M., MELEADY, P., MOLLOY, K., JUNDI, B., BERGIN, D. A., MCCARTHY, C., MCELVANEY, O. J., WHITE, M. M., CLYNES, M., REEVES, E. P. & MCELVANEY, N. G. 2014. A neutrophil intrinsic impairment affecting Rab27a and degranulation in cystic fibrosis is corrected by CFTR potentiator therapy. *Blood,* 124**,** 999-1009.

PRULIÈRE-ESCABASSE, V., FANEN, P., DAZY, A. C., LECHAPT-ZALCMAN, E., RIDEAU, D., EDELMAN, A., ESCUDIER, E. & COSTE, A. 2005. TGF-β1

downregulates CFTR expression and function in nasal polyps of non-CF patients. *American Journal of Physiology - Lung Cellular and Molecular Physiology,* 288**,** L77-L83.

PUREN, A. J., FANTUZZI, G. & DINARELLO, C. A. 1999. Gene expression, synthesis, and secretion of interleukin 18 and interleukin 1β are differentially regulated in human blood mononuclear cells and mouse spleen cells. *Proceedings of the National Academy of Sciences of the United States of America,* 96**,** 2256-2261.

RATHMELL, J. C., HEIDEN, M. G. V., HARRIS, M. H., FRAUWIRTH, K. A. & THOMPSON, C. B. 2000. In the absence of extrinsic signals, nutrient utilization by lymphocytes is insufficient to maintain either cell size or viability. *Molecular Cell,* 6**,** 683-692.

RATJEN, F., BELL, S. C., ROWE, S. M., GOSS, C. H., QUITTNER, A. L. & BUSH, A. 2015. Cystic fibrosis. *Nat Rev Dis Primers,* 1**,** 15010.

RAYCHAUDHURI, N., DOUGLAS, R. S. & SMITH, T. J. 2010. PGE2 induces IL-6 in orbital fibroblasts through EP2 receptors and increased gene promoter activity: Implications to thyroid-associated ophthalmopathy. *PLoS ONE,* 5.

REGARD, L., MARTIN, C., ZEMOURA, L., GEOLIER, V., SAGE, E. & BURGEL, P. R. 2018. Peribronchial tertiary lymphoid structures persist after rituximab therapy in patients with cystic fibrosis. *Journal of Clinical Pathology*.

REGELMANN, W. E., SKUBITZ, K. M. & HERRON, J. M. 1991. Increased monocyte oxidase activity in cystic fibrosis heterozygotes and homozygotes. *American journal of respiratory cell and molecular biology,* 5**,** 27-33.

REINIGER, N., LEE, M. M., COLEMAN, F. T., RAY, C., GOLAN, D. E. & PIER, G. B. 2007. Resistance to Pseudomonas aeruginosa chronic lung infection requires cystic

fibrosis transmembrane conductance regulator-modulated interleukin-1 (IL-1) release and signaling through the IL-1 receptor. *Infect Immun,* 75**,** 1598-608.

REN, H. Y., GROVE, D. E., DE LA ROSA, O., HOUCK, S. A., SOPHA, P., VAN GOOR, F., HOFFMAN, B. J. & CYR, D. M. 2013. VX-809 corrects folding defects in cystic fibrosis transmembrane conductance regulator protein through action on membrane-spanning domain 1. *Molecular Biology of the Cell,* 24**,** 3016-3024.

RIMESSI, A., BEZZERRI, V., PATERGNANI, S., MARCHI, S., CABRINI, G. & PINTON, P. 2015. Mitochondrial Ca2+-dependent NLRP3 activation exacerbates the Pseudomonas aeruginosa-driven inflammatory response in cystic fibrosis. *Nat Commun,* 6**,** 6201.

RIORDAN, J. R. 2008. CFTR function and prospects for therapy. *Annu Rev Biochem,* 77**,** 701-26.

RIORDAN, J. R., ROMMENS, J. M., KEREM, B. S., ALON, N. O. A., ROZMAHEL, R., GRZELCZAK, Z., ZIELENSKI, J., LOK, S. I., PLAVSIC, N., CHOU, J. L., DRUMM, M. L., IANNUZZI, M. C., COLLINS, F. S. & TSUI, L. C. 1989. Identification of the cystic fibrosis gene: Cloning and characterization of complementary DNA. *Science,* 245**,** 1066-1073.

RODRÍGUEZ-NUEVO, A., DÍAZ-RAMOS, A., NOGUERA, E., DÍAZ-SÁEZ, F., DURAN, X., MUÑOZ, J. P., ROMERO, M., PLANA, N., SEBASTIÁN, D., TEZZE, C., ROMANELLO, V., RIBAS, F., SECO, J., PLANET, E., DOCTROW, S. R., GONZÁLEZ, J., BORRÀS, M., LIESA, M., PALACÍN, M., VENDRELL, J., VILLARROYA, F., SANDRI, M., SHIRIHAI, O. & ZORZANO, A. 2018. Mitochondrial DNA and TLR9 drive muscle inflammation upon Opa1 deficiency. *EMBO Journal,* 37.

ROLFE, M. W., KUNKEL, S. L., ROWENS, B., STANDIFORD, T. J., CRAGOE JR, E. J. & STRIETER, R. M. 1992. Suppression of human alveolar macrophage-derived cytokines by amiloride. *American journal of respiratory cell and molecular biology,* 6**,** 576-582.

ROMEO, G., DEVOTO, M. & GALIETTA, L. J. V. 1989. Why is the cystic fibrosis gene so frequent? *Human Genetics,* 84**,** 1-5.

ROMMENS, J. M., IANNUZZI, M. C., KEREM, B. S., DRUMM, M. L., MELMER, G., DEAN, M., ROZMAHEL, R., COLE, J. L., KENNEDY, D., HIDAKA, N., ZSIGA, M., BUCHWALD, M., RIORDAN, J. R., TSUI, L. C. & COLLINS, F. S. 1989. Identification of the cystic fibrosis gene: Chromosome walking and jumping. *Science,* 245**,** 1059-1065.

RON-HAREL, N., SANTOS, D., GHERGUROVICH, J. M., SAGE, P. T., REDDY, A., LOVITCH, S. B., DEPHOURE, N., SATTERSTROM, F. K., SHEFFER, M., SPINELLI, J. B., GYGI, S., RABINOWITZ, J. D., SHARPE, A. H. & HAIGIS, M. C. 2016. Mitochondrial Biogenesis and Proteome Remodeling Promote One-Carbon Metabolism for T Cell Activation. *Cell Metabolism,* 24**,** 104-117.

ROOS, D. & LOOS, J. A. 1973. Changes in the carbohydrate metabolism of mitogenically stimulated human peripheral lymphocytes. II. Relative importance of glycolysis and oxidative phosphorylation on phytohaemagglutinin stimulation. *Experimental Cell Research,* 77**,** 127-135.

ROTSCHILD, M., ELIAS, N., BERKOWITZ, D., POLLAK, S., SHINAWI, M., BECK, R. & BENTUR, L. 2005. Autoantibodies against bactericidal/permeability-increasing protein (BPI-ANCA) in cystic fibrosis patients treated with azithromycin. *Clinical and Experimental Medicine,* 5**,** 80-85.

ROWCZENIO, D. M., PATHAK, S., AROSTEGUI, J. I., MENSA-VILARO, A., OMOYINMI, E., BROGAN, P., LIPSKER, D., SCAMBLER, T., OWEN, R., TROJER, H., BAGINSKA, A., GILLMORE, J. D., WECHALEKAR, A. D., LANE, T., WILLIAMS, R., YOUNGSTEIN, T., HAWKINS, P. N., SAVIC, S. & LACHMANN, H. J. 2017. Molecular genetic investigation, clinical features and response to treatment in 21 patients with Schnitzlers syndrome. *Blood*.

SAVIC, S., DICKIE, L. J., WITTMANN, M. & MCDERMOTT, M. F. 2012. Autoinflammatory syndromes and cellular responses to stress: Pathophysiology, diagnosis and new treatment perspectives. *Best Practice and Research: Clinical Rheumatology,* 26**,** 505-533.

SCAMBLER, T., HOLBROOK, J., SAVIC, S., MCDERMOTT, M. F. & PECKHAM, D. 2018. Autoinflammatory disease in the lung. *Immunology*.

SCHINDLER, T., MICHEL, S. & WILSON, A. W. M. 2015. Nutrition Management of Cystic Fibrosis in the 21st Century. *Nutrition in Clinical Practice,* 30**,** 488-500.

SCHIOTZ, P. O., EGESKJOLD, E. M., HOIBY, N. & PERMIN, H. 1979. Autoantibodies in serum and sputum from patients with cystic fibrosis. *Acta Pathologica et Microbiologica Scandinavica - Section C Immunology,* 87**,** 319-324.

SCHLESINGER, N. 2014. Anti-interleukin-1 therapy in the management of gout. *Current Rheumatology Reports,* 16**,** 398.

SCHMIDT, C., HÖCHERL, K., SCHWEDA, F., KURTZ, A. & BUCHER, M. 2007. Regulation of renal sodium transporters during severe inflammation. *Journal of the American Society of Nephrology,* 18**,** 1072-1083.

SCHROEDER, B. C., CHENG, T., JAN, Y. N. & JAN, L. Y. 2008. Expression Cloning of TMEM16A as a Calcium-Activated Chloride Channel Subunit. *Cell,* 134**,** 1019-1029.

SCHULTZ, A., PUVVADI, R., BORISOV, S. M., SHAW, N. C., KLIMANT, I., BERRY, L. J., MONTGOMERY, S. T., NGUYEN, T., KREDA, S. M., KICIC, A., NOBLE, P. B., BUTTON, B. & STICK, S. M. 2017. Airway surface liquid pH is not acidic in children with cystic fibrosis. *Nature Communications,* 8.

SCUDIERI, P., CACI, E., BRUNO, S., FERRERA, L., SCHIAVON, M., SONDO, E., TOMATI, V., GIANOTTI, A., ZEGARRA-MORAN, O., PEDEMONTE, N., REA, F., RAVAZZOLO, R. & GALIETTA, L. J. V. 2012. Association of TMEM16A chloride channel overexpression with airway goblet cell metaplasia. *Journal of Physiology,* 590**,** 6141-6155.

SENA, L., LI, S., JAIRAMAN, A., PRAKRIYA, M., EZPONDA, T., HILDEMAN, D., WANG, C. R., SCHUMACKER, P., LICHT, J., PERLMAN, H., BRYCE, P. & CHANDEL, N. 2013. Mitochondria Are Required for Antigen-Specific T Cell Activation through Reactive Oxygen Species Signaling. *Immunity,* 38**,** 225-236.

SETH, R. B., SUN, L., EA, C. K. & CHEN, Z. J. 2005. Identification and characterization of MAVS, a mitochondrial antiviral signaling protein that activates NF-κB and IRF3. *Cell,* 122**,** 669-682.

SHI, H., WANG, Y., LI, X., ZHAN, X., TANG, M., FINA, M., SU, L., PRATT, D., BU, C. H., HILDEBRAND, S., LYON, S., SCOTT, L., QUAN, J., SUN, Q., RUSSELL, J., ARNETT, S., JUREK, P., CHEN, D., KRAVCHENKO, V. V., MATHISON, J. C., MORESCO, E. M., MONSON, N. L., ULEVITCH, R. J. & BEUTLER, B. 2016. NLRP3 activation and mitosis are mutually exclusive events coordinated by NEK7, a new inflammasome component. *Nat Immunol,* 17**,** 250-8.

SHI, J., ZHAO, Y., WANG, K., SHI, X., WANG, Y., HUANG, H., ZHUANG, Y., CAI, T., WANG, F. & SHAO, F. 2015. Cleavage of GSDMD by inflammatory caspases determines pyroptotic cell death. *Nature,* 526**,** 660-5.

SIMONIN-LE JEUNE, K., LE JEUNE, A., JOUNEAU, S., BELLEGUIC, C., ROUX, P. F., JAGUIN, M., DIMANCHE-BOITRE, M. T., LECUREUR, V., LECLERCQ, C., DESRUES, B., BRINCHAULT, G., GANGNEUX, J. P. & MARTIN-CHOULY, C. 2013. Impaired Functions of Macrophage from Cystic Fibrosis Patients: CD11b, TLR-5 Decrease and sCD14, Inflammatory Cytokines Increase. *PLoS ONE,* 8.

SINGH, A. K., ALANI, S., BALUT, C., FAN, Y., GAO, W., GRESZLER, S., JIA, Y., LIU, B., MANELLI, A., SEARLE, X., SWENSEN, A., VORTHERMS, T., YEUNG, C., CONRATH, K., WANG, X. & TSE, C. 2016. Discovery and characterization of ABBV/GLPG-2222, a novel first generation CFTR corrector. *Pediatr. Pulmonol.,* 51**,** 264-265.

SINHA, C., ZHANG, W., MOON, C. S., ACTIS, M., YARLAGADDA, S., ARORA, K., WOODROOFE, K., CLANCY, J. P., LIN, S., ZIADY, A. G., FRIZZELL, R., FUJII, N. & NAREN, A. P. 2015. Capturing the Direct Binding of CFTR Correctors to CFTR by Using Click Chemistry. *ChemBioChem,* 16**,** 2017-2022.

SOLOMON, G. M., MARSHALL, S. G., RAMSEY, B. W. & ROWE, S. M. 2015. Breakthrough therapies: Cystic fibrosis (CF) potentiators and correctors. *Pediatric Pulmonology,* 50**,** S3-S13.

SORIO, C., BUFFELLI, M., ANGIARI, C., ETTORRE, M., JOHANSSON, J., VEZZALINI, M., VIVIANI, L., RICCIARDI, M., VERZÈ, G., ASSAEL, B. M. & MELOTTI, P. 2011. Defective CFTR expression and function are detectable in blood monocytes: Development of a new blood test for cystic fibrosis. *PLoS ONE,* 6.

SORIO, C., MONTRESOR, A., BOLOMINI-VITTORI, M., CALDRER, S., ROSSI, B., DUSI, S., ANGIARI, S., JOHANSSON, J. E., VEZZALINI, M., LEAL, T., CALCATERRA, E., ASSAEL, B. M., MELOTTI, P. & LAUDANNA, C. 2016. Mutations of cystic fibrosis transmembrane conductance regulator gene cause a

monocyte-selective adhesion deficiency. *American Journal of Respiratory and Critical Care Medicine,* 193**,** 1123-1133.

SOSNAY, P. R., SIKLOSI, K. R., VAN GOOR, F., KANIECKI, K., YU, H., SHARMA, N., RAMALHO, A. S., AMARAL, M. D., DORFMAN, R., ZIELENSKI, J., MASICA, D. L., KARCHIN, R., MILLEN, L., THOMAS, P. J., PATRINOS, G. P., COREY, M., LEWIS, M. H., ROMMENS, J. M., CASTELLANI, C., PENLAND, C. M. & CUTTING, G. R. 2013. Defining the disease liability of variants in the cystic fibrosis transmembrane conductance regulator gene. *Nat Genet,* 45**,** 1160-7.

SRIVASTAVA, S., PELLOSO, D., FENG, H., VOILES, L., LEWIS, D., HASKOVA, Z., WHITACRE, M., TRULLI, S., CHEN, Y. J., TOSO, J., JONAK, Z. L., CHANG, H. C. & ROBERTSON, M. J. 2013. Effects of interleukin-18 on natural killer cells: Costimulation of activation through Fc receptors for immunoglobulin. *Cancer Immunology, Immunotherapy,* 62**,** 1073-1082.

STOFFELS, M. & KASTNER, D. L. 2016. Old Dogs, New Tricks: Monogenic Autoinflammatory Disease Unleashed. *Annu Rev Genomics Hum Genet*.

STOKES, C. A., KAUR, R., EDWARDS, M. R., MONDHE, M., ROBINSON, D., PRESTWICH, E. C., HUME, R. D., MARSHALL, C. A., PERRIE, Y., O'DONNELL, V. B., HARWOOD, J. L., SABROE, I. & PARKER, L. C. 2016. Human rhinovirus-induced inflammatory responses are inhibited by phosphatidylserine containing liposomes. *Mucosal Immunol*.

STREB, H., IRVINE, R. F., BERRIDGE, M. J. & SCHULZ, I. 1983. Release of Ca2+from a nonmitochondrial intracellular store in pancreatic acinar cells by inositol-1,4,5-trisphosphate. *Nature,* 306**,** 67-69.

SU, X., LOONEY, M. R., SU, H. E., LEE, J. W., SONG, Y. & MATTHAY, M. A. 2011. Role of CFTR expressed by neutrophils in modulating acute lung inflammation and injury in mice. *Inflamm Res,* 60**,** 619-32.

SUBRAMANIAN, N., NATARAJAN, K., CLATWORTHY, M. R., WANG, Z. & GERMAIN, R. N. 2013. The adaptor MAVS promotes NLRP3 mitochondrial localization and inflammasome activation. *Cell,* 153**,** 348-361.

SUTTERWALA, F. S., MIJARES, L. A., LI, L., OGURA, Y., KAZMIERCZAK, B. I. & FLAVELL, R. A. 2007. Immune recognition of Pseudomonas aeruginosa mediated by the IPAF/NLRC4 inflammasome. *J Exp Med,* 204**,** 3235-45.

SWEENEY, C. M., TOBIN, A. M. & KIRBY, B. 2011. Innate immunity in the pathogenesis of psoriasis. *Archives of Dermatological Research,* 303**,** 691-705.

TANG, A., SHARMA, A., JEN, R., HIRSCHFELD, A. F., CHILVERS, M. A., LAVOIE, P. M. & TURVEY, S. E. 2012. Inflammasome-mediated IL-1beta production in humans with cystic fibrosis. *PLoS One,* 7**,** e37689.

TANG, T., SCAMBLER, T. E., SMALLIE, T., CUNLIFFE, H. E., ROSS, E. A., ROSNER, D. R., O'NEIL, J. D. & CLARK, A. R. 2017. Macrophage responses to lipopolysaccharide are modulated by a feedback loop involving prostaglandin E_2, dual specificity phosphatase 1 and tristetraprolin. *Scientific Reports,* 7.

TANG, X. X., OSTEDGAARD, L. S., HOEGGER, M. J., MONINGER, T. O., KARP, P. H., MCMENIMEN, J. D., CHOUDHURY, B., VARKI, A., STOLTZ, D. A. & WELSH, M. J. 2016. Acidic pH increases airway surface liquid viscosity in cystic fibrosis. *Journal of Clinical Investigation,* 126**,** 879-891.

TANNAHILL, G. M., CURTIS, A. M., ADAMIK, J., PALSSON-MCDERMOTT, E. M., MCGETTRICK, A. F., GOEL, G., FREZZA, C., BERNARD, N. J., KELLY, B.,

FOLEY, N. H., ZHENG, L., GARDET, A., TONG, Z., JANY, S. S., CORR, S. C., HANEKLAUS, M., CAFFREY, B. E., PIERCE, K., WALMSLEY, S., BEASLEY, F. C., CUMMINS, E., NIZET, V., WHYTE, M., TAYLOR, C. T., LIN, H., MASTERS, S. L., GOTTLIEB, E., KELLY, V. P., CLISH, C., AURON, P. E., XAVIER, R. J. & O'NEILL, L. A. 2013a. Succinate is an inflammatory signal that induces IL-1beta through HIF-1alpha. *Nature,* 496**,** 238-42.

TANNAHILL, G. M., CURTIS, A. M., ADAMIK, J., PALSSON-MCDERMOTT, E. M., MCGETTRICK, A. F., GOEL, G., FREZZA, C., BERNARD, N. J., KELLY, B., FOLEY, N. H., ZHENG, L., GARDET, A., TONG, Z., JANY, S. S., CORR, S. C., HANEKLAUS, M., CAFFREY, B. E., PIERCE, K., WALMSLEY, S., BEASLEY, F. C., CUMMINS, E., NIZET, V., WHYTE, M., TAYLOR, C. T., LIN, H., MASTERS, S. L., GOTTLIEB, E., KELLY, V. P., CLISH, C., AURON, P. E., XAVIER, R. J. & O'NEILL, L. A. J. 2013b. Succinate is an inflammatory signal that induces IL-1β through HIF-1α. *Nature,* 496**,** 238-242.

TARIQUE, A. A., SLY, P. D., HOLT, P. G., BOSCO, A., WARE, R. S., LOGAN, J., BELL, S. C., WAINWRIGHT, C. E. & FANTINO, E. 2017. CFTR-dependent defect in alternatively-activated macrophages in cystic fibrosis. *Journal of Cystic Fibrosis,* 16**,** 475-482.

TAYLOR, P. C. & SIVAKUMAR, B. 2005. Hypoxia and angiogenesis in rheumatoid arthritis. *Current Opinion in Rheumatology,* 17**,** 293-298.

TAYLOR, P. R., BONFIELD, T. L., CHMIEL, J. F. & PEARLMAN, E. 2016. Neutrophils from F508del cystic fibrosis patients produce IL-17A and express IL-23 - dependent IL-17RC. *Clin Immunol*.

TECLE, T., TRIPATHI, S. & HARTSHORN, K. L. 2010. Defensins and cathelicidins in lung immunity. *Innate Immunity,* 16**,** 151-159.

TSCHOPP, J. & SCHRODER, K. 2010. NLRP3 inflammasome activation: The convergence of multiple signalling pathways on ROS production? *Nat Rev Immunol,* 10**,** 210-5.

VAETH, M., MAUS, M., KLEIN-HESSLING, S., FREINKMAN, E., YANG, J., ECKSTEIN, M., CAMERON, S., TURVEY, S. E., SERFLING, E., BERBERICH-SIEBELT, F., POSSEMATO, R. & FESKE, S. 2017. Store-Operated Ca2+Entry Controls Clonal Expansion of T Cells through Metabolic Reprogramming. *Immunity*.

VAETH, M., ZEE, I., CONCEPCION, A. R., MAUS, M., SHAW, P., PORTAL-CELHAY, C., ZAHRA, A., KOZHAYA, L., WEIDINGER, C., PHILIPS, J., UNUTMAZ, D. & FESKE, S. 2015. Ca<sup>2+</sup> signaling but not store-operated Ca<sup>2+</sup> entry is required for the function of macrophages and dendritic cells. *Journal of Immunology,* 195**,** 1202-1217.

VALDIVIESO, A. G. & SANTA-COLOMA, T. A. 2013. CFTR activity and mitochondrial function. *Redox Biol,* 1**,** 190-202.

VAN 'T WOUT, E. F., VAN SCHADEWIJK, A., VAN BOXTEL, R., DALTON, L. E., CLARKE, H. J., TOMMASSEN, J., MARCINIAK, S. J. & HIEMSTRA, P. S. 2015. Virulence Factors of Pseudomonas aeruginosa Induce Both the Unfolded Protein and Integrated Stress Responses in Airway Epithelial Cells. *PLoS Pathog,* 11**,** e1004946.

VAN DE WEERT-VAN LEEUWEN, P. B., VAN MEEGEN, M. A., SPEIRS, J. J., PALS, D. J., ROOIJAKKERS, S. H., VAN DER ENT, C. K., TERHEGGEN-LAGRO, S. W., ARETS, H. G. & BEEKMAN, J. M. 2013. Optimal complement-mediated phagocytosis of Pseudomonas aeruginosa by monocytes is cystic fibrosis transmembrane conductance regulator-dependent. *Am J Respir Cell Mol Biol,* 49**,** 463-70.

VAN DEN BOSSCHE, J., BAARDMAN, J. & DE WINTHER, M. P. J. 2015. Metabolic characterization of polarized M1 and M2 bone marrow-derived macrophages using real-time extracellular flux analysis. *Journal of Visualized Experiments,* 2015.

VAN DER HEIJDEN, R. A., SHEEDFAR, F., MORRISON, M. C., HOMMELBERG, P. P. H., KOR, D., KLOOSTERHUIS, N. J., GRUBEN, N., YOUSSEF, S. A., DE BRUIN, A., HOFKER, M. H., KLEEMANN, R., KOONEN, D. P. Y. & HEERINGA, P. 2015. High-fat diet induced obesity primes inflammation in adipose tissue prior to liver in C57BL/6j mice. *Aging,* 7**,** 256-268.

VAN DER MERWE, J. Q., OHLAND, C. L., HIROTA, C. L. & MACNAUGHTON, W. K. 2009. Prostaglandin E2 derived from cyclooxygenases 1 and 2 mediates intestinal epithelial ion transport stimulated by the activation of protease-activated receptor 2. *Journal of Pharmacology and Experimental Therapeutics,* 329**,** 747-752.

VAN GOOR, F., HADIDA, S., GROOTENHUIS, P. D. J., BURTON, B., STACK, J. H., STRALEY, K. S., DECKER, C. J., MILLER, M., MCCARTNEY, J., OLSON, E. R., WINE, J. J., FRIZZELL, R. A., ASHLOCK, M. & NEGULESCU, P. A. 2011. Correction of the F508del-CFTR protein processing defect in vitro by the investigational drug VX-809. *Proceedings of the National Academy of Sciences of the United States of America,* 108**,** 18843-18848.

VELTMAN, M., STOLARCZYK, M., RADZIOCH, D., WOJEWODKA, G., DE SANCTIS, J. B., DIK, W. A., DZYUBACHYK, O., ORAVECZ, T., DE KLEER, I. & SCHOLTE, B. J. 2016. Correction of lung inflammation in a F508del CFTR murine cystic fibrosis model by the sphingosine-1-phosphate lyase inhibitor LX2931. *American Journal of Physiology - Lung Cellular and Molecular Physiology,* 311**,** L1000-L1014.

VENKATAKRISHNAN, A., STECENKO, A. A., KING, G., BLACKWELL, T. R., BRIGHAM, K. L., CHRISTMAN, J. W. & BLACKWELL, T. S. 2000. Exaggerated activation of nuclear factor-kappaB and altered IkappaB-beta processing in cystic fibrosis bronchial epithelial cells. *Am J Respir Cell Mol Biol,* 23**,** 396-403.

WAINWRIGHT, B. J., SCAMBLER, P. J., SCHMIDTKE, J., WATSON, E. A., LAW, H. Y., FARRALL, M., COOKE, H. J., EIBERG, H. & WILLIAMSON, R. 1985. Localization of cystic fibrosis locus to human chromosome 7cen-q22. *Nature,* 318**,** 384-385.

WAINWRIGHT, C. E., ELBORN, J. S., RAMSEY, B. W., MARIGOWDA, G., HUANG, X., CIPOLLI, M., COLOMBO, C., DAVIES, J. C., DE BOECK, K., FLUME, P. A., KONSTAN, M. W., MCCOLLEY, S. A., MCCOY, K., MCKONE, E. F., MUNCK, A., RATJEN, F., ROWE, S. M., WALTZ, D., BOYLE, M. P., GROUP, T. S. & GROUP, T. S. 2015. Lumacaftor-Ivacaftor in Patients with Cystic Fibrosis Homozygous for Phe508del CFTR. *N Engl J Med,* 373**,** 220-31.

WATT, A. P., COURTNEY, J., MOORE, J., ENNIS, M. & ELBORN, J. S. 2005. Neutrophil cell death, activation and bacterial infection in cystic fibrosis. *Thorax,* 60**,** 659-664.

WEBER, A. J., SOONG, G., BRYAN, R., SABA, S. & PRINCE, A. 2001. Activation of NF-kappaB in airway epithelial cells is dependent on CFTR trafficking and Cl- channel function. *Am J Physiol Lung Cell Mol Physiol,* 281**,** L71-8.

WEKELL, P., KARLSSON, A., BERG, S. & FASTH, A. 2016. Review of autoinflammatory diseases, with a special focus on periodic fever, aphthous stomatitis, pharyngitis and cervical adenitis syndrome. *Acta Paediatrica, International Journal of Paediatrics,* 105**,** 1140-1151.

WELCH, E. M., BARTON, E. R., ZHUO, J., TOMIZAWA, Y., FRIESEN, W. J., TRIFILLIS, P., PAUSHKIN, S., PATEL, M., TROTTA, C. R., HWANG, S.,

WILDE, R. G., KARP, G., TAKASUGI, J., CHEN, G., JONES, S., REN, H., MOON, Y. C., CORSON, D., TURPOFF, A. A., CAMPBELL, J. A., CONN, M. M., KHAN, A., ALMSTEAD, N. G., HEDRICK, J., MOLLIN, A., RISHER, N., WEETALL, M., YEH, S., BRANSTROM, A. A., COLACINO, J. M., BABIAK, J., JU, W. D., HIRAWAT, S., NORTHCUTT, V. J., MILLER, L. L., SPATRICK, P., HE, F., KAWANA, M., FENG, H., JACOBSON, A., PELTZ, S. W. & SWEENEY, H. L. 2007. PTC124 targets genetic disorders caused by nonsense mutations. *Nature,* 447**,** 87-91.

WEN, H., TING, J. P. & O'NEILL, L. A. 2012. A role for the NLRP3 inflammasome in metabolic diseases--did Warburg miss inflammation? *Nat Immunol,* 13**,** 352-7.

WEYLER, R. T., YURKO-MAURO, K. A., RUBENSTEIN, R., KOLLEN, W. J. W., REENSTRA, W., ALTSCHULER, S. M., EGAN, M. & MULBERG, A. E. 1999. CFTR is functionally active in GnRH-expressing GT1-7 hypothalamic neurons. *American Journal of Physiology - Cell Physiology,* 277**,** C563-C571.

WHITSETT, J. A. & ALENGHAT, T. 2015. Respiratory epithelial cells orchestrate pulmonary innate immunity. *Nat Immunol,* 16**,** 27-35.

WILSCHANSKI, M., MILLER, L. L., SHOSEYOV, D., BLAU, H., RIVLIN, J., AVIRAM, M., COHEN, M., ARMONI, S., YAAKOV, Y., PUGATCH, T., COHEN-CYMBERKNOH, M., MILLER, N. L., REHA, A., NORTHCUTT, V. J., HIRAWAT, S., DONNELLY, K., ELFRING, G. L., AJAYI, T. & KEREM, E. 2011. Chronic ataluren (PTC124) treatment of nonsense mutation cystic fibrosis. *European Respiratory Journal,* 38**,** 59-69.

XU, H., YANG, J., GAO, W., LI, L., LI, P., ZHANG, L., GONG, Y. N., PENG, X., XI, J. J., CHEN, S., WANG, F. & SHAO, F. 2014. Innate immune sensing of bacterial modifications of Rho GTPases by the Pyrin inflammasome. *Nature,* 513**,** 237-241.

YANG, D., HE, Y., MUNOZ-PLANILLO, R., LIU, Q. & NUNEZ, G. 2015. Caspase-11 Requires the Pannexin-1 Channel and the Purinergic P2X7 Pore to Mediate Pyroptosis and Endotoxic Shock. *Immunity,* 43**,** 923-32.

YANG, J., ZHAO, Y., SHI, J. & SHAO, F. 2013a. Human NAIP and mouse NAIP1 recognize bacterial type III secretion needle protein for inflammasome activation. *Proc Natl Acad Sci U S A,* 110**,** 14408-13.

YANG, Y. D., CHO, H., KOO, J. Y., TAK, M. H., CHO, Y., SHIM, W. S., PARK, S. P., LEE, J., LEE, B., KIM, B. M., RAOUF, R., SHIN, Y. K. & OH, U. 2008. TMEM16A confers receptor-activated calcium-dependent chloride conductance. *Nature,* 455**,** 1210-1215.

YANG, Z., FUJII, H., MOHAN, S. V., GORONZY, J. J. & WEYAND, C. M. 2013b. Phosphofructokinase deficiency impairs atp generation, autophagy, and redox balance in rheumatoid arthritis T cells. *Journal of Experimental Medicine,* 210**,** 2119-2134.

YARON, J. R., GANGARAJU, S., RAO, M. Y., KONG, X., ZHANG, L., SU, F., TIAN, Y., GLENN, H. L. & MELDRUM, D. R. 2015. K(+) regulates Ca(2+) to drive inflammasome signaling: dynamic visualization of ion flux in live cells. *Cell Death Dis,* 6**,** e1954.

ZAIDI, T., MOWREY-MCKEE, M. & PIER, G. B. 2004. Hypoxia increases corneal cell expression of CFTR leading to increased Pseudomonas aeruginosa binding, internalization, and initiation of inflammation. *Investigative Ophthalmology and Visual Science,* 45**,** 4066-4074.

ZASŁONA, Z., PALSSON-MCDERMOTT, E. M., MENON, D., HANEKLAUS, M., FLIS, E., PRENDEVILLE, H., CORCORAN, S. E., PETERS-GOLDEN, M. & O'NEILL, L. A. J. 2017. The induction of Pro-IL-1β by lipopolysaccharide requires endogenous prostaglandin E$_2$ production. *Journal of Immunology,* 198**,** 3558-3564.

ZHANG, J. Z., LIU, Z., LIU, J., REN, J. X. & SUN, T. S. 2014. Mitochondrial DNA induces inflammation and increases TLR9/NF-κB expression in lung tissue. *International Journal of Molecular Medicine,* 33**,** 817-824.

ZHANG, Q., RAOOF, M., CHEN, Y., SUMI, Y., SURSAL, T., JUNGER, W., BROHI, K., ITAGAKI, K. & HAUSER, C. J. 2010. Circulating mitochondrial DAMPs cause inflammatory responses to injury. *Nature,* 464**,** 104-107.

ZHANG, W., ZHANG, X., ZHANG, Y. H., STOKES, D. C. & NAREN, A. P. 2016. Lumacaftor/ivacaftor combination for cystic fibrosis patients homozygous for Phe508del-CFTR. *Drugs of Today,* 52**,** 229-237.

ZHAO, Y., YANG, J., SHI, J., GONG, Y. N., LU, Q., XU, H., LIU, L. & SHAO, F. 2011. The NLRC4 inflammasome receptors for bacterial flagellin and type III secretion apparatus. *Nature,* 477**,** 596-600.

ZHOU, Z., DUERR, J., JOHANNESSON, B., SCHUBERT, S. C., TREIS, D., HARM, M., GRAEBER, S. Y., DALPKE, A., SCHULTZ, C. & MALL, M. A. 2011. The ENaC-overexpressing mouse as a model of cystic fibrosis lung disease. *Journal of Cystic Fibrosis,* 10**,** S172-S182.

ZHOU, Z., TREIS, D., SCHUBERT, S. C., HARM, M., SCHATTERNY, J., HIRTZ, S., DUERR, J., BOUCHER, R. C. & MALL, M. A. 2008. Preventive but not late amiloride therapy reduces morbidity and mortality of lung disease in βENaC-overexpressing mice. *American Journal of Respiratory and Critical Care Medicine,* 178**,** 1245-1256.

ZU, X. L. & GUPPY, M. 2004. Cancer metabolism: Facts, fantasy, and fiction. *Biochemical and Biophysical Research Communications,* 313**,** 459-465.